11 MARCH 1967

K-11-67-1

FINAL REPORT

A STUDY OF HYDROGEN SLUSH AND/OR HYDROGEN GEL UTILIZATION

Contract NAS 8-20342

VOLUME II

SYSTEMS OPTIMIZATION AND VEHICLE APPLICATION STUDIES

CRYOGENIC STAGE PROGRAMS

LOCKHEED MISSILES & SPACE COMPANY / SUNNYVALE, CALIFORNIA

66-21.1

11 MARCH 1967

K-11-67-1

FINAL REPORT

A STUDY OF HYDROGEN SLUSH AND/OR HYDROGEN GEL UTILIZATION

Contract NAS 8-20342

VOLUME II

SYSTEMS OPTIMIZATION AND VEHICLE APPLICATION STUDIES

Prepared for

NATIONAL AERONAUTICS AND SPACE ADMINISTRATION
GEORGE C. MARSHALL SPACE FLIGHT CENTER
HUNTSVILLE, ALABAMA

CRYOGENIC STAGE PROGRAMS

LOCKHEED MISSILES & SPACE COMPANY / SUNNYVALE, CALIFORNIA

FOREWORD

The study described in this report was conducted by Lockheed Missiles & Space Company (LMSC) under Contract NAS 8-20342 for the George C. Marshall Space Flight Center (MSFC), National Aeronautics and Space Administration, Huntsville, Alabama. All study efforts were performed under the technical direction of Mr. A. L. Worlund of the Fluid Thermal Systems Branch of the Propulsion and Vehicle Engineering Laboratory.

Results of the Hydrogen Slush and/or Hydrogen Gel Utilization Study are published in two volumes:

Volume I – Handbook of Physical and Thermal Property Data for Hydrogen
Volume II – Systems Optimization and Vehicle Application Studies

Primary contributors to the study and reports were:

- Project Manager: C. W. Keller
- Thermodynamics: T. C. Nast, R. P. Warren, W. S. Williams, D. R. Elgin
- Propellant Dynamics: Dr. G. Vliet
- Propulsion Analysis: G. W. Coutts
- Performance Analysis: P. J. Van Zytveld
- Systems Analysis: H. L. Jensen, W. B. Zeber, E. F. Costa
- Design: R. B. Seger
- Instrumentation: R. M. Kocher

Close coordination was maintained throughout the study contract with Mr. D. B. Chelton and Mr. D. B. Mann of the National Bureau of Standards (NBS), Institute for Materials Research, Cryogenics Division, where a related analytical and experimental program on slush-hydrogen characteristics is in progress.

Technical opinions and data regarding the J-2 and RL10 rocket engines, the Saturn V/S-IVB propulsion stage, and its hydrogen chilldown pumping system were contributed during the study by:

- Rocketdyne, a Division of North American Aviation, Inc.
- Pratt & Whitney Aircraft, a Division of United Aircraft Corporation
- Douglas Missiles and Space Division of Douglas Aircraft Company
- Pesco Products, a Division of Borg-Warner Corporation

CONTENTS

ILLUSTRATIONS

TABLES

NOTATION

Basic Symbols			International Units	English Units
a	=	liquid-vapor interface area	cm^2	ft^2
d	=	tank diameter	m	ft
g_c	=	gravitational constant	9.807 m/sec^2	32.2 ft/sec^2
k	=	thermal conductivity of propellant	w/m° K	Btu/hr ft° R
ℓ	=	length	m	ft
m	=	molecular weight	Dimensionless	
n	=	number of variables in a system	Dimensionless	
$\bar{q}$	=	solar heat load near earth	1,397 w/m^2	443 Btu/hr ft^2
q	=	heat rate per unit area	w/m^2	Btu/hr ft^2
q'	=	heat rate per unit length	w/m	Btu/hr ft
r	=	equivalent tank radius (3V/A) or	m	ft
	=	engine mixture ratio (O/F)	Dimensionless	
$\bar{r}$	=	equivalent tank radius $(A/4\pi)^{1/2}$	m	ft
s	=	slope of hydrogen pressure-temperature curve plotted on log coordinates	Dimensionless	
v	=	specific volume	m^3/kg	ft^3/lb
A	=	tank surface area	m^2	ft^2
C	=	specific heat capacity of H_2	joules/gm° K	Btu/lb° R
		or		
	=	a constant	Dimensionless	
$\bar{C}$	=	mass absorption coefficient	1/kg	1/lb
C*	=	characteristic velocity used to describe engine performance	m/sec	ft/sec
G	=	gas or vapor state	Dimensionless	
H	=	enthalpy of liquid H_2	joules/gm	Btu/lb

Basic Symbols			International Units	English Units
H'	=	enthalpy of solid H_2	joules/gm	Btu/lb
H_2	=	hydrogen	Dimensionless	
He	=	helium	Dimensionless	
I	=	gamma penetration rate	photon/sec	photon/sec
I_{sp}	=	specific impulse	m/sec	lb-sec/lb
K	=	thermal conductivity of insulation	w/m°K	Btu/hr ft°R
K'	=	a constant for calculating gamma radiation penetration	photon/sec	photon/sec
L	=	liquid state	Dimensionless	
	=	latent heat for hydrogen	joules/gm	Btu/lb
M	=	mass	kg	lb
$\dot{M}$	=	mass transfer rate	kg/hr m^2	lb/hr ft^2
P	=	pressure	Newton/m^2	psia
Q	=	gross heating rate	watt	Btu/hr
	=	volumetric flowrate	m^3/min	gpm
$\overline{Q}$	=	total heat energy content	joules	Btu
R	=	universal gas constant	8.3143 joules/°K mol	1,544 ft/°R
$\overline{R}$	=	thermal resistance of an evacuated space	0.01579 °K/w	0.00833 hr°R/Btu
S	=	solid state	Dimensionless	
T	=	temperature	°K	°R
T*	= =	ullage gas temperature that yields zero mass transfer across interface	°K	°R
V	=	tank volume	m^3	ft^3
	=	velocity	m/sec	ft/sec
W	=	total hydrogen or system weight	kg	lb

Basic Symbols			International Units	English Units
$\dot{W}$	=	flowrate	kg/hr	lb/hr
X	=	ratio of solid to sum of liquid and solid mass	Dimensionless	
Z	=	mass transfer parameter	Dimensionless	
α	=	thermal diffusivity of hydrogen = $k/\rho C_P$	cm^2/sec	ft^2/sec
$\bar{\alpha}$	=	solar absorptivity of a white painted surface = 0.19	Dimensionless	
β	=	angle of misalignment of vehicle thrust axis with respect to the sunline	radians	deg
γ	=	ratio of heat capacities for hydrogen = C_P/C_V	Dimensionless	
δ	=	insulation thickness	cm	ft
	=	tolerance increment of a variable (prefix)	Dimensionless	
Δ	=	discrete increment of a particular variable (prefix)	Dimensionless	
ϵ	=	dielectric constant of H_2	Dimensionless	
η	=	volume fraction of tank occupied by liquid and solid	Dimensionless	
θ	=	time	hr	hr
θ^*	=	time when optimum insulation thickness results in zero boiling	hr	hr
μ	=	ratio of initial to final mass = $e^{\Delta V/I_{sp}g_c}$	Dimensionless	
ρ	=	density	kg/m^3	lb/ft^3

Subscripts

1	=	initial conditions
	=	first engine firing
2	=	final conditions
	=	saturated conditions after pressurization
	=	second engine firing
3	=	conditions near liquid-vapor interface after pressurization
a	=	average conditions at tank inlet
b	=	average conditions within tank
c	=	average conditions at tank outlet
d	=	tank bulkhead or dome
f	=	fusion
i	=	a particular engine firing
	=	a particular system tolerance
j	=	a particular time step during which hydrogen weight and heating rate are approximately constant
ℓ	=	liquid
m	=	melted
n	=	total number of engine firings
p	=	penetrations through tank insulation for structural supports and plumbing
s	=	solid
t	=	total
v	=	vapor
	=	vaporatization
w	=	tank sidewall
y	=	hydrogen component in a mixture
z	=	helium component in a mixture
AD	=	adiabatic
B	=	boiling
BO	=	boiloff
G	=	gross

Subscripts (Continued)

I = inert
I = insulation
IP = impulse propellant
M = mission duration
N = time step just prior to propellant boiling
N = time of initial boiling
P = hydrogen propellant
UP = impulse propellant used to orient the hydrogen ullage for venting
PL = payload
R = residual
T = tank
V = volume dependent

	Analytical Groups	International Units	English Units
insulation optimization analysis	$\phi_N = \frac{W_{P_N} BF}{A\rho_I L_v} (XL_f + \Delta H)$	m	ft
	$\alpha = \frac{K\Delta T BF}{\rho_I L_v}$	m^2/hr	ft^2/hr
	$q^* = \frac{Q_p}{KA\Delta T}$	m^{-1}	ft^{-1}
system tolerance and performance analyses	$BF = \frac{\sum_{i=0}^{n} W_{BO_i} \left[\frac{1}{\mu_i} \cdot \frac{1}{\mu_{i+1}} \cdots \frac{1}{\mu_n}\right]}{W_{BO}}$	Dimensionless	
	$\mu = e^{\Delta V/I_{sp}g_c}$	Dimensionless	

$$C1 \equiv \sqrt{\rho_v k_v C_{P_v} \frac{C_{P_\ell}}{\rho_\ell k_\ell}} \frac{T_2 - T_3}{L_v}$$

$$C2 \equiv \frac{C_{P_\ell}(T_2 - T_1)}{\sqrt{\pi}\, L_v}$$

$$C3 \equiv \sqrt{\frac{\rho_\ell k_\ell C_{P_v}}{C_{P_\ell} \rho_v k_v}}$$

$$C1_v \equiv \sqrt{\rho_v k_v C_{P_v}} = P_2^{1/2} \sqrt{\frac{k_v C_{P_v}}{RT}}$$

} Dimensionless

$$C3_v \equiv \sqrt{\frac{C_{P_v}}{\rho_v k_v}} = P_2^{-1/2} \sqrt{\frac{C_{P_v} RT}{k_v}}$$

$$C_\ell \equiv \sqrt{\frac{\rho_\ell k_\ell}{C_{P_\ell}}}$$

} Dimensionless

Section 1
INTRODUCTION AND SUMMARY

The study of Hydrogen Slush and/or Hydrogen Gel Utilization constitutes the first formal investigation of subcooled liquid and slush hydrogen fuels for space vehicle applications. Results of this study program are reported in two volumes. The first volume contains the physical and thermal property data for hydrogen used in the study. Complete property data from the triple-point to the critical point are included. In the second volume, all the details of the technical effort are presented, including parametric analysis of effects on vehicle systems and application of subcooled hydrogen to three study vehicles.

This study program was conducted by Lockheed Missiles & Space Company (LMSC) for the George C. Marshall Space Flight Center (MSFC). Objectives of the program were to:

- Extend the basic technology required to employ subcooled hydrogen fuels effectively for space propulsion
- Develop the capabilities needed to design, analyze, and evaluate new vehicle systems and to adapt existing vehicle systems to utilize these fuels
- Determine potential benefits resulting from use of these fuels

To meet these objectives the 12-month program was conducted in three phases: propellant property survey, systems optimization studies, and vehicle application studies. In Phase I, all available property data on subcooled (including slush) and gelled hydrogen were compiled for later use in Phases 2 and 3. Because it was determined that insufficient data were available on hydrogen gels, it was recommended by LMSC and approved by MSFC that the study concentrate on triple-point hydrogen. In Phase 2, effects of using triple-point hydrogen were investigated on vehicle subsystem designs in parametric fashion. These effects were then evaluated for each

of the affected vehicle subsystems before the Phase 3 vehicle application studies were undertaken. These vehicle subsystems are:

- Propellant Management
- Propulsion
- Insulation
- Venting
- Pressurization

Phase 1 and 2 efforts culminated in Phase 3, the application of triple-point and slush hydrogen to three space vehicles. These vehicles are the Saturn V S-IVB, the Lunar Mission Vehicle, and the Earth Orbital Hydrogen Tanker.

The Saturn V S-IVB application was based on performance of an advanced lunar logistics mission. In this concept, the S-IVB would be modified from the existing Saturn V Apollo booster stage to a cargo-landing vehicle. This would require integration of a landing gear, additional propulsion, and additional system equipment. The mission profile selected for study included a direct launch and ascent from earth, a 72-hr lunar transit, two lunar orbits, a Hohmann-transfer descent, and a throttled landing. The Lunar Mission Vehicle application was based on performance of a selected advanced Apollo mission. The Lunar Mission Vehicle was defined as a cryogenic service module for a 21-day lunar mission that would include 17 days in lunar orbit for the service module and 14 days of astronaut stay-time on the lunar surface. The Earth Orbital Tanker application study was conducted for a typical 120-day earth-orbit storage mission. The tanker would be launched into a low earth orbit with subsequent adjustment to a higher orbit altitude, coast in that orbit for the 120-day storage period, then provide transfer of the stored hydrogen into a receiving vehicle.

1.1 STUDY RESULTS

In conducting Phase 1 it was found that all of the fundamental physical and thermal properties of hydrogen needed to properly perform Phases 2 and 3 were available

in the literature. It was further found that additional data regarding triple-point hydrogen flow characteristics ultimately will be needed to conduct detail design of flight subsystems. Close coordination between MSFC, Lockheed, and the National Bureau of Standards (NBS) during the course of this program has ensured that these data will be forthcoming from the current MSFC-sponsored experimental program at the NBS Cryogenic Engineering Laboratory in Boulder, Colorado. Figure 1-1 is a photograph of slush hydrogen production using the freeze-thaw process; this photo was taken by NBS in the early phases of that program. Triple-point liquid and slush of varying quality are shown. In the study program undertaken by Lockheed, triple-point liquid and 50-percent slush mixtures were emphasized.

The compilation of hydrogen property data performed in Phase 1, and later used in Phases 2 and 3, included data from triple-point to critical pressures. This compilation appears in Volume I as a "Handbook of Physical and Thermal Property Data for Hydrogen."

In Phase 2 the analytical techniques normally employed to design vehicle subsystems for liquid hydrogen applications were extended to account for phenomena occurring with use of triple-point hydrogen. Unique analytical techniques were developed, as needed, during the course of Phase 2.

The propellant management studies included investigations of tank loading and draining, and review of candidate hydrogen quantity and slush quality measurement techniques. It was found that recirculation of triple-point liquid or slush hydrogen from ground supply dewars to the flight tankage is the best method to control the quality of hydrogen during ground operations. It was also found that maintenance of a partial pressure of helium in the ullage space is the preferred technique to prevent tank implosion during ground operations and ascent. For vehicles requiring an early engine firing after launch, this helium pressurant can be maintained to provide part of the engine start pressurant requirement. Conversely, for vehicles requiring long-term storage and/or later firings, it is best to vent the initial ground helium pressurant during ascent.

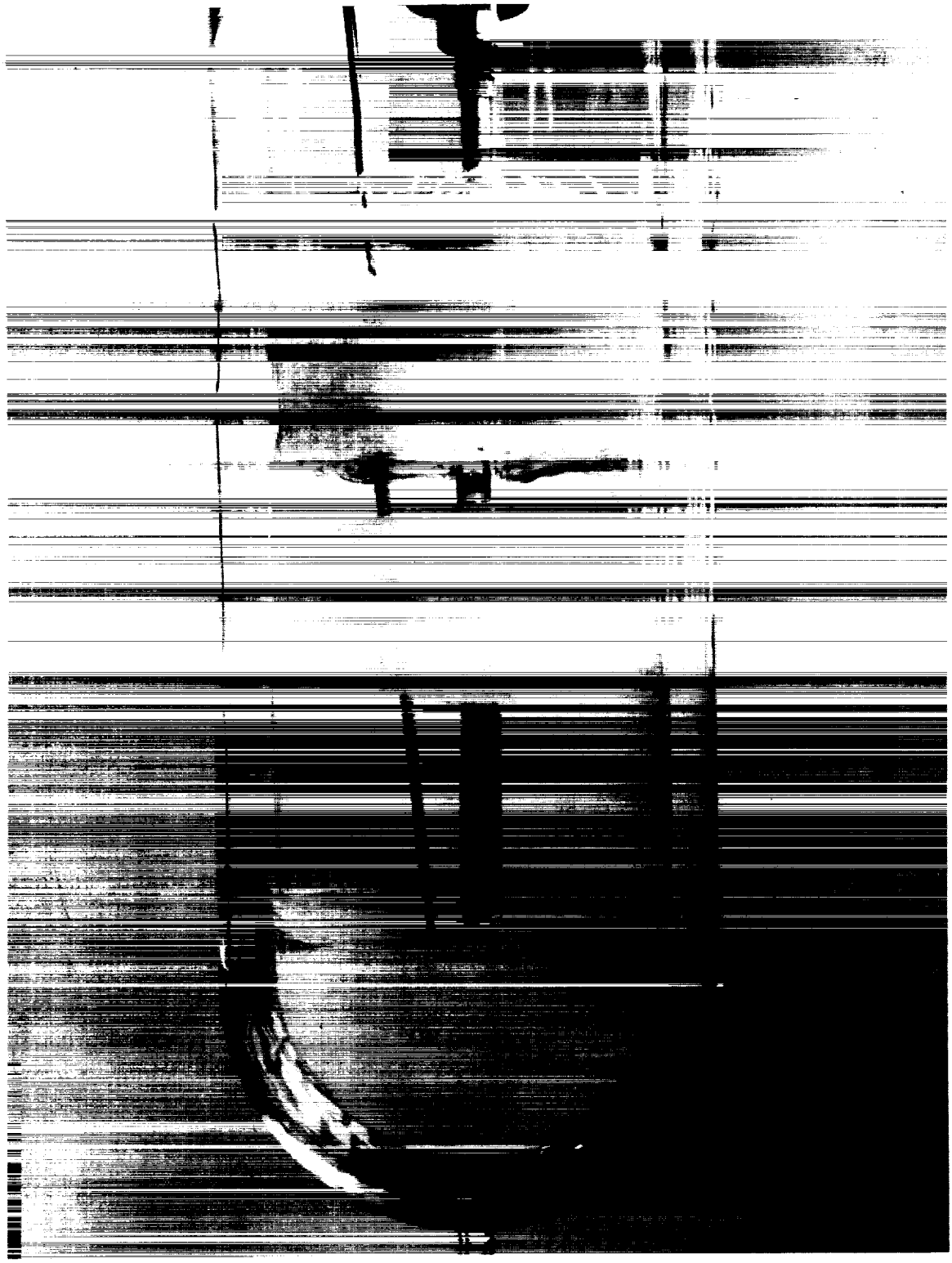

Fig. 1-1 Freeze-Thaw Production Process (From NBS Report 8881)

An assessment of payload degradation resulting from tolerances on instrumentation measurements indicated that much higher penalties are incurred for a given inaccuracy in measuring slush hydrogen quantity than for the same inaccuracy in measuring its quality. The penalty is approximately an order of magnitude greater for a tolerance on quantity measurements. For example, a 1-percent error in measuring loaded hydrogen quantity results in a loss of 97.1 kg (214 lb) of payload for the Saturn V S-IVB lunar mission, but an equal percentage error in measuring loaded quality results in a loss of only 6.6 kg (14.6 lb) of payload.

The engine systems associated with this study contract are the Rocketdyne 205K J-2 and the Pratt and Whitney 15K RL10 engines. The scope of the Lockheed effort on propulsion system effects was limited to discussions with engine and pump company specialists. Their opinions were that even if homogeneous slush mixtures were fed to the pumps and engines, erosive action of the solid hydrogen would not take place in the engine pumps and that solid particles would melt before reaching the engine injector.

As an integral part of the Phase 2 efforts, Lockheed recommended that use of a screen near the tank bottom region could effectively permit retention of solid particles and allow only the triple-point liquid to flow to the engine. This technique was demonstrated by the NBS under the MSFC-sponsored program.

The results of the propulsion systems evaluation indicate that tests to confirm technical opinions obtained during this program would be needed prior to utilization of slush hydrogen in existing engine systems.

In the analysis of insulation systems it was found that space-heating of triple-point hydrogen fuels is approximately 3 to 6 percent higher than that for saturated liquid because of the slight increase in temperature difference between the tank and its environment. There are no unique ground hold requirements imposed upon the insulation system resulting from use of subcooled hydrogen. Where multilayer insulation is used, it may be applied with or without a substrate. While use of the substrate does reduce the heat flow to the hydrogen during ground hold, it has only

a small effect on recirculation rates of the slush or triple-point hydrogen. For those mission durations and thermal environments requiring venting with an optimized design, equal insulation thicknesses result independent of the initial hydrogen condition. For shorter mission durations, optimum thicknesses are different for each initial hydrogen condition. For this case, optimum thicknesses become thinner as the degree of subcooling is increased.

Results of pressurization and venting system studies indicate that use of a mixer system located in the hydrogen tank is desirable where subcooled hydrogen fuels are employed. When a cyclic venting mode is used, or when no venting is required, the mixer provides the best method to ensure uniform saturation and proper control of the venting sequences. Startup pressurant quantity requirements can be considerably higher where subcooled hydrogen is utilized compared with standard liquid hydrogen. As a result, for vehicles using subcooled hydrogen which require engine firings between the vents, it is desirable to adequately predict the ullage pressure history so that startup pressurant quantities can be properly defined. For the types of vehicles investigated in this study program it was determined that helium is the best repressurizing medium for engine startup and that use of warm hydrogen vapor from the engine bleed system is best for expelling the liquid hydrogen during the firing. These conclusions are identical whether subcooled hydrogen fuels or saturated liquid is assumed.

The most important results from Phase 3 are shown in Tables 1-1 and 1-2. The data presented in Table 1-1 show that relatively large payload gains can be realized from use of subcooled hydrogen for the Saturn V S-IVB vehicle over that obtained when saturated LH_2 is assumed. For example, dry landed payload weights obtained with use of the triple-point fuels are approximately 32 to 40 percent (1630 to 2060 kg, 3590 to 4540 lb) higher than those obtained with use of saturated liquid. The two basic reasons for this are (1) the liquid-fueled reference vehicle design is not optimized for this mission of 76 hr, and (2) use of a large quantity of hydrogen soon after liftoff for the translunar firing permits loading of a greater initial quantity of hydrogen

Table 1-1

SUMMARY OF SATURN S-IVB AND LUNAR MISSION VEHICLE APPLICATION STUDY RESULTS

Initial Hydrogen Condition	Liquid Saturated Above 1 Atmosphere	Triple-Point Liquid	50% Liquid-Solid Mixture
Saturn V S-IVB Vehicle:			
Tanked Propellant Weight, kg (lb)	105,548 (232,690)	112,352 (247,690)	113,500 (250,220)
Optimum Mixture Ratio	5.5	4.8	4.2
Optimum Common Bulkhead Insulation Thickness, cm (in.)	7.6 (3.0)	7.6 (3.0)	7.6 (3.0)
Dry Landed Payload Weight, kg (lb)	5,131 (11,311), Ref.	6,760 (14,902)	7,191 (15,853)
Increase in Payload Weight, kg (lb)	0 (0)	1,629 (3,591)	2,060 (4,542)
%	0	31.7	40.2
Lunar Mission Vehicle (LMV):			
Tanked Propellant Weight, kg (lb)	12,846 (28,320)	12,700 (27,999)	12,685 (27,966)
Constant Mixture Ratio	5.0	5.0	5.0
Optimum Insulation Thickness, cm (in.)	1.78 (0.70)	1.60 (0.63)	0.79 (0.31)
Lunar Excursion Module (Payload) Weight, kg (lb)	18,514 (40,816), Ref.	18,740 (41,313)	18,799 (41,443)
Increase in Payload Weight, kg (lb)	0 (0)	225 (497)	284 (627)
%	0	1.22	1.54

Table 1-2

SUMMARY OF EARTH ORBITAL TANKER VEHICLE APPLICATION STUDY RESULTS

Initial Hydrogen Condition		Liquid Saturated Above 1 Atmosphere	Triple-Point Liquid	50% Liquid-Solid Mixture
Delivery of Saturated Liquid Before Transfer	Case 1: $K = 3.5 \times 10^{-7}$ w/cm °K (2×10^{-5} Btu/hr ft °R):			
	Optimum Insul. Thickness, cm (in.)	3.81 (1.50)	1.04 (0.41)	0.64 (0.25)
	Boiloff Hydrogen Weight, kg (lb)	4,441 (9,790)	0 (0)	0 (0)
	Delivered Hydrogen Weight, kg (lb)	106,914 (235,700) Ref.	110,139 (242,810)	110,275 (243,110)
	Increase in Delivered Weight, kg (lb)	0 (0)	3,225 (7,110)	3,361 (7,410)
	%	0	3.0	3.1
	Case 2: $K = 1.7 \times 10^{-6}$ w/cm °K (1×10^{-4} Btu/hr ft °R):			
	Optimum Insul. Thickness, cm (in.)	6.35 (2.50)	5.08 (2.00)	3.18 (1.25)
	Boiloff Hydrogen Weight, kg (lb)	14,334 (31,600)	0 (0)	0 (0)
	Delivered Hydrogen Weight, kg (lb)	102,328 (225,590), Ref.	108,075 (238,260)	109,018 (240,340)
	Increase in Delivered Weight, kg (lb)	0 (0)	5,747 (12,670)	6,691 (14,750)
	%	0	5.6	6.5
Delivery of Saturated Liquid After Transfer and Cool-down of Receiver	Case 3: $K = 3.5 \times 10^{-7}$ w/cm °K (2×10^{-5} Btu/hr ft °R):			
	Optimum Insul. Thickness, cm (in.)	3.81 (1.50)	2.54 (1.00)	1.27 (0.50)
	Boiloff Hydrogen Weight, kg (lb)	12,830 (28,290)	0 (0)	0 (0)
	Delivered Hydrogen Weight, kg (lb)	98,522 (217,200), Ref.	109,272 (240,900)	109,953 (242,400)
	Increase in Delivered Weight, kg (lb)	0 (0)	10,750 (23,700)	11,431 (25,200)
	%	0	10.9	11.6

(for example, 16 percent more for a slush-fueled vehicle),thus realizing the potential benefit offered by the higher slush density.

Examination of the Lunar Mission Vehicle study results in Table 1-1 shows that modest payload gains are obtained with use of subcooled fuels when based on the total Lunar Excursion Module weight. For example, payload gains of 1.22 to 1.54 percent were calculated over that possible with saturated LH_2.

Other important conclusions can be drawn. It is significant that venting is not required for optimum vehicle designs for the 21-day mission duration when either triple-point liquid or 50-percent slush is used. This permits an operational simplicity and reliability approaching those for vehicles using earth-storable propellants, but with the higher specific impulse of cryogenic propellants. Lastly, it should be noted that if the payload gains obtained with use of subcooled hydrogen fuels were applied strictly to additional life-support and data-gathering functions, the relative gains with respect to those for a saturated liquid-fueled vehicle would be much greater than indicated.

The results of applying triple-point liquid and 50-percent slush hydrogen to the Earth Orbital Tanker are presented in Table 1-2. Three basic sets of design conditions were studied. In the first two, the tanker designs were optimized to provide maximum quantity of hydrogen in the tanker for transfer at the end of 120 days earth orbital storage. The liquid hydrogen was saturated at 17.2 N/cm^2 (25 psia) after the 120-day duration for all initial hydrogen loading conditions. Thermal performance of the multilayer insulation on the tanker was based on two insulation design conditions, namely, idealized performance with an effective thermal conductivity of 3.5×10^{-7} w/cm°K (2×10^{-5} Btu/hr ft° R) and degraded performance with a thermal conductivity of 1.7×10^{-6} w/cm°K (10^{-4} Btu/hr ft° R). The third vehicle design condition investigated was based on optimizing tanker design to maximize hydrogen delivered to the receiver tank. In this case, the final condition of the hydrogen after transfer and chilldown of the receiver tank was 17.2 N/cm^2 (25 psia) saturated liquid. The receiver tank volume was sized for the quantity of delivered propellant.

This third case is considered the most practical design condition; however, receiver characteristics were assumed since they have not been defined elsewhere. The first two cases were studied to isolate the effect of insulation thermal conductivity.

For the first case where maximum tanker delivery capability was sought (Case 1), Table 1-2 data indicate a 3-percent increase (3225 kg, 7110 lb) in delivered hydrogen can be obtained by using triple-point liquid and a 3.1-percent increase (3361 kg, 7410 lb) where 50-percent slush is used as compared with 11.7 N/cm^2 (17 psia) saturated hydrogen. Specifically, this applies where calorimeter-measured insulation conductivity data for multilayer insulation could be achieved on the flight hardware. It is apparent that there is a relatively small improvement in performance with use of the subcooled liquid hydrogen. The difference between slush and triple-point liquid is even smaller.

The effect of using a less effective insulation (Case 2) is shown to essentially double the improvement in delivered hydrogen. A conclusion reached from careful consideration of these data is that a better performance improvement is achievable with use of subcooled hydrogen where nonideal insulation performance is expected.

For the third case studied, i.e., maximization of hydrogen in the receiver, marked improvements in performance with use of subcooled hydrogen are evident from Table 1-2 data. An increase of 10,750 kg (23,700 lb) delivered hydrogen was obtained where triple-point liquid is initially loaded compared with an initial loading of 11.7 N/cm^2 (17 psia) saturated liquid. An additional 680 kg (1500 lb) is gained by loading 50-percent slush hydrogen instead. The more obvious advantages of triple-point liquid should not overshadow the added performance payoff obtained from slush hydrogen.

1.2 CONCLUSIONS

Two major conclusions were obtained from the study:

- Use of triple-point liquid or slush hydrogen can significantly extend the mission capability of existing hydrogen-fueled vehicles.

- Elimination of venting triple-point liquid or slush hydrogen for most earth-orbit and lunar mission vehicles permits an operational simplicity approaching that for earth-storable-fueled vehicles, but with the superior specific impulse of cryogenic propellants.

Use of triple-point liquid or slush hydrogen provides increased payload compared with use of atmospheric saturated hydrogen as fuel. The largest payload payoff for application of triple-point hydrogen was found where existing vehicle hardware, designed for modest mission requirements, is applied to a more complex mission of longer space duration. As anticipated, for the three vehicle applications studied, the largest performance improvements were obtained upon substituting triple-point liquid for atmospheric saturated liquid. A smaller additional performance gain is obtained where 50-percent slush is used.

It is significant that venting is not required for optimum vehicle designs for both the service module and tanker missions when either triple-point or slush hydrogen is used. This permits an operational simplicity and reliability approaching those for vehicles using earth-storable propellants, but with the higher specific impulse of cryogenic propellants.

As improved performance in existing and future hydrogen-fueled vehicles is desired, use of the highest possible solid content for slush will be sought. The current MSFC/NBS experimental program has demonstrated that solid-liquid mixtures up to 40 percent can be handled with relatively the same ease as the triple-point liquid. No apparent differences in ground support equipment are required in producing triple-point liquid or solid using the vacuum technique or in transferring either triple-point liquid or slush to the flight tank. The added performance improvement warrants serious consideration of slush hydrogen at least for solid-liquid mixtures up to approximately 60 percent. This value represents the current NBS estimate of the maximum settled quality of aged slush mixtures.

1.3 RECOMMENDATIONS

The following recommendations are made based on results of this study program:

- Additional vehicle studies are warranted and should be undertaken to determine the potential benefits and problem areas that would be encountered if subcooled liquid and slush hydrogen were applied to other existing and proposed vehicles.
- A subscale test program should be undertaken to verify transfer, storage, and use of these subcooled hydrogen fuels in flight-type propellant tankage. The test program should have these objectives:
  - Confirmation of the recirculation technique for tank loading and ground hold
  - Correlation of predicted and measured flow variables, such as supply quality, rate, and loaded quality during ground-hold operations
  - Demonstration that helium partial pressurant can be used to stabilize a flight-weight tank shell containing triple-point liquid or slush hydrogen in an atmospheric pressure environment
  - Demonstration that quantity and quality measurements can be made in the flight-type tank within the accuracies required for space vehicle applications
  - Simulation of launch, ascent, and propellant draining environments and operations to demonstrate controllability of a flight-type system
- Additional data regarding engine and pump performance for triple-point liquid hydrogen use should be obtained from industry
- Additional basic research and development should be continued with regard to quality- and quantity-sensing instrumentation

Section 2
SYSTEMS OPTIMIZATION STUDIES

2.1 TECHNICAL APPROACH

Prior to conducting vehicle application studies, many systems optimization studies were performed. These general studies were directed toward the preliminary design and anlysis of those vehicle systems that optimize and operate differently with use of hydrogen fuel at different initial conditions, e.g., standard saturated liquid, triple-point liquid, and slush. The following general procedure was used in conducting these studies:

- Basic system functions were related to physical-thermal properties of hydrogen.
- Limiting conditions and problem areas peculiar to each system were defined.
- Preliminary design and analysis techniques were developed.
- Parametric equations were derived (if applicable).
- Optimum system characteristics were determined.
- Results were applied to the three study vehicles.

General parametric investigations were used to determine optimum system characteristics whenever possible. However, for certain systems, an investigation of alternate candidates was more appropriate than numerical solution of equations. For example, the study of quantity- and quality-sensing instrumentation was conducted in this manner. Emphasis was then placed on selecting the most promising candidates for future studies.

Since the most critical problems associated with use of subcooled liquid and slush hydrogen are encountered during tank fill and ground hold, this prelaunch phase of operations was investigated first. Ascent and orbital flight were then investigated, in that order.

Applications of liquid hydrogen initially saturated at near atmospheric pressure, initially triple-point liquid hydrogen, and initially 50-percent slush hydrogen were compared in each of the system studies. Discussions on each investigation are presented in this section in approximately the same order that the investigations were conducted during the contract period.

2.2 PROPELLANT MANAGEMENT STUDIES

Effective design and operation of propellant management systems for liquid- or slush-hydrogen fueled vehicles require provision for many key functions. Of these, the most significant with respect to the fuel system are: (1) loading of liquid or liquid-solid hydrogen into the fuel tank on the launch pad, (2) measurement of hydrogen quantity (mass) and quality (solid content) in the fuel tank during tank fill and ground hold, (3) maintenance or upgrading of hydrogen quality during ground hold for slush-fueled vehicles, (4) measurement of hydrogen quantity in the fuel tank during flight, (5) flow of hydrogen to the propulsion system during firings, and (6) adjustment of the mixture ratio during firings to uniformly deplete both propellants at final burnout. The latter function is normally accomplished by modulation of the oxidizer flow rate at the feed pump. Reasonable tolerances on hydrogen quantity and quality must be maintained by the propellant management system in providing each of the functions described above.

General investigations relating to propellant management were conducted in three specific areas during the contract period: (1) tank fill and ground hold. (2) system tolerance effects, and (3) instrumentation for quantity and quality measurements.

Preliminary analysis (see subsection 2.7) shows that solid hydrogen particles settle to the bottom of flight vehicle tanks within a few minutes after the tank recirculation ceases. National Bureau of Standards (NBS) studies confirm this rapid settling phenomenon. The bulk liquid above the settled solid then behaves much the same as does the saturated liquid in existing LH_2-fueled vehicles, at least during launch and ascent. For this reason slosh dynamics are similar for liquid- and slush-fueled vehicles.

2.2.1 Tank-Fill and Ground-Hold Study

Filling the fuel tank of hydrogen-fueled vehicles involves transient chilldown of GSE transfer and fill lines, tank structure, and insulation. After this, the approximately steady-state ground-hold heat flux can be balanced by continuous or intermittent topping, recirculation, or refrigeration of the hydrogen. Since these processes are well understood for saturated liquid hydrogen, efforts in this study were directed to the slush case. Here,the analysis was generalized to treat any solid content, so that the particular case of triple-point liquid is simply one with zero-slush quality.

Three techniques were investigated analytically for loading, maintaining, and upgrading liquid-solid mixtures of hydrogen in flight-weight tankage during ground operations. These techniques are: recirculation, injection of helium vapor, and operation of a cold-helium heat exchanger. Combinations of these techniques were also investigated.

2.2.1.1 Recirculation

This technique can be accomplished with continuous or intermittent flow of a two-phase mixture of hydrogen into the stage tank through the fill line from a GSE dewar. Simultaneously, there would be a return flow of liquid out of the stage tank and into the dewar through a liquid-return line. The circulation would probably be accomplished with a pump-induced flow. The energy balance between the slush flow into the tank, the liquid flow out of the tank, and the heat flow into the tank can be adjusted to change the average quality of the mixture within the tank. This is accomplished by adjusting either the quality of the supply, the rate of flow, or both.

Figure 2-1 shows a typical recirculation system such as that described. The liquid-solid mixture in the tank is maintained at a total pressure of 1 atm or greater (to preclude buckling of the tank shell) by a partial pressure of helium vapor in the ullage space. The hydrogen mixture is maintained essentially at a triple-point temperature of 13.803 °K (24.85°R) and a partial pressure of 7.04×10^3 N/m^2 (1.02 psia).

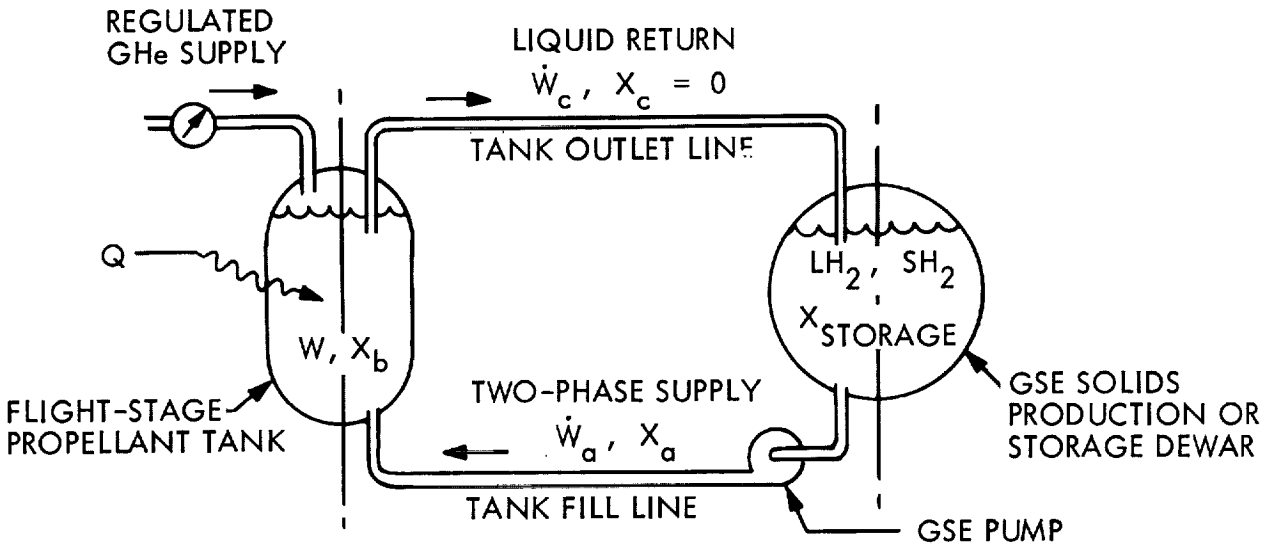

Fig. 2-1 Schematic of a Typical Slush Recirculation System

Chilldown of Vacuum-Jacketed Transfer Lines. The existing liquid hydrogen transfer line for the Saturn V launch facility at Kennedy Space Center (KSC) is approximately 457 m (1,500 ft) in length. To cool this line from ambient to cryogenic temperature, approximately 105 joules/gm (45 Btu/lb) must be removed from the stainless steel inner wall of the line. Assuming that this wall is approximately 15 cm (6 in.) in diameter and 1.52 mm (0.060 in.) thick, approximately 6.125×10^5 joules (177 Btu) must be removed from each meter (foot) of length to cool it. This results in a total line heat capacity of approximately 2.81×10^8 joules (2.66×10^5 Btu), which is small compared with the total ground-hold heat transfer.

Because of the relatively low heat capacity of stainless steel at low temperature, the enthalpy rise in hydrogen used to cool the line is approximately the same for all initial hydrogen conditions. As a result, there is no significant difference in the quantity of hydrogen required to cool the line for transfer of saturated liquid, triple-point liquid, or 50 percent slush hydrogen.

Melting of Solid in Vacuum-Jacketed Transfer Lines. Manufacturers' literature indicates that a heat flux of approximately 8.65 w/m (9 Btu/hr ft) is typical for lines of the

type described above. A flux of 26 w/m (27 Btu/hr ft) was used in the analysis to allow for degradation at joints, fittings, etc. With a latent heat of vaporization of 58.15 joules/gm (25 Btu/lb), the rate at which solid is melted during transfer is then approximately equal to $q'\ell/L_f$ or 735 kg/hr (1,620 lb/hr).

The melt rate can also be expressed as the product of the change in quality within the transfer line ΔX and the total mass flow rate $\dot{W}$. Then

$$\dot{W} = \frac{\dot{W}_m}{\Delta X} = \frac{q'\ell}{L_f \Delta X} \tag{2.1}$$

At the same time, the mass flow rate required to balance the ground-hold heat load on the vehicle fuel tank is

$$\dot{W} = \frac{Q}{L_f (X_1 - \Delta X)} \tag{2.2}$$

where X_1 is the initial supply quality.

Equating (2.1) and (2.2)

$$\frac{q'\ell}{L_f \Delta X} = \frac{Q}{L_f (X_1 - \Delta X)} \quad \text{or} \quad \frac{\Delta X}{X_1} = \frac{1}{1 + \frac{Q}{q'\ell}} \tag{2.3}$$

Equation (2.3) can be used to calculate the quality loss in the transfer line for any vehicle as a function of the intial slush-supply quality, the steady-state heat loads on the vehicle fuel tank and the transfer line, and the length of the transfer line.

Chilldown of a Vehicle Fuel Tank. Approximately 140 joules/gm (60 Btu/lb) must be extracted from an aluminum tank wall to cool it from room temperature to hydrogen temperature. Assuming an aluminum tank wall with a density of 2.77 gm/cm^3 (0.1 lb/in.^{3}), the total energy that must be absorbed to chill it is approximately 389 joules/cm^3

(6 Btu/in.^{3}) of tank material volume. The absorption of this amount of heat by the hydrogen does not impose severe requirements on the recirculation system, regardless of the initial condition of the hydrogen. For example, the total heat absorbed in chilldown of a 6.1-m (20-ft) diameter spherical tank with a 3.05-mm (0.120-in.) wall thickness is approximately 1.35×10^8 joules (128,000 Btu). For typical vehicles, this amount of energy is only a small fraction of the total absorbed during ground hold.

Steady-State Recirculation. Equal mass flow into and out of a vehicle hydrogen tank (constant-loaded propellant weight) is of practical interest for steady-state ground-hold operations. For this case, the required flow rate can be calculated as a function of the desired average quality in the tank, the quality of the two-phase supply, the geometry of the propellant tank, and the steady-state heat flux into the tank. Using the constant-flow assumption, a convenient expression was obtained for determining the required flow rate in terms of a "recirculation period." This is defined as the time required to completely replenish the mass of the propellant mixture in the tank at that particular flow rate.

By making an energy balance on the slush-tankage system over time $\Delta\theta$ and manipulating algebraically, the following relation is obtained

$$\frac{\dot{W}}{W} = \frac{qA}{X_a L_f \rho_{b2} \eta_2 V} + \frac{\Delta X_b}{\Delta\theta X_a} \qquad (2.4)$$

Since A/V is the important geometry characteristic, any tank can be treated as an "equivalent sphere" so that $A/V = 3/r$. Equation (2.4) then becomes

$$\frac{\dot{W}}{W} = \frac{3q}{X_a L_f \rho_{b2} \eta_2 r} + \frac{\Delta X_b}{\Delta\theta X_a} \qquad (2.5)$$

The recirculation period can be calculated by taking the reciprocal of Eq. (2.5).

2.2.1.2 Injection of Helium Vapor

This technique can be used to cool saturated liquid, form solids, maintain subcooled liquid or slush, and upgrade slush quality in a flight-weight hydrogen tank once it has been loaded with saturated liquid. Tank fill is therefore accomplished using standard procecures and was not an object of study in this investigation.

Using this technique, helium vapor is supplied from the launch facility through a transfer line to the vehicle. A flow of make-up liquid hydrogen is also supplied. The helium and make-up hydrogen are injected into the bulk hydrogen at the bottom of the tank. A mixture of helium and hydrogen vapor is simultaneously vented from the tank ullage space. A practical ground-hold system would require a closed loop to permit recovery of the helium supply. As with the recirculation system, an energy balance between the flow of helium vapor into the tank, make-up liquid hydrogen flow into the tank, mixed vapor flow vented from the tank, and heat flow into the tank, can be adjusted to vary the quality of the solid-liquid hydrogen mixture within desired limits.

Figure 2-2 shows schematically a typical helium injection system. Here, again, a total pressure of 1 atm or greater is maintained in the ullage space by increasing the partial pressure of helium as the hydrogen partial pressure diminishes with cooling.

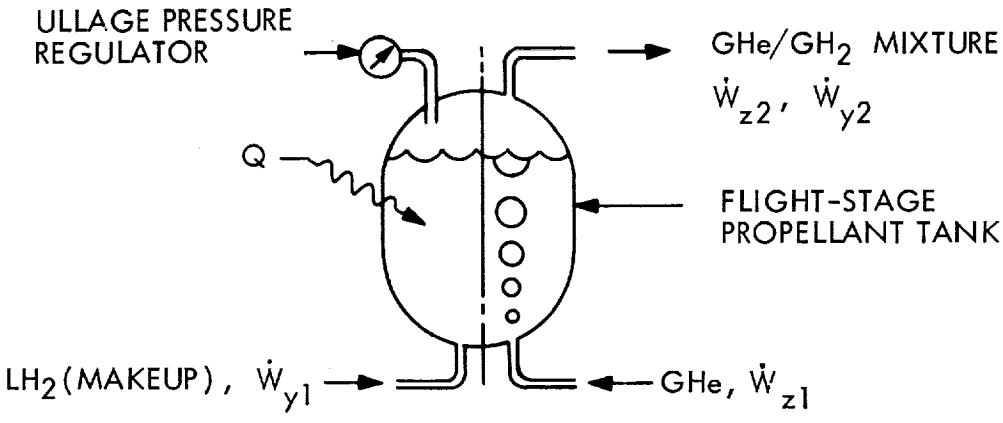

Fig. 2-2 Schematic of a Typical Helium Injection System

Transient Cooldown. Using the helium injection technique, hydrogen liquid is cooled by simultaneous exchange of heat with the helium and evaporation of the hydrogen into the helium bubbles. The energy balance for the transient condition was written to determine helium mass flow rates needed to cool liquid hydrogen from relatively warm temperatures down to a desired triple-point condition. The resulting expression is

$$(\dot{W}H)_{yz1} - (\dot{W}H)_{yz2} + Q = \frac{d\,(WCT)_y}{d\theta} \qquad (2.6)$$

By substitution and $\dot{W}_1 = \dot{W}_2$, Eq. (2.6) becomes

$$\dot{W}_y\,[C_y\,(T_{y1} - T) - L_v] + \dot{W}_z\,C_z\,(T_{z1} - T) + Q = (WC)_y\,\frac{dT}{d\theta} \qquad (2.7)$$

Further substitution of thermodyanmic relationships yields

$$\dot{W}_z \left\{ \frac{C_y\,(T_{y1} - T) - L_v}{\frac{m_z}{m_y}\left[\frac{P_1}{P_y(T_{y1})}\left(\frac{T}{T_{y1}}\right)^{-s}-1\right]} + C_z(T_{z1} - T) \right\} + Q = (WC)_y\,\frac{dT}{d\theta} \qquad (2.8)$$

For the cooldown, or transient case, the variables in Eq. (2.8) were separated and integrated with respect to both temperature and time for several combinations of initial and final conditions.

Equation (2.8) was put in dimensionless form and integrated numerically for an appropriate range of the variables involved. Some results are presented in Fig. 2-3.

Steady-State Helium Injection. A case of practical interest for steady-state operations is again one where the tanked hydrogen mass is held constant. Required helium and

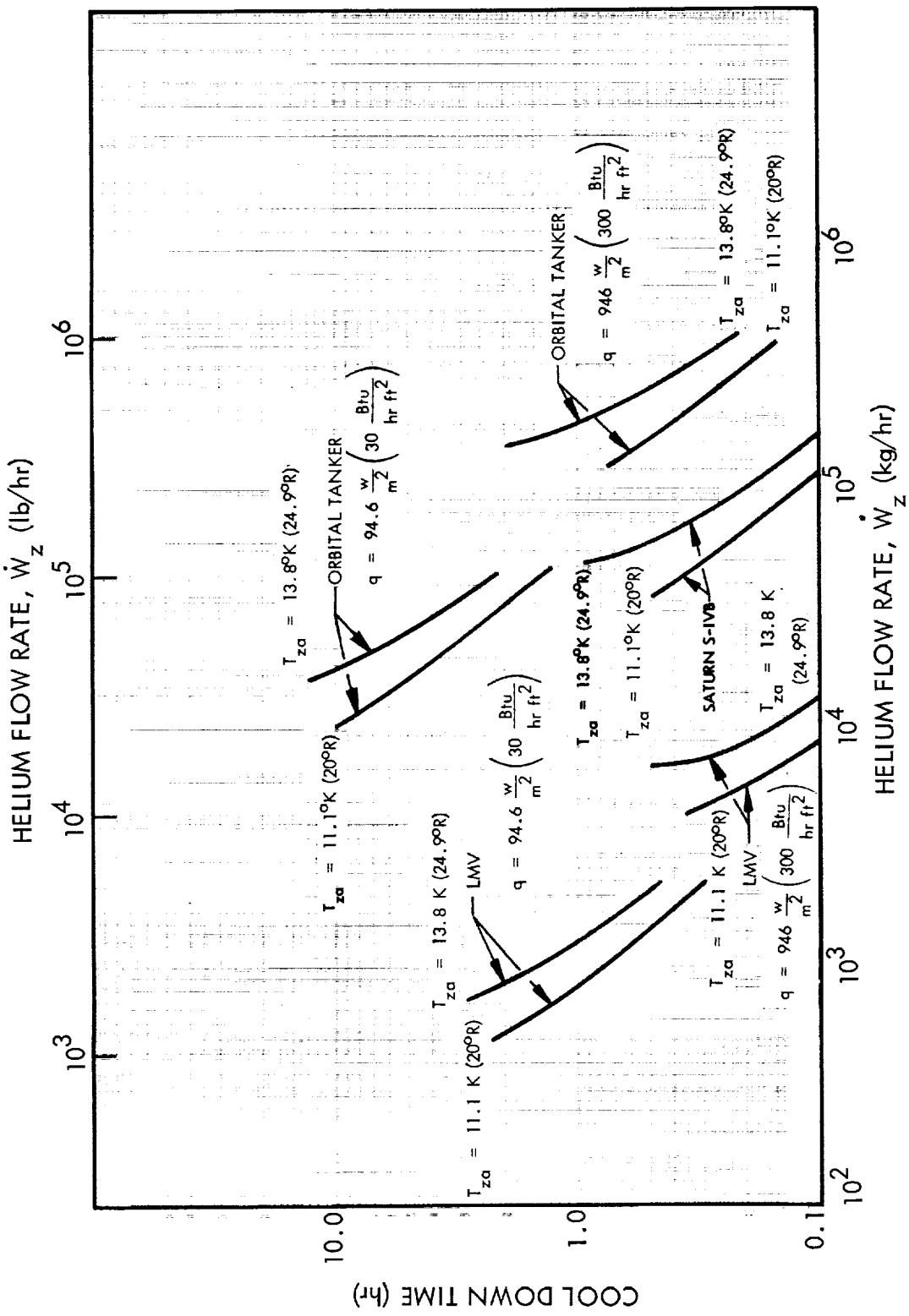

Fig. 2-3 Cooldown of Liquid Hydrogen From 20.3°K to 13.8°K (36.6°R to 24.9°R) With Helium Injection

make-up hydrogen flow rates are calculated as a function of the desired final quality in the tank, the inlet temperature of the helium, the temperature of the hydrogen, and the geometry and heat flux properties of the tank and its insulation system.

The steady-state energy balance is

$$(\dot{W}H)_1 - (\dot{W}H)_2 + Q = 0 \qquad (2.9)$$

Applying Dalton's law and substituting into Eq. (2.9) the following expression is obtained:

$$\left[\left(\frac{m_y}{m_z}\right)\left(\frac{\Delta H_y}{\frac{P_2}{P_y} - 1}\right) + \Delta H_z\right] \dot{W}_z + Q = 0 \qquad (2.10)$$

The pressure-temperature relationship for hydrogen is applied in Eq. (2.10) to provide the data shown graphically in Fig. 2-4. The quantity of helium vapor required to maintain the hydrogen propellant at any desired temperature can be determined from this plot.

Solid Formation With Helium Injection. A flow of helium in excess of that shown in Fig. 2-4 for the triple-point temperature value of 13.803° K (24.85° R) is required to form hydrogen slush in the propellant tank. Analysis indicates that the ratio of total additional pounds of helium to the total additional heat removed is identical to the ratio of helium flow rate to total heat flow into the stored propellant for the steady-state case. The latter quantity is the ordinate of Fig. 2-4. The additional helium needed to form the slush is then

$$W_z = \left(\frac{\dot{W}_z}{Q}\right)_{T = 13.8°K\ (24.9°R)} W_y X_{b2} L_f \qquad (2.11)$$

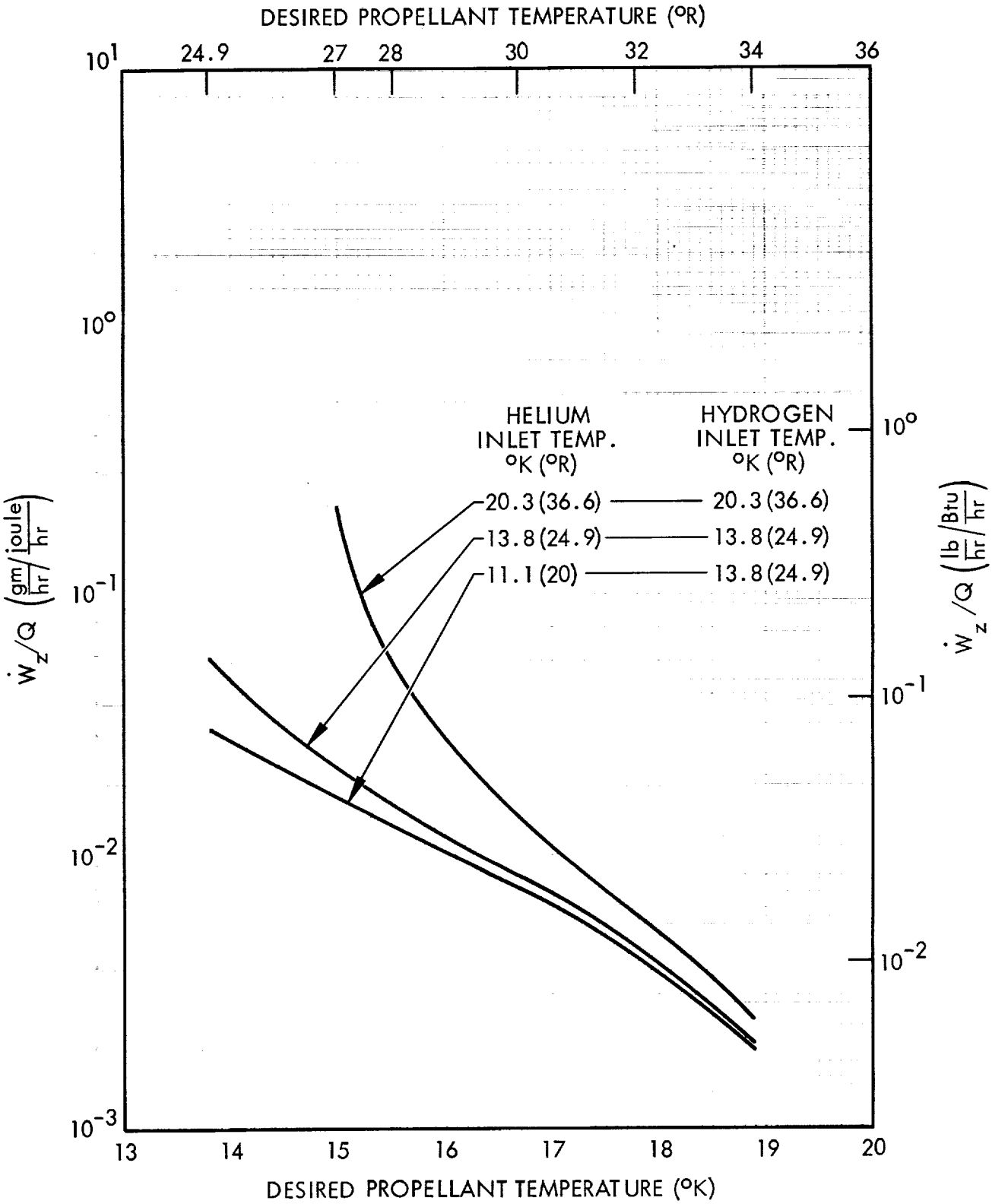

Fig. 2-4 Helium Flow Required to Maintain Hydrogen Propellant at Desired Temperature

When the desired slush quality is achieved, the helium flow can be reduced to the value indicated in Fig. 2-4 at 13.8° K (24.9° R); thereafter, the solid-liquid ratio will be maintained.

2.2.1.3 Operation of a Cold-Helium Heat Exchanger

This technique can be used to perform the same functions noted for the injection of helium vapor, i.e., (1) cooling saturated liquid that was previously loaded into the tank using conventional liquid fill procedures, (2) forming solids in the tank, (3) maintaining subcooled liquid or slush in the tank, and (4) upgrading slush quality in the tank.

Using this technique, cooling is accomplished by continuous or intermittent flow of GSE-supplied helium vapor through heat-exchanger tubes located in or attached to the propellant tank. The process depends on the thermal potential of helium that is supplied at a temperature equal to or below the triple-point temperature of hydrogen. The efficiency of the method can be markedly dependent on maintaining controllable heat transfer coefficients through the tube walls. In this analysis, the effect of solid hydrogen build-up on tube walls is not included.

The heat exchanger tubes can be placed in the bulk propellant within the tank cavity, attached to the tank wall but within the insulation envelope, or placed in a "blanket" or "cocoon" that envelopes the vehicle shell during ground hold. For the latter case, the blanket would be removed prior to liftoff.

The energy balance between the flow of helium vapor into and out of the heat exchanger and the heat flow into the tank/heat-exchanger system can be adjusted to vary the quality of the solid-liquid hydrogen mixture within desired limits. Both the temperature of the helium supply and the rate of flow can be utilized to accomplish the desired balance.

A typical cold-helium heat-exchanger system is shown schematically in Fig. 2-5. The hydrogen mixture is maintained at its triple-point temperature and pressure. A partial pressure of helium vapor in the tank ullage space serves to prevent buckling of the tank wall, as with the other techniques studied previously.

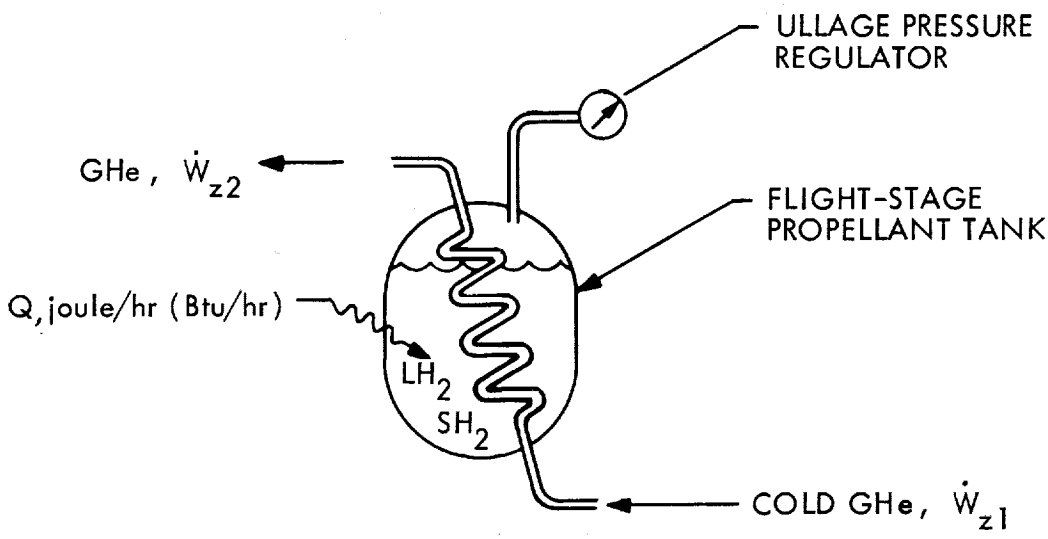

Fig. 2-5 Schematic of a Typical Cold-Helium Heat-Exchanger System

The instantaneous energy balance at any point in time yields

$$Q + \dot{W}_z (H_{z1} - H_{z2}) = \frac{d(WCT)_y}{d\theta} \tag{2.12}$$

Assuming that both W_y and C_y are constant and that the exit temperature of the helium is equal to the hydrogen temperature, Eq. (2.12) becomes

$$Q + \dot{W}_z \left(H_{z1} - H_{z(T)}\right) = (WC)_y \frac{dT}{d\theta} \tag{2.13}$$

where $H_{z(T)}$ indicates that H is to be evaluated at T.

Transient Cooldown. In the cooldown, or transient case, the variables in the right side of Eq. (2.13) are separated and integrated with respect to both temperature and time. The resulting cooldown time as a function of $\dot{W}_z$ is given in Fig. 2-6 for the study vehicles.

Steady-State Operation. In the steady-state case, the applied refrigeration balances the heat load Q and the right side of Eq. (2.13) is taken as zero. For spherical tanks, substituting into Eq. (2.13), and evaluating $\bar{r}$ versus $\dot{W}_z/q$, the results are plotted in Fig. 2-7.

Solid Formation With the Cold Helium Heat Exchanger. A flow of helium through the heat exchanger in excess of that shown in Fig. 2-7 is required to form hydrogen solids in the propellant tank at the triple-point temperature of 13.803°K (24.85°R). The heat transferred per pound of helium varies with the temperature difference between final and inlet conditions. Equating this energy to the latent heat of fusion for hydrogen, the additional weight of helium needed to form solid hydrogen, of quality fraction X, is then

$$W_z = \frac{L_f}{\Delta \bar{Q}_z} X W_y = 4.01 X W_y \qquad (2.14)$$

When the desired slush quality is reached, the helium flow can be reduced to the value indicated in Fig. 2-7; thereafter, the solid-liquid ratio will be maintained.

2.2.1.4 Selection of a Preferred Technique

Ranking of candidate tank loading and ground maintenance techniques requires careful consideration of influences on practical vehicle design and performance and on selection of ground support and launch complex equipment. For the latter, factors such as cost, development time, safety requirements, and support-system reliability enter into the determination. It is the intent of this study program to provide recommendations on the candidate techniques based on practicability and effects on vehicle design

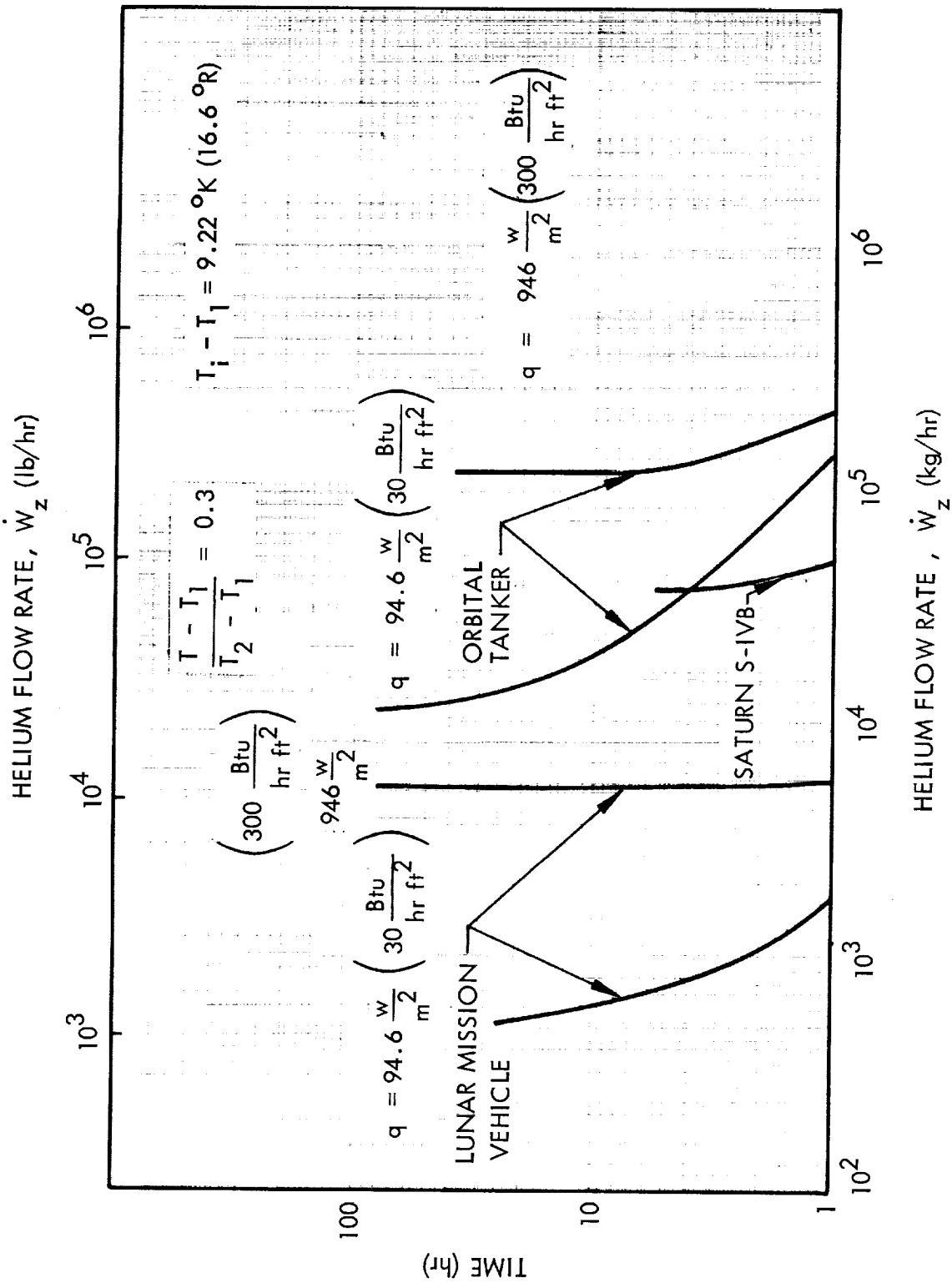

Fig. 2-6 Time to Cool Down Hydrogen Tank With Helium Heat Exchanger

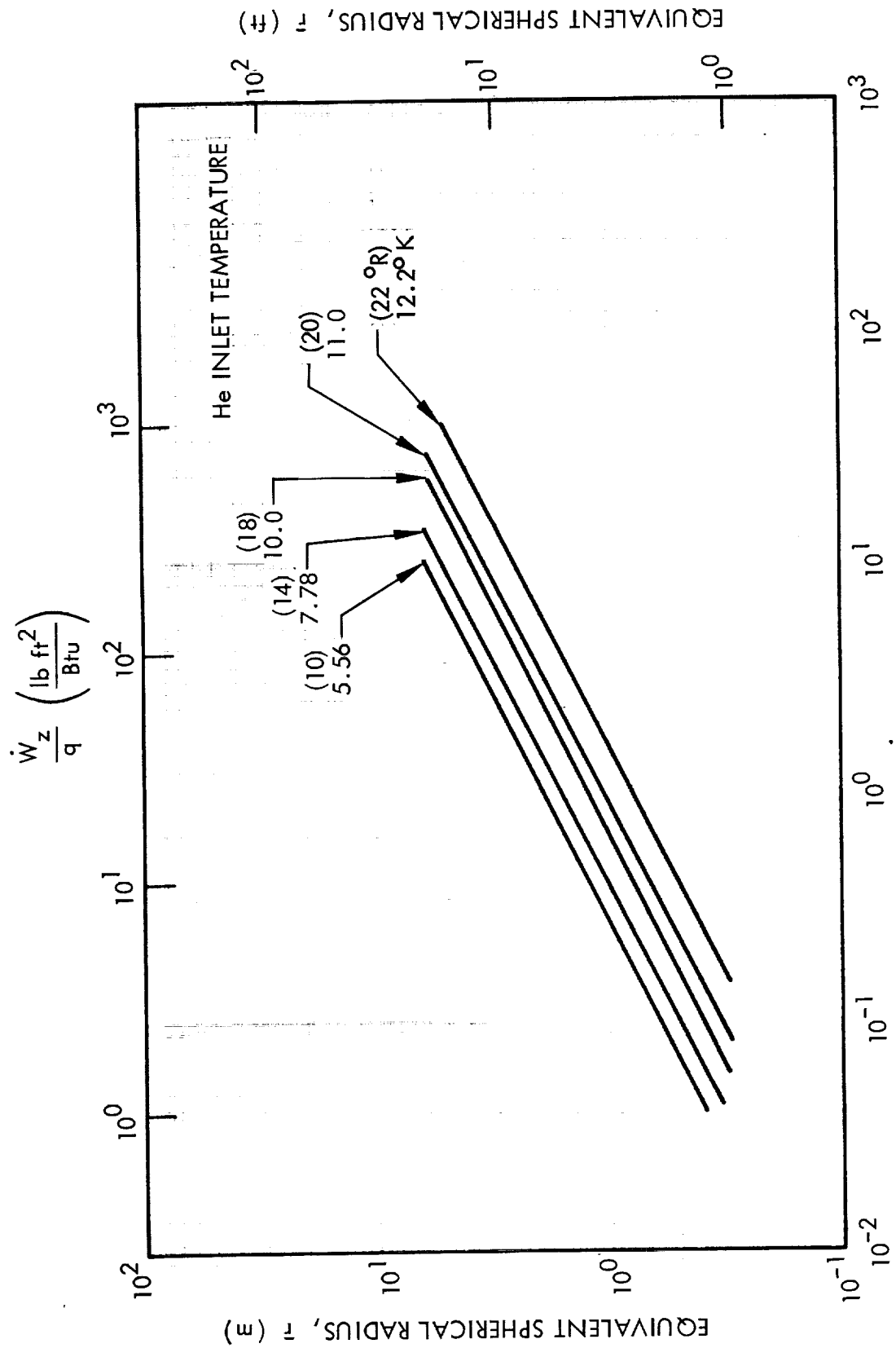

Fig. 2-7 Helium Refrigeration Requirements to Maintain Triple-Point Mixtures of Hydrogen

and performance, with some consideration given to GSE requirements. MSFC will also evaluate the effects of these techniques on GSE requirements, and will arrive at an independent ranking.

A determination of flow characteristics for each of the candidate systems was evaluated for each vehicle (Refer to Sections 3, 4, and 5). Examining the flow rates and total quantities presented, it is apparent that significant design and operational problems could arise from use of any of the systems studied. This is particularly true for large vehicles such as the Saturn S-IVB and the Earth Orbital Tanker.

Flow rates calculated for recirculation tank fill and ground maintenance systems appear to be within the capability of the existing Saturn V launch complex transfer line. However, a new slush production and/or storage facility and additional transfer equipment are required. Also, vehicle modifications are required to provide a liquid-return line, control valve, and disconnect.

Flow rates calculated for injection of helium vapor to form and maintain slush mixtures in the vehicle tanks clearly require additional GSE facilities to store, transfer, and recover the large quantities of helium indicated. Also required are distribution manifolds inside the vehicle tank and relatively large diameter ground vent lines from the tank. The latter requirement results because the maximum differential pressure between the vehicle tank and the helium recovery facility is necessarily limited to about 2 atm.

Flow rates calculated for operation of a cold-helium heat exchanger appear to be excessive in terms of GSE facility and vehicle requirements.

Combinations of the recirculation and helium injection techniques were also studied. Four variations of these techniques are listed below, ranging from recirculation only to helium injection only. They have been ranked according to the considerations noted above, with the most promising listed first.

(1) A recirculation system in which slush is transferred into the flight tank from a ground system supply through the normal tank fill line. Liquid hydrogen is then returned to the facility through a separate line (to be added to existing vehicles). The same system is employed during the ground-hold period.

(2) A combination system in which slush is transferred into the flight tank initially from a ground system supply through the normal tank fill line. After the tank is loaded to the desired quality and quantity of SH_2, helium vapor is injected into the propellant through the fill line or a separate GHe supply line. During this ground-hold phase, make-up liquid is supplied through either a separate smaller line or the fill line (if the GHe supply is separate). A liquid-return line is not necessary.

(3) A combination system similar in all respects to system (2) described above, except that a liquid-return line is provided to allow initial loading of higher quality mixtures.

(4) A basic helium injection system in which standard saturated liquid at approximately 1 atm is transferred into the flight tank from a ground system supply through the normal tank fill line. Helium vapor is then injected into the propellant as described for system (2), and SH_2 is formed and maintained in the flight tank.

It appears that use of recirculation for loading and ground hold [system (1) above] is the most practical and strightforward technique. The primary advantages that can be gained using this technique include the following:

- Higher confidence in a successful application, since much has been learned about producing and transferring mixtures with predictable characteristics
- Slush mixtures loaded in this manner are equally suitable for either the "homogeneous mixture" or the "filtered liquid" concepts of propulsion system utilization*
- Higher confidence in measuring the loaded slush quantity and quality

*The "homogeneous mixture" concept requires that relatively small solid particles be formed in a ground-system dewar, transferred into and stored in the flight propellant tank, and fed into the engine feed system while uniformly suspended in a slurry. The "filtered liquid" concept, on the other hand, presumes that solids, independent of origin or size, remain in the flight propellant tank until they are melted and only triple-point liquid is fed to the engine system.

The disadvantages of system (1) include the following:

- Requirements for additional large-diameter line and umbilical for returning the liquid to the ground system
- A partial pressure of helium vapor must be provided and carefully controlled at all times to prevent implosion of the tank

Advantages inherent with use of the helium-injection technique [system (4) above] include the following:

- Slush can be produced and maintained in the flight tank without transfer of the solids through long lines and without danger of tank implosion.
- Only minor modifications to existing stages (such as S-IVB) are required to provide a make-up LH_2 line.
- A new slush production and/or storage facility at the launch complex is not required.

On the other hand, the helium injection technique has the following significant disadvantages:

- Considerable design uncertainties exist because the characteristics of the resulting solids are not well known.
- The ground systems facility required to supply and reclaim large amounts of helium at low temperatures will probably be complex and costly.
- The slush mixture produced with this method may be suitable only for the "filtered liquid" propulsion usage concept.
- Measurements of quantity and quality may be difficult or impossible within required tolerances.

The two combination techniques [systems (2) and (3) above] are simply compromises of the two basic techniques, which are intended to yield most of the advantages while minimizing the disadvantages.

Consideration of quantity and quality instrumentation is important to selection of a tank loading and ground maintenance technique. It is not certain that these factors can be determined with sufficient accuracy in a tank being thermally conditioned with a sizable flow of helium vapor bubbles.

Further consideration is not recommended for use of the cold-helium heat-exchanger technique for the following reasons:

- Extremely high helium-vapor flow rates needed are of such a magnitude that serious GSE design problems are evident.
- Estimated weights of heat exchangers to accommodate these high flow rates make use of this technique unfeasible for flight systems.
- Uncertainty in knowledge of the formation of solid hydrogen near the heat-exchanger surfaces dictates low design confidence in defining heat-transfer coefficients and efficiency of the heat exchanger.

2.2.2 System Tolerance Effects Study

Payload penalties result from the operation of any space vehicle at nonoptimum values of propellant weight, mixture ratio, etc. For hydrogen-fueled vehicles, these factors are directly affected by hydrogen mass and solid content, tank operating temperatures and pressures, and heat transfer into the hydrogen. Therefore, instrumentation and controls are provided to measure and regulate these quantities within reasonable tolerances during tank fill, ground-hold, launch, ascent, and orbital-flight phases. Predesign knowledge of the payload penalties that will result from specified tolerances is necessary to select and install adequate instruments and controls. This study was directed toward a comparison of tolerance effects for hydrogen at various initial conditions.

Parametric equations were derived to define general relationships between significant system tolerances and resulting performance penalties. Maximum usable payload was the only performance criterion used. Booster capability was assumed to be the

minimum required to inject vehicles of specified weight, or less, into appropriate trajectories at fixed requisite velocities. Each of the significant system tolerances was then identified, and specific equations were written relating penalties and tolerances. The payload penalties were then evaluated and compared for those tolerances that could result in different penalties for liquid- and slush-hydrogen systems.

The net effect of system tolerances on payload weight depends completely on the course of action selected to correct or account for them. For example, tolerances on the mass of hydrogen in the flight tank will affect impulse propellant, boiloff, residual propellant, etc., by different amounts, depending on the correction mode. Possibilities for correction include active propellant utilization system control to vary the mixture ratio and a bias of loaded propellants prior to launch. Only the first-mentioned possibility was studied for each parameter tolerance in this investigation.

2.2.2.1 General System Tolerance-Payload Penalty Relationships

The ratio of initial system weight to final system weight for any propulsive stage firing in space is

$$\frac{W_1}{W_2} = \mu = e^{\Delta V / I_{sp} g_c} \tag{2.15}$$

The initial and final weights can be written as

$$W_1 = W_I + W_{PL} + W_P = W_I + W_{PL} + \sum_{i=0}^{n} W_{IP_i} + \sum_{i=0}^{n} W_{BO_i} + W_R \tag{2.16}$$

$$W_2 = W_I + W_{PL} + W_R \tag{2.17}$$

where W_{BO_i} is defined as the boiloff preceding the i^{th} firing. Rearranging Eq. (2.16) to evaluate the payoad weight, one obtains

$$W_{PL} = W_1 - W_I - \sum_{i=0}^{n} W_{IP_i} - \sum_{i=0}^{n} W_{BO_i} - W_R \qquad (2.18)$$

An expansion of the impulse propellant weight term yields

$$\sum_{i=0}^{n} W_{IP_i} = W_1\left(1 - \frac{1}{\mu_i} \cdot \frac{1}{\mu_{i+1}} \cdots \frac{1}{\mu_n}\right) - W_{BO}(1 - BF) \qquad (2.19)$$

where

$$\text{Boiloff Factor (BF)} = \frac{\sum_{i=0}^{n} W_{BO_i}\left(\frac{1}{\mu_i} \cdot \frac{1}{\mu_{i+1}} \cdots \frac{1}{\mu_n}\right)}{W_{BO}}$$

Then, substituting into Eq. (2.18), writing in differential form, and then simplifying, one obtains

$$\Delta W_{PL} = \frac{\Delta W_1}{\left(\mu_1 \cdot \mu_2 \cdots \mu_n\right)} - \Delta W_I - BF\Delta W_{BO} - \Delta W_R + W_2 \ln\left(\mu_i \cdot \mu_2 \cdots \mu_n\right)\frac{\Delta I_{sp}}{I_{sp}} \qquad (2.20)$$

For a mission with a single engine firing, the term

$$\left(\frac{1}{\mu_1} \cdot \frac{1}{\mu_2} \cdots \frac{1}{\mu_n}\right)$$

becomes $1/\mu$ as does the boiloff factor. For this case, Eq. (2.20) simplifies to

$$\Delta W_{PL} = \frac{\Delta W_1}{\mu} - \Delta W_I - \frac{\Delta W_{BO}}{\mu} - \Delta W_R + W_2 \ln \mu \frac{\Delta I_{sp}}{I_{sp}} \qquad (2.21)$$

Equations (2.20) and (2.21) are used in this investigation to evaluate ΔW_{PL} for propulsive vehicles such as the S-IVB and the lunar mission vehicle. For a nonpropulsive stage, such as the earth orbital tanker, no propulsion system effects are considered. In this case, the usable payload is the propellant available for transfer at the end of the orbit storage period; Eqs. (2.20) and (2.21) then simplify to

$$\Delta W_{PL} = \Delta W_1 - \Delta W_I - \Delta W_{BO} - \Delta W_R \qquad (2.22)$$

If the boiloff is dropped during booster thrust, boiloff weight is multiplied by a dropped weight factor, which is dependent on booster characteristics.

2.2.2.2 Specific System Tolerance-Payload Penalty Relationships

Tolerances on sensing accuracy for the following system parameters were considered in evaluating Eqs. (2.20), (2.21), and (2.22):

- Loaded hydrogen quantity (mass)
- Loaded hydrogen quality (solid fraction)
- In-flight hydrogen quantity (mass)
- Hydrogen tank ground-vent pressure
- Hydrogen tank flight-vent pressure
- Hydrogen expulsion pressure
- Hydrogen tank heat load

The necessary relationships for each parameter are discussed in the order given in the paragraphs that follow. Vehicle and mission peculiarities are noted where they occur.

Loaded-Hydrogen Quantity Sensing. The loaded propellant weight W_P and, therefore, the initial total system weight W_1 can vary by a maximum of δW_P if the tolerance on loaded propellant mass is taken as $\pm \delta W_P/2$. The propulsive-stage payload weight depends directly on the minimum propellant weight to achieve a given mission velocity increment. Also, the sum of the payload and maximum propellant weights for any stage (synonomous terms for a tanker stage) is limited by a given mission booster capability. This analysis assumes that the entire loading tolerance exists on the fuel side. The resulting off-optimum mixture ratio r for a propulsive stage degrades the specific impulse, and a maximum ΔW_{PL} penalty is obtained for a given δW_P tolerance. Neglecting the small influence of W_P on tank (dry inert) weight, boiloff weight, and propellant residual weight for a propulsive stage, Eq. (2.20) becomes

$$\Delta W_{PL} = \frac{-\delta W_P}{\left(\mu_1 \cdot \mu_2 \cdots \mu_n\right)} + W_2 \ln \left(\mu_1 \cdot \mu_2 \cdots \mu_n\right)\left(\frac{\Delta I_{sp}}{\Delta r}\right)\left(\frac{r \Delta W_{IP}}{I_{sp} W_P}\right) \quad (2.23)$$

where $(\Delta I_{sp}/\Delta r)$ and specific impulse can be obtained from engine performance data, r is the nominal propellant mixture weight ratio, W_P is the total loaded hydrogen weight, δW_P is the loaded propellant mass tolerance, and ΔW_{IP} is the decrement of available impulse propellant equal to δW_P.

For a tanker stage, the maximum payload penalty can be obtained from Eq. (2.22) which reduces to

$$\Delta W_{PL} = \Delta W_1 = -\delta W_P \quad (2.24)$$

The payload penalty that results from a propellant mass-loading tolerance varies for slush-fueled and liquid-fueled systems only insofar as δW_P varies due to the instrumentation and measurement techniques employed.

Loaded-Hydrogen Quality Sensing. This parameter, by definition, applies only to a slush-fueled system. The major effect of introducing a tolerance on fuel quality δX

is the resulting change in heat absorption capability that affects boiloff. For propulsive stages only, secondary effects are imposed on available impulse propellant, mixture ratio, and, consequently, on specific impulse. The maximum payload penalty occurs for a decrease in slush quality since the resulting increased boiloff reduces the propellant payload directly for a tanker and reduces the available impulse propellant, with subsequent degradation of the specific impulse for propulsive stages. The change in boiloff hydrogen for any stage is

$$\Delta W_{BO} = \frac{L_f W_P \delta X}{L_v} \tag{2.25}$$

Also, the term $\Delta I_{sp}/I_{sp}$ can be expressed for the propulsive stage case as

$$\frac{\Delta I_{sp}}{I_{sp}} = - \left(\frac{\Delta I_{sp}}{\Delta r}\right)\left(\frac{r}{I_{sp}}\right)\left(\frac{\Delta W_{BO}}{W_{IP}}\right) \tag{2.26}$$

where ΔW_{BO} and W_{IP} are for hydrogen only.

Neglecting small influences of δX on initial vehicle weight, tank weight, residual propellant weight, and boiloff factor, and combining Eqs. (2.20), (2.25), and (2.26), the payload penalty for propulsive stages due to quality tolerance becomes

$$\Delta W_{PL} = \frac{- L_f W_P \delta X BF}{L_v} - W_2 \ln\left(\mu_1 \cdot \mu_2 \cdots \mu_n\right)\left(\frac{\Delta I_{sp}}{\Delta r}\right)\left(\frac{r}{I_{sp}}\right)\left(\frac{\Delta W_{IP}}{W_{IP}}\right) \tag{2.27}$$

where $\Delta W_{IP} = \Delta W_{BO}(BF - 1)$.

The corresponding payload penalty for tanker stages is

$$\Delta W_{PL} = -\Delta W_{BO} = -\frac{L_f W_P \delta X}{L_v} \qquad (2.28)$$

In-Flight Hydrogen Quantity Sensing. A tolerance in measuring this parameter, which is applicable to propulsive stages only, results in increased residuals at burnout. The maximum payload penalty is given by

$$\Delta W_{PL} = -\Delta W_R \qquad (2.29)$$

where $\Delta W_R = \delta W_P$, the in-flight mass tolerance.

The payload penalty that results from this tolerance differs for slush-fueled and liquid-fueled systems only if the accuracy of measurement differs. This characteristic is identical to that indicated for the loaded-hydrogen quantity.

Hydrogen Tank Ground Vent Pressure Sensing. This parameter measurably degrades performance for a liquid-fueled system only. For a slush-fueled system, the temperature and partial pressure of the hydrogen are maintained constant at the triple-point prior to launch. Any ground vent pressure-sensing tolerance, therefore, can affect only the partial pressure of the inert helium pressurant. A small variation in helium pressure at liftoff exerts a negligible influence on the total pressurant requirement, and, hence, on the payload. The maximum payload penalty for the liquid-fueled system occurs for an increase in ground vent pressure. Since a higher saturation pressure at liftoff dictates lower heat absorption capability after that time, the resulting increased boiloff directly decreases the tanker propellant payload and reduces the available impulse propellant, with subsequent degradation of the specific impulse, for propulsive stages.

The maximum payload penalty for a propulsion stage can then be calculated by combining Eqs. (2.20) and (2.26).

$$\Delta W_{PL} = -\Delta W_{BO} BF - W_2 \ln\left(\mu_1 \cdot \mu_2 \cdots \mu_n\right)\left(\frac{\Delta I_{sp}}{\Delta r}\right)\left(\frac{r}{I_{sp}}\right)\left(\frac{\Delta W_{IP}}{W_{IP}}\right) \quad (2.30)$$

where $\Delta W_{IP} = \Delta W_{BO}(BF - 1)$.

Similarly, the payload penalty for a tanker stage can be obtained from Eq. (2.22)

$$\Delta W_{PL} = -\Delta W_{BO} = -\left(\frac{dH_{sat}}{dP_{sat}}\right)\left(\frac{\delta P W_P}{L_v}\right) \quad (2.31)$$

Hydrogen Tank Flight Vent Pressure Sensing. A tolerance on flight vent pressure also affects the heat absorption capability, but unlike that described for the ground vent value. In this case, the effect is on the saturation pressure at which venting occurs. Therefore, the final result is identical for both liquid-fueled and slush-fueled systems except the varying sensing accuracy.

The maximum payload penalty for a flight vent pressure tolerance occurs with a decrease in pressure. This effect is opposite to that for the ground vent pressure tolerance because the lower saturation pressure at venting decreases the total heat absorption capability. The resulting increased boiloff again decreases the tanker propellant payload directly (when in-flight venting is used) and reduces the available impulse propellant, with subsequent degradation of the specific impulse for propulsive stages. The increase in boiloff for all stages can be determined using Eq. (2.31), except that W_P is the hydrogen weight remaining when the vent condition is reached. Also, the maximum payload penalty for the tanker stage can be obtained from that equation. For propulsive stages, two independent changes in specific impulse result from the changes in mixture ratio and in final hydrogen temperature for successive firings. The maximum payload penalty in this instance is represented by:

$$\Delta W_{PL} = -\Delta W_{BO}\, BF - W_2 \ln (\mu_1 - \mu_2 \cdots \mu_n)\left(\frac{\Delta I_{sp}}{\Delta r}\right)\left(\frac{r}{I_{sp}}\right)\left(\frac{\Delta W_{IP}}{W_{IP}}\right) \qquad (2.32)$$

$$+ W_2 \ln (\mu_1 \cdot \mu_2 \cdots \mu_n)\left(\frac{\Delta I_{sp}}{I_{sp}}\right)_T \Delta T \qquad (2.32)$$

Hydrogen Explusion Pressure Sensing. The operation of the hydrogen tank pressure regulator is expected to be identical for liquid-fueled and slush-fueled systems. Tolerances on sensing and controlling this pressure will exist; therefore, for this investigation, they need not be determined since the net effect on payload will not vary for the liquid and slush systems.

Hydrogen Tank Heat Load Sensing. A considerable tolerance will exist on this parameter for any flight system. Errors in estimating insulation performance, predicting penetration heat leaks, predicting environmental heat loads, etc., are all contributing factors. Increases in total heat load are manifested in corresponding increases in boiloff propellant weight. This directly reduces the tanker payload and decreases propulsive-stage payload through effects on available impulse propellant, mixture-ratio shift, and subsequent degradation of specific impulse as noted previously for other parameters that affect boiloff.

The payload penalties that result from the uncertainty in hydrogen tankage heat load, evaluated with Eqs. (2.20 and 2.22) for propulsive and tanker stages, respectively, are

$$\Delta W_{PL} = -\Delta W_{BO}\, BF - W_2 \ln (\mu_1 \cdot \mu_2 \cdots \mu_n)\left(\frac{\Delta I_{sp}}{\Delta r}\right)\left(\frac{r}{I_{sp}}\right)\left(\frac{\Delta W_{IP}}{W_{IP}}\right) \qquad (2.33)$$

and

$$\Delta W_{PL} = -\Delta W_{BO} \qquad (2.34)$$

where

$$\Delta W_{BO} = \frac{\delta Q}{L_v} \text{ and } \Delta W_{IP} = \Delta W_{BO} (BF - 1)$$

2.2.2.3 Total System Payload Penalty

The total acceptable payload penalty for a given stage system and mission depends on many factors. However, for the vehicle applications studied during this program, individual payload penalties that resulted from predicted tolerances on each variable (mass, quality, pressure, etc.) were combined using a root mean square probability that all of the predicted worst tolerances would occur during a given mission. Results are presented for each vehicle in Sections 3, 4, and 5.

2.2.3 Instrumentation for Quantity and Quality Measurements

Knowledge of hydrogen quantity (mass) and slush quality (solid fraction) within predictable tolerances is mandatory for effective design and operation of stages that use liquid or slush hydrogen as fuel. Mass can be measured directly or deduced from measurements of occupied volume and density. Solid fraction is a unique function of density, which can also be measured directly or deduced; in this case, from measurements of mass and occupied volume. In any case, a minimum of two fundamental measurements are required to obtain both mass and solid fraction.

Applicable gaging devices and systems must therefore be capable of measuring volume, mass, or density of the solid and/or liquid; or the ullage vapor; or gross average conditions within the entire tank. Where direct measurements are not practical, independent measurements of pressure, temperature, interface height, etc., can be applied through precalibrated or known relationships to obtain propellant-occupied volume, mass,or density.

There are two basic environments in which these measurements of hydrogen are to be made. The first is with its 1-g gravitational force, moderate temperature and pressure

extremes, and the very extensive mechanical equipment and electrical power available to maintain liquid and solid hydrogen within a wide range of state points for indefinite periods of time. The second environment is that of space, with additional problems imposed by low gravity, solar radiation, Van Allen belt radiation, meteoroid impact, and vacuum. Other problems include those imposed by the inaccessibility of an orbiting stage and the lack of orbiting equipment with which to maintain the liquid and solid hydrogen at even one or two state points.

Many techniques have been proposed and investigated for gaging the quantity and quality of liquid-solid mixtures of hydrogen at rest in a cryostat and flowing through a tank fill line. Some techniques are especially suitable for earth-based equipment and tests, and other techniques are suitable for low-g operation.

2.2.3.1 Literature Search

A thorough search of the literature was conducted to examine the state of the art with respect to gaging systems in general. Particular attention was focused on the applicability and limitations of each system as applied to mixtures of liquid and solid hydrogen. Candidate systems that could be used for a flight vehicle are as follows:

Primarily Volume-Measuring Systems

- Point-level sensing
- Volumetric flowmeter
- Acoustic and mechanical resonant frequency

Primarily Mass-Measuring Systems

- Gamma-ray attenuation
- Pulsed x-ray tube
- Direct weighing
- Mass flowmeter

Primarily Density-Measuring Systems

- Parallel-plate capacitance
- Radio frequency
- Differential pressure

- Optical
- Buoyant force
- Ultrasonic
- Linear momentum
- Angular momentum
- Rotating paddle

The systems or techniques were grouped according to whether they primarily measure volume, mass, or density. In reality, some systems measure a combination of these. The basic principles of operation of each candidate system and the significant features or limitations of the more promising ones were extracted from the literature and are presented in the following paragraphs.

Point-Level Gaging System. Liquid-level sensors suitable for determining the liquid-vapor interface of hydrogen are available commercially and include the following:

- Magnetostrictive – Measures the difference in acoustic damping between a liquid and a vapor to detect the common interface
- Optical – Employs a liquid-level transducer containing a light source and a light-sensitive cell to measure differences in prism-reflected light through the liquid and the vapor, thereby detecting the interface
- Capacitance – Measures the difference in dielectric constant between the liquid and vapor to detect the interface

Characteristics and limitations of the point-level gaging system are as follows

- This technique is indirect in that only the height of the interface between the liquid or liquid-solid and the vapor is measured. The relationship between volume and interface level depends upon careful calibration of the system.
- Use of this system is limited to a gravity environment such as that present on the launch pad where the propellant is oriented with respect to the vehicle axis and the interface is flat.

- Measurements of interface height can be very accurate if the interface is quiescent. This precludes accurate measurements during rapid tank filling and periods of active boiling or turbulence.
- Detection of the interface height between liquid and settled slush can be accomplished by adjusting electronic circuitry for the optical and capacitance type sensors.

Volumetric Flowmeter Gaging System. One common type of this device is presently used to determine volumetric flow rates of gases by measuring the rates of rotation of a positive displacement impeller. In principle, at least, the volumetric flow rates of liquids, solids, or mixed-state fluids could also be obtained; however, a great reduction in friction losses is important so that flow characteristics are not seriously affected by the measuring mechanism. The primary disadvantages of volumetric flowmeters are: (1) fluid properties must also be measured so that mass flow rates can be inferred and (2) suitable mixed-state devices, needed for an application to slush systems, are not presently available.

Acoustic Gaging System. This system measured the acoustic pressure change in a tank containing ullage vapor and liquid or solid propellant by periodically perturbing the tank volume with acoustic energy generated by a vibrating bellows or piston. The compliance of the solid/liquid-vapor mixture in the tank is analogous to an electrical capacitor whose characteristics can be related to mixture pressure, volume, and specific heat. Likewise, acoustic resistances are analogous to electrical resistances. Thus, ullage volumes may be observed by differences in acoustic impedance in the tank with respect to a reference volume. The equation indicating ullage volume in the main tank then reduces to the relationship of a constant multiplied by the reference frequency.

Characteristics and limitations of the acoustic gaging system are as follows:

- Volume variation of ullage vapor is measured; therefore, many errors can be encountered in the determination of liquid propellant volume because of the nonhomogeneous mixing between pressurization gas and ullage vapor, which varies the ratio of specific heats and affects the accuracy of the system.

Also, under certain conditions of rapid pressurization, a stabilization time will be required because temperature gradients in the vapor substantially affect its acoustic propagation characteristics.

- A reference volume, analogous to one arm of an electronic bridge circuit, must be used. To obtain accurate measurement, the temperature and pressure in the reference and gaging volume must be kept the same, increasing construction, maintenance, and testing problems.
- The system cannot be used during loading because it is nearly impossible to maintain equivalent gas characteristics in the ullage and reference volumes.

Gamma-Ray Attenuation Gaging System. In this system, gamma rays are emitted by a radioisotope source mounted on the tank. Some of the rays pass through the tank walls and liquid container volume and arrive at a detector mounted opposite the source. The empty tank is used to calibrate the tare. With propellant present, the signal strength decreases due to absorption of the radiation by the liquid, vapor, and/or solid mass in the tank. The detector then converts the gamma rays into electrical signals for computer processing.

Characteristics and limitations of the gamma-ray attenuation gaging system are as follows:

- For a ground-based gaging system, a single source and detector arrangement can be used. This would require that the source and detector be translated up and down along the tank and back and forth in one quadrant of the tank, obtaining an average density over the entire fluid volume. This approach would require that a relatively large source strength be employed, thereby causing inconvenient restraints to be imposed on ground operations procedures.
- For a flight-type system that would require gaging under a low-gravity environment, a gamma-ray system would be difficult to implement. Several sources and detectors would have to be strategically placed around the tank to provide a uniform radiation flux within the tank. This would most certainly require solid-state detectors to keep weight to a reasonably low value, which would further complicate sensitivity and discrimination requirements. Also, this

system is subject to inherent errors resulting from imposition of background radiation such as Van Allen belt radiation in earth orbit.

Pulsed X-ray Tube Gaging System: This system consists of an x-ray tube source, solid-state detection subsystem, and data processing subsystem. The system uses the attenuation of electromagnetic radiation by the liquid, vapor, and solid hydrogen propellant contained in the tank. With the tank empty, the signal output of the detection subsystem sets the zero level, which compensates for all fixed masses, such as tank walls, insulation, plumbing standpipes, etc., between the source and detectors. As propellant is added, the detector signal level is reduced because the x-rays are absorbed by the propellant. Maximum accuracy and sensitivity of the system are reached when the tank is empty.

The pulsed x-ray tube system contains no internal moving parts. Available equipment, including the x-ray tube, is of rugged construction and proven service life. System stability and accuracy can be increased by use of a reference detector which is shielded from the x-ray source subsystem. The detector compensates for thermal noise, variations in emitted x-ray flux, space radiation noise, and drift in the output electronics. Also, the pulsed x-ray tube can be shut off except when interrogated and a series of tanks can be interrogated without danger of crosstalk.

Characteristics and limitations of the pulsed x-ray tube gaging system are as follows:

- This system could be effectively employed for ground-based operations by using a single x-ray tube and a single detector diametrically opposed, and by vertically translating and horizontally rotating the coupled system to scan the contents of the tank. In this manner, an average mass quantity could be obtained.

- The system has a distinct advantage over a radioisotope system, in that it can be turned on or off when required; however, protection against the radiation environment must be provided. Relatively large radiation sources are required to ensure that sufficient penetrating radiation is received by the detector on the opposite side of a large, full hydrogen tank.

- For an in-flight function this approach seems to be less attractive than for a ground-based system, since a complete mapping or averaging technique, similar to the radioisotope method, would have to be employed to operate in low-gravity environments. Many x-ray generating devices would have to be placed on the tank, creating difficult implementation problems and resulting in reduced reliability.

Direct Weighing Gaging System. This can be accomplished either by weighing the GSE propellant storage tanks or the launch vehicle. Load cells for such systems measure either mechanical strain or change in electrical resistivity as a function of applied load. Extremely accurate weight measurements are attainable in practice. Although direct weighing has not generally been considered as a field technique, it has served as a primary calibration standard and has been used for some vehicles on the launch pad. Some advantages of the method are simplicity of equipment, repeatability, and lack of dependence on nonhomogeneous properties of the fluid. Disadvantages include the difficult system problems incurred due to the severe size and weight of vehicles such as those in the Saturn family.

Mass Flowmeter Gaging System. Several different basic principles of operation have been used to develop devices that can determine mass flow rate. The simplest approach has been to deduce mass flow by correlating volume flow measurements with density obtained from an independent measure of temperature or pressure. Such a device is, of course, restricted to measuring single-state fluid flow. Another flowmeter presently under development measures viscous drag of the flowing material to obtain a combined function of drag coefficient, flow velocity, and density in one section of the meter. The output signal is obtained from an electrical grid sensor mounted in the flow stream. Fluid density is then determined by correlating measurements of dielectric constant using a capacitive sensor, located in a separate portion of the meter. A third type measures the inertial reactance to torque imposed on rotating turbines by the mass of flowing material.

Flexibility is the primary advantage of a mass flowmeter system. The net mass flowing into and out of a tank can be monitored throughout tank loading, launch, and flight. Flow through fill, vent, and feed lines can be independently recorded by using a flowmeter in each line. The primary disadvantages are those noted for volumetric flowmeters, i.e., the accumulative effects of inherent tolerances and the lack of availability of a proven system for use with multistate fluid flow.

Parallel-Plate Capacitance-Gaging System. These systems measure the dielectric constant of the gas, liquid, or solid in a volume of defined geometry. The dielectric constant ϵ of a material is given by the ratio of the capacitance of a condenser, with the material as dielectric, to the capacitance of a condenser of the same linear dimensions with no dielectric (vacuum). The known relationship between dielectric constant of the fluid being measured and the geometric volume can be used to determine the quantity of liquid versus gas in that volume. This technique is well established and performs very well in systems where the location of the liquid is well known with relation to the volume being measured, e.g., in a tank on the launch pad. For a nonhomogeneous fluid such as slush hydrogen, a network of capacitors would be required. This is relatively easy to install in small laboratory tanks, but are heavy and difficult to install in large tanks.

To be useful under low-gravity conditions, a capacitance-gaging system must include a capacitor structure in the storage tank such that a quantity of liquid will cause the same effect on measured capacitance regardless of its location. This is necessary because it must be assumed that liquid distribution can be completely undefined. Therefore, field strength throughout the tank must be uniform within the accuracy expected from the tank portion of the system.

Characteristics and limitations of the capacitance-gaging system are as follows:

- Nonhomogeniety and/or low-gravity conditions require complex in-tank capacitor structures. For accuracy, small spacings would be required between

active elements throughout the tank to ensure a sufficiently uniform electrostatic field. The mechanical problems appear to be excessive; the structure must withstand vibration and slosh forces without major deformation. The two capacitor structures must be mechanically supported through electrical insulators at many points to permit use of lightweight elements.

- Surface tension (capillary) effects cause liquids under zero-gravity conditions to collect in areas that have a high surface-to-volume ratio. These effects cause the liquid to build up in thickness on the capacitor elements where the field strength is greatest. This can cause errors since the capacitance measurement is no longer accurately related to liquid quantity in adjacent areas.
- Vibration may cause capacitor elements to move with respect to each other, resulting in errors unless signal conditioning is used to filter out all the signals caused by vibration.

Radio-Frequency Gaging System. The radio-frequency gaging system interprets the changing resonant frequency of an enclosed metallic structure (the tank) containing dielectric material (the propellant) as a measure of the density of propellant in the propellant tank. For certain tank configurations, it is possible to obtain accurate gaging by exciting a single RF mode and measuring the frequency shift due to variation in propellant quantity. For irregularly shaped tanks, or tanks with baffling and internal structures, problems are encountered in obtaining a single RF mode that is stable over the entire fill range of interest. However, if the tank is illuminated with many resonant frequencies, the net effect is to produce an approximately uniform distribution of RF energy in the tank. The number of modes present over a selected frequency band can be counted and the information used as a measure of propellant quantity. The importance of the mode-counting system is that, primarily, measurement does not depend on tank geometry or propellant distribution. Irregularly shaped tanks lend themselves

more to this technique than do regularly shaped structures. This technique has the following characteristics:

- Adaptable to any tank shape
- Independent of propellant location
- Operates during fuel loading or withdrawal
- Instrumentation (except for probes) is external to the tank
- Multitank gaging is feasible with one signal conditioning unit
- High sensitivity is possible
- High potential accuracy is possible

Limitations of the RF gaging system are as follows:

- Fluid orientation effects could affect the amplitude of the modes to be counted, making mode counting more difficult.
- Differentiating electronics and triggering devices required to count modes have deadbands that can add to the difficulty in counting.
- At present, the manner in which solid particles affect the transverse electrical and magnetic modes is not understood completely.

Differential Pressure Gaging System. This method measures the pressure of a vertical column of the mixture, which gives the density and the height of the column. Advantages of this system include relatively simple equipment, small component size, and the possibility of field applications. It is applicable only in a gravity environment.

Optical Gaging System. In this method of density determination, a light beam (including ultraviolet and infrared wave lengths) is passed through the fuel tank and the intensity is measured on the opposite side. The spectral absorption of the transmitted light can be related to the density of the mixture. Although there are many advantages to this system, the scattering of light by the solid hydrogen particles presents a severe problem which must be solved before the system could become practical.

Buoyant-Force Gaging System. Density of a fluid can be measured by the buoyant force that it exerts on a submerged plummet. This method is ideally suited for static laboratory use and involves relatively simple equipment; however, it is applicable only in a gravity environment. The disadvantages are slow response, poor sensitivity, and the need for a homogeneous mixture.

Ultrasonic Gaging System. In this method, the impedance of a vibrating crystal in the fluid is measured and related to the fluid density. This method is not suitable for non-homogeneous mixtures or for a turbulent medium, and therefore cannot be used in a slush mixture.

Linear-Momentum Gaging System. Fluid density can be determined by measuring linear fluid flow rate and momentum. This system is not applicable to static density measurement because it requires a mechanism for controlled stirring of the fluid.

Angular-Momentum Gaging System. Density of a fluid can be obtained by measuring the angular momentum as the fluid rotates, and relating this momentum to density. As with the rotating paddle method, density is measured while uniformly mixing the fluid. Equipment required is relatively simple. Disadvantages of this method include the presence of bulky moving parts in the fluid.

2.2.3.2 Evaluation of Specific Systems

A preliminary investigation of instrumentation and measurement techniques applicable to subcooled liquid or slush hydrogen is discussed in this subsection. In this investigation, three different techniques of determining quantity and quality during tank loading and ground hold were briefly considered. All of the methods entail measurements of propellant-occupied volume using point-level sensors that depend on precalibrated volume-level relationships. Propellant mass measurements for these techniques require integrating mass flow rates into and out of the tank using flowmeters, direct weighing using load cells, or use of a nucleonic gaging system.

Mass and Quality Determination Using Flowmeters and Point-Level Sensors. In the first system considered, mass flowmeters are mounted in both the slush supply and liquid-recirculation lines and are used to monitor continuously the net mass in the tank. The volume occupied is monitored by liquid-level sensors, assuming the flight tank was previously calibrated for volume. Aerojet-General (Ref. 2.1) has shown that it is possible to calibrate a tank volume to 0.05 percent of full capacity.

Volume occupied by a liquid-solid propellant mixture can be expressed in terms of total propellant mass, solid fraction, and the specific volumes of the liquid and solid:

$$V_{(\ell + s)} = W\left[Xv_s + (1 - X)v_\ell\right] = W\left[X(v_s - v_\ell) + v_\ell\right] \qquad (2.35)$$

Since v_ℓ for hydrogen is an order of magnitude greater than $X(v_s - v_\ell)$, the specific volume V/W of the mixture can be approximated by v_ℓ in Eq. (2.35). Using this approximation of specific volume for the mixture, the tolerance in quality can be expressed as

$$dX = \frac{\left(d\dot{W}'\left(\frac{\theta}{\theta'}\right) - dV'\right)}{1 - v_s/v_\ell} \qquad (2.36)$$

where $d\dot{W}' = d\dot{W}/\dot{W}$ = flowmeter tolerance as a fraction of mass flowrate, $\theta' = V\eta/\dot{W}v_\ell$ = time to fill the occupied volume at a flow rate $\dot{W}$ and $dV' = dV/\eta V$ = volume tolerance as a fraction of occupied volume.

Also, the allowable flowmeter tolerance fraction, which indicates its required accuracy, can be expressed as

$$d\dot{W}' = \frac{\left(1 - \frac{v_s}{v_\ell}\right)(dX) + (\pm dV')}{\theta/\theta'} \qquad (2.37)$$

The application of mass flowmeters can be best illustrated with representative numbers. For example, $d\dot{W}' = 0.1$ percent (0.001) at the end of the fill period (where $\theta/\theta' = 1.0$) if dV' is taken as 1 percent (0.01) and dX as 10 percent (0.10). This low value of $d\dot{W}'$ indicates that a very accurate flowmeter is required. Further examination of Eq. (2.37) shows that even if the volumetric sensing error were reduced, the allowable flowmeter tolerance fraction is still very low. In the above examples, $d\dot{W} = 1.1$ percent (0.011) for $dV' = 0$ and $dX = 10$ percent. The resulting allowable tolerance fraction is likewise very low if greater accuracy in quality is required. In this case, $d\dot{W}' = 0.11$ percent (0.0011) for $dV' = 0$ and $dX = 1.0$ percent.

As discussed in NBS Report 8879, calibration of flowmeters for slush service has not yet been accomplished. Thus, while it is theoretically feasible to determine the mass, and therefore the solid fraction, this method is probably not practical for a flight system since the accuracy requirements on the flowmeters appear to be much too stringent.

Very accurate measurements of tank volume are possible using point-level sensors. NBS Report 8879 cites that both optical and capacitive point-level sensors can be adjusted to sense the phase interfaces for triple-point liquid hydrogen, settled slush hydrogen, or stirred slush hydrogen. Previous NBS references state that the total band of sensing inaccuracy using these sensors for liquid hydrogen is on the order of 0.030 in. The error in volume determination dV varies only with the error in measured interface level and the tank radius. For example, dV in the Saturn S-IVB hydrogen tank is approximately 4.25×10^4 cm^3 (1.5 ft^3) if the error in measured interface level is assumed to be 1.27 mm (0.050 in). This amounts to a volume tolerance dV/V of about 0.015 percent.

Mass and Quality Determination Using Direct Weighing and Point-Level Sensors. At many vehicle test stands and launch complexes, propellants are weighed directly, either by weighing the GSE propellant storage tanks or the entire gross launch vehicle. The load cells for such systems measure either mechanical strain or change in electrical resistivity to monitor the gravitational forces. Weight measurements accurate to ± 0.05 percent of reading to 10 percent of full scale are common (Ref. 2.2).

For cryogenic vehicle systems such as those used with the Saturn V , this method of determining propellant weight can be enhanced considerably if the load cell is installed in the interstage structure between stages. For the Saturn S-IVB stage, for example, the uncertainties introduced by makeup or vented propellants and frost in lower stages can be completely avoided. Further, the gross liftoff weight of the S-IVB stage plus the items above it in the Apollo configuration is only about 5.7 percent of the total vehicle gross weight at liftoff. This means that the respective errors in weighing are also related by this percentage. Assuming that additional inherent errors result in a weighing system with a net accuracy of ±0.10 percent of reading to 10 percent of full scale, the uncertainty in propellant weight for the Saturn S-IVB stage is approximately 16 kg (36 lb) for the interstage weighing system and approximately 290 kg (640 lb) for the total vehicle weighing system. Volume occupied by propellant may again be measured with point-level sensors for this concept of quantity and quality control. The above discussion under "Mass and Quality Determination Using Flowmeters and Point-Level Sensors" applies.

Mass and Quality Determination Using a Nucleonics Gaging System. This method depends upon placing gamma emitters and detectors in a precalculated array on the outer tank surface. Theoretically, such a system can be used at all levels of acceleration. Various equations describing the process can be reduced to

$$I = K'e^{-\bar{C}W} \tag{2.38}$$

As with other systems discussed, this method requires an accurate precalibration of tank volume.

A serious consideration with respect to radiation mass measurement is reliability in the Van Allen belt. This, of course, does not affect the use of such a system for prelaunch measurements. The high cost of such a system could be minimized by arranging the emitter/detector array in a separable blanket outside the stage external shell. Removal of the blanket prior to liftoff would also avoid a possible radiation hazard considering range safety requirements.

Instrumentation Study Summary and Recommendations. The results of the System Tolerance Effects Study (subsection 2.2.2) indicate that an acceptable tolerance for sensing loaded propellant mass is on the order of 1 or 2 percent of that mass if a 5-percent total payload degradation is assumed. In addition, a tolerance of approximately 10 to 15 percent on sensing loaded-propellant solid fraction for slush was shown to be acceptable with the same assumptions applied. Because the acceptance sensing tolerances are this large, it is reasonable to conclude that several of the candidate systems could work equally well. Therefore, the objectives of the present study contract (i.e., development of preliminary design techniques and assessment of resulting benefits obtained with use of subcooled or slush hydrogen) were pursued independent of instrumentation development.

Based on existing knowledge of volume, mass, and density sensing techniques, the following systems show the most promise for development for use with subcooled or slush hydrogen systems:

- Point-level sensing to obtain volume
- Either gamma radiation (or x-ray) attenuation, mass flowmeters, or direct weighing to measure mass
- Radio-frequency techniques to measure density

It is recommended that development work be continued on these systems, and possibly others.

2.3 PROPULSION STUDY

Initial contacts were made early in the study program with representatives of the Rocketdyne Division of North American Aviation, Inc., the Pratt & Whitney Aircraft Division of United Aircraft Corporation, and the Pesco Products Division of the Borg-Warner Corporation, to discuss engine and pump operating characteristics with use of subcooled liquid and slush hydrogen. In addition, further discussions were conducted periodically with both engine companies throughout the contract period.

A substantial portion of the engine and pump operating characteristics and supporting data presented in this section was obtained from these contacts. Propulsion anslysis performed during the study was essentially that required to apply these data to the S-IVB and Lunar Mission Vehicle studies.

2.3.1 Engine Characteristics and Performance

Estimates of the effects of subcooled liquid and slush hydrogen usage on engine operation and performance are described in subsequent paragraphs. The specific propulsion systems considered are the 205K J-2* and the 15K RL10A3-7,** identified with the S-IVB/ LASS mission concept, and the 15K RL10A3-3** employed on the Lunar Mission Vehicle.

Rocketdyne 205K J-2 Engine. The J-2 rocket engine, shown in Fig. 2-8, is a high-performance upper stage propulsion system featuring a tubular-wall, bell-shaped high-altitude thrust chamber, independent turbine-driven propellant pumps, a single oxygen/ hydrogen gas generator supplying gas to the two turbines in series, and a propellant utilization system. The basic engine uses a tank-head start system with augmented spark ignition (ASI), is rated at 910,000 N (205,000 lbf) ± 3-percent thrust with a nominal vacuum specific impulse of 4,175 m/sec (426 sec), and operates nominally at a propellant mixture ratio (oxidizer/fuel) of 5.0:1 ± 2 percent. For the S-IVB/ LASS mission evaluation, Douglas Aircraft Co. selected the 205K nominal engine, which yields 985,000 N (222,000 lbf) ± 3-percent thrust at a mixture ratio of 5.4:1 ± 2 percent. In this study analysis, the 910,000 N (205,000 lbf) nominal thrust engine was also used with variable mixture ratios, and a temperature range of 13.803° K (24.85° R) to 20.55° K (37° R) was considered. Use of subcooled liquid propellant is discussed first, followed by slush considerations.

Engine performance based on temperature is estimated in Figs. 2-9, 2-10, and 2-11 for the basic engine.*** Using a nominal engine balance without temperature calibration,

*205K at a 5.0 to 1 mixture ratio, and 230K at a 5.5 to 1 mixture ratio.
**15K at a 5.0 to 1 mixture ratio and 15.3K at a 5.5 to 1 mixture ratio.
***Engine performance for the Qual. II engine used in the S-IVB application study is shown in Figs. 3-6, 3-7, and 3-8.

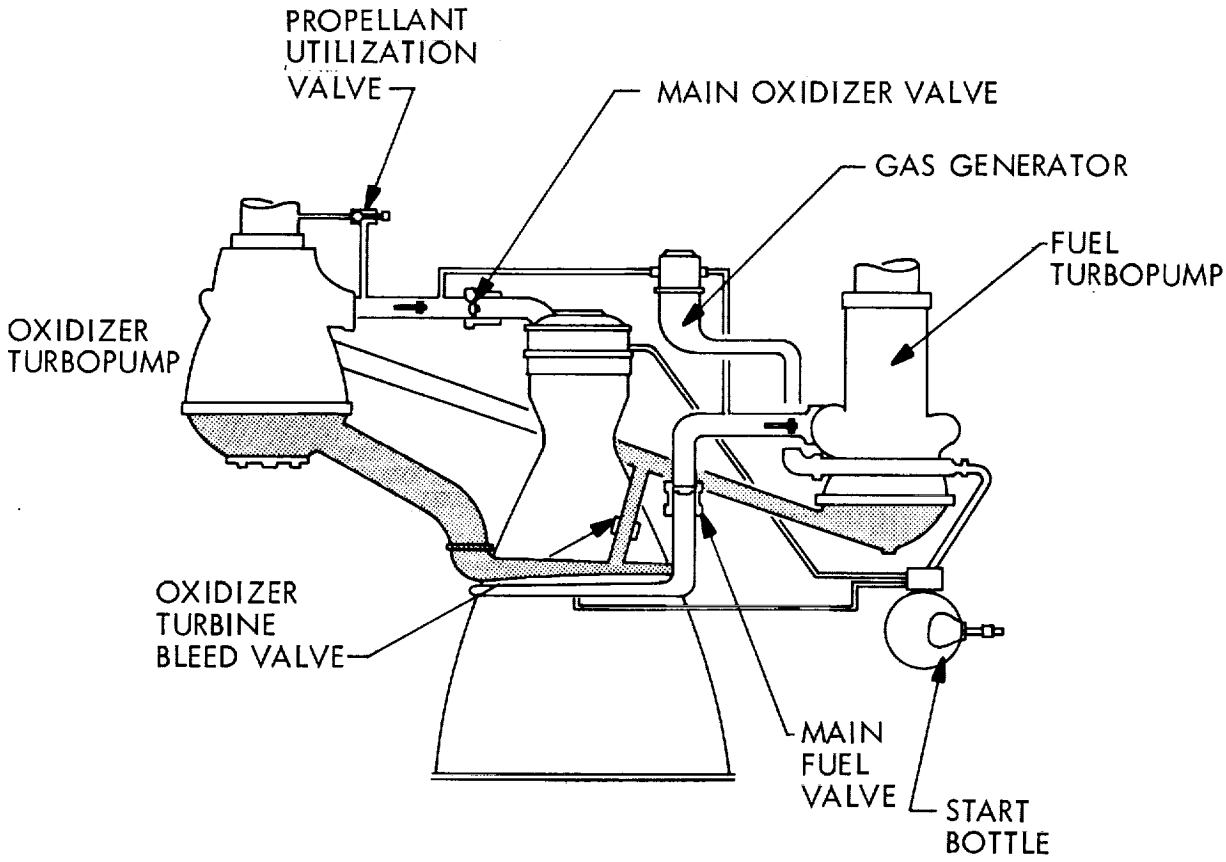

Fig. 2-8 J-2 Engine Schematic (205K Thrust)

the thrust, specific impulse, and chamber pressure increase, reaching a maximum at 17.8° K (32° R), and then decrease to nominal at 20.55° K (37° R). Similarly, the engine mixture ratio decreases, reaching a minimum at 17.8° K (32° R), and then increases. Also shown are the results of the analysis which considered engine balance with recalibration at each different hydrogen engine inlet temperature. In this case, the engine operates at the same volumetric flow rate as in the nominal case. Using this approach, the engine balance is recalibrated to operate at the desired hydrogen temperature and at the weight flow rates, mixture ratio, and chamber pressure resulting from the constraint of constant volumetric flow rates. The specific impulse and thrust vary inversely with hydrogen temperature in the temperature range of interest. On the other hand, the engine mixture ratio varies directly with these quantities in the constant volumetric flowrate approach.

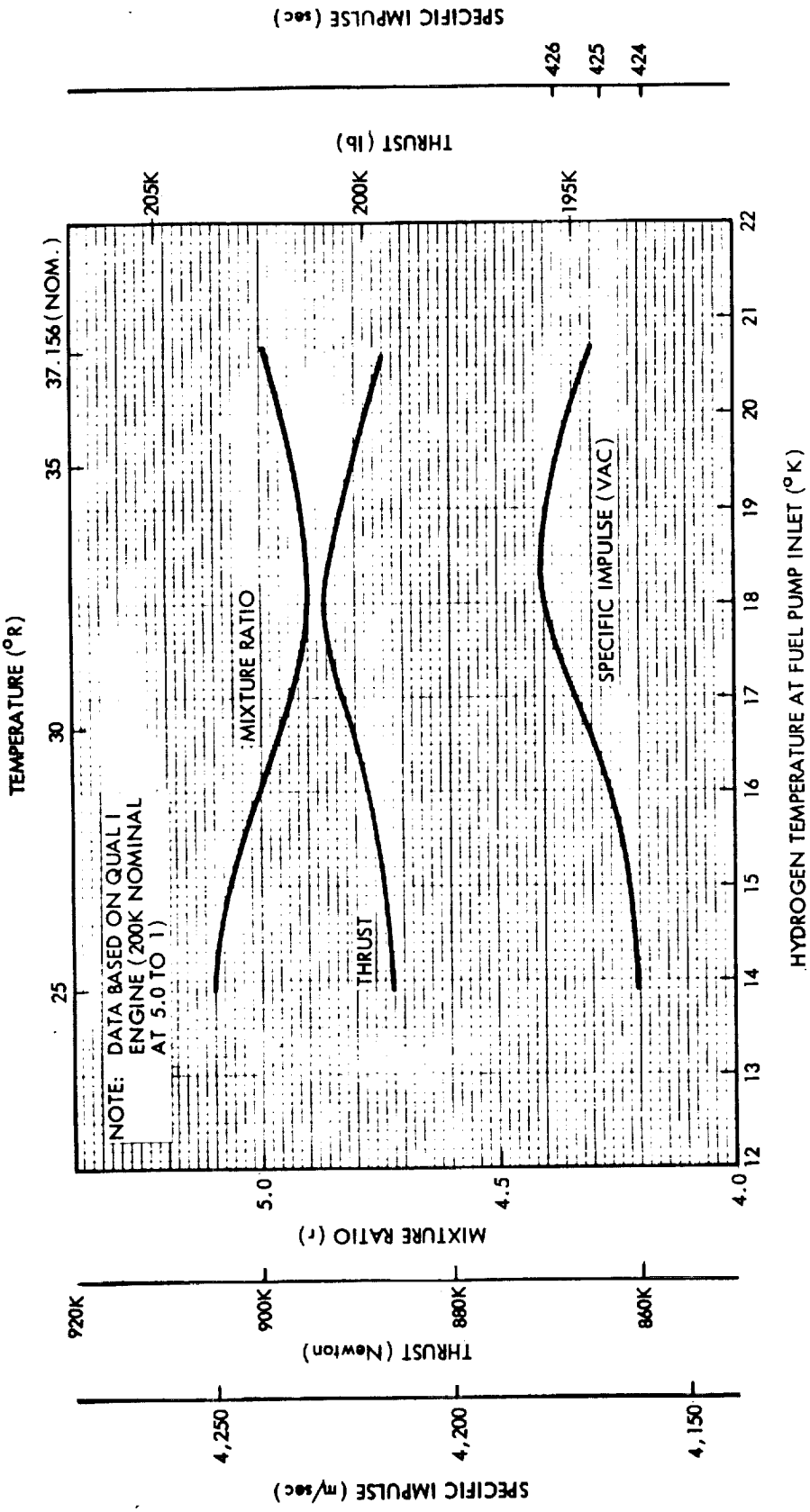

Fig. 2-9 Preliminary J-2 Engine Thrust and Specific Impulse Without Temperature Calibration

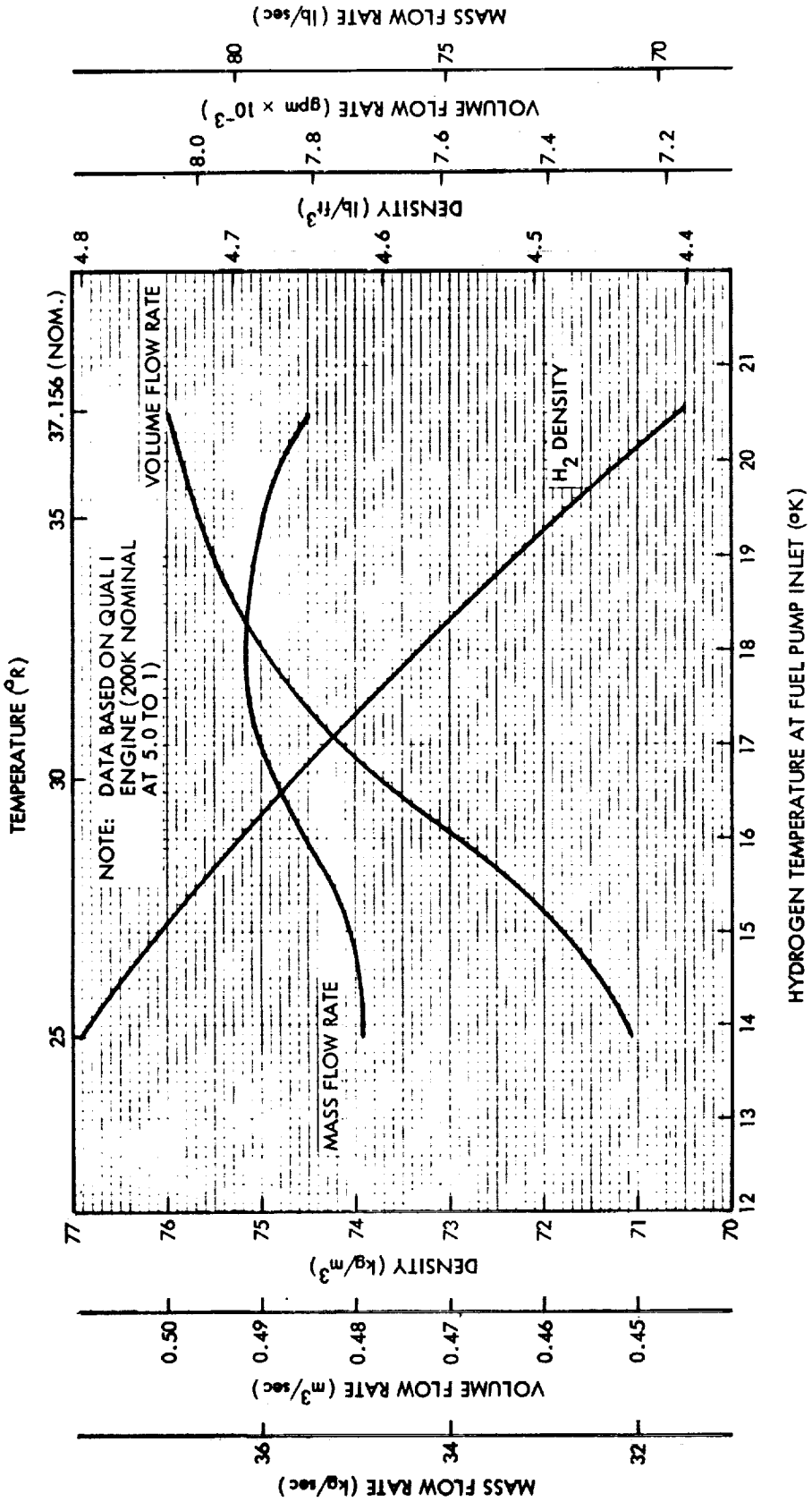

Fig. 2-10 Preliminary J-2 Engine Flow Characteristics Without Temperature Calibration

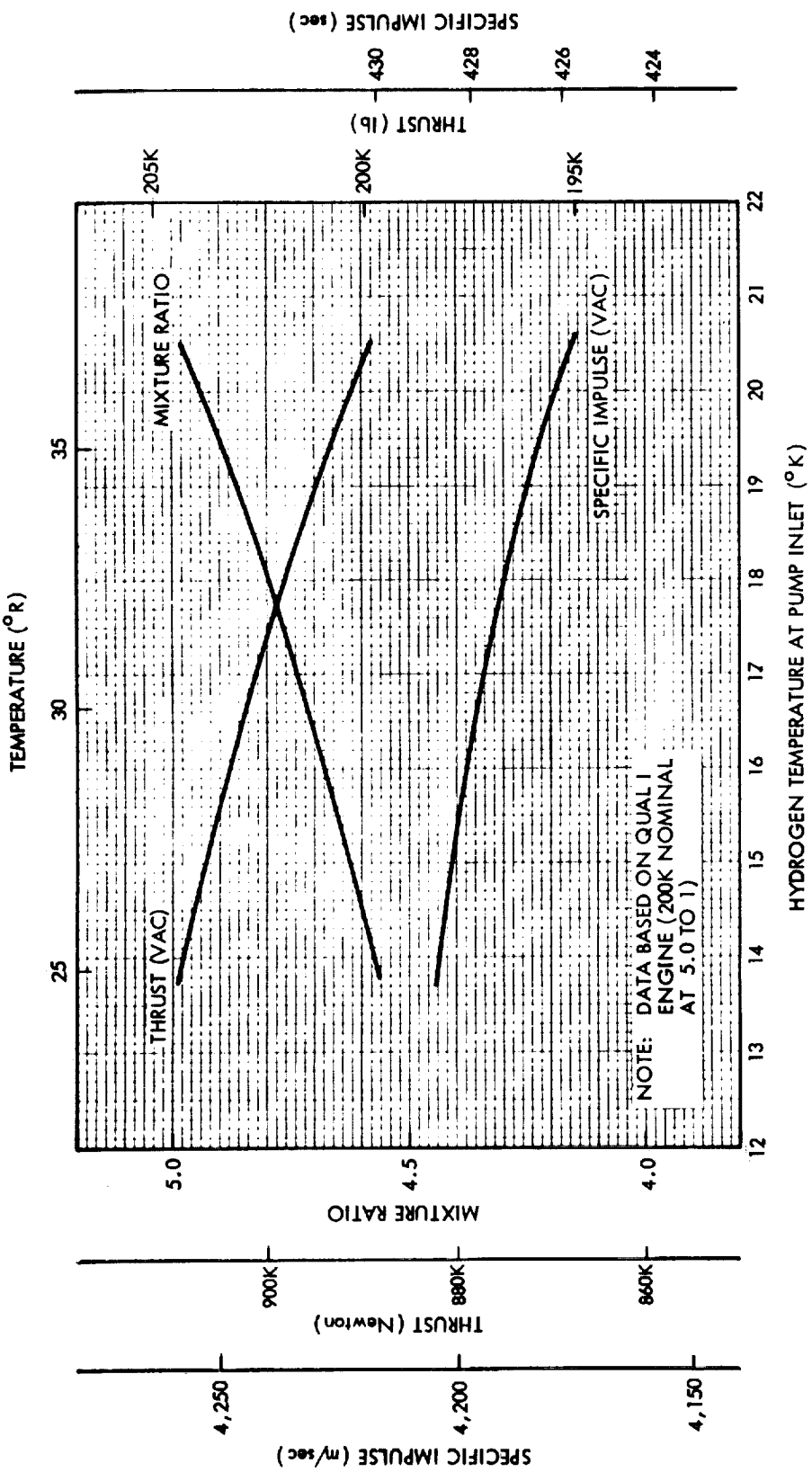

Fig. 2-11 Preliminary J-2 Engine Performance With Temperature Calibration (Constant Volumetric Flowrate)

Two important factors which must be considered when using subcooled liquid or slush hydrogen are: the effect on the cooling capability of the fuel at lower temperature and the effect on current injector design and performance with use of a lower temperature (higher density) fuel. A preliminary investigation of thrust-chamber cooling indicates that engine cooling capability will not be influenced significantly for moderate subcooled conditions. A small loss in characteristic velocity (C*) does result for subcooled temperatures in the triple-point region.

The following areas are recommended for futher detailed investigation by the engine contractor to confirm the effects of subcooling:

- Thrust-chamber injector stability during transition and mainstage firing
- Ignition in the gas generator combustor and in the engine with ASI
- Clearances in engine valves and turbopumps
- Maximum thrust at low mixture ratios (which might exceed the structural limitations of the engine)
- Flight instrumentation temperature transducer range changes
- Effect of lower temperature on engine inlet ducting and associated gimbal restraints

A preliminary evaluation of the effect of slush usage was analyzed by Rocketdyne. It was predicted that no deleterious effects would be experienced in the engine systems due to erosion from solid particles. It was hypothesized that there is only a slight probability of small solid hydrogen crystals, from 1 to 3 mm in diameter, reaching the injector during engine operation. This condition could exist even considering the "crushing" effect in the pump. There is a distinct probability that solid hydrogen particles could flow to the injector during the start transient and chilldown sequence, in which case start instability or rough combustion could take place.

The following areas of detailed test investigation with respect to slush are required to confirm engineering theory if the "homogenous mixture" concept is to be used:

- Dead-headed slush in the engine inlet ducting
- Velocity loss in the turbopump due to minimal inducer and impeller clearances

- The effect of "ice-bridging" in the ASI bleed line and the flowmeter
- Operation of the main hydrogen propellant valve and engine check valves
- The effect of "ice-bridging" at the gas generator orifice and control valve

Pratt & Whitney Aircraft 15K RL10A3-7 and RL10A 3-3 Engines. These engines are regeneratively cooled and turbopump-fed with single-thrust chambers and have a rated thrust of 66,600 N (15,000 lbf) ±2 percent. A simplified schematic for the RL10A3-7 engine is shown in Fig. 2-12. The propellant pumps are turbine driven through the use of an expander cycle, which utilizes fuel flow circulated through the pump, and the tubular-wall, bell-shaped, high-altitude thrust chamber. Both engines are capable of altitude restart, and propellant flow is controlled using propellant utilization systems and mixture-ratio adjustment valves at a nominal oxidizer/fuel mixture ratio of 5.0:1 ±2 percent. The resulting nominal specific impulse is 4,350 m/sec (444 sec); standard fuel temperature and pressure relationship is nominally 21.54° K (38.8° R) and 21.35 N/cm (32.4 psia). In their S-IVB/LASS Vehicle Study, Douglas used the RL10A3-7 at a mixture ratio of 5.4:1 ±2 percent. This results in a slight decrease in characteristic velocity C* and exhaust velocity V_e. This engine is throttleable from 66,600 N (15,000 lbf) down to 6,660 N (1,500 lbf) thrust at a total pump inlet pressure of 20.7 N/cm (30 psia) and can also be operated in the tank-head idle mode at a total inlet pressure of 13.79 N/cm (20 psia).

A lack of complete performance data on these engines required that LMSC use generalized analyses of potential problem areas. In consideration of the temperature drop at the pump inlet from 21.1° K (38° R) to 13.803° K (24.85° R), it is apparent that nominal calibration will be required on these engine systems due to the expander cycle turbine drive. The first effect of subcooled liquid use is found downstream of the pump, at the fuel pump discharge cooldown valve, where the cooldown time is reduced for any given initial propellant condition. Additional fuel pump trim does not appear to be needed at the present time because of the temperature rise of approximately 10.55° K (18.5° R) through the pumping cycle. The cooling capability of the propellant in the thrust chamber will not significantly affect engine operation; however, the engine experiences a slight shift in mixture ratio and nominal thrust with temperature. These effects are estimated in Fig. 2-13 where it can be seen that they are negligible.

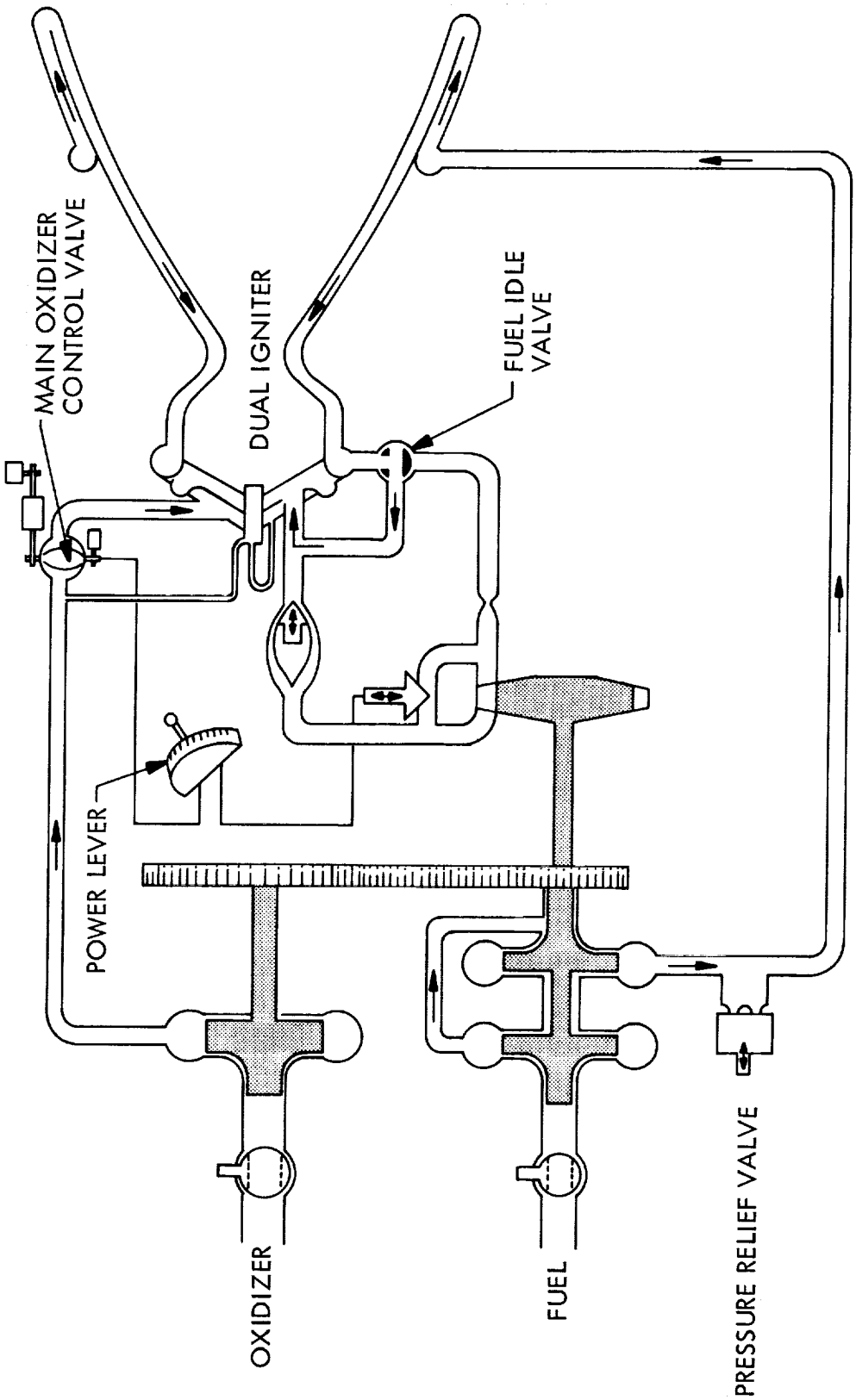

Fig. 2-12 Preliminary Propellant Flow Schematic of RL10 Variable-Thrust Engine With Low Idle

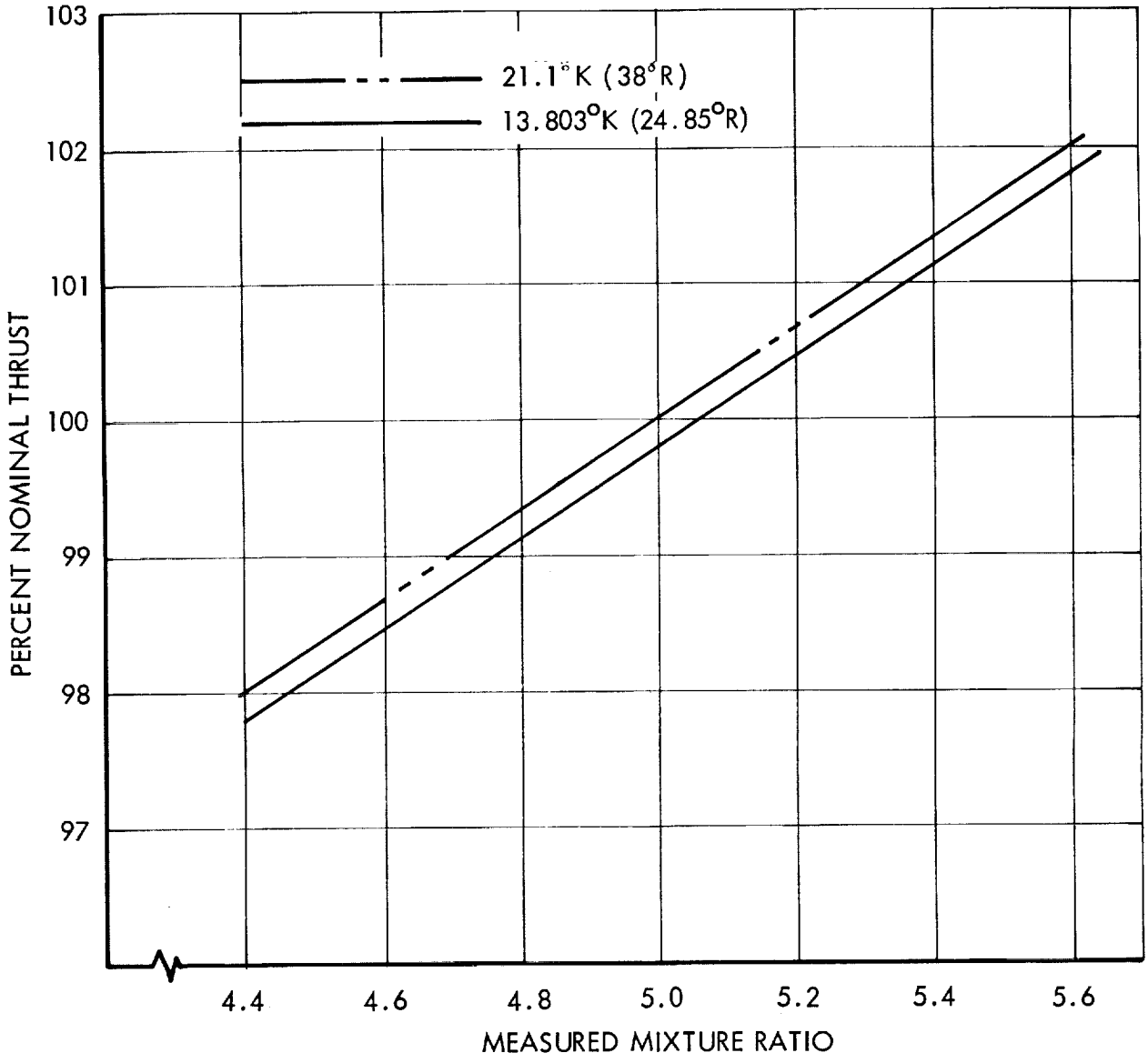

Fig. 2-13 Estimated Effect of Temperature on Mixture Ratio and Nominal Thrust for the RL10 Engine

Figure 2-14 shows the estimated effect of temperature on the percent nominal specific impulse at the measured mixture ratio.* Again, the effect is minor and the engine operation will still be within the rated nominal thrust tolerance of ±2 percent.

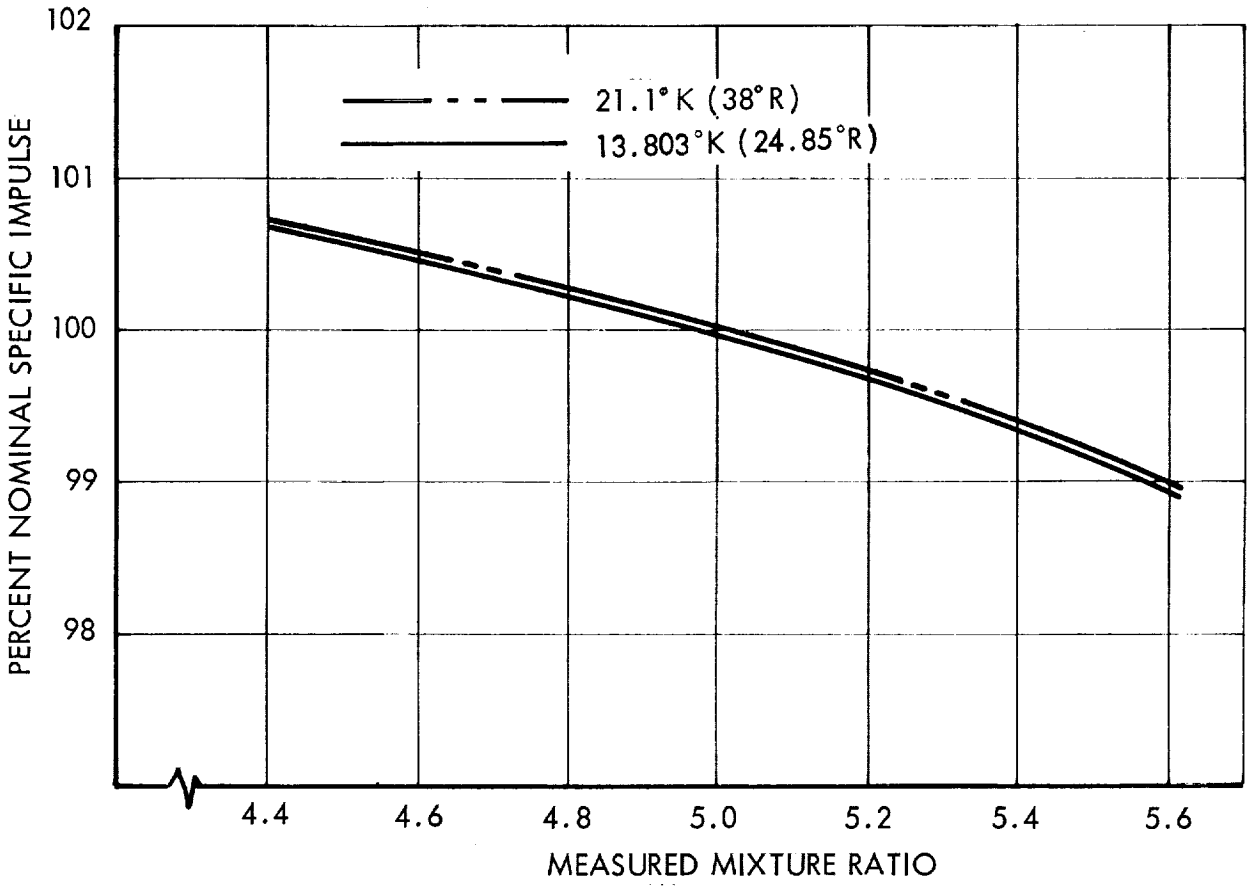

Fig. 2-14 Estimated Effect of Temperature on Mixture Ratio and Percent Nominal Specific Impulse for the RL10 Engine

Adjustment of mixture ratio and thrust control can be accomplished using present operational techniques, although a problem may exist in the final engine firing sequences when the subcooled propellant warms up to approximately 20.55° K (37° R). Detailed engine analysis accompanied by hardware testing is required to finalize engine operational efficiencies and effects on estimated propellant residuals.

*Engine performance for the RL10 engines that were used in the S-IVB/LASS and Lunar Mission Vehicle Application studies is given in Sections 3.3 and 4.3., respectively.

Technical opinions from Pratt & Whitney representatives concerning effects of solid hydrogen in the engine system were obtained, but require substantiation by analysis or test. It appears that very little erosive action, if any, will take place during engine firing, although engine operation could be impaired, resulting in hard starts, off-mixture-ratio operation, and increased ΔP. The following areas of investigation are cited to fully clarify and confirm systems analysis on both RL10 engines:

- Dead-headed slush in the inlet ducting and primarily in the "Y" duct to the engines
- Variation in throttling dual-engine combinations due to subcooled liquid and solid propellants
- "Ice-bridging" effect in cooldown valves, orifices, and igniter system utilization

2.3.2 Chilldown Pump Characteristics

The S-IVB vehicle presently uses a tank-mounted pump (PESCO Model No. 144668) for chilldown prior to engine burn. The requirement for this pump exists for the chilldown sequence in the LASS concept. The motor is of a "wet-run" design and, as such, requires circulation of liquid hydrogen through the pump motor during operation and immersion in liquid hydrogen during fill, launch hold, and ascent. Operation and output of this pump would not be affected either by exposure to, or by immersion in, slush hydrogen, although minor modifications to the impeller and housing would probably be required. Impeller vane clearances now range between 2.195 mm (0.090 in.) and 2.54 mm (0.10 in.), with a pump efficiency of approximately 60 percent. If the assumption is made that aged solid crystals are approximately 3 mm (0.120 in.) in size, then the clearance probably must be increased to reduce high breakaway torque and housing erosion. To minimize these effects, clearances should be increased to 5.09 mm (0.20 in.) and 6.34 mm (0.25 in.), respectively, resulting in a nominal decrease in efficiency to 50 to 55 percent. It will also be necessary to eliminate labyrinth passages, where they exist, to minimize the possibility of crystal adherence and buildup during static and dynamic flow. To reduce contemplated additional friction, it may be necessary

to provide nonmetallic liners or plating on the inner pump passages. This thickness can be minimal and would not cause additional pump ΔP.

The unit presently mounted outside the S-IVB tank provides an appreciable heat short to the propellant. To maintain high-quality slush in the tank, it is essential that a technique be evaluated for mounting the entire unit inside the tank. It was the manufacturer's (PESCO) suggestion that this could be readily accomplished at an early date. The present mounting flange, shown in Fig. 2-15, can be modified so that structural mounting to the internal tank wall can be accomplished during stage assembly. Electrical connections can be made through suitable cryogenic connectors and associated plumbing can then be installed. Although final systems analyses were not performed, the chilldown pump could possibly be used for recirculation during launch hold and ascent, thereby eliminating or reducing stratification in the tank. This would require a change from a two-way tank to a three-way control valve, allowing the extra port for recirculation in the tank. A second option would be to maintain the same valving, and bleed off part of the chilldown flow to the tank for circulation during the chilldown phase. In future analyses, if it appears that chilldown requirements for both the RL10A and J-2 engines would exceed the existing pump capability of 85.2×10^{-4} m^3/sec (135 gpm), uprating of the pump should include one of the above-noted recommendations regarding slush-hydrogen recirculation.

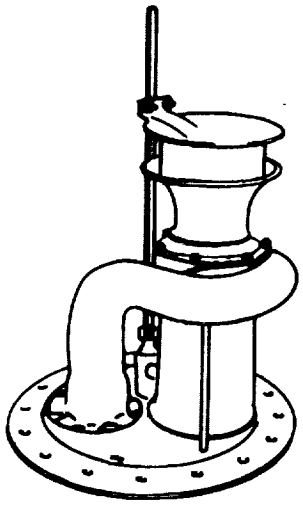

Fig. 2-15 Existing S-IVB Chilldown Pump

2.4 INSULATION STUDY

Optimization of the insulation system for a liquid-hydrogen-fueled or slush-hydrogen-fueled stage, as with any other cryogenic stage, depends upon the criterion used. For this investigation, the primary assumptions were:

- Stage payload is maximized with fixed velocity increments.
- Maximum gross stage weight is limited by booster capability.

- The hydrogen tank is vented at a saturated pressure and temperature significantly above those of the loaded propellant.
- Separate independent insulation and venting systems are employed for the oxidizer tank.

The gross stage weight can be expressed as:

$$W_G = W_{PL} + W_{IP} + W_{BO} + W_I + W_T + W_{INS} \qquad (2.39)$$

The variation in payload weight with insulation thickness can be otained by differentiating Eq. (2.39) with respect to thickness. The approximate optimum insulation thickness that corresponds to maximum stage payload weight can then be determined by equating the differentiated equation to zero and solving for the corresponding thickness. Extensive mathematical manipulation is required to do this and to incorporate the heat absorption capability of subcooled liquid or slush hydrogen. An alternative procedure was used in the study to predict the approximate optimum insulation thicknesses in preliminary analyses for each vehicle.

A more comprehensive determination of optimum insulation thickness was also obtained for each vehicle application study. This was accomplished by numerically evaluating insulation, tank, inert and boiloff weights for a number of specific insulation thicknesses. The total integrated weight index was then plotted as a function of insulation thickness to obtain the optimum and to show the effect of nonoptimum thicknesses. Secondary effects, such as tank-wall cooldown, pressurization gas heating, etc., which could not be considered in the preliminary analysis described, were included using the numerical technique.

The deviation of equations used in the preliminary optimization of insulation thickness for each study vehicle is presented in the following paragraphs. Results of the preliminary optimization using these equations and the final optimization using the numerical technique are presented in Sections 3, 4, and 5.

The weight of boiloff propellant and insulation are first-order functions of insulation thickness. Other terms in Eq. (2.39) reflect only secondary influences of thickness. The optimization technique presented here consists of equating to zero the sum of the differentials of these two weight terms with respect to insulation thickness and solving for the thickness. Also included are the effects of heating initially subcooled liquid or slush hydrogen to the final vent conditions and of venting boiloff hydrogen prior to accelerating the stage. This optimization process is only approximate, since the effects of insulation thickness on the other weight terms of Eq. (2.39) are not considered. However, a more exact solution can be obtained by subsequently adjusting the total propellant and tank weights so that they correspond to the calculated boiloff, and then recalculating the optimum thickness. This is accomplished within the constraints of a fixed gross stage weight and fixed velocity increment. Resulting boiloff propellant and insulation weight terms are then differentiated and again solved for the optimum thickness. The true optimum is obtained when further iterations produce a negligible change in thickness.

The potential to increase enthalpy from an initially subcooled liquid or slush condition to a saturated liquid condition can be equated to the actual enthalpy gain of the bulk propellant as shown by

$$XL_f + \Delta H = \left(\frac{KA\Delta T}{\delta} + Q_p\right) \sum_{j=1}^{N} \frac{\theta_j}{W_{P_j}} \qquad (2.40)$$

From Eq. (2.40), it can be seen that boiling will start at the conclusion of the N^{th} time step.

The time of initial boiling is

$$\theta_N = \frac{\phi_N}{\alpha\left(q^* + \frac{1}{\delta}\right)} - W_{P_N} \sum_{j=1}^{N-1} \frac{\theta_j}{W_{P_j}} \tag{2.41}$$

where

$$\phi_N = \frac{W_{P_N}\, BF}{A\rho_I L_v}\left(XL_f + \Delta H\right)$$

$$\alpha = \frac{K\Delta T\, BF}{\rho_I L_v}$$

$$q^* = \frac{Q_p}{KA\Delta T}$$

The total boiloff that occurs after θ_N is

$$W_{BO} = \frac{\alpha \rho_I A}{BF}\left(q^* + \frac{1}{\delta}\right)\left(\theta_M - \sum_{j=1}^{N} \theta_j\right) \tag{2.42}$$

By differentiating the boiloff and insulation weight with respect to insulation thickness, combining, and solving for thickness yields

$$\delta_{OPT} = \left\{\alpha\left[\theta_M - \sum_{j=1}^{N-1} \theta_j\left(1 - \frac{W_{P_N}}{W_{P_j}}\right)\right]\right\}^{1/2} \tag{2.43}$$

Equation (2.43) is the expression for insulation thickness that will always result in a minimum sum of insulation and equivalent boiloff weights. It provides the true optimum insulation thickness for all mission durations only if the propellant is loaded and vented

at the same enthalpy level. In such cases, all heat transferred into the propellant tank results in boiloff. This boiloff appears in Eq. (2.43) as a positive quantity, and is therefore real and permissible. However, for cases where the propellant is vented after an enthalpy gain compared to that of the loaded propellant, Eq. (2.43) is discontinuous below certain mission durations. This occurs because the resulting boiloff quantity in the discontinuous region is negative and is therefore not real or permissible.

The true optimum thickness in this region will permit heating of the propellant precisely to its boiling point at the saturated-vent conditions for any mission duration in that region. This thickness can be obtained by defining the boiling period θ_B as

$$\theta_B = \theta_M - \sum_{j=1}^{N} \theta_j = 0 \tag{2.44}$$

The expression for optimum thickness that results from combining Eqs. (2.41) and (2.44) is

$$\delta_{OPT} = \frac{1}{\dfrac{\phi_N/\alpha}{\theta_M - \displaystyle\sum_{j=1}^{N-1} \theta_j \left(1 - \frac{W_{P_N}}{W_{P_j}}\right)} - q^*} \tag{2.45}$$

The general form of the curves obtained by plotting the loci of points calculated from Eqs. (2.43) and (2.45) versus mission duration is shown in Fig. 2-16. For different initial and final propellant enthalpy conditions, the true optimum thickness is the smaller of the values given by these two equations.

The mission duration at which Eqs. (2.43) and (2.45) yield identical results is

$$\theta_M^* = \frac{2\phi q^* + 1 \pm (1 + 4\phi q^*)^{1/2}}{2\alpha q^{*2}} \tag{2.46}$$

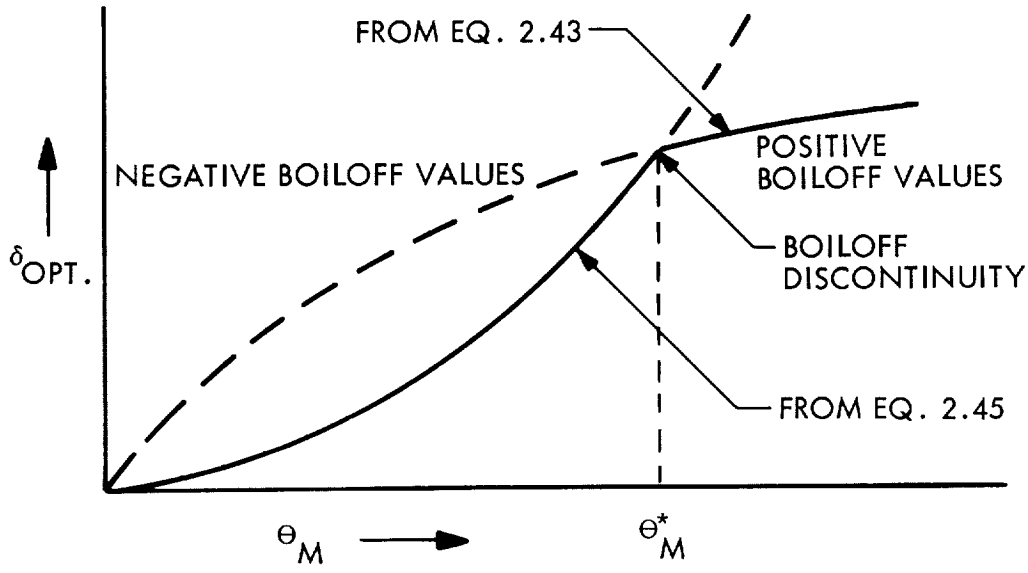

Fig. 2-16 General Solution of the Insulation Optimization Equations

2.5 VENTING STUDY

Venting of a hydrogen tank can be accomplished with either continuous or periodic (cyclic) venting. The latter technique was assumed for all analyses performed in this study. This was done to disassociate the complexities of continuous venting in low-gravity environments from the comparison of performance for various initial conditions of the hydrogen.

Equations were derived that describe the general energy balances present during periodic venting and self-pressurization cycles:

$$\overline{Q}_{vent} = \left(\overline{Q}_{\ell_1} - \overline{Q}_{\ell_2}\right) + \left(\overline{Q}_{v_1} - \overline{Q}_{v_2}\right) \tag{2.47}$$

$$\Delta\overline{Q}_{stored} = \left(\overline{Q}_{\ell_2} - \overline{Q}_{\ell_1}\right) + \left(\overline{Q}_{v_2} - \overline{Q}_{v_1}\right) \tag{2.48}$$

where

$\overline{Q}_{vent}$ = energy removed from the system during venting

$\overline{Q}_{\ell_1}$ = energy content of the initial liquid mass

$\overline{Q}_{\ell_2}$ = energy content of the final liquid mass

$\overline{Q}_{v_1}$ = energy content of the initial vapor mass

$\overline{Q}_{v_2}$ = energy content of the final vapor mass

$\Delta\overline{Q}_{stored}$ = total energy absorbed in self-pressurization of the saturated system from an initial to a final pressure

Equations (2.47 and 2.48) were expanded and solved during the study for tank sizes and a general range of initial and final cycle pressures. From this analysis, values of final liquid mass, initial vapor mass, final vapor mass in the tank, and vapor mass vented overboard were expressed in terms of initial liquid mass, initial total mass, and total tank volume for the vent cycle that was described by Eq. (2.47):

$$M_{\ell_2} = \overline{A}\, M_{\ell_1} - \overline{B}V \tag{2.49}$$

$$M_{vent} = \overline{C}\, M_{\ell_1} + \overline{D}V \tag{2.50}$$

$$M_{v_1} = M_{t_1} - M_{\ell_1} \tag{2.51}$$

$$M_{v_2} = M_{t_1} - M_{\ell_2} - M_{vent} \tag{2.52}$$

where $\overline{A}$ through $\overline{D}$ are functions of initial and final pressure.

Figures 2-17 through 2-20 present the solutions of coefficients $\overline{A}$ through $\overline{D}$ that were obtained in the analysis. They apply to any tank for the pressure range shown.

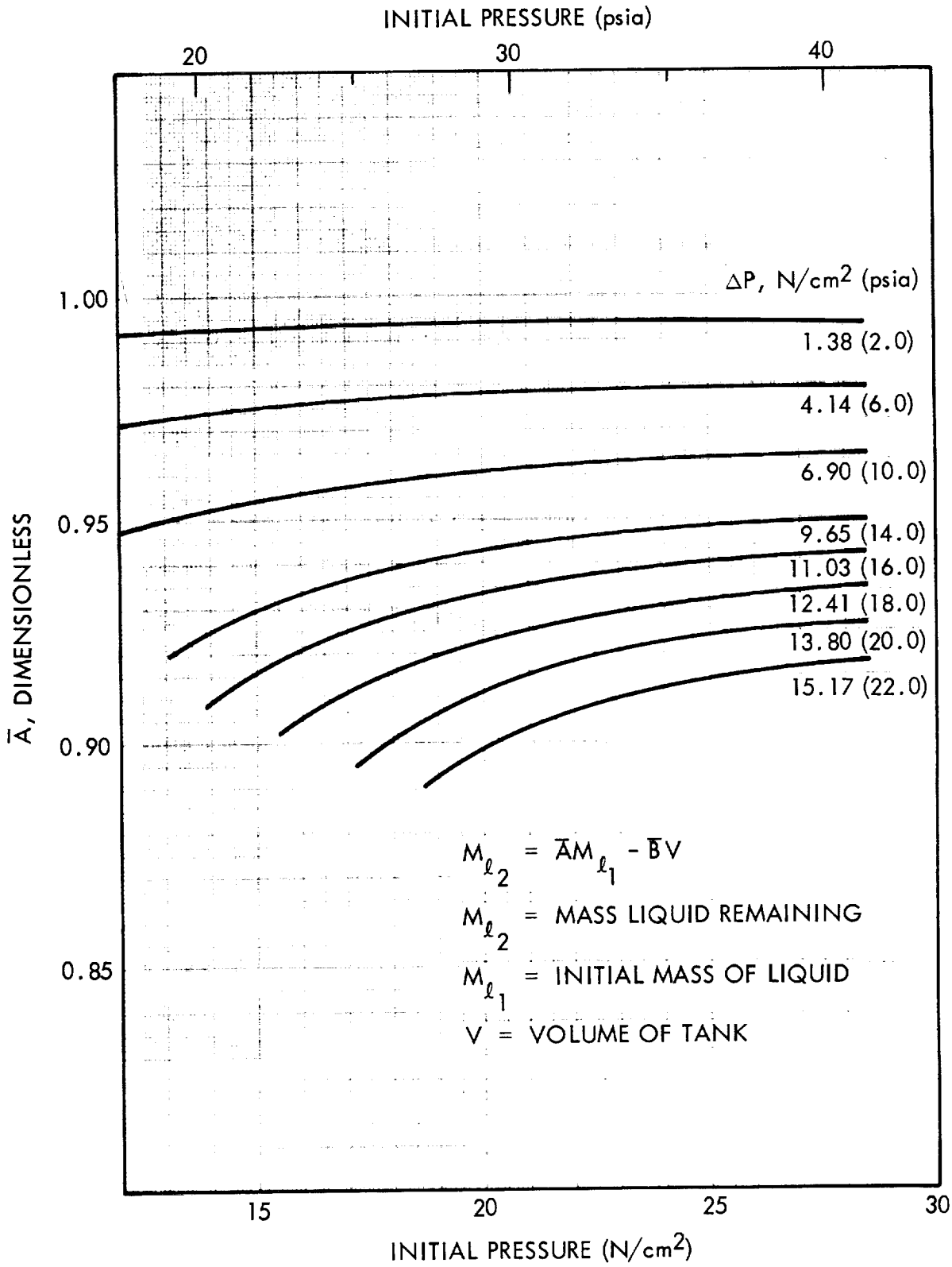

Fig. 2-17 Coefficient for Mass of Liquid Hydrogen Remaining After Vent ($\bar{A}$)

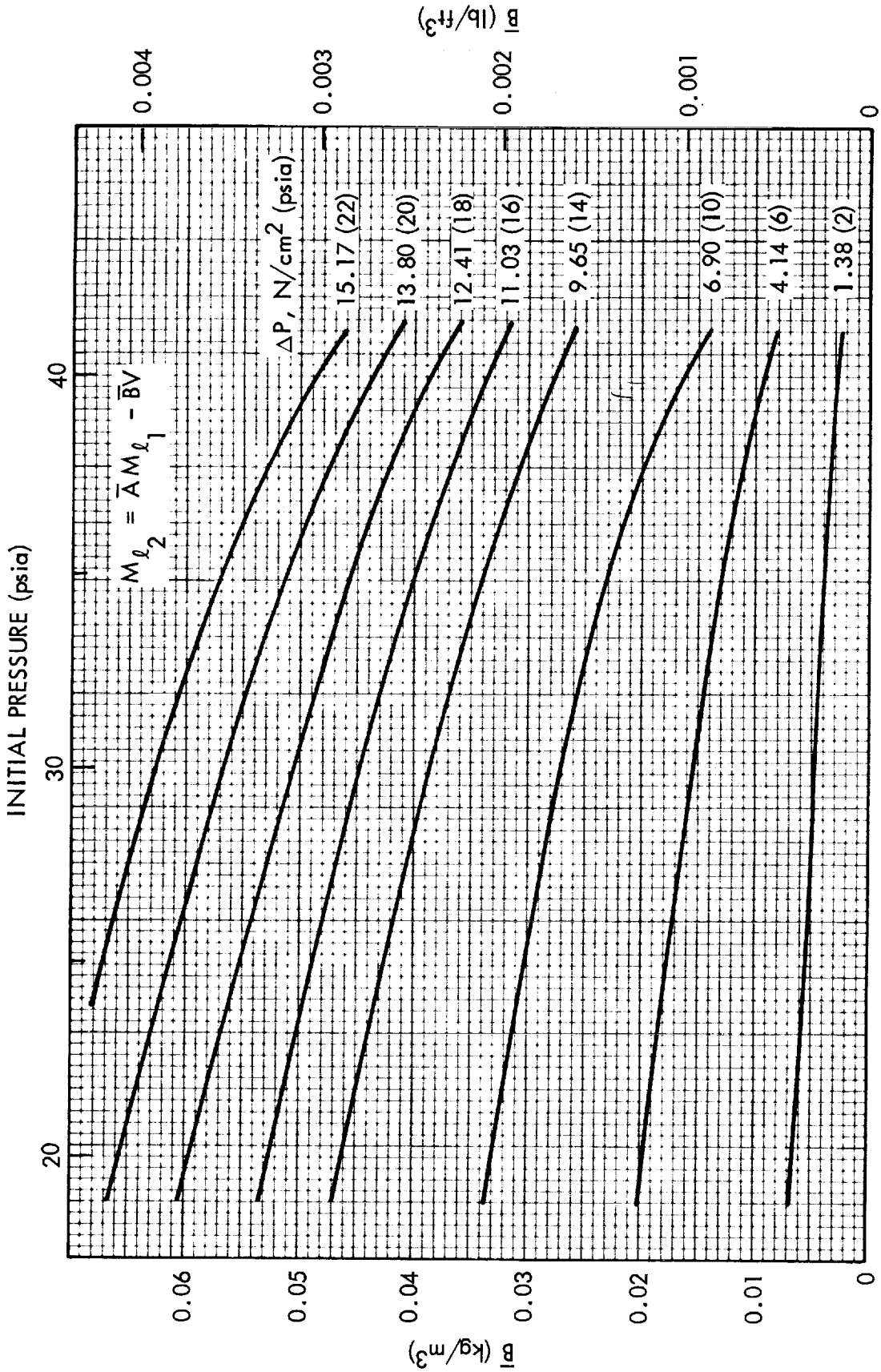

Fig. 2-18 Coefficient for Mass of Liquid Hydrogen Remaining After Vent ($\bar{B}$)

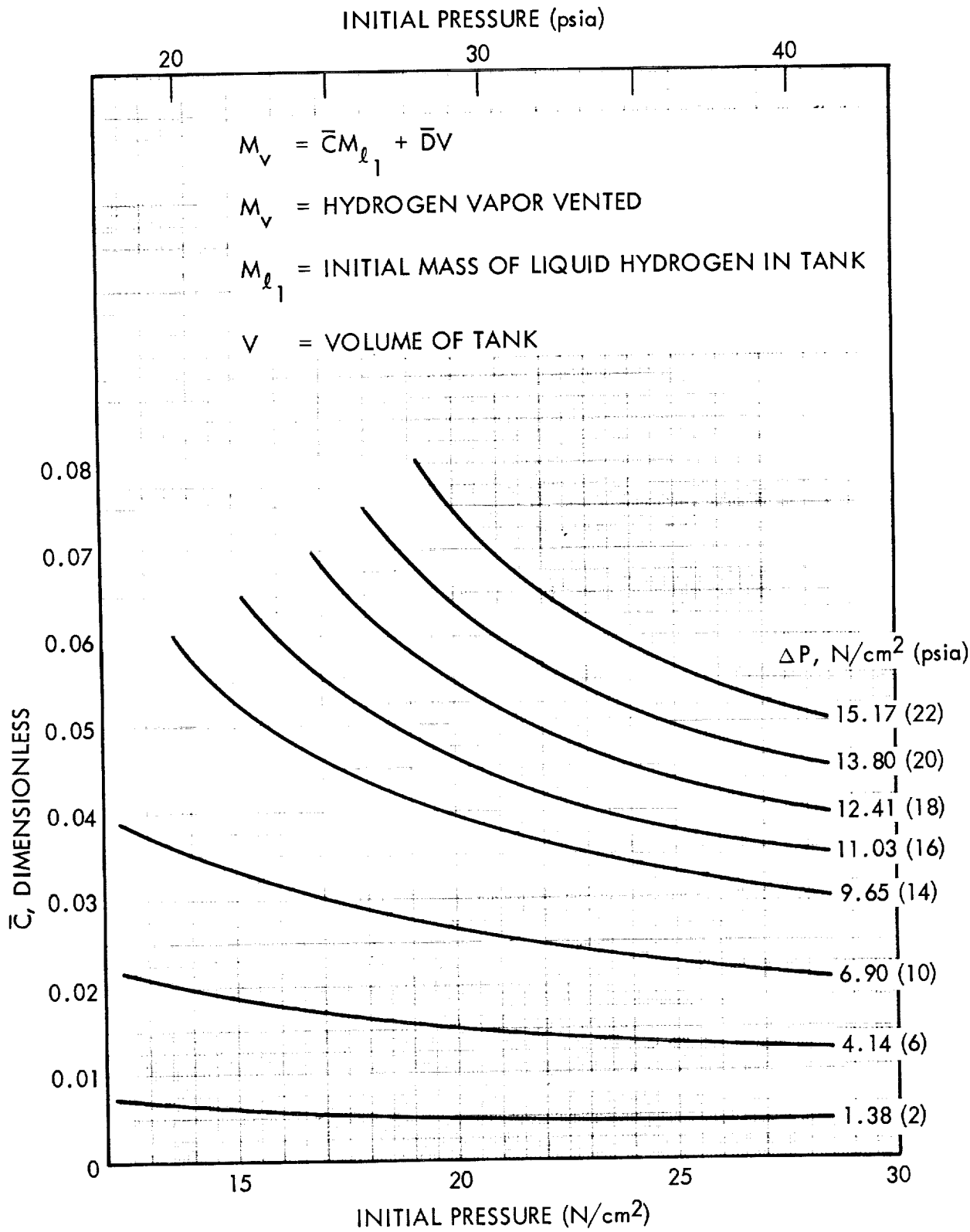

Fig. 2-19 Coefficient for Mass of Vapor Hydrogen Vented ($\bar{C}$)

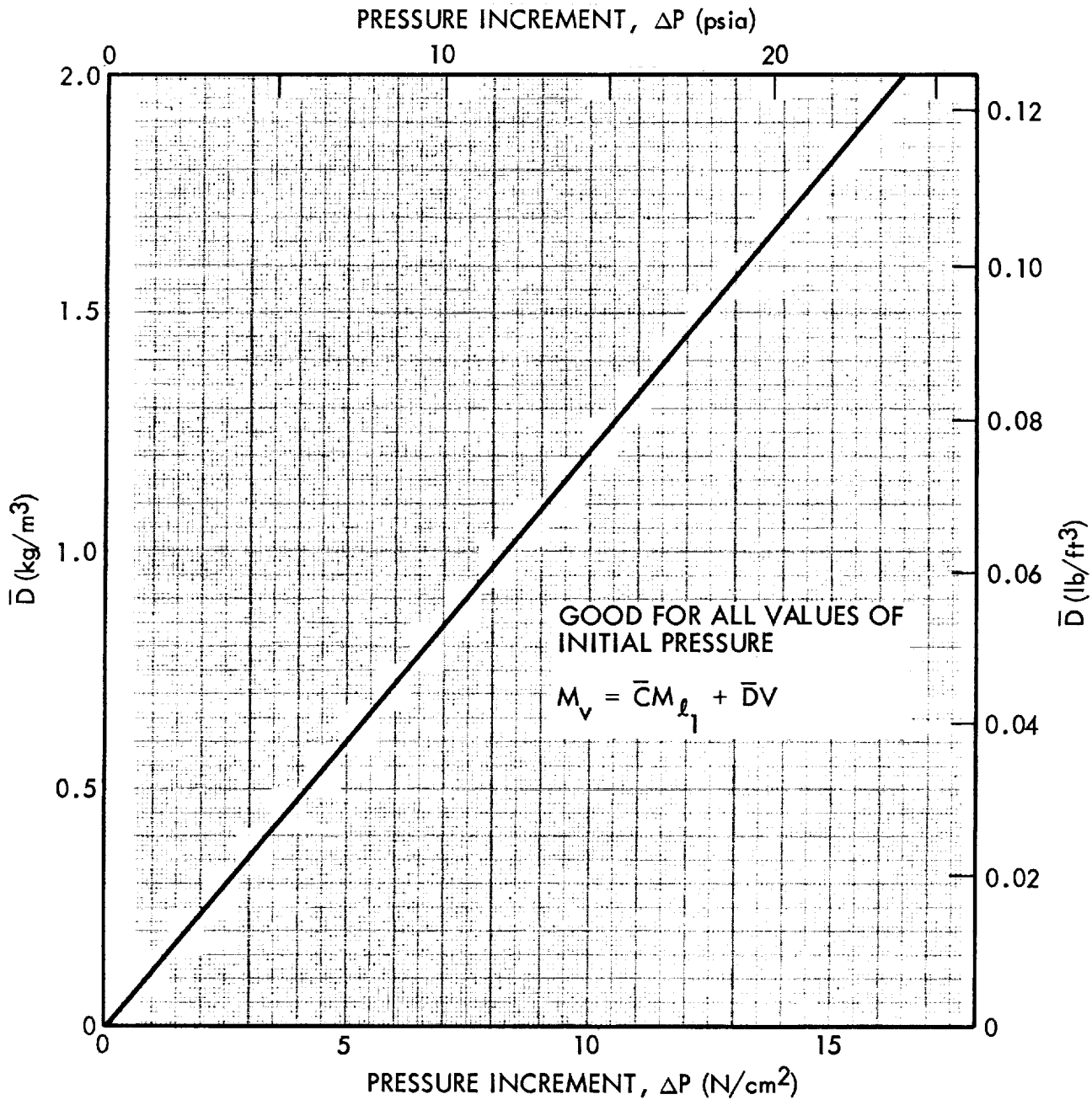

Fig. 2-20 Coefficient for Mass of Vapor Hydrogen Vented ($\bar{D}$)

Energy stored during a self-pressurization cycle, final liquid mass in the tank at the end of the cycle, and initial and final vapor masses in the tank are expressed in terms of initial liquid mass and initial total mass present at the beginning of the self-pressurization cycle described by Eq. (2.48):

$$\Delta\bar{Q}_{Stored} = \bar{E}\, M_{\ell_1} + \bar{F}V \tag{2.53}$$

$$M_{\ell_2} = \bar{G}\, M_{\ell_1} + \bar{H}V \tag{2.54}$$

$$M_{v_1} = M_{t_1} - M_{\ell_1} \tag{2.55}$$

$$M_{v_2} = M_{t_1} - M_{\ell_2} \tag{2.56}$$

where $\bar{E}$ through $\bar{H}$ are functions of initial and final pressures.

Figure 2-21 presents the solution of Eq. (2.53) that resulted from the analysis. Coefficients $\bar{E}$ and $\bar{F}$ were obtained in generating Fig. 2-21, but are not shown since the total relationship of stored energy to initial and final pressures is needed directly. This technique permits use of the figure to obtain the stored heat energy for known pressure limits, or to obtain one pressure limit if the stored heat energy and the other limit are known. Figure 2-21 applies only to the S-IVB since its particular tank volume was used in calculating the values shown.

The coefficients $\bar{G}$ and $\bar{H}$ are given by

$$\bar{G} = \left(1 - \frac{\rho_{v_1}}{\rho_{\ell_1}}\right) \Bigg/ \left(1 - \frac{\rho_{v_2}}{\rho_{\ell_2}}\right) \tag{2.57}$$

$$\bar{H} = \left(\rho_{v_1} - \rho_{v_2}\right) \Bigg/ \left(1 - \frac{\rho_{v_2}}{\rho_{\ell_2}}\right) \tag{2.58}$$

2.6 PRESSURIZATION STUDY

Systems using helium and/or hydrogen pressurants were investigated during this study program. Both pressurants were considered for initial pressurization prior to launch and for repressurization to start the engines in space. Preliminary studies indicated

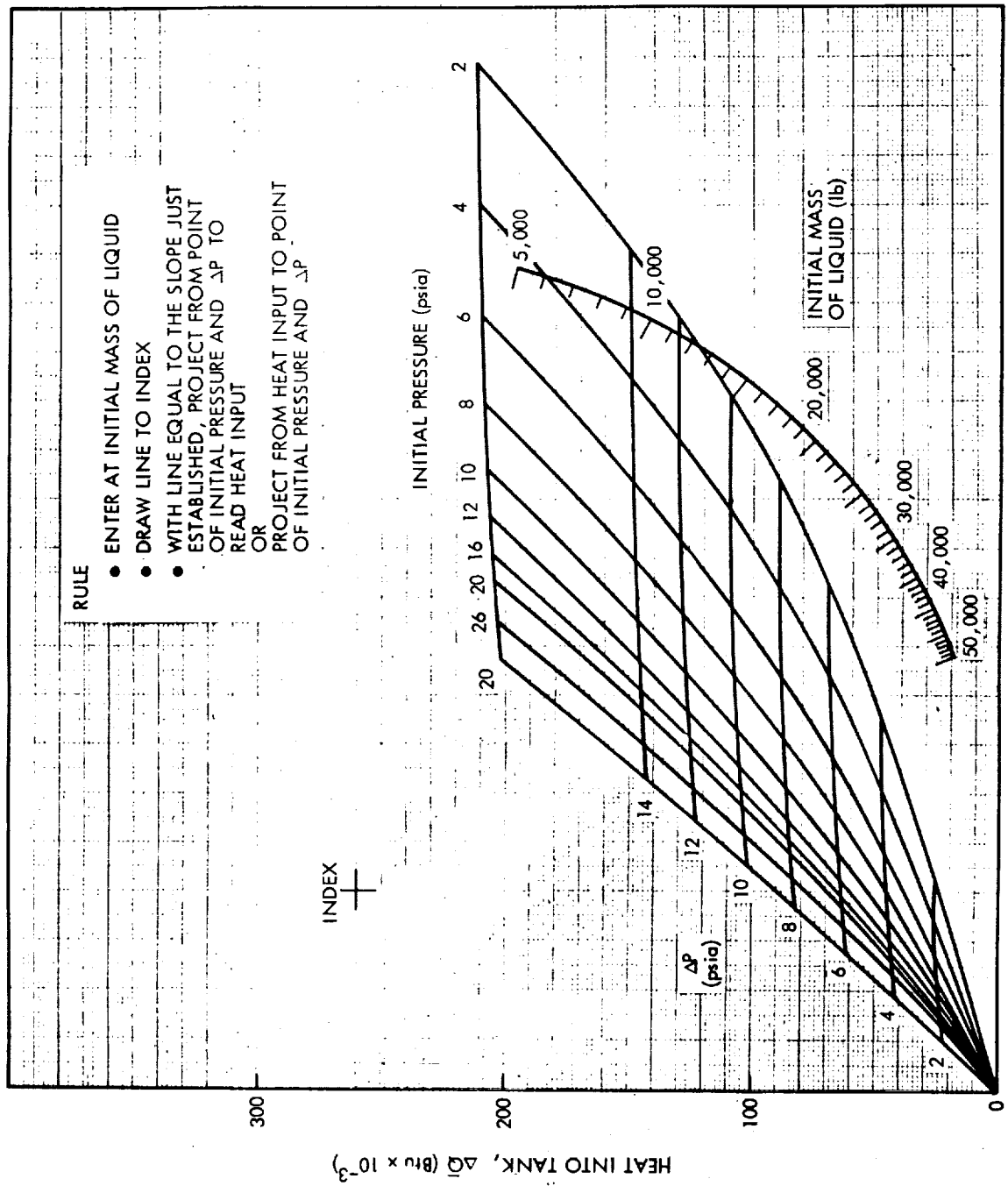

Fig. 2-21 Relationship for Heat Transfer and Pressure in the S-IVB Hydrogen Tank

that systems which use only helium pressurant for these functions are lighter and more reliable. Therefore, such systems were selected for final study analysis. However, only hydrogen pressurant systems were considered for expulsion of the fuel during engine firings because this pressurant can be obtained from engine bleed, which results in a considerable saving of hardware weight. Primary variables that affect pressurization system optimization in general are pressurant injection temperature and mode of storage.

Flight weight hydrogen tanks require that atmospheric or greater internal pressure be maintained to prevent buckling of the tank shell during ground operations and ascent. Saturated hydrogen vapor pressure for subcooled liquid or slush, which is approximately 0.7 N/cm^2 (1 psia) at the triple-point condition, is well below atmospheric pressure. Analyses performed during the study assumed use of a partial pressure of helium vapor to provide the total pressure required during ground and ascent operations.

Differences in pressurant-gas requirements resulting from use of subcooled liquid or slush hydrogen are due to the following:

- A tendency toward greater condensation (hydrogen pressurant only) on the liquid surface
- Additional pressure drops in the system unique to the slush condition
- A necessity to start the engines early in the mission when the saturated hydrogen vapor pressure is substantially below the tank pressure required to start (mission dependent)
- A smaller volume per unit-mass-expulsion-rate requirement due to increased density of the subcooled fuels

2.6.1 Increased Condensation Rates for Hydrogen Pressurants

The first consideration, that of higher condensation rates (or reduced evaporation), has been previously investigated (Refs. 2-3, 2-4, and 2-5) analytically and experimentally. Results of these investigations are applicable to systems that use subcooled hydrogen propellant.

In terms of increased system weight, the penalties are more significant for pressurization of an ullage with hydrogen vapor for engine startup than for expulsion,

because the vapor for startup normally would be stored in an ambient storage bottle, while for expulsion it comes from engine bleed. The hardware weight required to store hydrogen vapor at ambient conditions can be significant, while engine bleed is essentially free.

Results of Computer Analysis. Typical values of mass transfer at the interface during engine firing are presented in Fig. 2-22. Predicted values were obtained from the Rocketdyne pressurization computer program for the translunar firing of the S-IVB/LASS mission. Results show a slightly larger mass evaporated for the saturated liquid case than for the triple-point liquid or slush case. The difference in pressurant gas required is negligible for vehicle performance considerations. The total pressurant gas weight for the translunar firing expulsion is approximately 73 kg (160 lb).

Results of Other Analyses. The model chosen to study condensation prior to application of the Rocketdyne computer code was selected after a literature search. This model is conservative in that it predicts a larger mass transfer than would occur. The selected model assumes that the liquid and vapor exist initially at some uniform temperature. At time zero, the pressure is suddenly raised by the introduction of pressurant gas into the upper region of the ullage. A higher uniform temperature is assumed to result from adiabatic compression of the ullage gas.

The analysis used in the application of this model was derived by Thomas and Morse (Ref. 2-3). Essentially, separate solutions of transient heat conduction equations for the liquid and vapor were coupled by boundary conditions at the traveling interface. The resulting pair of coupled second-order partial differential equations were then simplified. A pair of ordinary second-order differential equations resulted which have for their solution the real root of a transcendental equation. To avoid the difficulties of a numerical solution, an approximate polynomial solution (Ref. 2-3), based on the idealization of a thermal boundary layer thickness, was developed. Subsequently, a computer program was developed by Olsen (Ref. 2-4) to solve the transcendental equation. An alignment chart that permits a graphic solution of the transcendental equation was then developed by O'Loughlin (Ref. 2-5). The results presented in the following paragraphs were obtained with the aid of this alignment chart.

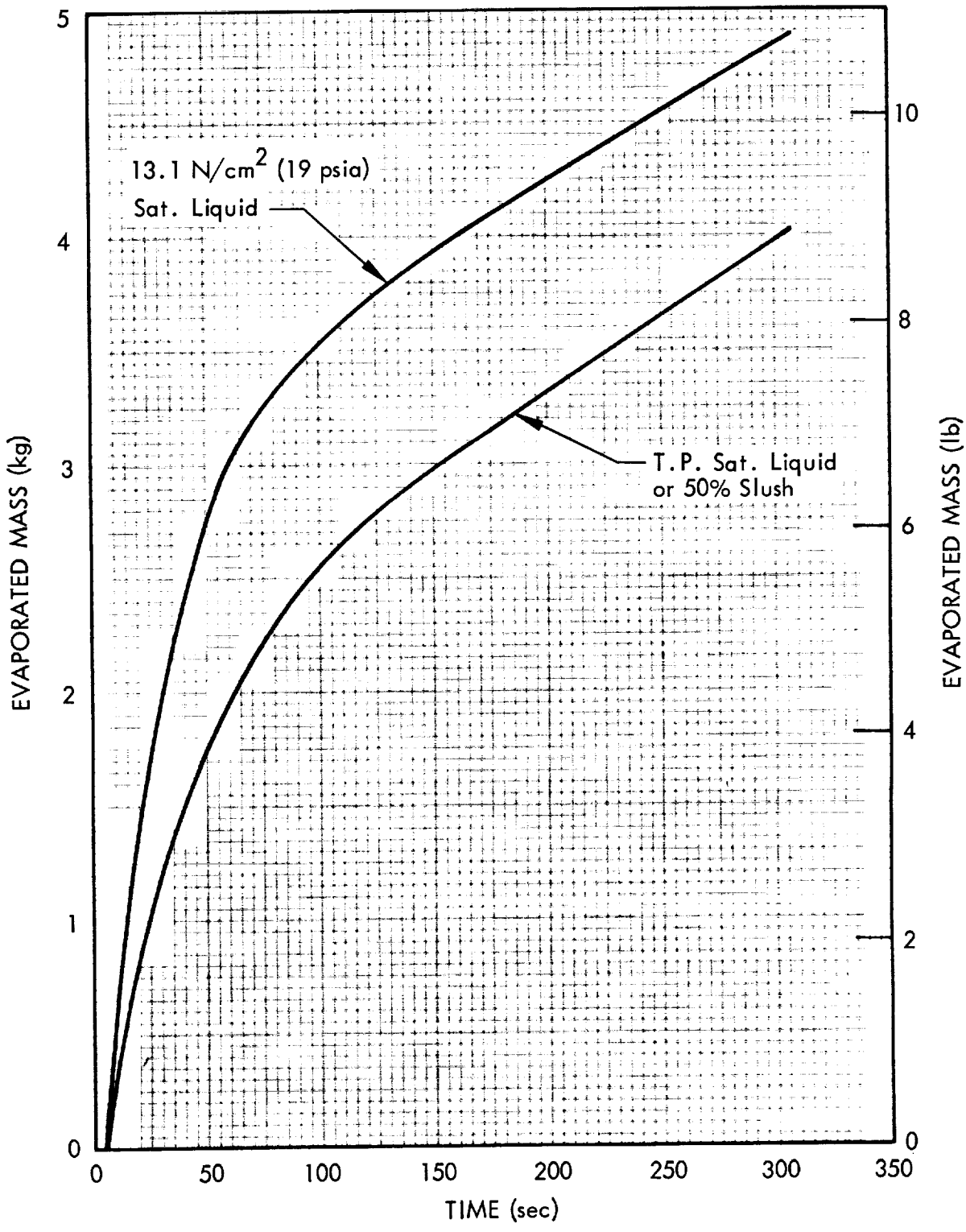

Fig. 2-22 Comparison of Interface Evaporation Rates During Translunar Injection Firing of the S-IVB/LASS for Various Liquid Conditions

From the solution a bulk gas temperature, T_3^* may be determined such that there is no net mass transfer at the interface. For bulk gas temperatures greater than T_3^*, evaporation will result; for temperatures less than T_3^*, condensation will occur.

With a diffuser in the tank inlet so that little or no mixing occurs, the bulk gas temperature will correspond closely to the adiabatic compression temperature T_{Ad}. This will, in general, be much lower than either the inlet temperature or T_3^*. Therefore, mixing of the ullage gas will be desirable in most cases because this will result in higher temperatures near the interface, along with reduced condensation. Such results have been verified by tests referred to in Ref. 2-4.

The relations for T_3^* and T_{Ad} are as follows:

$$\frac{T_3^* - T_2}{T_2 - T_1} = \sqrt{\frac{(k\rho C_p)_\ell}{(k\rho C_p)_v}} \tag{2.59}$$

$$\frac{T_{Ad}}{T_1} = \left(\frac{P_2}{P_1}\right)^{\frac{\gamma - 1}{\gamma}} \tag{2.60}$$

These two temperatures are listed in Table 2-1 for four specific conditions. Note the large effect of the initial liquid temperature on T_3^*.

Table 2-1

BULK PRESSURANT GAS AND ASSOCIATED ADIABATIC COMPRESSION TEMPERATURES

T_1, °K (°R)	P_2, N/cm^2 (psia)	T_3^*, °K (°R)	T_{Ad}, °K (°R)
13.84 (24.9)	11.7 (17)	135.7 (244)	53.9 (97)
13.84 (24.9)	19.3 (28)	140.1 (252)	43.9 (79)
20.35 (36.6)	11.7 (17)	28.4 (51)	27.2 (49)
20.35 (36.6)	19.3 (28)	58.4 (105)	21.7 (39)

The solution obtained from the alignment chart is given in terms of three constants which are defined as follows:

$$C1 \equiv \sqrt{\rho_v k_v C_{P_v} \frac{C_{P_\ell}}{\rho_\ell k_\ell}} \frac{T_2 - T_3}{L_v} \tag{2.61}$$

$$C2 \equiv \frac{C_{P_\ell} (T_2 - T_1)}{\sqrt{\pi}\, L_v} \tag{2.62}$$

$$C3 \equiv \sqrt{\frac{\rho_\ell k_\ell C_{P_v}}{C_{P_\ell} \rho_v k_v}} \tag{2.63}$$

The solution is facilitated by breaking down these groups into subgroups involving just liquid or vapor terms. The vapor terms in Eqs. (2.61 and 2.63) are grouped as follows:

$$C1_v \equiv \sqrt{\rho_v k_v C_{P_v}} \tag{2.64}$$

$$C3_v \equiv \sqrt{\frac{C_{P_v}}{\rho_v k_v}} \tag{2.65}$$

Making use of the ideal gas law yields:

$$C1_v = P_2^{1/2} \sqrt{\frac{k_v C_{P_v}}{RT}} \tag{2.66}$$

$$C3_v = P_2^{-1/2} \sqrt{\frac{C_{P_v} RT}{k_v}} \tag{2.67}$$

The properties and temperatures in Eqs. (2.66 and 2.67) should be evaluated at the arithmetic average between T_2 and T_3. A group common to C1 and C3, which involves only liquid properties, is defined as C_ℓ and is

$$C_\ell \equiv \sqrt{\frac{\rho_\ell k_\ell}{C_{P_\ell}}} \tag{2.68}$$

C_ℓ should be evaluated at the mean of T_1 and T_2. The heat capacity in the parameter C2 should be evaluated at the average of T_1 and T_2, whereas the latent heat of vaporization in both C1 and C2 should be evaluated at T_2. For a set of property groups C1, C2, and C3, the alignment chart yields a dimensionless mass transfer parameter Z such that

$$M = \frac{a dM}{d\theta} = -a\rho_\ell \sqrt{\frac{\alpha_\ell}{\theta}}\ Z \tag{2.69}$$

and

$$M = a\int_0^\theta \frac{dM}{d\theta}\, d\theta = -2\rho_\ell a\sqrt{\alpha_\ell \theta}\, Z = -2C_\ell \sqrt{\theta}\, Z a \tag{2.70}$$

If the rate of mass transfer is desired, then Eq. (2.69) is used. The total mass transferred from time zero is given by Eq. (2.70).

Values of the parameter Z were determined for four systems as a function of the gas temperature in the vicinity of the interface. The four systems consist of liquid initially at temperatures of 13.803° K (24.85° R) and 20.35° K (36.6° R), which are suddenly pressurized to 11.7 N/cm^2 (17 psia) and 19.3 N/cm^2 (28 psia). The product of $2ZC_\ell$ is plotted in Fig. 2-23 for the four systems. Note that for the lower pressurant temperatures, the mass transfer is predominately condensation with 13.803° K (24.85° R) liquid and evaporation with the 20.35° K (36.6° R) liquid.

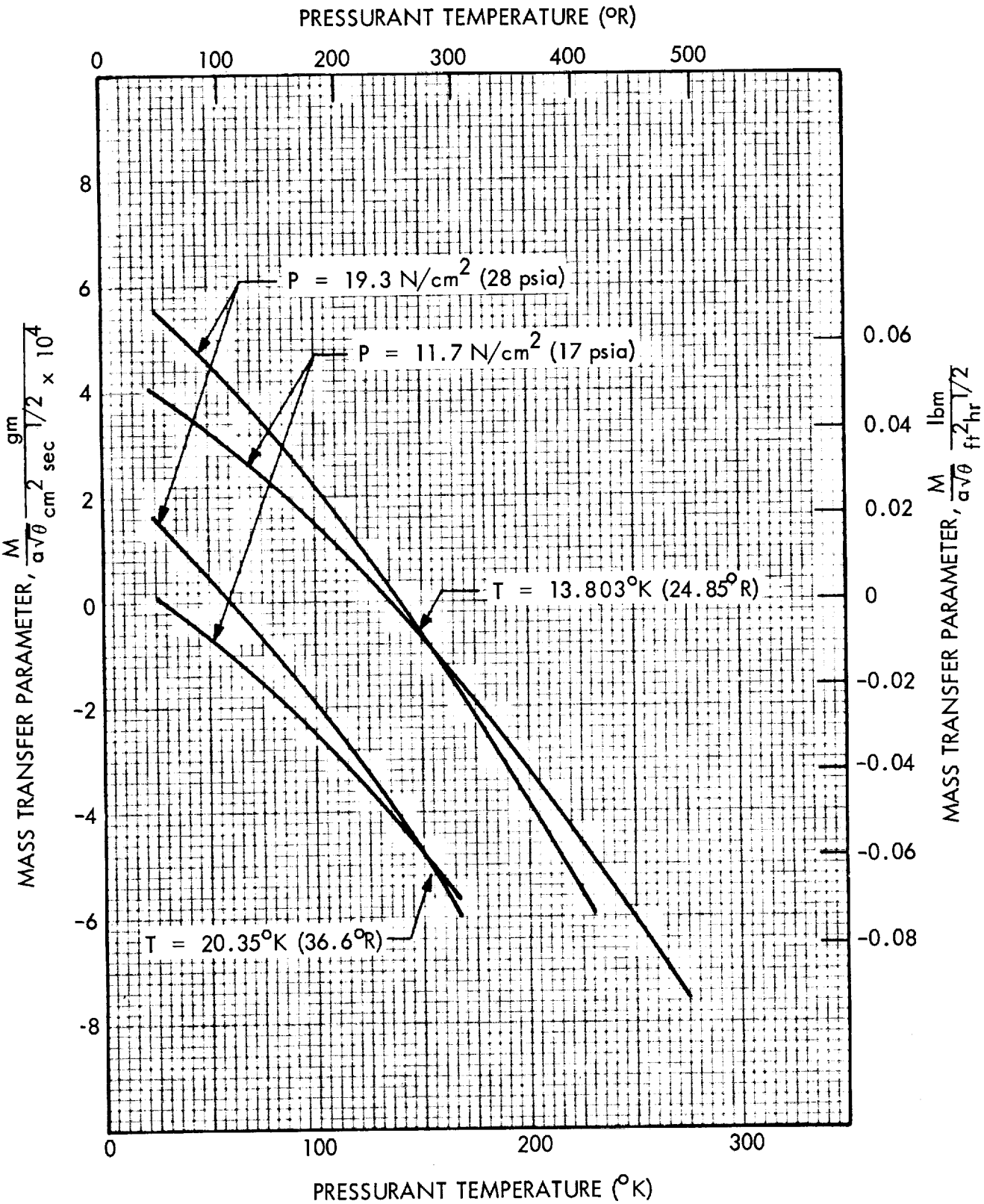

Fig. 2-23 Mass Transfer in a Suddenly Pressurized Hydrogen Liquid-Vapor System

To make use of Fig. 2-23 for a specific design, the temperature of the gas near the interface must be specified. However, to be conservative, the adiabatic compression temperature was used for T_3. Using the result from Fig. 2-23 for $T_3 = T_{Ad}$, the total quantity of mass transferred is plotted as a function of time in Fig. 2-24.

The magnitude and direction of the mass transfer in a suddenly pressurized saturated hydrogen system are quite sensitive to the bulk liquid temperature, as shown above. These effects can be summarized as follows:

- For a liquid hydrogen system initially saturated at 20.35°K (36.6°R), condensation is predicted at the liquid-vapor interface when hydrogen pressurant is introduced at a temperature of approximately 27.8° to 55.6°K (50° to 100°R), or below (depending on the final pressure). Evaporation is predicted at this interface for higher pressurant temperatures.
- For a triple-point liquid or slush hydrogen system initially saturated at 13.803°K (24.85°R), condensation is predicted at the interface when hydrogen pressurant is introduced at a temperature of approximately 139°K (250°R) or below. Again, evaporation is predicted for higher pressurant temperatures.

When the bulk gas temperature after pressurizing is conservatively assumed to be equal to the adiabatic compression temperature, it can be seen that condensation will occur at the interface for system initially saturated at 20.35°K (36.6°R) or 13.803°K (24.85°R). However, the magnitude of condensation is much greater for the 13.803°K (24.85°R) system. For example, in 0.1 hr, the predicted mass condensed per unit of interface area is 76.2 gm/cm^2 (0.168 lb/ft^2) for 13.803°K (24.85°R) liquid or slush compared to 25.6 gm/cm^2 (0.0565 lb/ft^2) for 20.35°K (36.6°R) liquid if both were initially saturated and then pressurized to 19.3 N/cm^2 (28 psia). This condensed quantity is three times greater for 13.803°K (24.85°R) systems, and becomes approximately 13 times greater if both initially saturated systems were pressurized to 11.7 N/cm^2 (17 psia) rather than 19.3 N/cm^2 (28 psia).

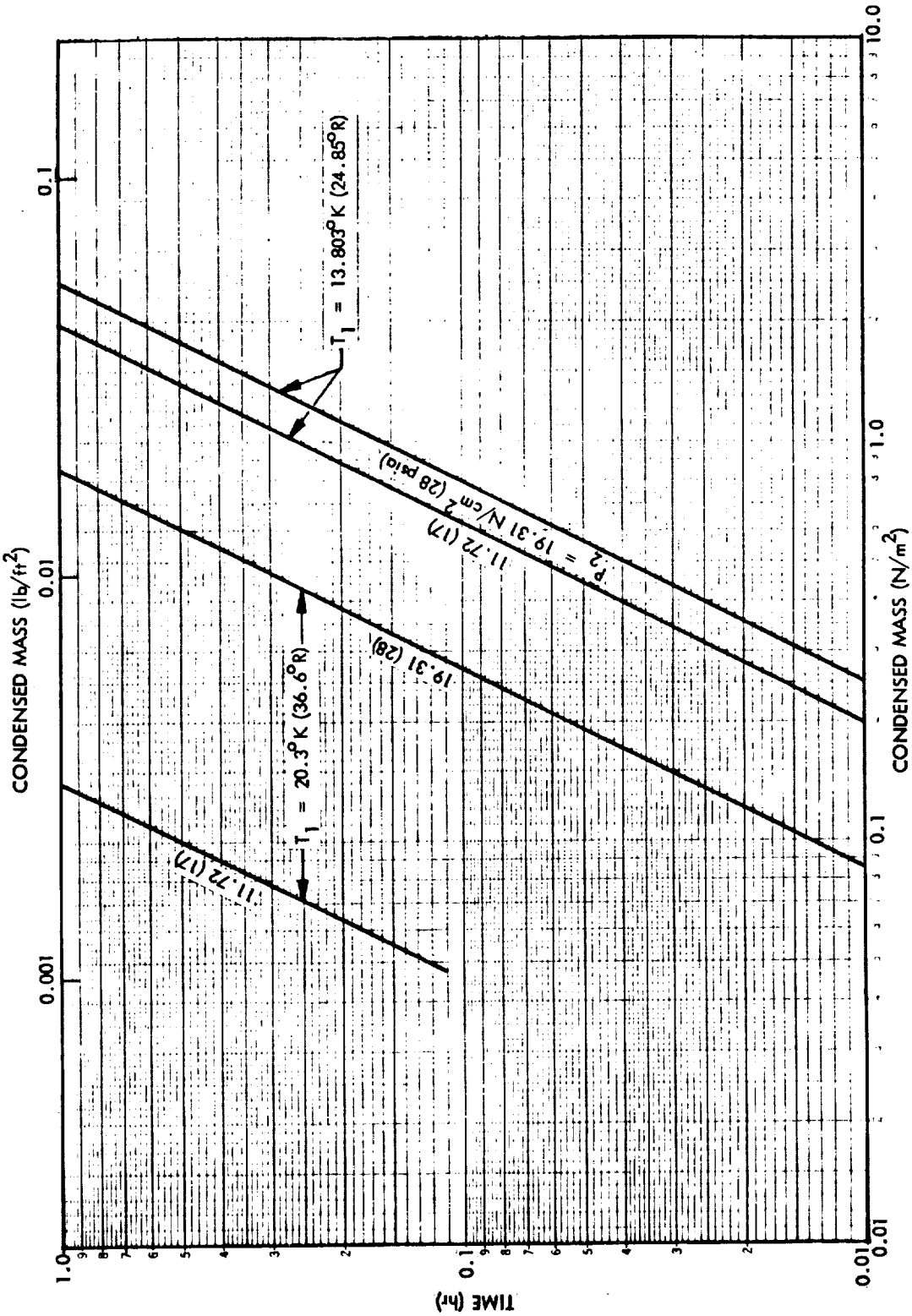

Fig. 2-24 Mass Transfer With $T_3 = T_{Ad}$

2.6.2 Additional Pressure Drops in Slush Systems

Additional pressure drops in a system using slush hydrogen result from the following:

- Presence of a screen on strainer that is being used to prevent solids from entering the engine
- Draining of liquid through the solids

These small additional pressure drops will result in a requirement for a higher ullage pressure only if the pressure delivered at the pump is to be maintained at a fixed value. If the pressure requirements can be modified at the pump inlet, a penalty will not result. Cavitation of the liquid entering the pump is not a problem because the liquid would be highly subcooled.

These additional pressure drops are estimated to be very small; however, they have not been quantitatively evaluated because of the lack of appropriate experimental data.

2.6.3 Increased Pressurant Requirements Due to Low Hydrogen Vapor Pressure

The third consideration, unlike the first two, is highly mission dependent. If an engine firing is required comparatively early in the mission when the low hydrogen vapor pressure results in a low total ullage pressure, a large incremental pressure requirement exists for pre-pressurization. The ullage pressure history shows this case for the first midcourse correction firing for the S-IVB/LASS mission. This is discussed in detail in Section 3. These studies indicate that other S-IVB/LASS mission events are not penalized because of low vapor pressure, since the propellant has had sufficient time to heat before the next major event, which is lunar braking.

2.6.4 Effect of Increased Density of Subcooled Hydrogen

The final effect which was investigated is that due to differences in propellant density. Since triple-point liquid and slush hydrogen have higher densities than saturated liquid, their volumentric flow rates are reduced during an engine firing, and pressurant

requirements are correspondingly reduced, given a fixed mass of expelled propellant. That is, the pressurant mass per pound of propellant expelled is reduced for hydrogen in the triple-point liquid and slush condition.

A comparison of pressurant requirements for saturated liquid, triple-point liquid and slush (applicable when the solids are screened out) during translunar firing of S-IVB/LASS is presented in Fig. 2-25. These results, obtained using the Rocketdyne program, include the effects of heat exchange with the tank walls and the internal insulation, two-component gas diffusion (helium and hydrogen) in the ullage space, and mass and heat transfer at the interface. The results show the combined and opposing effects of less evaporation at the interface (shown in Fig. 2-22) and lower volumetric flow rate for the subcooled condition.

Inspection of these results shows that the effect of lower volumetric flow rate (greater subcooled density) dominates and that less pressurant gas is required during translunar firing for subcooled liquid and slush.

2.6.5 Summary of Results

The following observations are based on analyses performed during the study:

- Pressurant required for use of subcooled hydrogen can be less than for saturated liquid hydrogen under some conditions, e.g., the translunar injection firing of the S-IVB/LASS vehicle.
- Repressurization requirements for engine starts early in a mission may lead to large increases in the total pressurant requirement. This is shown by the requirements of first midcourse correction for the S-IVB/LASS vehicle. The Lunar Mission Vehicle, on the other hand, does not require increased pressurant because the engine firings do not occur until late in the mission, when the propellant vapor pressure has increased to near its maximum value.
- In general, the effects of condensation (or reduced evaporation), liquid density, and additional pressure drops unique to the subcooled condition appear to be minor. The primary effects are mission unique.

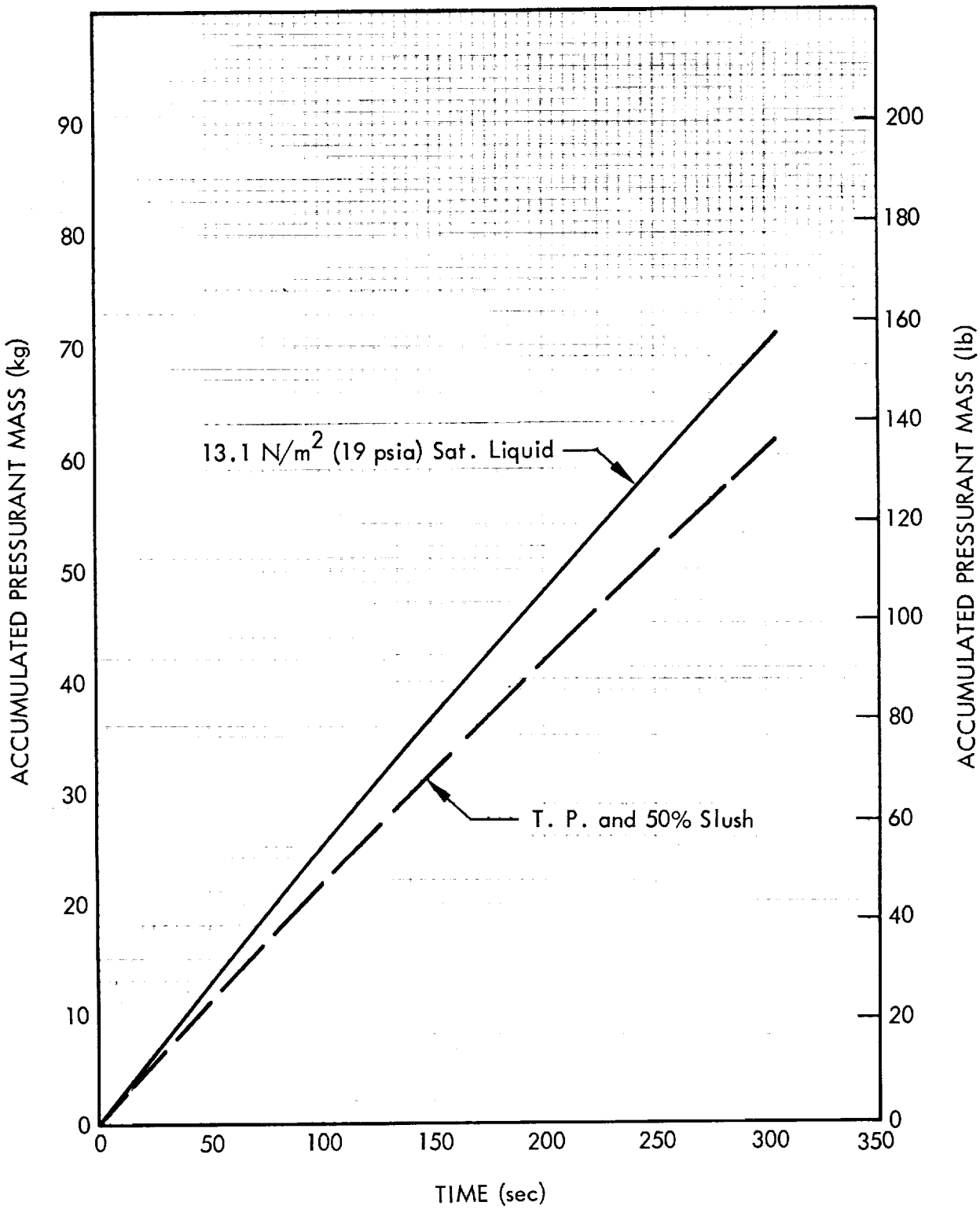

Fig. 2-25 Accumulated Mass of Pressurant Required for S-IVB/LASS Translunar Injection Firing

2.7 COMPUTER-CODE CORRELATIONS

Behavior of helium vapor and hydrogen solid, liquid, and vapor components in the fuel tank of hydrogen-fueled vehicles is extremely complex. However, an understanding of fundamental behavior characteristics is a prerequisite for investigations of propellant management and pressurization systems such as those performed during this study program. Therefore, computer-code correlations were used to substantiate trends, effects, and conclusions obtained from the analyses of these systems. A discussion of the codes used and the major results of their use is given below.

2.7.1 Stratification Flow-Model Code Application

Solid-particle settling, natural convection in the boundary layer, and mass and energy balances resulting in stratification within a liquid-solid hydrogen mixture were studied using a modified version of the "Asymmetric Nuclear Heating Computer Program" (Ref. 2-6). Modifications to the program were accomplished using Lockheed Independent Development funds in support of the contract study. Application of the modified program was funded within the contract budget.

To reduce the time required to modify the existing program, certain features not required for immediate slush studies were stripped out before the modifications were made. Therefore, the stripped version of the program, which was then modified and used to study slush effects, does not include nuclear heating in the bulk or boundary layer, asymmetric wall heating, or variable wall heating.

The modified computer code was applied to studies of propellant behavior during ground hold, launch, and ascent. Environmental characteristics and tank geometry typical of the three study vehicles were used in these computer studies.

Significant conclusions arrived at as a result of the computer studies include the following:

- Settling of the solids will occur within a few minutes after tank fill or when recirculation is terminated.

- Stratification of the surface liquid layers is considerably greater for initially subcooled liquid or liquid-solid mixtures than for initially saturated liquid under a pressure of approximately one atmosphere.

These effects are shown in Fig. 2-26 using the Saturn S-IVB as an example. Data are presented for time = 0 (mixed model) and time = 750 to 800 sec (engine firing).

2.7.2 Rocketdyne-Epstein Pressurization Code Application

Correlation of study results from application of the stratified flow model and the Rocketdyne-Epstein pressurization code shows that the latter program is better suited for studies of ullage gas behavior and pressurization requirements. Therefore, the Rocketdyne code was used in the pressurization studies as discussed in subsection 2.6.

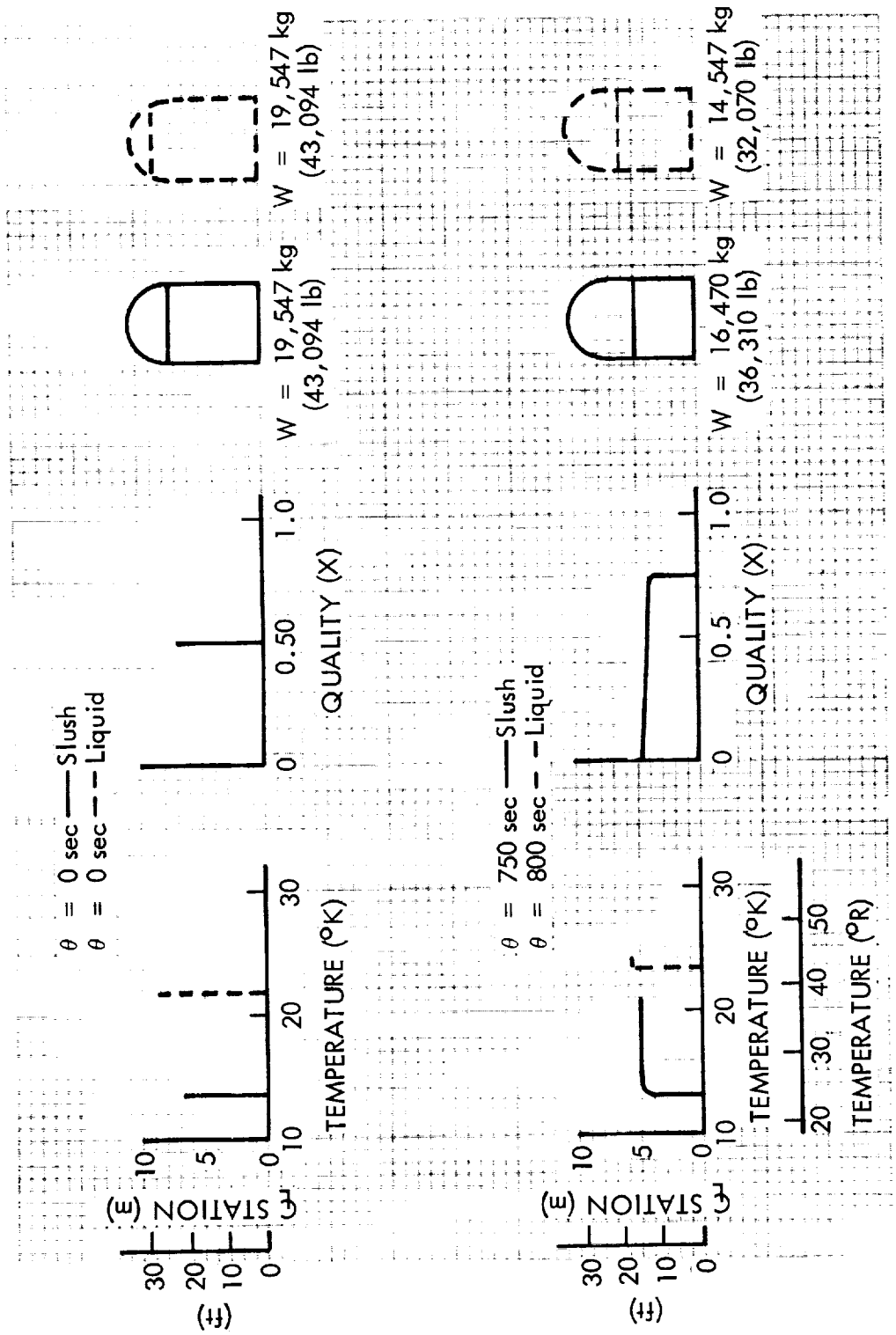

Fig. 2-26 S-IVB/LASS Bulk Fluid Temperature and Solids Distribution

Section 3
SATURN S-IVB APPLICATION STUDIES

3.1 VEHICLE/MISSION CHARACTERISTICS

An advanced lunar logistics mission was specified by MSFC for S-IVB application studies during this contract program. This vehicle/mission concept was originally defined by Douglas Missiles and Space Systems Division of Douglas Aircraft Company in a previous effort. The final report of the Douglas work, entitled "Lunar Applications of a Spent S-IVB/IU Stage (LASS)," was taken as the baseline reference for this study (Ref. 3-1).

The baseline vehicle is fueled with liquid hydrogen initially saturated at 13.1 N/cm^2 (19 psia). Figure 3-1 shows the vehicle configuration selected by Douglas. The mission profile specified in that work was modified for this program to permit a better comparison of resulting performance with that from the Lockheed MIMOSA studies for MSFC (Ref. 3-2).

Existing Saturn V/S-IVB/IU vehicles require a number of significant modifications to perform the LASS mission using saturated liquid hydrogen. Figure 3-2, reproduced from the Douglas report, shows the most significant of the modifications which were investigated in their work. Some additional changes are required to effectively use subcooled liquid or slush hydrogen with this vehicle/mission concept. A summary of modifications which apply to S-IVB/LASS vehicles fueled with hydrogen at all initial conditions is presented below. Items which apply to a particular initial hydrogen condition are so noted:

- Installation of two RL10A-3-7 engines, including gimbal systems and plumbing, to supplement the J-2 engine
- Installation of a four-leg landing gear, including cables, deployment mechanisms, and a hydraulic system

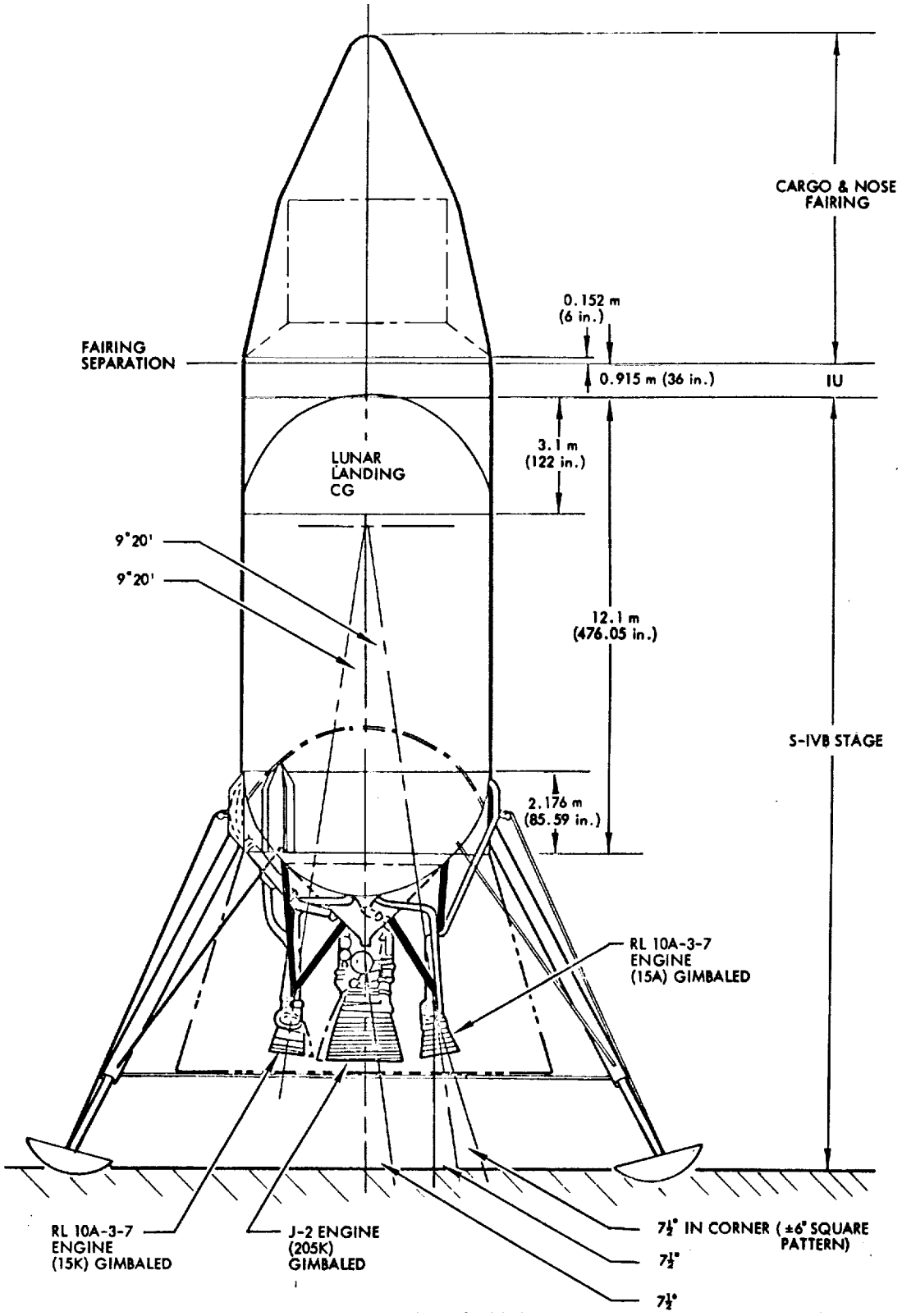

Fig. 3-1 Selected Saturn S-IVB/LASS Vehicle Configuration (from Douglas Report 56365P, ref. 3-1)

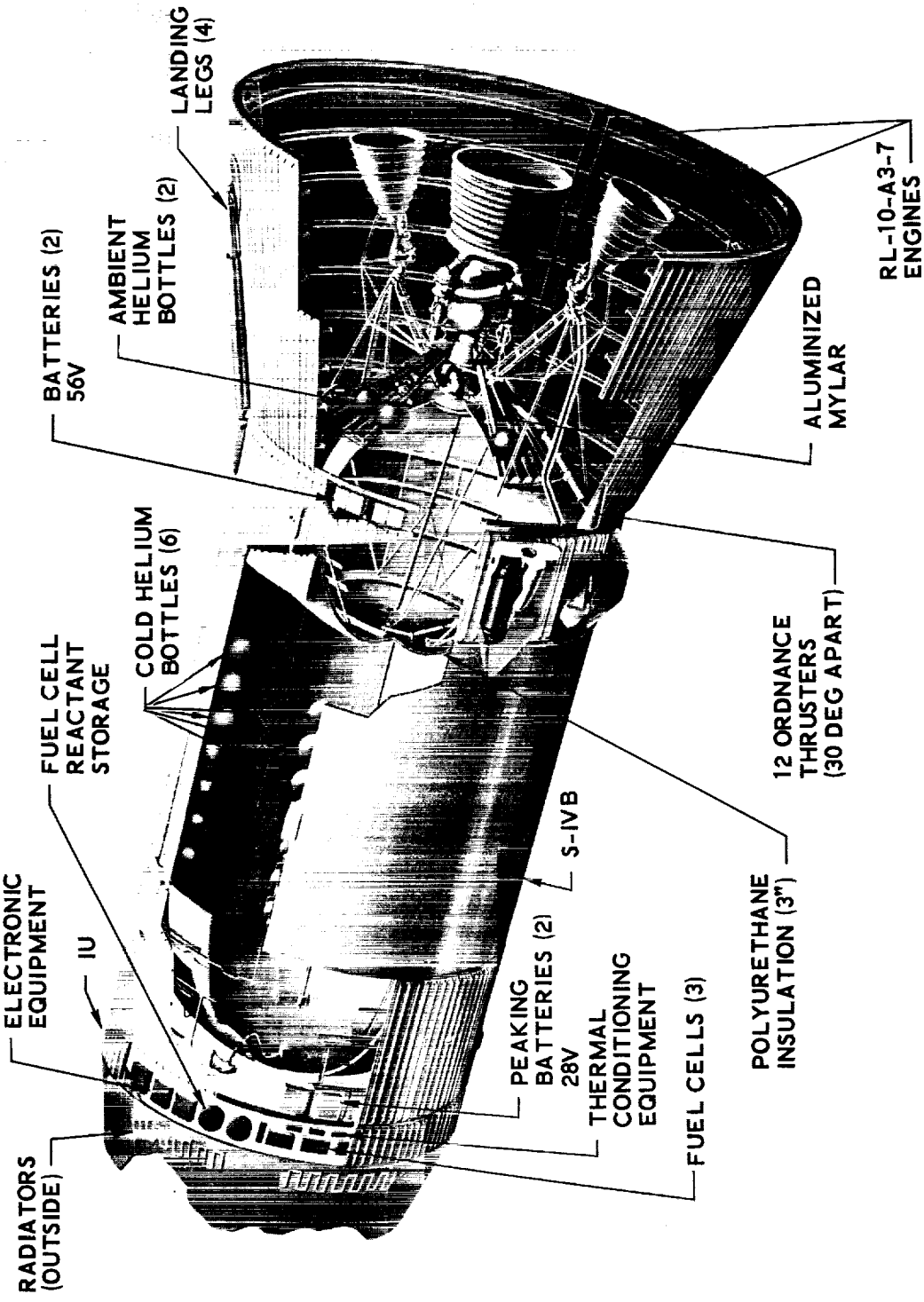

Fig. 3-2 Saturn S-IVB Vehicle Modified for LASS (from Douglas Presentation PP 147, Ref. 3-4)

- Installation of polyurethane foam insulation on the common tank bulkhead
- Installation of an aluminized Mylar multilayer insulation blanket on the engine thrust cone
- Installation of additional cold helium bottles for pressurizing the O_2 and H_2 tanks (number varies with initial hydrogen condition)
- Installation of additional ambient helium (or hydrogen) bottles to provide H_2 tank pressurant for secondary firings, and additional helium bottles for pneumatic valve service
- Installation of structural supports for the RL10 engines, additional helium bottles, and other additional equipment
- Installation of additional power, electronics, and thermal conditioning equipment in the Instrument Unit (IU) and Auxiliary Propulsion System (APS) modules
- Deletion of two existing 320-N (72-lb) thrust ullage rockets from the APS modules
- Modification of the existing S-II stage separation system
- Installation of a liquid-return line, for the slush-fueled vehicle only, and additional instrumentation and wiring for both the subcooled liquid- and slush-fueled vehicles

As noted above, the LASS mission profile selected for this study was modified from that proposed by Douglas. Mission operations, and the corresponding velocity requirements, were made consistent with those from NASA-sponsored MIMOSA studies at Lockheed. In general, the mission requirements used are more stringent than those specified by Douglas. This results in somewhat lower payload weights, but in a higher probability of mission success. Pertinent features of the selected mission profile include:

- Direct ascent to translunar injection from Earth (no Earth parking orbit)
- Transit time of 72 hours
- Injection into a 148.3-km (80-nm) lunar orbit for two revolutions
- Hohmann-transfer descent to the lunar surface at a preselected site
- Throttled hover and landing, nominally at 76 hours after injection from Earth

Operation of the S-IVB/IU for LASS differs from that for the standard Apollo mission in the following important respects:

- The vehicle is oriented during translunar coast with the engines pointed toward the sun, except for propulsive and venting functions, by use of the APS modules.
- Propellants are settled for engine starts and hydrogen tank venting by ignition of the RL10 engines in a tank-head-idle pressure-fed mode (zero NPSP).
- Venting of hydrogen is accomplished with a series of cyclic vents, performed after orienting the propellants. Each cycle is initiated by a tank pressure sensor.

3.2 PROPELLANT MANAGEMENT SYSTEM

Analytical methods obtained from the propellant management system optimization studies described in Section 2 of this report were applied to the S-IVB vehicle and LASS mission. These studies included: (1) tank fill and ground hold, (2) system tolerance effects, and (3) instrumentation for quantity and quality measurements. Resulting system characteristics and effects unique to the S-IVB are discussed in this section.

The existing S-IVB propellant management system design was reviewed to determine its approximate compatibility with use of subcooled liquid and slush hydrogen. An estimate of the areas which will require detailed analysis prior to actual hardware modifications for use of these subcooled fuels is listed below:

- Engine suction line screen and baffling
- Temperature sensors
- Quality meters
- Recirculation disconnect
- Recirculation control valve
- Recirculation liquid-return line
- Additional capacitors on LH_2 mass probe

- Chilldown pump screen
- Additional three-way valve for chilldown pump circulation, header, and control
- GHe/GH_2 scavenge system
- Improved chilldown pump mounting (internal)

3.2.1 Tank Fill and Ground Hold

Preliminary analysis was performed to determine approximate requirements for: (1) filling the S-IVB fuel tank with triple-point liquid or slush hydrogen on the launch pad, (2) maintaining the hydrogen fuel which was initially loaded in either of these conditions during ground hold, and (3) forming or upgrading the quality of slush in the vehicle tank during ground operations. Transient as well as steady-state requirements were determined in the analysis. Recirculation, injection of helium vapor, and operation of a cold-helium heat exchanger were the three techniques evaluated in this preliminary analysis.

The following S-IVB vehicle characteristics were assumed for the preliminary analysis:

- Loaded hydrogen weight = 19,822 kg (43,700 lb)
- Steady-state ground-hold heat rate = 2.27×10^5 w (12,900 Btu/min = 7.74×10^5 Btu/hr)

Results of the preliminary analysis are summarized in Table 3-1. Inspection of the data presented in this table shows that a continuous flow velocity of approximately 4.57 m/sec (15 ft/sec) is required through the existing 15.24-cm (6-in.) diameter fill line to supply the 24,177 kg/hr (53,300 lb/hr) SH_2 flow rate necessary to maintain 50-percent slush using recirculation. Compared with this, a flow velocity of approximately 54.86 m/sec (180 ft/sec) of 11.11°K (20°R) GHe is required through the 15.24 cm (6-in.) line to achieve the 26,309 kg/hr (58,000 lb/hr) flow rate indicated for steady-state slush maintenance using helium injection. An approximate velocity of 73.15 m/sec (240 ft/sec) is required to supply the 34,020 kg/hr (75,000 lb/hr) flow rate

Table 3-1

PREDICTED HYDROGEN TANK FILL AND GROUND HOLD REQUIREMENTS FOR THE SATURN V/S-IVB

Technique	Recirculation	GHe Injection	Cold GHe Heat Exchanger
Transient Cooldown:			
T_1 of LH_2, °K (°R)	–	20.33 (36.6)	20.33 (36.6)
T_2 of LH_2, °K (°R)	–	13.83 (24.9)	13.83 (24.9)
T_1 of GHe, °K (°R)	–	11.11 (20.0)	11.11 (20.0)
GHe Flowrate, kg/hr (lb/hr)	–	34,020 (75,000)	47,174 (104,000)
Cooldown Time, hr	–	0.55	1.0
Steady-State Operation to Maintain Triple Point Liquid or Slush:			
Degradation in transfer line, $\Delta X/X_1$	0.05	–	–
H_2 Flowrate for X_a = 50%, X_{b_2} = 50%, kg/hr (lb/hr)	24,177 (53,300)	–	–
Recirculation Period, hr	0.82	–	–
20°R GHe Flowrate, kg/hr (lb/hr)	–	26,309 (58,000)	56,246 (124,000)
Slush Formation in Vehicle Tank:			
20°R GHe required to form 50% slush, kg (lb)	–	18,552 (40,900)	39,690 (87,500)

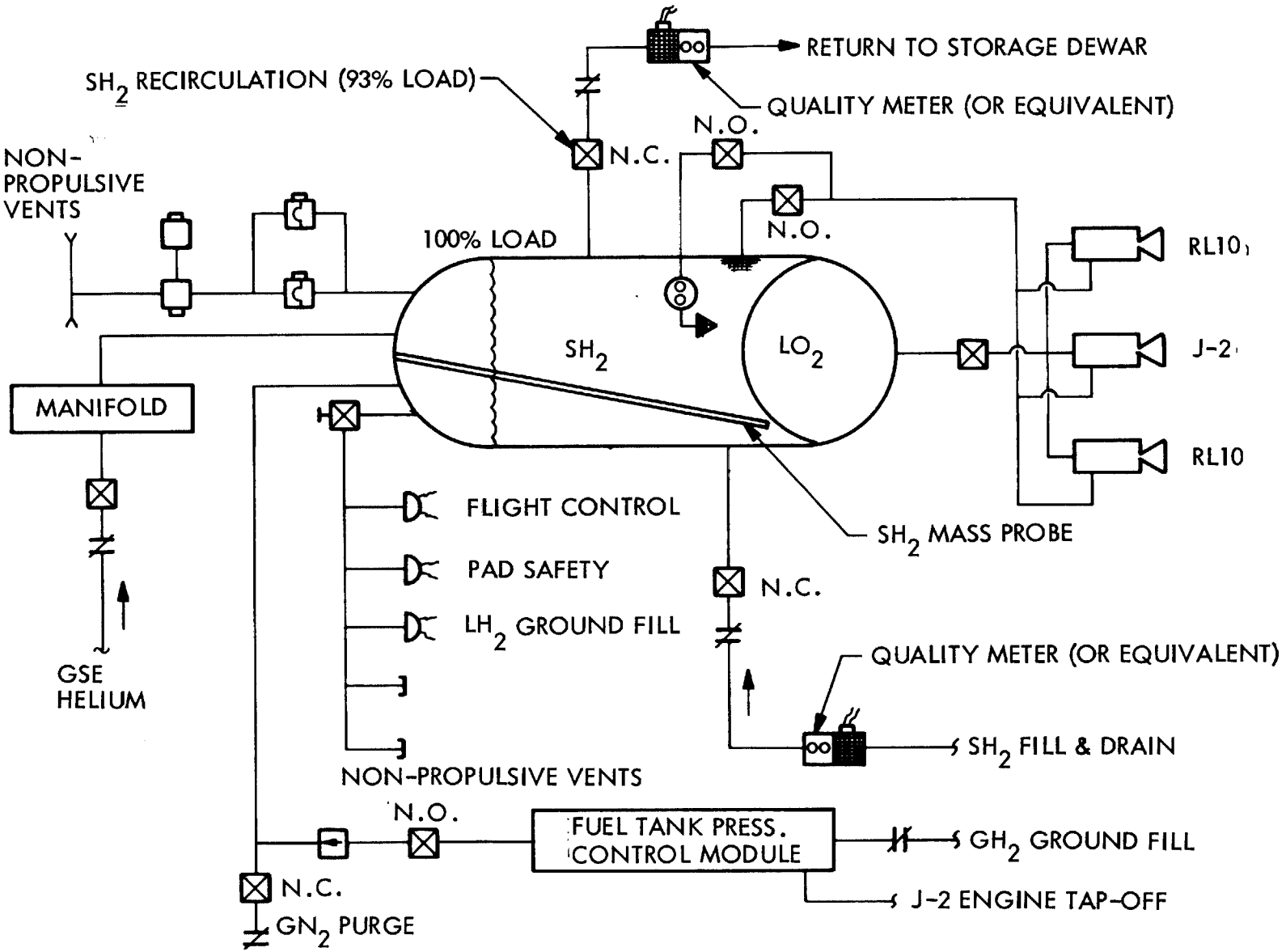

Fig. 3-3 Schematic of a Slush Hydrogen Loading and Recirculation System for the S-IVB

needed to cool a tank of liquid hydrogen from 20.33° K (36.6° R) to the triple point. It can be seen from this comparison that the flow rate and velocity which result from use of recirculation are entirely feasible. Those rates and velocities associated with helium injection would seem to make the design of an injection manifold, a vent line, and the GSE facility very difficult. In addition, the highly turbulent conditions in the tank resulting from large helium flow rates needed for the injection technique would impose severe requirements on quantity- and quality-sensing instrumentation.

Further, the indicated flow rates and velocities required for use of a cold-helium heat exchanger appear unfeasible since they are approximately double those needed for helium injection. Therefore, the results of this analysis for the S-IVB vehicle indicate that recirculation is the preferred technique for filling the fuel tank with subcooled liquid or slush hydrogen and for quality maintenance during ground hold.

Figure 3-3 shows a schematic of a typical recirculation system which could be used to load and maintain subcooled hydrogen in the S-IVB stage. The following paragraph describes a preliminary tank loading procedure for the S-IVB.

S-IVB propellant loading is presently accomplished by automatic programming; therefore, slush loading will require conversion of the loading console located on the Launch Umbilical Tower. In this study, an attempt was made to maintain as much of the present loading program as possible, thereby reducing additional thermal stresses in the internal insulation and a potential problem of tank implosion. The numerical data presented are typical for hydrogen slush loading of 50-percent average quality in the flight article at 13.83° K (24.9° R) with a density of 81.7 kg/m^3 (5.1 lb/ft^3).

The following loading sequence depicts a preliminary recirculation technique for loading and maintaining slush of 50-percent average quality.

Sequence	Operation	Comments
1.0	Begin GN_2 purge of LH_2 tank; cool tank to 77.77° K (140° R) at 13.2 N/cm^2 ± 0.69 N/cm^2 (19.1 ± 1 psia).	Present practice for LH_2 system

2.0	When tank temperature sensors stabilize at 77.77° K (140° R) for minimum of 3 minutes, initiate GHe purge at 77.77° K (140° R) and 13.2 N/cm^2 ± 0.69 N/cm^2 (19.1 ± 1 psia) until tank volume is 99% GHe; maintain inert condition in tanks until verification for loading is received.	Present practice for LH_2 system
3.0	Assure that dewar slush (SH_2) quality is nominally 50% before transfer is begun. Note: Dewar slush of any quality that can be readily transferred in a line can be used to upgrade propellant in the flight tank to an average quality of 50% by properly adjusting the supply and liquid-return flow rates.	New procedure for typical 50% quality slush system
4.0	Begin slow fill at 500 gpm (158.76 kg/min or 350 lb/min SH_2) maintaining 13.2 N/cm^2 ± 2.76 N/CM^2 (19.1 ± 4 psia) tank pressure at 5% load.	Present practice for LH_2 system
5.0	Initiate fast fill with SH_2 at 13.83°K (24.9°R) and 3000 gpm (920.8 kg/min or 2030 lb/min) to 93% load. Maintain tank pressure with GHe at 13.2 N/cm^2 (19.1 ± 1 psia) during fill.	Present practice for LH_2 system, except for additional GHe requirement
6.0	Begin SH_2 slow fill at 1270 gpm (403.7 kg/min or 890/lb/min) to 100% load. Maintain tank pressure with GHe at 13.2 N/cm^2 ± 0.69 N/cm^2 (19.1 ± 1 psia) during fill.	Final fill rate equalized to that required for ground-hold maintenance
7.0	When liquid level approaches S-IVB station 512, open SH_2 recirculation valve (estimated S-IVB station 500), permitting liquid flow to storage dewar.	New procedure for slush system

	Return flow will approximate 403.7 kg/min LH_2 (890 lb/min LH_2). Continue recirculation until SH_2 inlet and SH_2/LH_2 outlet quality-meter outputs are constant, and the fuel mass probe registers 100% load.	
8.0	Continue recirculation during launch hold with nominal 50% quality slush at maximum of 1270 gpm (403.7 kg/min or 890 lb/min) to maintain 100% load; monitor quality instrumentation and SH_2 mass probe.	New procedure for slush system
9.0	Approximately 90 seconds prior to lift-off, close fill, recirculation, and vent valves and pressurize tank to 21.03 N/cm^2 ± 0.35 N/cm^2 (30.5± 0.5 psia) with GHe.	Present practice for LH_2 system

3.2.2 System Tolerance Effects Study

Significant payload penalties will result from instrumentation and design tolerances associated with measurements of (1) loaded hydrogen quantity, (2) loaded quality or solid fraction, (3) in-flight hydrogen quantity, (4) ground-vent pressure, (5) flight vent pressure, and (6) total heat rate to the hydrogen. Equations which relate payload penalty magnitude to tolerance magnitudes were developed and are summarized in subsection 2.2.2 of this report. Figure 3-4 presents individual payload penalties as a function of tolerance magnitude which resulted from preliminary evaluation of the equations for the S-IVB/LASS vehicle.

From inspection of these data, it may be noted that payload is most sensitive to the quantity of hydrogen available in flight. Slightly smaller penalties result from errors in measuring loaded hydrogen quantity. Payload is then considerably less sensitive to variations in predicted heating rate, slush quality, flight-vent pressure, and ground-vent pressure, in that order.

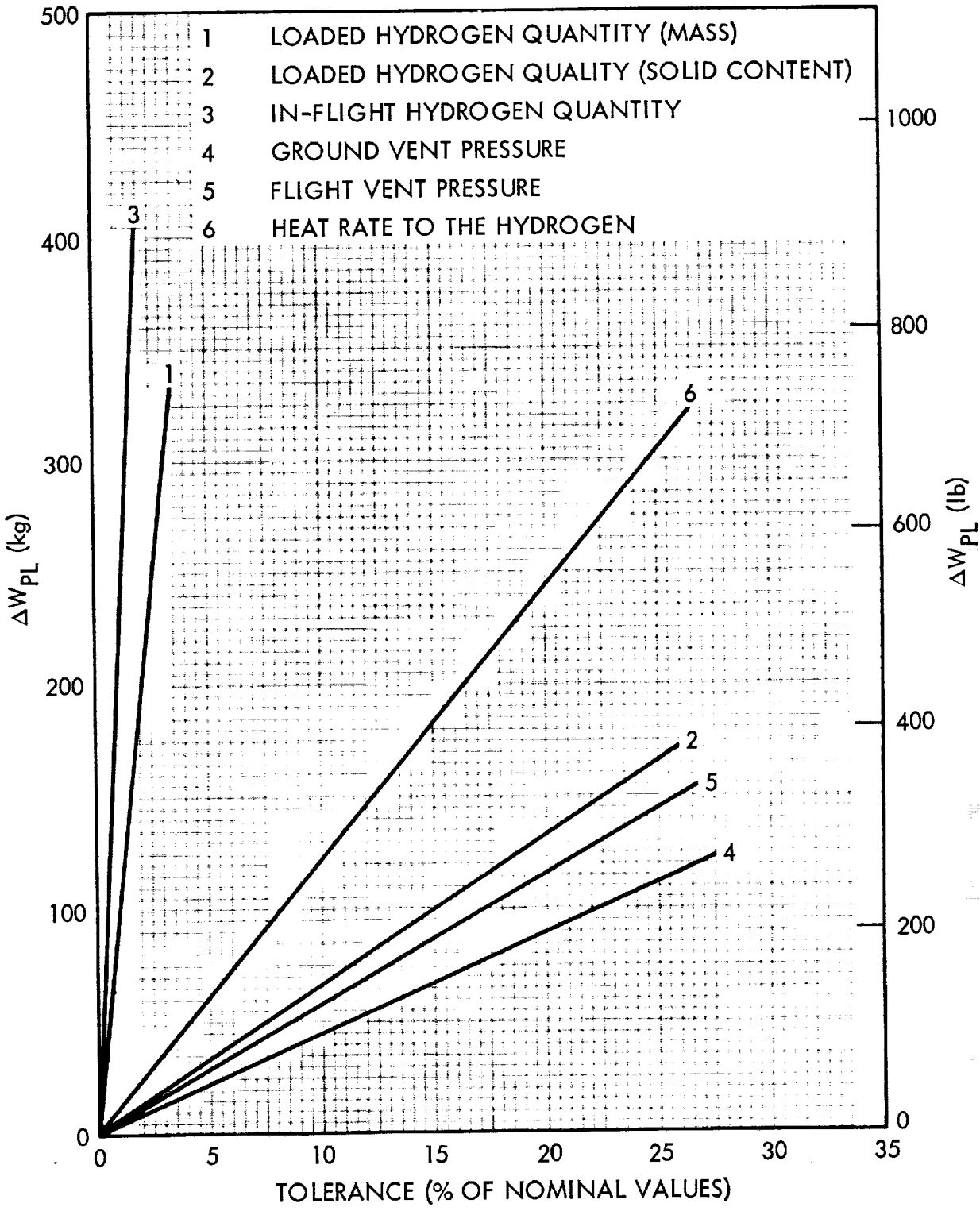

Fig. 3-4 Payload Penalties Resulting from Saturn V/S-IVB System Tolerances; Liquid- or Slush-Fueled Vehicles

Using the data from Fig. 3-4, individual and total system payload penalties were obtained for presently predicted state-of-the-art tolerances. The total penalty was calculated using a root-mean-square combination of the individual values. Results are given in Table 3-2. This preliminary analysis shows that the system penalty is essentially the same for both liquid-and slush-fueled vehicles. The penalties are similar because the insulation thickness does not optimize differently for slush and liquid. The increased payload penalties for both, as a percentage of nominal payload, result because the S-IVB was not originally designed or optimized for an extended mission duration. The LASS mission profile therefore presents a severe design condition insofar as hydrogen storability and tolerance effects are concerned. If it were determined later that the 10 percent plus penalties shown are unacceptably high, more accurate instrumentation and measurement techniques would be required for this stage and mission.

3.2.3 Instrumentation Requirements

Significant modifications are required in Saturn V/S-IVB instrumentation and control components to provide for measurements of quantity and quality where subcooled liquid and slush fuels are used. However, existing propellant management and propellant utilization system instrumentation was assumed to satisfy requirements for the saturated liquid hydrogen-fueled [13.1 N/cm^2 (19 psia)] LASS vehicle. For study purposes, it was necessary to roughly define these modifications so that system inert weights could be estimated.

For use of triple-point liquid, only minor modifications to the existing system were assumed. These are (1) replacement or recalibration of temperature sensors and (2) replacement or recalibration of capacitance probes.

For use of liquid-solid mixtures, additional modifications were assumed. These are (1) installation of a liquid recirculation line, control valve, and disconnect, (2) replacement or recalibration of temperature and capacitance sensors, (3) installation of a gamma radiation (or X-ray) attenuation system, and (4) installation of a screen

Table 3-2

PAYLOAD PENALTIES RESULTING FROM PREDICTED HYDROGEN SYSTEM TOLERANCES FOR THE SATURN S-IVB/ LASS VEHICLE

Variable	Nominal Value	Predicted Tolerance (%)	Tolerance Value	Payload Penalty kg (lb)
Loaded H_2 Quantity	19,822 kg (43,700 lb)	1	198.22 kg (437 lb)	97.07 (214)
Loaded H_2 Solid Fraction	50%	10	N.A./5%	N.A./66.23 (N.A./146)
In-Flight H_2 Quantity	Variable	2	396.9 kg (875 lb)	391 (862)
Ground Vent Pressure	13.1 N/cm^2 (19 psia)	5	0.655 N/cm^2/NA (0.95 psia/N.A.)	N.A./21.3 (N.A./47)
Flight Vent Pressure	19.31 N/cm^2 (28 psia)	5	0.965 N/cm^2 (1.4 psia)	28.58 (63)
Heat Rate to H_2	4,688 w (16,000 Btu/hr)	25	1172 w (4000 Btu/hr)	303.9 (670)
Total System Payload	4,867 kg (10,730 lb)	10.4/10.5	–	505.76/509.85 (1115/1124)

Note: When two values are given, the first applies to liquid-fueled systems and the second to slush-fueled systems; single values apply to both.

near the tank outlet to filter and retain solid hydrogen particles in the tank during explusion of liquid for engine firings.

Although modifications would also be required for other vehicle instrumentation, no definition was made during this study because weight differences are assumed to be negligible.

3.3 PROPULSION SYSTEM

The primary propulsion system for the Saturn S-IVB/LASS vehicle combines the existing J-2 engine installation and two additional RL10 engines, as described in subsection 3.1. A schematic of the combined system is shown in Fig. 3-5.

Three full-thrust firings are required for the LASS mission. These provide (1) translunar injection, (2) retro into lunar orbit, and (3) braking during descent to the lunar surface. Both the J-2 and the two RL10 engines are assumed to operate at an optimum fixed mixture ratio for each of these firings. The mixture ratios used in the analysis were selected from a range which is feasible for J-2 and RL10 engine operation. Nominal limits are 4.5 to 1, minimum, (oxygen to hydrogen) and 5.5 to 1, maximum. Selected ratios were those that result in maximum payload weights for each initial hydrogen condition. Since hydrogen is conserved by the use of the initially subcooled liquid or slush, the optimum mixture ratios are lower for these cases. Values of thrust and specific impulse as a function of mixture ratio and hydrogen temperature were estimated for study purposes. Figures 3-6 through 3-8 present these estimated values.

In addition to the full-thrust firings discussed above, a number of throttled firings of the RL10 engines only are required to perform the LASS mission. Two firings at 10 percent of full thrust are assumed for the first midcourse correction and for deorbit to achieve the Hohmann-transfer descent. Hover and landing are accomplished by throttling the RL10 engines to provide a total thrust equal to the total equivalent vehicle weight in the lunar gravitational environment. The second midcourse correction

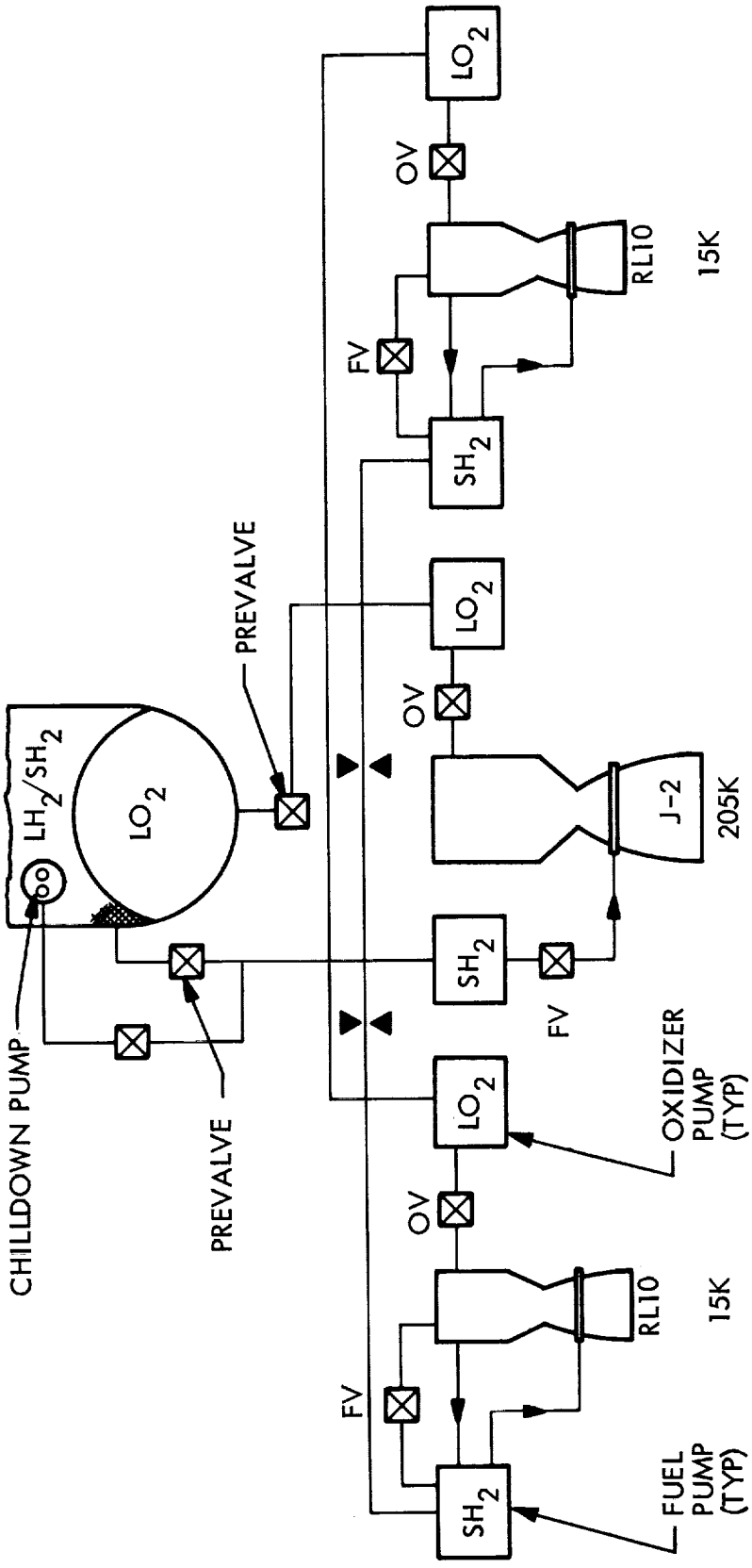

Fig. 3-5 Saturn V/S-IVB Propulsion Schematic for LASS

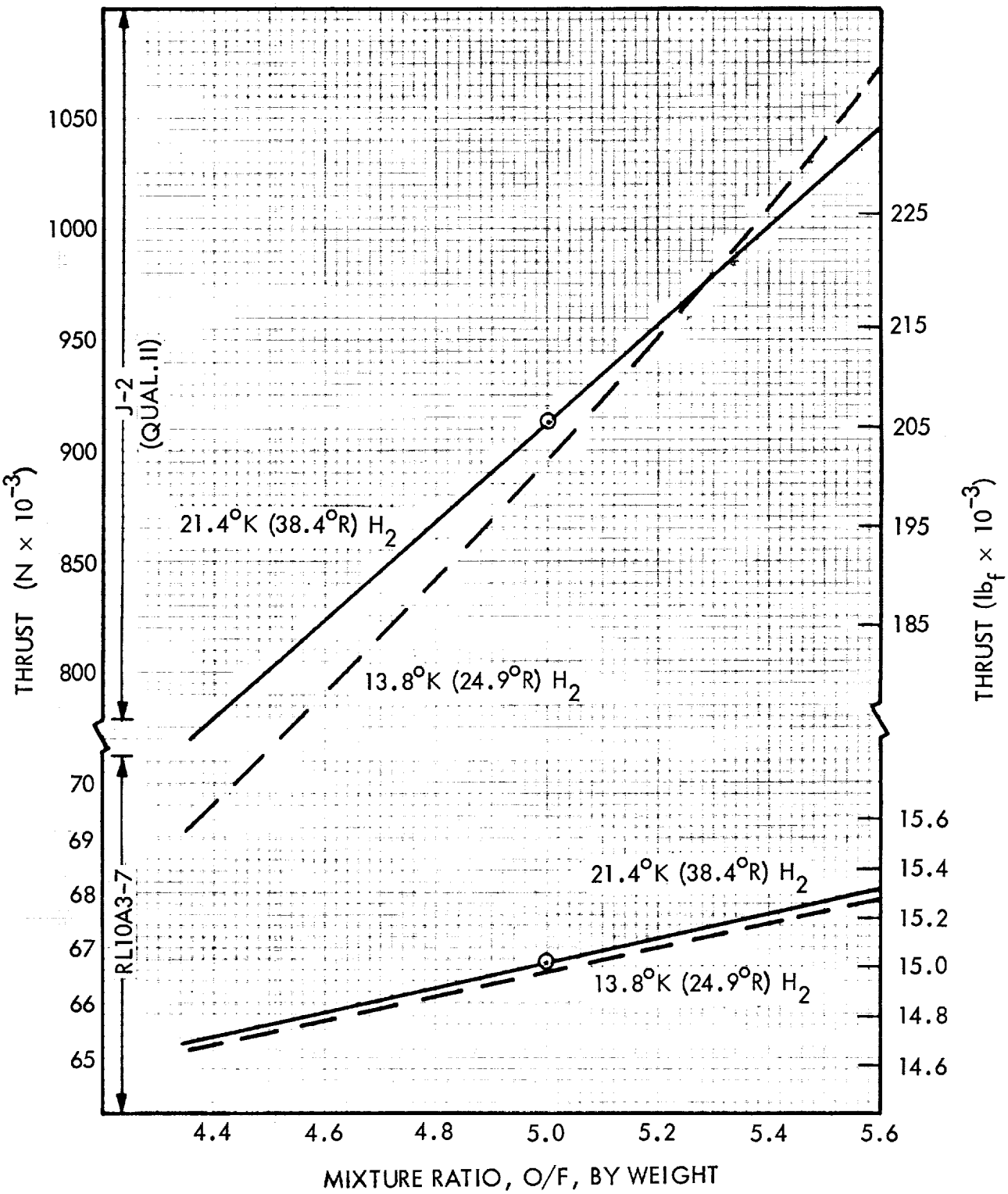

Fig. 3-6 Estimated Thrust vs. Mixture Ratio for S-IVB/LASS Vehicle

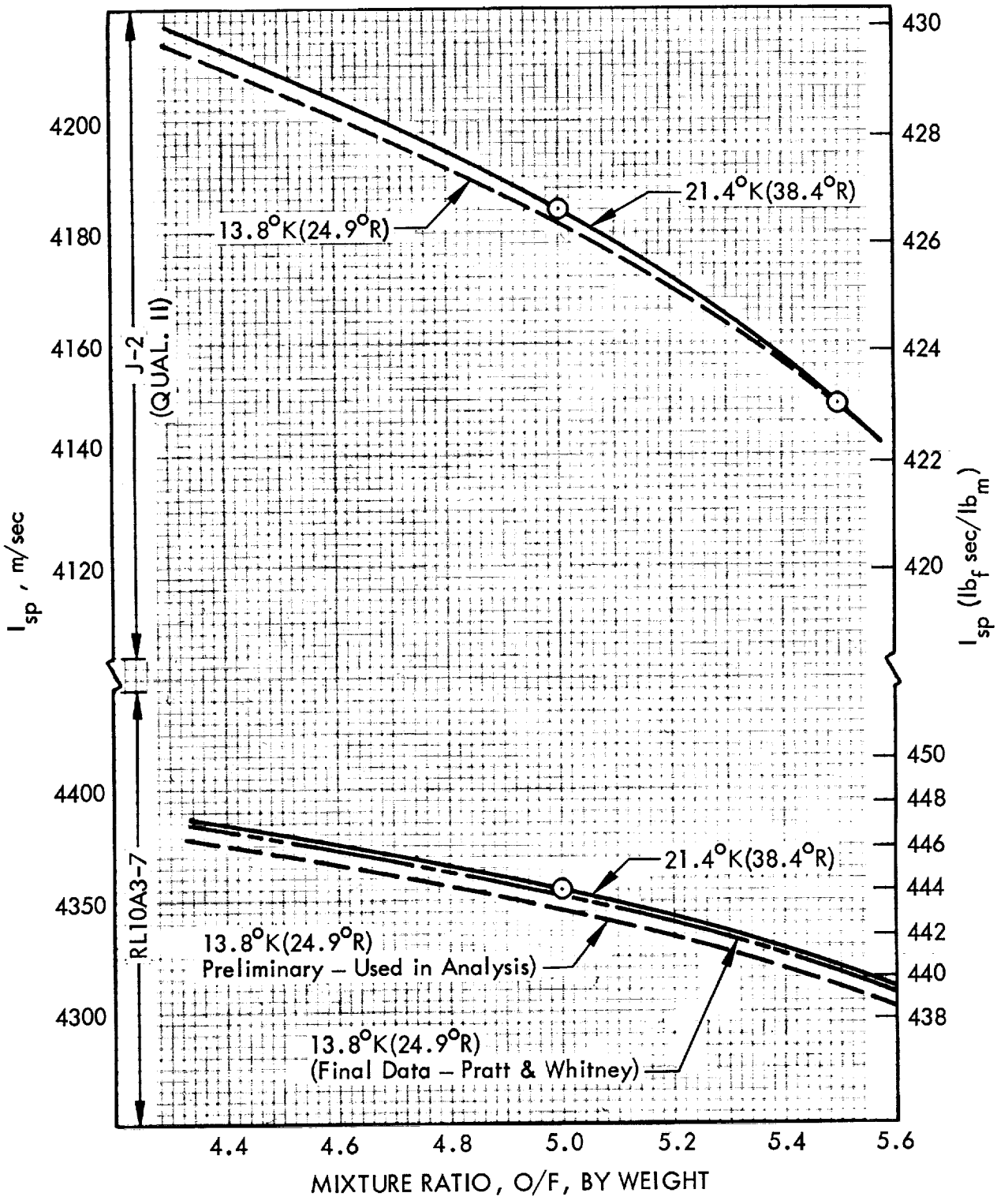

Fig. 3-7 Estimated I_{sp} vs. Mixture Ratio for S-IVB/LASS Vehicle

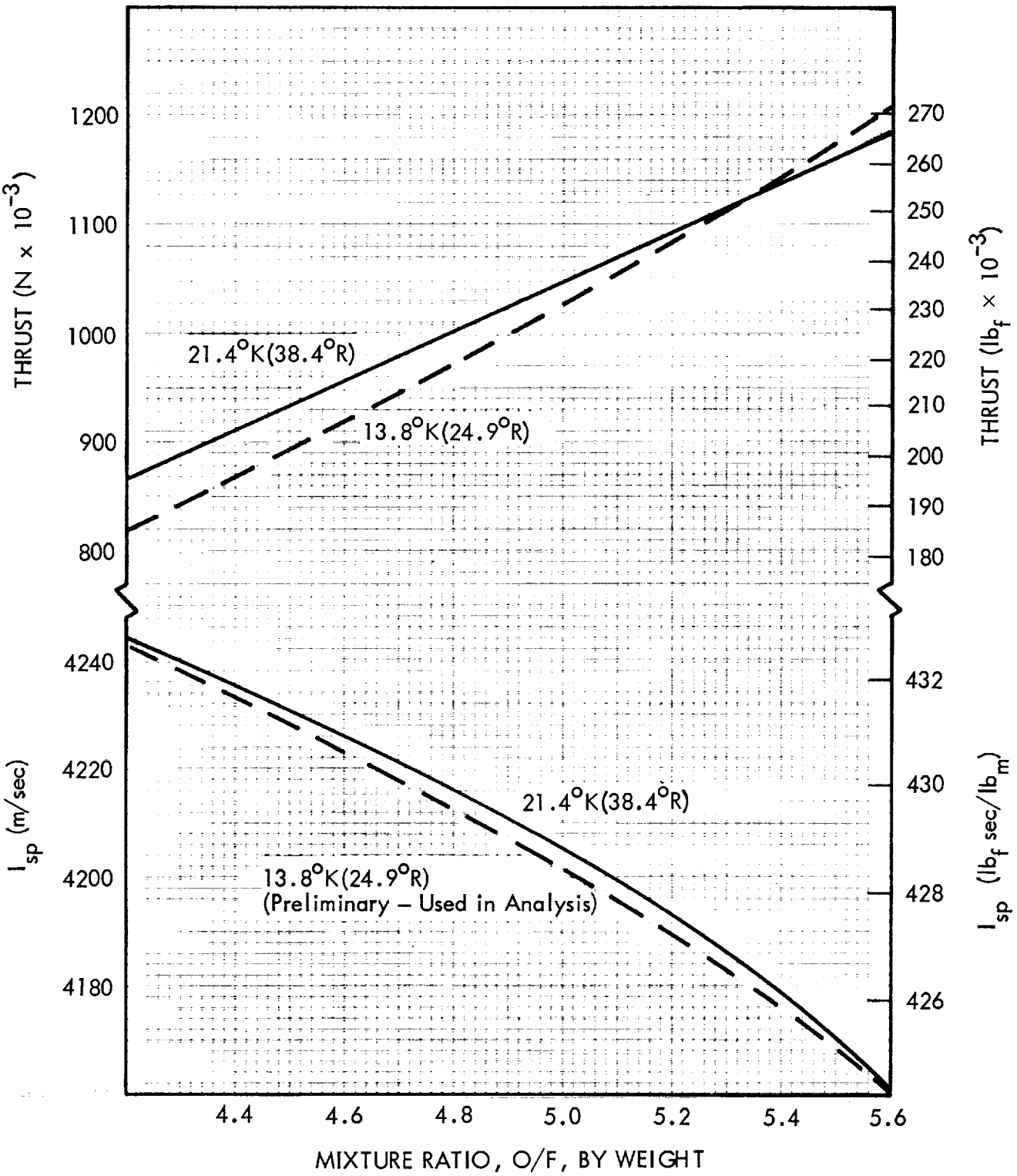

Fig. 3-8 Estimated Performance for J-2 (Qual II)/RL10A3-7 Engine Combination for S-IVB/LASS

firing and numerous ullaging firings to settle propellants for engine starts and venting are provided by using the RL10's in a tank-head idle mode. All throttled firings of the RL10 engines were analyzed at a nominal mixture ratio of 5.0 to 1, regardless of the initial hydrogen condition being considered.

Table 3-3 presents a summary of the propulsion system requirements and characteristics resulting from the S-IVB/LASS performance analyses. Details of propellant usage and venting are given in other sections of this report.

3.4 INSULATION SYSTEM

The S-IVB hydrogen tank insulation is an internal foam composite (Ref. 3-3) consisting of (1) a reinforced polyurethane foam core weighing 83.3 kg/m^3 (5.2 lb/ft^3); (2) a No. 116 fiberglass cloth liner impregnated with polyurethane resin weighing 0.269 kg/m^2 (0.055 lb/ft^2); (3) a wiped-on coat of polyurethane resin sealer weighing 0.0537 kg/m^2 (0.011 lb/ft^2); and (4) the bond between the foam core and the tank wall, estimated at 0.293 kg/m^2 (0.060 lb/ft^2). The average density, therefore, varies with thickness.

A preliminary optimization of the insulation was obtained using the method described in subsection 2.4. A more comprehensive determination was then obtained by a numerical evaluation of insulation and boiloff weights for several values of insulation thickness. In the latter analysis, tank-wall cooldown, pressurant heating, and other secondary effects were considered.

3.4.1 Preliminary Optimization

The nested-tank design of the Saturn S-IVB stage results in different heating rates to the hydrogen through the tank sidewall and through the common bulkhead. The pertinent aspects of the thermal environment, the resulting heat transfer, and the optimization of thicknesses are therefore treated separately in the discussion that follows. All preliminary calculations are based on a single firing into lunar orbit, since the earth

Table 3-3

SUMMARY OF SELECTED PROPULSION SYSTEM REQUIREMENTS AND CHARACTERISTICS FOR THE S-IVB/LASS MISSION

Event	Nominal Time of Initiation	Event Duration (sec)	Basis	Engine(s)	Percent of Full Thrust	Req'd NPSP N/cm^2 (psia)	Line and Accel. Losses N/cm^2 (psia)	Total Req'd Ullage Pressure, N/cm^2 (psia)	Initial H_2 Condition	Nominal Thrust, N (lb)	Nominal I_{sp}, m/sec (sec)	Mixture Ratio (O/F by wt.)	Hydrogen Flowrate, kg/sec (lb/sec)
Prop. settling for inject. firing	Liftoff + 558 sec	1.6	DAC guidelines	2 Thiokol TX-280 solids	–	–	–	–	–	30,246 (6,800)	–	–	–
Translunar inject. firing	Liftoff + 560 sec	254	DAC guidelines	J-2 + 2 RLIO's	100	2.8 (4)	2.1 (3)	20.7 (30)	Sat. at 13.1 N/cm^2 (19 psia)	1,158,704 (260,500)	4168 (425)	5.5	42.8 (94.3)
Translunar inject. firing	Liftoff + 560 sec	334	DAC guidelines	J-2 + 2 RLIO's	100	2.8 (4)	2.1 (3)	20.7 (30)	Sat at T. P.	973,667 (218,900)	4213.1 (429.6)	4.8	39.9 (87.9)
Translunar Inject. firing	Liftoff + 560 sec	371	DAC guidelines	J-2 + 2 RLIO's	100	2.8 (4)	2.1 (3)	20.7 (30)	50% Slush	894,048 (201,000)	4227.8 (431.1)	4.5	38.5 (84.8)
Prop. settling for venting	(as req'd – see venting anal)	120 (ea)	DAC guidelines	2 RLIOA-3-7's	2	0 (0)	Negl.	13.8 (20)	All	2,669 (600)	4020 (410)	5.0	0.111 (0.244)
Prop. settling for MCC firing	10 hr	240	DAC guidelines	2 RLIOA-3-7's	2	0 (0)	Negl.	13.8 (20)	All	2,669 (600)	4020 (410)	5.0	0.111 (0.244)
First MCC firing	10 hr	319 to 344	DAC guidelines	2 RLIOA-3-7's	10	1.2 (0.3)	0.5 (0.7)	20.7 (30)	All	13,344 (3,000)	4266 (435)	5.0	0.52 (1.15)
Second MCC firing	50 hr	86 to 94	DAC guidelines	2 RLIOA-3-7's	2	0 (0)	Negl.	13.8 (20)	All	2,669 (600)	4020 (410)	5.0	0.111 (0.244)
Prop. settling for retro firing	72 hr	420	MIMOSA guidelines	2 RLIOA-3-7's	2	0 (0)	Negl.	13.8 (20)	All	2,669 (600)	4020 (410)	5.0	0.111 (0.244)
Orbit retro firing	72 hr	37	MIMOSA guidelines	J-2 + 2 RLIO's	100	2.8 (4)	2.1 (3)	20.7 (30)	Sat. at 13.1 N/cm^2 (19 psia)	1,158,704 (260,500)	4168 (425)	5.5	42.8 (94.3)
Orbit retro firing	72 hr	46	MIMOSA guidelines	J-2 + 2 RLIO's	100	2.8 (4)	2.1 (3)	20.7 (30)	Sat. at T. P.	999,466 (224,700)	4217 (430)	4.8	40.9 (90.1)
Orbit retro firing	72 hr	51	MIMOSA guidelines	J-2 + 2 RLIO's	100	2.8 (4)	2.1 (3)	20.7 (30)	50% slush	931,411 (209,400)	4230.7 (431.4)	4.5	40.1 (88.3)
Prop. settling for deorbit	75 hr	240	MIMOSA guidelines	2 RLIOA-3-7's	2	0 (0)	Negl.	13.8 (20)	All	2,669 (600)	4020 (410)	5.0	0.111 (0.244)
Deorbit firing	75 hr	41 to 46	MIMOSA guidelines	2 RLIOA-3-7's	10	0.2 (0.3)	0.5 (0.7)	20.7 (30)	All	13,344 (3,000)	4266 (435)	5.0	0.52 (1.15)
Prop. settling for braking	76 hr	420	MIMOSA guidelines	2 RLIOA-3-7's	2	0 (0)	Negl.	13.8 (20)	All	2,669 (600)	4020 (410)	5.0	0.111 (0.244)
Braking firing	76 hr	47	MIMOSA guidelines	J-2 + 2 RLIO's	100	2.8 (4)	2.1 (3)	20.7 (30)	Sat. at 13.1 N/cm^2 (19 psia)	1,158,704 (260,500)	4168 (425)	5.5	42.8 (94.3)
Braking firing	76 hr	58	MIMOSA guidelines	J-2 + 2 RLIO's	100	2.8 (4)	2.1 (3)	20.7 (30)	Sat. at T. P.	999,466 (224,700)	4217 (430)	4.8	40.9 (90.1)
Braking firing	76 hr	66	MIMOSA guidelines	J-2 + 2 RLIO's	100	2.8 (4)	2.1 (3)	20.7 (30)	50% slush	931,411 (209,400)	4230.7 (431.4)	4.5	40.1 (88.3)
Hover and landing firing	76 hr	184	MIMOSA guidelines	2 RLIOA-3-7's	27.1	1.4 (2)	1.4 (2)	20.7 (30)	Sat. at 13.1 N/cm^2 (19 psia)	36,176 (8,133)	4335 (442)	5.0	1.39 (3.07)
Hover and landing firing	76 hr	191	MIMOSA guidelines	2 RLIOA-3-7's	28.9	1.4 (2)	1.4 (2)	20.7 (30)	Sat. at T. P.	38,506 (8,657)	4335 (442)	5.0	1.48 (3.26)
Hover and landing firing	76 hr	184	MIMOSA guidelines	2 RLIOA-3-7's	30.8	1.4 (2)	1.4 (2)	20.7 (30)	50% slush	41,055 (9,230)	4335 (442)	5.0	1.58 (3.48)

escape firing occurs very early and therefore exerts only a small influence on insulation optimization.

The S-IVB stage is assumed to be oriented during the earth-lunar transit phase with the engine pointed toward the sun. Such orientation is feasible in practice only within the limits of the angular cone resulting from attitude control system tolerances and an optimized dead band. For this analysis, a constant average angular displacement is assumed. The net heat transfer into and away from the tank sidewall exposed to the sun is, of course, zero. The term which describes the heat re-radiated from that surface can be neglected since the surface temperature is only approximately 17 to 22°K (30 to 40°R). The heat which is conducted through the sidewall insulation to the propellant must then equal the absorbed solar energy. For the combination of insulation thermal conductivity and surface absorptivity of the S-IVB stage, it can be seen that the sidewall heating rate is relatively independent of the sidewall foam insulation thickness for small changes to that thickness. For this preliminary analysis then, the heating rate through the tank sidewall is

$$Q_w = \frac{\pi}{180} \bar{\alpha} \bar{q} \beta d\ell = 795 \beta \qquad (3.1)$$

The above value for sidewall heating rate compares favorably with the range of values presented by Douglas (Ref. 3-4).

The S-IVB common bulkhead separates the oxygen and hydrogen tankage volumes with a nearly constant temperature differential. Since the foam insulation is in series with the evacuated space between the bulkhead skins, the expressions that define the optimization parameters are slightly different from those developed in subsection 2.4. Heat transfer through the bulkhead can be conveniently expressed as a function of the differential temperature and the combined resistance of the foam insulation and the evacuated space. The length of the boiling period is given by Eq. (3.2):

$$\theta_B = \theta_M - \frac{W_P(XL_f + \Delta H)}{\frac{\Delta T}{\bar{R} + \frac{\delta_d}{KA_d}} + Q_w + Q_p} \tag{3.2}$$

The resulting total boiloff hydrogen weight is then

$$W_{BO} = \frac{\Delta T \theta_M}{\left(\bar{R} + \frac{\delta_d}{KA_d}\right) L_v} - \frac{W_P(XL_f + \Delta H)}{L_v} \tag{3.3}$$

And, the differential of boiloff weight with respect to bulkhead insulation thickness is

$$\frac{dW_{BO}}{d\delta_d} = \frac{\Delta T \theta_M}{KA_d L_v \left(\bar{R} + \frac{\delta_d}{KA_d}\right)^2} \tag{3.4}$$

Combining $dW_I/d\delta_d = \rho_I A_d$ with Eq. (3.4), and solving for the thickness yields

$$\delta_d(\text{opt}) = \left(\alpha \theta_M\right)^{1/2} - KA_d \bar{R} \tag{3.5}$$

Similarly, the expression for thickness which yields zero boiling is

$$\delta_d(\theta_B = 0) = \frac{1}{\frac{\phi}{\alpha \theta_M} - q^*} - KA_d \bar{R} \tag{3.6}$$

The solution of Eqs. (3.5) and (3.6) for θ_M^* yields the same result as that obtained from the equations derived in subsection 2.4.

For preliminary evaluations, the angle between the vehicle centerline and the sun vector, β, is assumed to be 2 degrees. The optimum bulkhead insulation thicknesses together with the resulting boiloff weights and other related parameters are summarized in Table 3-4 for initially saturated liquid at 13.1 N/cm^2 (19 psia), and for 50% slush.

It is interesting to compare the optimum conditions shown in Table 3-4 with those that result if the bulkhead insulation were designed to yield zero boiloff. That thickness, from Eq. (3.6), is 7.90 cm (3.1 in.) for initially 50% slush. The associated bulkhead insulation weight is then 694 kg (1530 lb). The corresponding payload penalty is approximately 124.7 kg (275 lb) and could be even less if the inert weights of vent hardware were deleted.

3.4.2 Final Optimization

Discussion of the final S-IVB insulation optimization for the LASS mission is separated into (1) Heat Transfer Considerations, and (2) Final Optimization Procedure and Results.

3.4.2.1 Significant Heat-Transfer Considerations

In order to determine heat-transfer rates and total heat absorbed by the S-IVB hydrogen tank, it is convenient to separate the LASS mission profile into four chronological time periods. These are (1) pre-pressurization, (2) ascent and cooldown, (3) lunar transit, and (4) lunar orbit, descent, and landing. Environmental heating is significantly different during each of these periods. A further differentiation can be made within each time period to show the distribution of heat transferred through the (1) forward dome and joint, (2) cylindrical sidewall, (3) aft dome, aft joint, and common bulkhead, (4) fill, drain, feed, and chill lines, (5) helium bottle supports, and (6) pressurization gases.

The thermal conductivity of polyurethane foam insulation is dependent upon its temperature and the degree of hydrogen permeation (Ref. 3-3). The values of thermal

Table 3-4

SUMMARY OF PRELIMINARY OPTIMIZED BULKHEAD INSULATION THICKNESSES AND RELATED QUANTITIES FOR THE SATURN S-IVB STAGE AND LASS MISSION

$Q_w + Q_p$	= 1425 w (4865 Btu/hr)
β	= 2 deg
K	= 3.46×10^{-4} w/cm °K (0.02 Btu/hr-ft-°R)
A_d	= 54.8 m^2 (590 ft^2)
W_P	= 6,350 kg (14,000 lb)
ΔT_d	= 69.44°K (125°R)
ρ_I	= 160.2 kg/m^3 (10 lb/ft^3)
θ_M	= 76 hr
Vent Pressure	= 26.2 N/cm^2 (38 psia)
BF	= 0.5

$q^* = 10.83\ m^{-1}$ (3.30 ft^{-1}) (for $Q_w + Q_p$)

$\alpha = 0.650 \times 10^{-4}\ m^2/hr$ ($0.700 \times 10^{-3}\ ft^2/hr$)

	Initially Sat. Liquid at 13.1 N/cm^2 (19 psia)		Initially 50% Solid at 0.703 N/cm^2 (1.02 psia)	
ϕ, m (ft)	0.0344	(0.113)	0.0991	(0.325)
θ_M^* (hr)	10.9		65.8	
δ_d (opt), cm (in.)	4.06	(1.6)	4.06	(1.6)
W_{BO}, kg (lb)	1787	(3940)	290	(640)
W_{Id}, kg (lb)	356	(785)	356	(785)
$W_I + BFW_{BO}$, kg (lb)	1250	(2755)	502	(1105)

conductivity used in this analysis, Fig. 3-9, were obtained by correlating data presented in the above reference with recent Douglas-originated data for the Saturn V/S-IVB Apollo stage. Where maximum and minimum values were presented, an arithmetic average was used.

It can be seen by examining available S-IVB data that heat transfer through the forward dome and tank penetrations is not significantly affected by insulation optimization. Therefore, only the common bulkhead and the aft dome/cylindrical sidewall insulation thicknesses were optimized in this analysis. Heat transfer through the forward dome, tank penetrations, and pressurization gases was considered in calculating total heat absorbed to determine boiloff. For the common bulkhead, the heating environment is essentially constant throughout the mission; therefore, the temperature differential and thermal conductivity are constant also. For the remaining tank components, heating environments, temperature differentials, and thermal conductivities all vary throughout the mission.

Pre-pressurization. The nominal countdown procedure for the Saturn V/S-IVB Apollo launch vehicle specifies that topping of the S-IVB hydrogen tank is terminated at from 50 to 90 sec before liftoff. Pre-pressurization of the hydrogen tank occurs at this time. For purposes of this analysis, a 90-sec period was assumed. Heat transferred into the hydrogen tank during this period results in heating of the bulk hydrogen and must therefore be considered in optimizing the insulation system.

Ascent and Cooldown. Tank temperature and effective thermal conductivity of the insulation increase rapidly between liftoff and maximum aerodynamic heating; they then gradually decrease to steady-state values during lunar transit. The sidewall cooldown period varies from approximately 2 hr for 1.02-cm (0.4-in.) thick insulation to approximately 12 hr for that 6.35 cm (2.5 in.) thick. Variations are greatest along the sidewall where the effect of aerodynamic heating is maximized. Similar (but smaller)variations occur along the aft dome which is shielded by the aft skirt and cooled by the oxygen tank. The forward dome experiences initial heating near the skirt joint, but the net effect is one of gradual cooling. Heating rate to the hydrogen

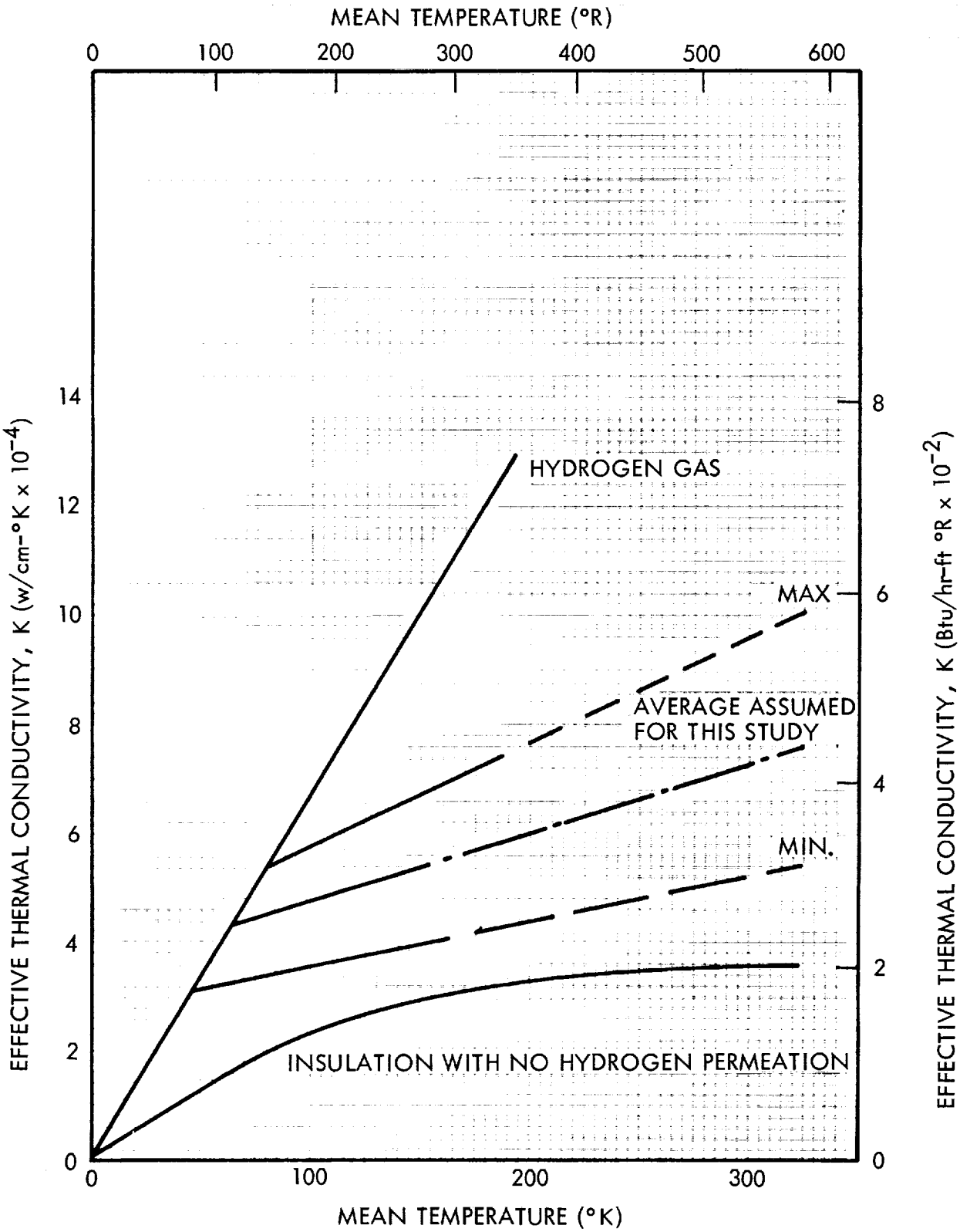

Fig. 3-9 Effective Thermal Conductivity of Saturn S-IVB Insulation as a Function of Temperature

is shown in Fig. 3-10 as a function of flight time and insulation conductance. Since conductance varies throughout the cooldown period, average values were calculated for this study. The insulation conductivity values used to calculate the average conductances during cooldown were those which correspond to the average insulation temperatures. The areas under the resulting heat-rate curves of Fig. 3-10 were then integrated to determine total heat transfer during the ascent and cooldown period corresponding to those particular values of conductance.

Lunar Transit. Tank sidewall insulation temperature and thermal conductivity vary during the lunar transit period as a function of vehicle centerline-sunline angle. An average steady-state angle of 1 degree was assumed for this analysis (Ref. 3-1). The corresponding steady-state heat flux through the sidewall insulation is approximately 392.6 w (1340 Btu/hr) (Ref. 3-1). Analysis indicates that the steady-state tank sidewall temperature and insulation conductivity which would yield this flux for a 2.54-cm (1.0-in.) insulation thickness are 25.6°K (46°R) and 1.73×10^{-3} w/cm°K (0.10 Btu/hr-ft-°R), respectively. Since negligible reradiation would occur for a tank temperature of 25.6°K (46°R), this flux is essentially independent of insulation thickness, and was therefore used for all thicknesses.

It can be shown that a significant heat transfer would result from increased solar heat flux incidence during brief periods of reorientation to accomplish midcourse corrections and venting. Therefore, an increment of total heat transfer was included in the analysis to account for this increase. The incremental flux used was 22,151 w (21 Btu/sec) for the reoriented periods only, conservatively assuming that the vehicle centerline is broadside to the sun for these periods.

Lunar Orbit, Descent, and Landing. Tank sidewall insulation temperature and thermal conductivity vary during the lunar orbit, descent, and landing period as a function of solar and lunar radiation fluxes, incidence angles, and the thermal properties of the external surface. Accurate calculation of the total heat transfer during this period can only be accomplished with the aid of a computer program. An approximation of

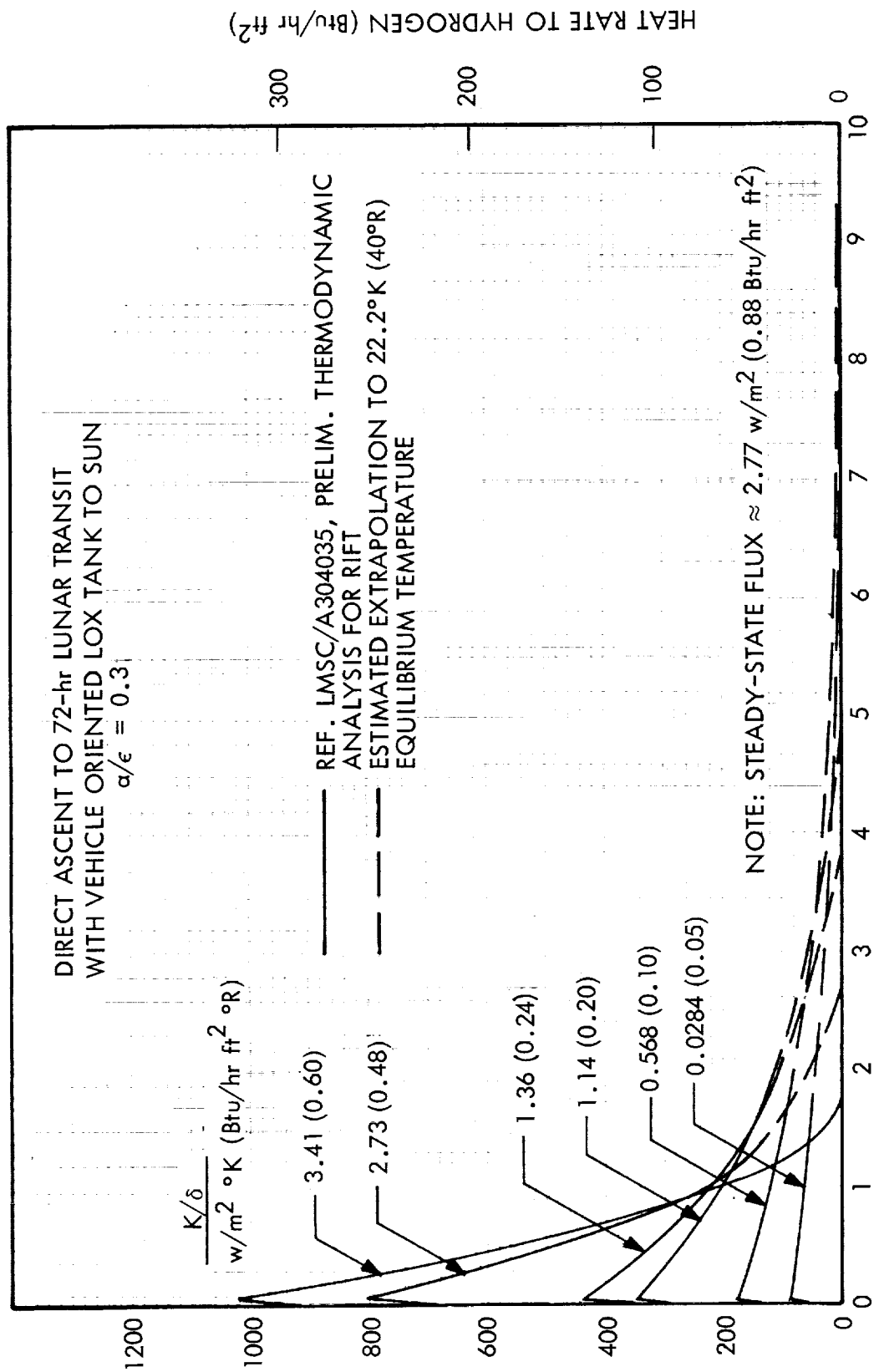

Fig. 3-10 Estimated Sidewall Heat Flux to Hydrogen for Saturn S-IVB/LASS Mission

heat transfer was made for this study by using the averaged absorbed heat flux for a vehicle in a noon lunar orbit as computed by such a machine program. The assumed surface properties included an emissivity of 0.92, a solar absorptivity of 0.16, and an infrared absorptivity of 0.92. The entire average absorbed heat flux of 187.3 w/m^2 (59.4 $Btu/hr-ft^2$) was assumed to result in heating of the hydrogen since the average surface temperature indicates that reradiation was relatively small compared to the total.

Total accumulated heat quantities absorbed by the hydrogen were calculated from the transient heating history described above. Results are presented in Figs. 3-11 through 3-14 for vehicles fueled with hydrogen at the three initial conditions of interest.

Total heat transfer to the hydrogen tank increases approximately 3.5 percent for triple-point liquid, and approximately 7.5 percent for 50% slush, over that corresponding to liquid saturated at 13.1 N/cm^2 (19 psia). These increases result from higher initial temperature differentials across the tank insulation system and from higher heat absorption from the pressurant gases introduced to start the engines and expel the hydrogen during firings.

Increases in temperature differential across the insulation range from 7.2°K (13°R) at tank pre-pressurization (90 sec before liftoff) to 0°K (0°R) after initial saturation at the vent pressure. Assuming a nominal initial hydrogen weight, initial saturation was predicted at approximately 22 hr for triple-point liquid and at approximately 44 hr for 50% slush. These times apply where 1-in. sidewall and 3-in. bulkhead insulation thicknesses are used in both cases. Subsequent to initial saturation times, heat transfer to the hydrogen is identical for all initial conditions.

A secondary effect, reflected in the data presented, results from slight decreases in insulation thermal conductivity for subcooled propellants during the early mission phases. These decreased conductivity values are due to lower average insulation temperatures caused by the cooler propellants. They tend to reduce the increased

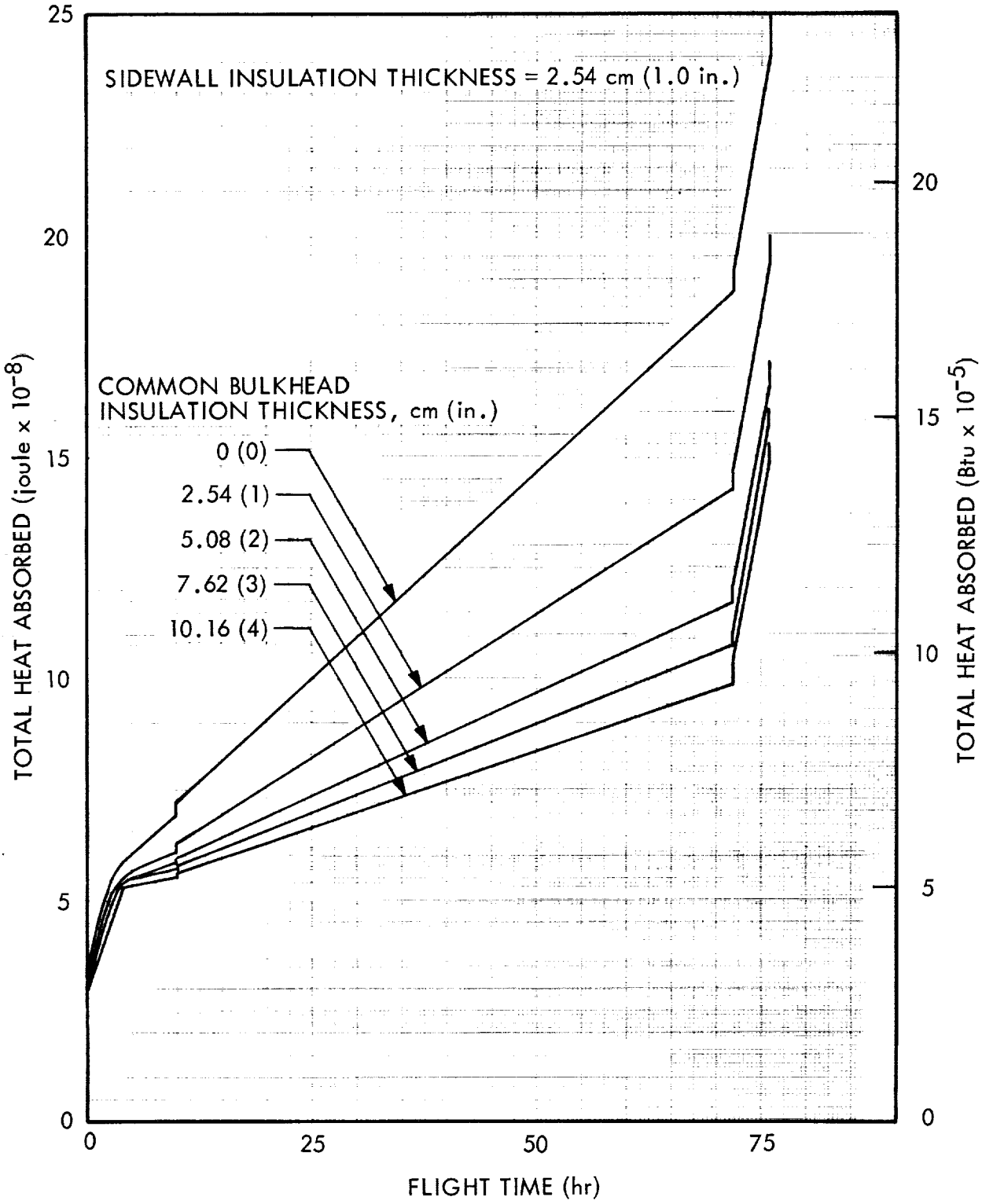

Fig. 3-11 Predicted Heat Transfer to the Hydrogen Tank; Saturated Liquid-Fueled S-IVB/LASS Mission

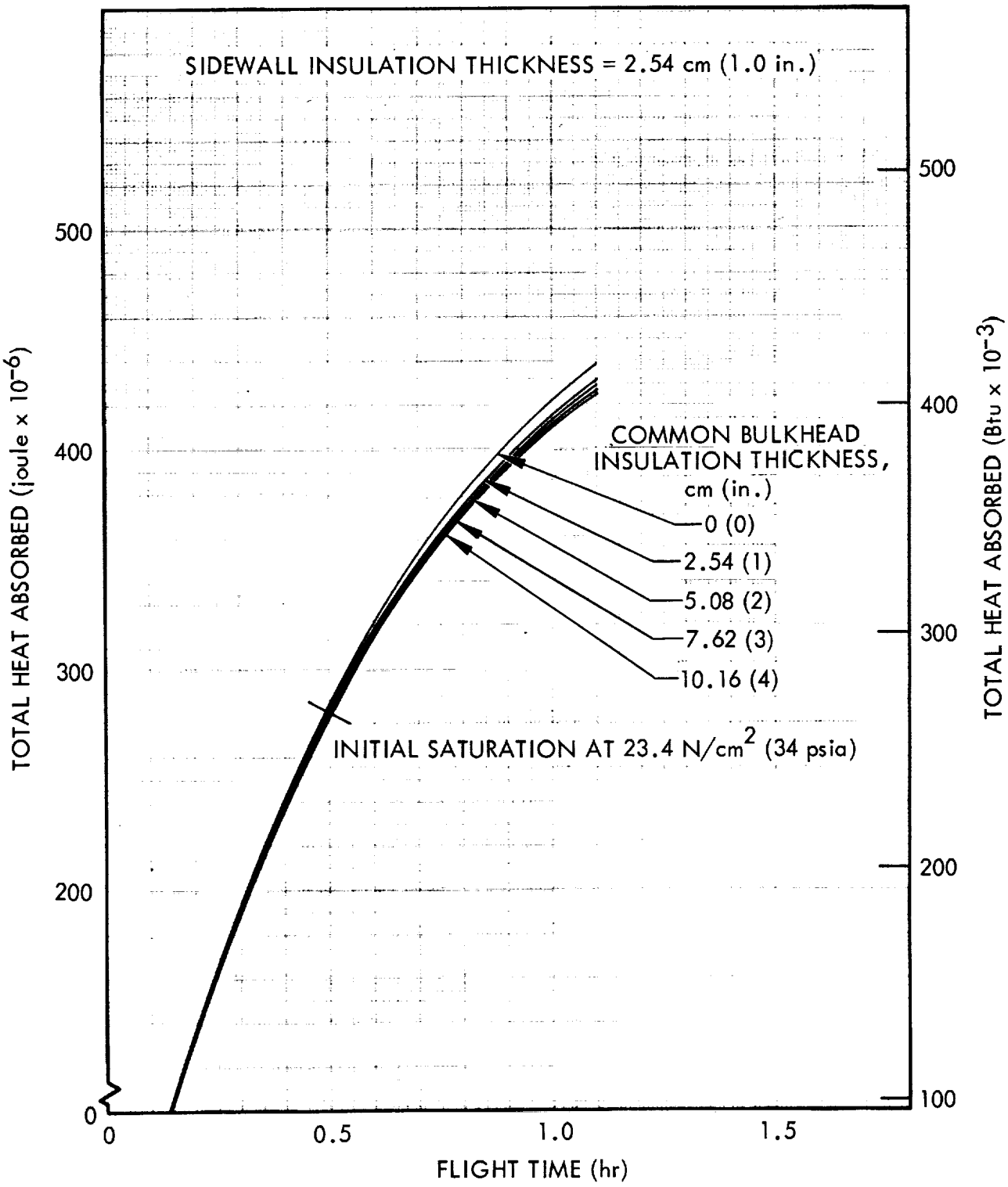

Fig. 3-12 Predicted Heat Transfer to the Hydrogen Tank During Ascent; Saturated Liquid-Fueled S-IVB/LASS Mission

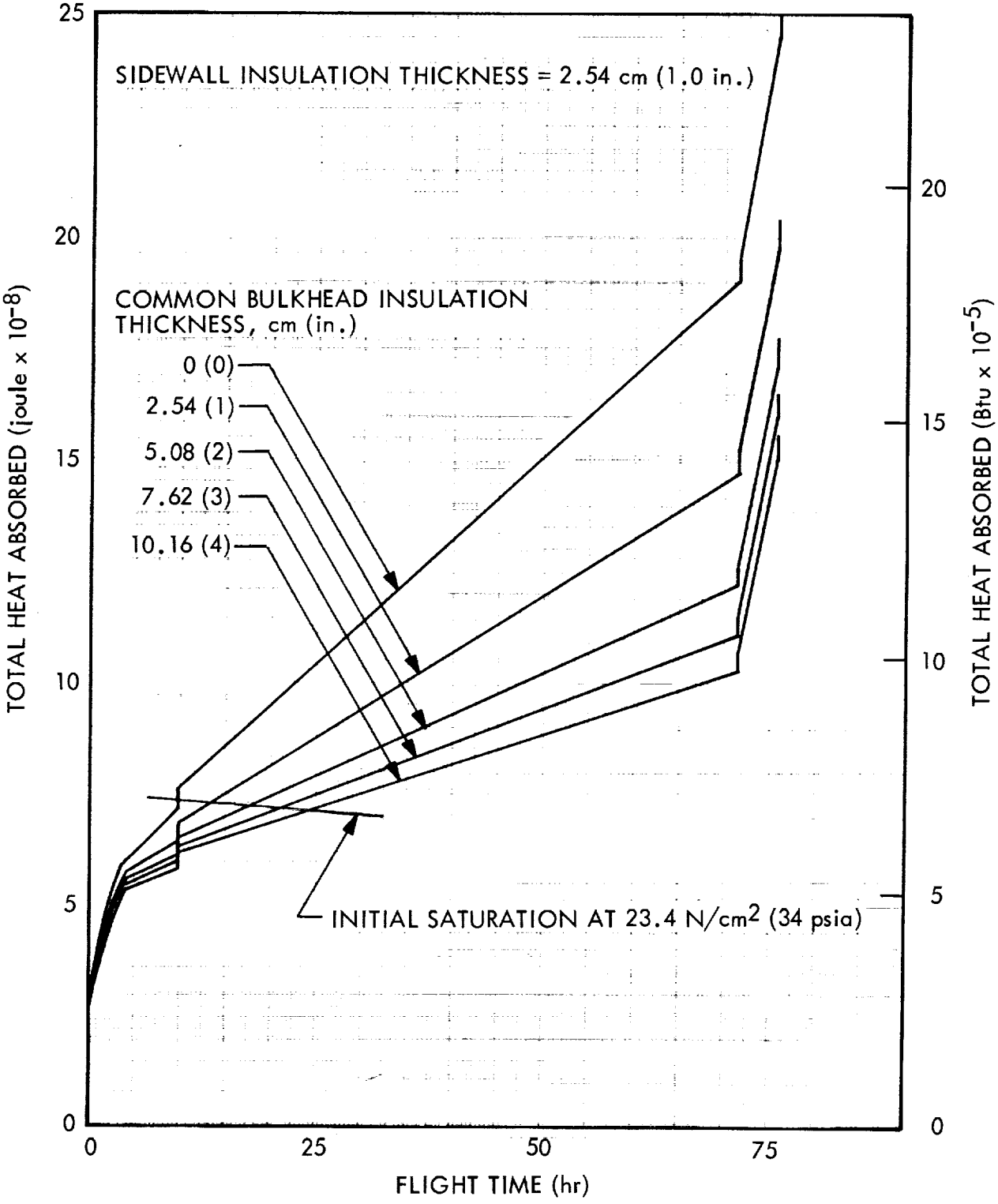

Fig. 3-13 Predicted Heat Transfer to the Hydrogen Tank; Triple-Point Liquid-Fueled S-IVB/LASS Mission

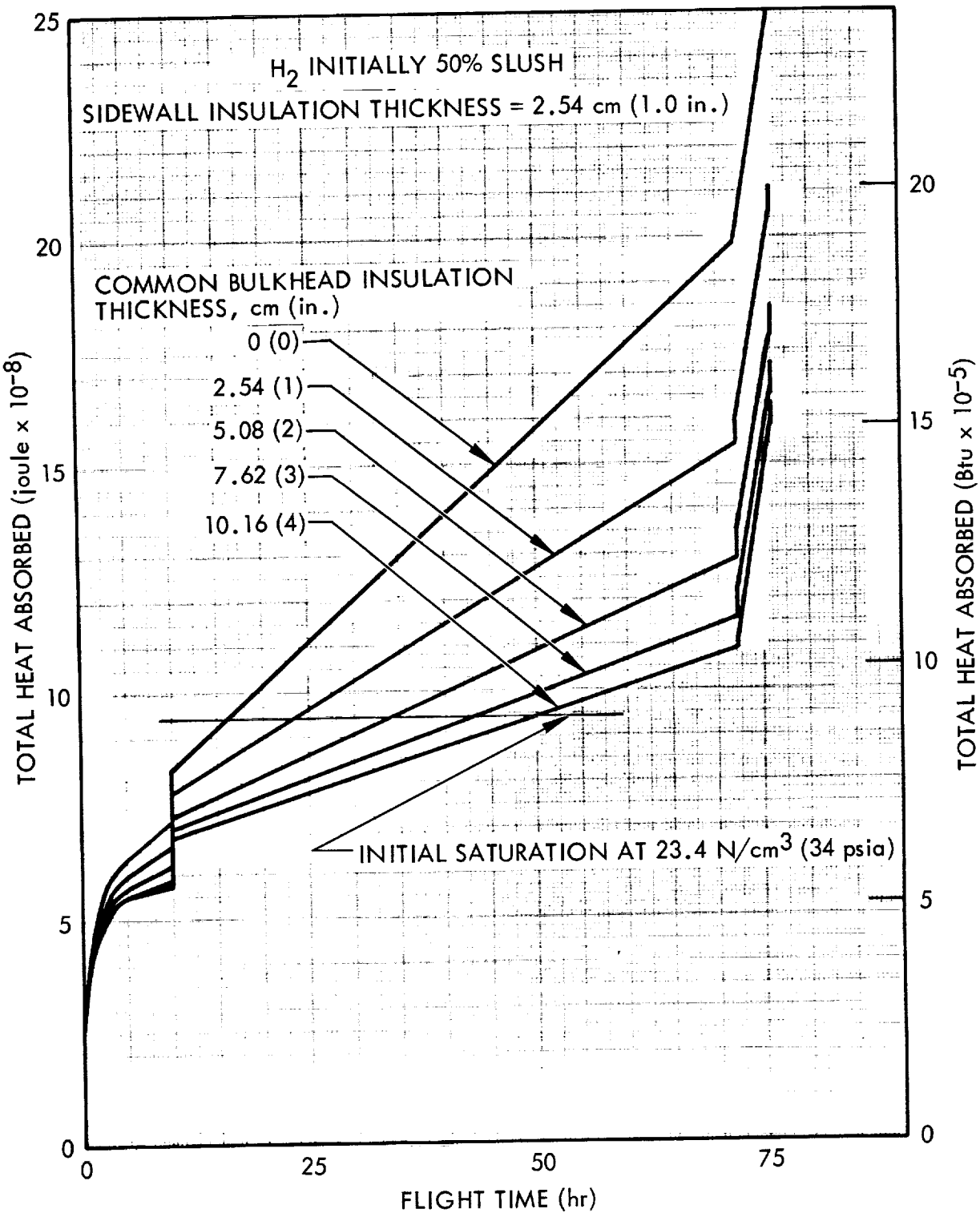

Fig. 3-14 Predicted Heat Transfer to the Hydrogen Tank; 50% Slush-Fueled S-IVB/LASS Mission

heat transfer caused by the higher temperature differentials. The variation of insulation thermal conductivity with average insulation temperature was taken from Fig. 3-9.

Heat absorption from pressurant gases varies with the type of pressurization system and the temperature of the pressurant gas. Table 3-5 presents typical values which were calculated for an all-hydrogen pressurization system. These values are reflected in the heating histories presented in Figs. 3-11 through 3-14.

Table 3-5

SUMMARY OF HEAT TRANSFERRED TO THE HYDROGEN FROM HYDROGEN GAS PRESSURANTS FOR THE S-IVB/LASS MISSION

Initial Condition	LH_2 Sat. at 19 psia Joules (Btu)	T.P. LH_2 Joules (Btu)	50% Slush H_2 Joules (Btu)
Pre-pressurization	2.2995×10^6 (2,180)	5.453×10^6 (5,170)	6.898×10^6 (6,540)
Translunar Firing	36.812×10^6 (34,900)	26.897×10^6 (25,500)	26.897×10^6 (25,500)
1st MCC	4.114×10^6 (3,900)	42.192×10^6 (40,000)	87.548×10^6 (83,000)
2nd MCC	0 (0)	0 (0)	0 (0)
Orbit Retro Firing	33.437×10^6 (31,700)	37.15×10^6 (35,220)	37.15×10^6 (35,220)
De-orbit Firing	5.327×10^6 (5,050)	4.831×10^6 (4,580)	4.831×10^6 (4,580)
Braking Firing	37.656×10^6 (35,700)	44.207×10^6 (41,910)	44.207×10^6 (41,910)

Note that heating histories for five different bulkhead insulation thicknesses are presented for a single sidewall insulation thickness. These data were ultimately used to optimize the bulkhead insulation thickness. A discussion of the optimization

procedure is given later, where it is shown that the selected sidewall insulation thickness depends upon factors other than minimum system weight.

3.4.2.2 Final Optimization Procedure and Results

Optimum insulation thickness for an existing vehicle such as the S-IVB is that which results in a minimum total effective weight of vented propellants plus insulation. Actual vented propellant weights must be multiplied by a boiloff factor for this purpose.

A simplified model was developed and used to predict vented (boiloff) hydrogen weights for the purpose of optimizing the insulation. This model assumed complete thermal mixing of the hydrogen throughout the mission. All heat absorbed by the system after pre-pressurization on the launch pad was assumed to raise the initial energy level of the liquid, or liquid-solid mixture, until saturated vent conditions were reached. The calculation to determine the time of initial venting included the effect of withdrawing impulse propellants for the translunar firing, midcourse corrections, etc. A summary of this calculation is given in Table 3-6 for the three initial hydrogen conditions of interest. The data presented is for a 3-in. common bulkhead insulation thickness and a 1-in. sidewall insulation thickness. Similar calculations were made for each of four other bulkhead insulation thicknesses and for three other sidewall insulation thicknesses.

After initial saturation at 23.443 N/cm^2 (34 psia) for a system pressurized with hydrogen gas only, all subsequent heat absorbed was assumed to result in vaporization of some of the liquid. An average heat of vaporization value was used which corresponds to the average of the initial and final vent pressures. For the cyclic venting mode previously established for the S-IVB, these pressures are 23.443 N/cm^2 (34 psia) and 13.79 N/cm^2 (20 psia), respectively. A portion of the hydrogen vapor thus produced after initial saturation was assumed to fill the additional ullage volume which resulted from liquid removal after that time. The remainder of the vaporized hydrogen was then assumed to vent overboard during the remainder of the mission. The total mass vented overboard was evaluated using the following equation:

Table 3-6

PRELIMINARY PREDICTION OF ENERGY ABSORPTION BY THE HYDROGEN PRIOR TO INITIAL VENTING: S-IVB/LASS[a]

Initial Hydrogen Condition	LH_2 Sat. at 13.1 N/cm^2 (19 psia)	LH_2 Sat. at T.P.	50% SH_2 at T.P.
Initial Energy Ref., joule/gm (Btu/lb)[b]	-248.9 (-107.0)	-309.1 (-132.9)	-338.2 (-145.4)
Initial Hydrogen Loaded, kg (lb)	19,547 (43,094)	19,547 (43,094)	19,547 (43,094)
Total Heat Input During Pre-press., joule (Btu)	14.366×10^6 (13,620)	17.809×10^6 (16,884)	19.254×10^6 (18,254)
Total Heat Input; Liftoff to Translunar Firing at 710 sec. joule (Btu)	12.221×10^7 (115,770)	10.946×10^7 (103,770)	11.912×10^6 (112,930)
Total Heat Input to Translunar Firing at 710 sec, joule (Btu)	13.648×10^7 (129,390)	12.727×10^7 (120,654)	13.837×10^7 (131,184)
Energy Increase to 710 sec, joule/gm (Btu/lb)	6.98 (3.00)	6.51 (2.80)	7.07 (3.04)
Energy Ref. at 710 sec, joule/gm (Btu/lb)	-241.90 (-104.00)	-302.61 (-130.10)	-331.13 (-142.36)
Energy Increment to Sat., joule/gm (Btu/lb) [c]	19.31 (8.30)	80.01 (34.40)	108.53 (46.66)
Heat Increment to Sat. at 23.44 N/cm^2 (34.0 psia) joule (Btu)	14.477×10^7 (137,250)	60.001×10^7 (568,838)	81.385×10^7 (771,570)
Total Heat Absorbed Prior to 1st Vent, joule (Btu)	28.125×10^7 (266,640)	72.728×10^7 (689,492)	95.222×10^7 (902,754)
Flight Time of 1st Vent (hr)	0.501	22.1	44.2
Total H_2 Mass Prior to 1st Vent, kg (lb)[d]	7.501 (16,536)	7,230 (16,093)	7,230 (16,093)
Liquid Mass, kg (lb)	6,954 (15,330)	6,737 (14,853)	6,737 (14,853)
Vapor Mass, kg (lb)	5,470 (1,206)	5,625 (1,240)	5,625 (1,240)

(a) 2.54 cm Sidewall Insulation and 7.62 cm Bulkhead Insulation (1.0 in. Sidewall Insulation and 3.0 in. Bulkhead Insulation)
(b) NBS Monograph 94
(c) Energy Reference = -222.59 joule/gm (-95.7 Btu/lb)
(d) Net remaining after impulse withdrawals

$$W_{BO} = \frac{Q_{total} - Q_{init.\ sat.}}{L_v\,(ave.)} - (M_{v_2} - M_{v_1}) \qquad (3.7)$$

The results of this S-IVB hydrogen tank insulation optimization are presented in Figs. 3-15 and 3-16. The sum of effective hydrogen boiloff plus insulation weight is shown in Fig. 3-15 as a function of sidewall and aft bulkhead insulation thickness for the initially saturated [at 13.1 N/cm^2 (19 psia)] liquid case. These data show that the true optimum sidewall and aft bulkhead insulation thickness is less than 1.27 cm (1/2 in.) considering effective weight. However, approximately 0.64 cm (1/4 in.) of insulation is required just to satisfy present Saturn V launch facility maximum vent rates and to prevent liquefaction during ground hold. Since the existing S-IVB vehicles are presently provided with a 2.54-cm (1-in.) thickness, this thickness was selected and used throughout the remainder of the study. It is noted that the weight penalty associated with 2.54 cm (1 in.) compared to 0.64 cm (1/4 in.) is approximately 258.6 kg (570 lb).

Figure 3-16 shows similar plots of effective weight versus common bulkhead insulation thickness for each of the three initial hydrogen conditions being studied. These data are given only for the selected 2.54 cm (1-in.) sidewall insulation thickness. The optimization shows very little difference in effective weight for thicknesses between 7.62 and 10.16 cm (3 and 4 in.). Therefore, a 7.62-cm (3-in.) thickness was selected for all propellant conditions. It is noted that the penalty associated with the 4.06-cm (1.6-in.) thickness previously predicted is on the order of 90.72 kg (200 lb). Since the total heat absorbed by the hydrogen was finally calculated to be greater than that predicted by the previous analysis, a greater optimum thickness was expected. The present analysis, therefore, confirms the previous analysis.

3.5 VENTING SYSTEM

Subsequent to optimization of the insulation, it was necessary to perform a more sophisticated analysis to determine the venting time history and the individual quantities

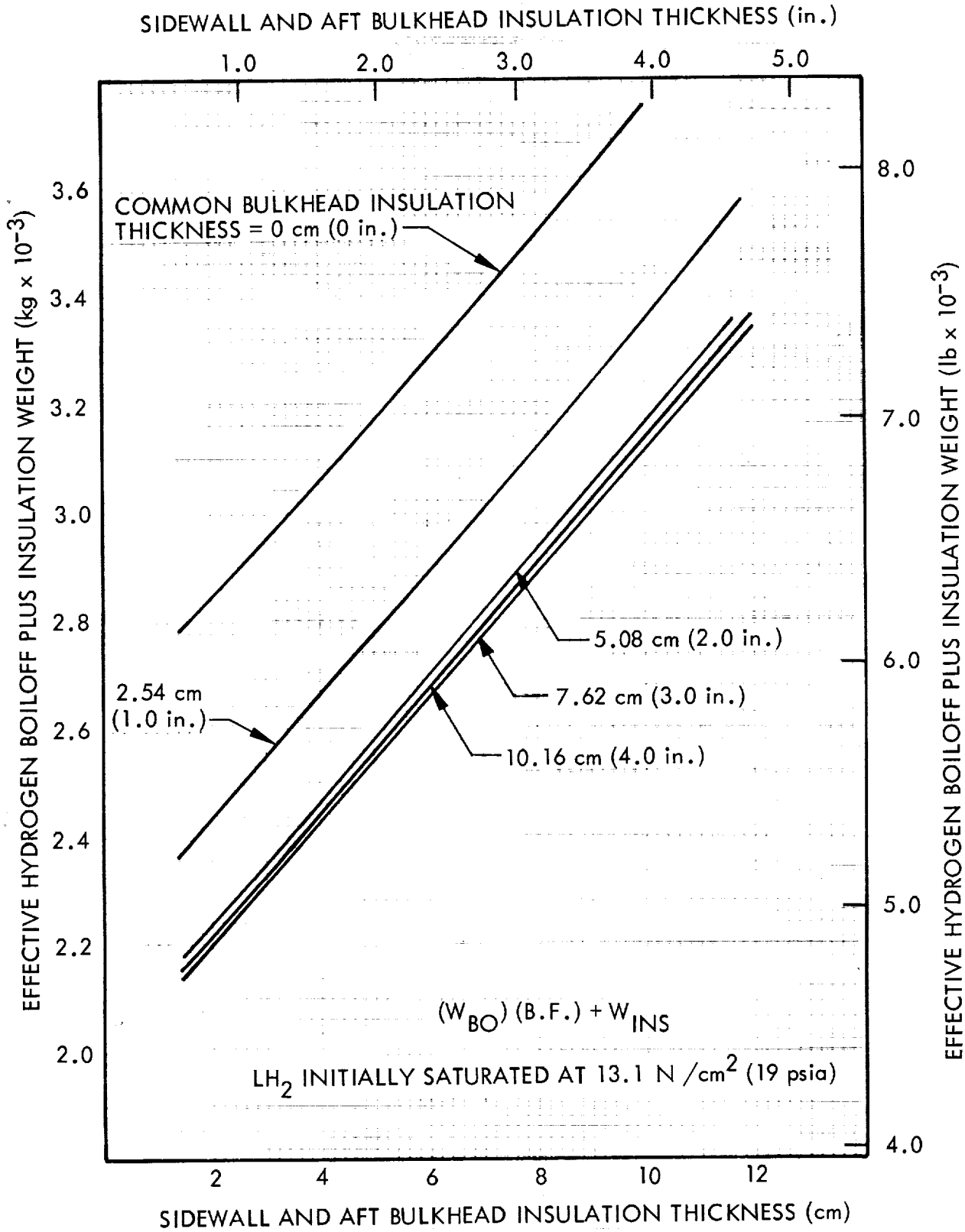

Fig. 3-15 Effective Hydrogen Boiloff Plus Insulation Weight as a Function of Sidewall Insulation Thickness for the Liquid-Fueled S-IVB/ LASS Mission

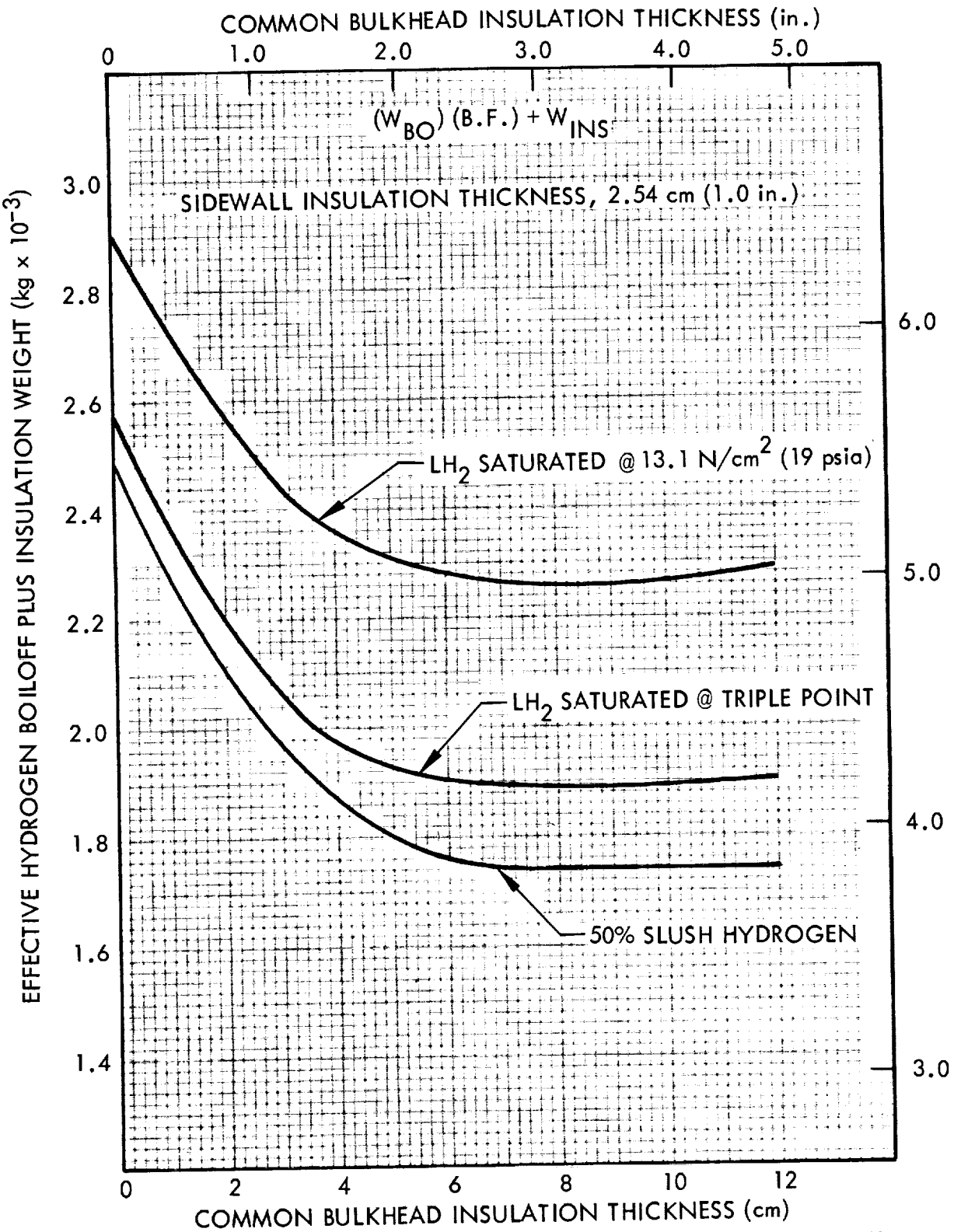

Fig. 3-16 Effective Hydrogen Boiloff Plus Insulation Weight as a Function of Bulkhead Insulation Thickness for the S-IVB/LASS Mission

of hydrogen lost overboard during each vent cycle. For this purpose, a second analytical model was developed and used. Again, complete thermal mixing of the hydrogen was assumed. In this second model, all heat absorbed by the hydrogen after initial saturation was distributed to both the liquid and the vapor. Energy balances were written describing the relationships involved. This was done in general terms for any vent period during which the tank pressure blows down from a given initial pressure to any desired final pressure. A description of the study and the results is given in subsection 2.5 of this report.

These generalized solutions were used to determine ullage pressure and venting histories for selected S-IVB/LASS vehicles fueled with saturated 13.1 N/cm^2 (19 psia) liquid, triple-point liquid, and 50% slush hydrogen. The selected design points were those resulting from a preliminary performance analysis to determine the vehicle gross weights, propellant loadings, and mixture ratios which would yield optimum performance. Self-pressurization and venting cycle pressure limits were then selected to minimize repressurization requirements for engine firings. Also, the venting pressure limits were selected to minimize total vented hydrogen weights. The resulting ullage pressures are presented as a function of mission time in Figs. 3-17 through 3-19, and a summary of vent characteristics is given in Table 3-7.

Development of the ullage pressure-time histories was based on present S-IVB operational procedures, modified as necessary for the LASS mission. To better understand these histories, major events for the saturated 13.1 N/cm^2 (19 psia) liquid-fueled vehicle are indicated in Fig. 3-17 by numbers in parentheses and are described below:

(1) Liquid hydrogen, saturated at 13.1 N/cm^2 (19 psia) is loaded into the S-IVB tank (present S-IVB procedure).

(2) Approximately 60 sec prior to liftoff, the S-IVB ullage is pressurized to approximately 20.7 N/cm^2 (30 psia) with 55.6°K (100°R) GHe from the ground facility (present S-IVB procedure).

(3) Ullage pressure may increase or decay during ascent boost, as shown by the dotted lines.

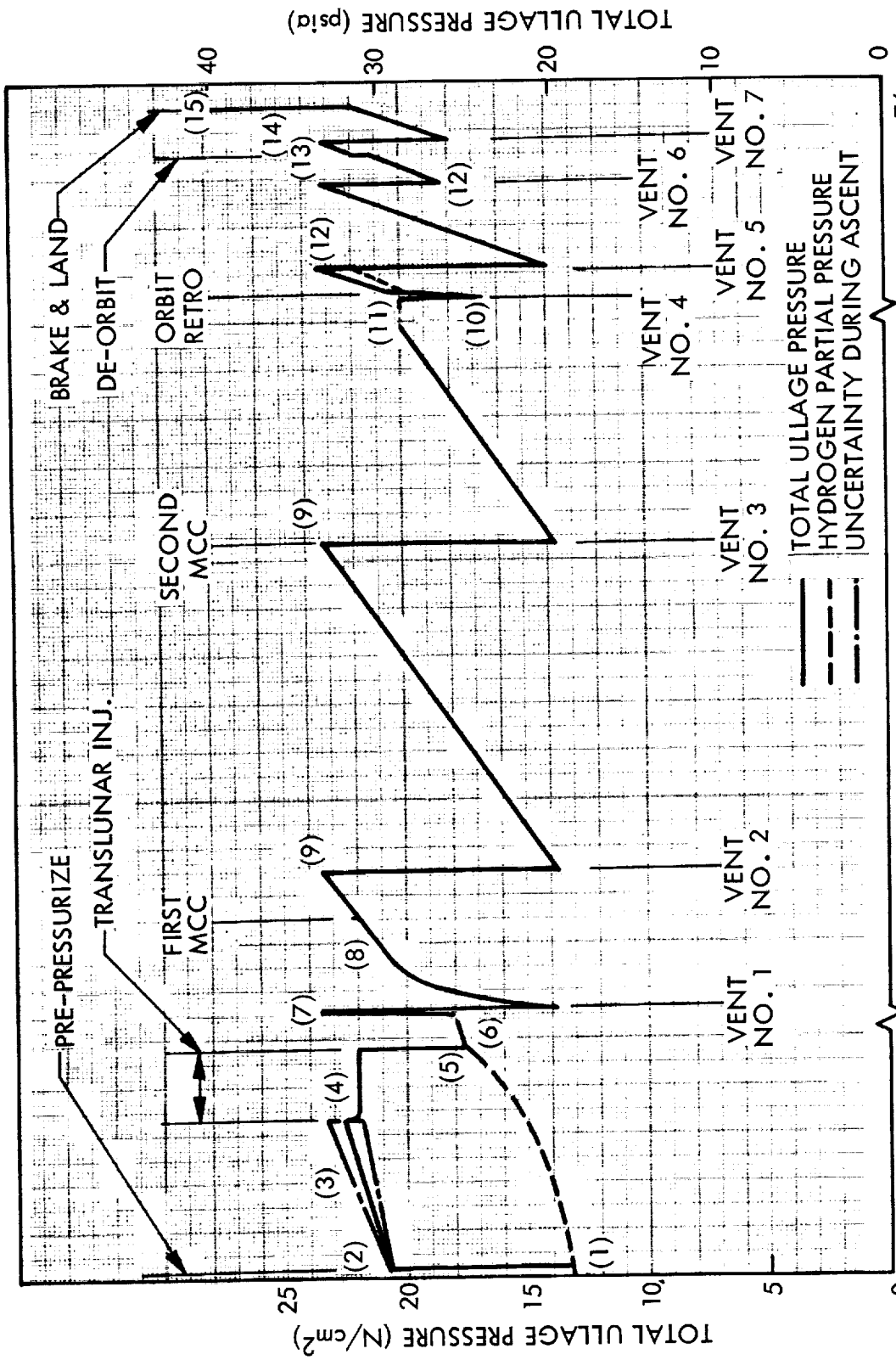

Fig. 3-17 Ullage Pressure-Time History for S-IVB/LASS Fueled With LH_2 Initially Saturated at 13.1 N/cm^2 (19 psia)

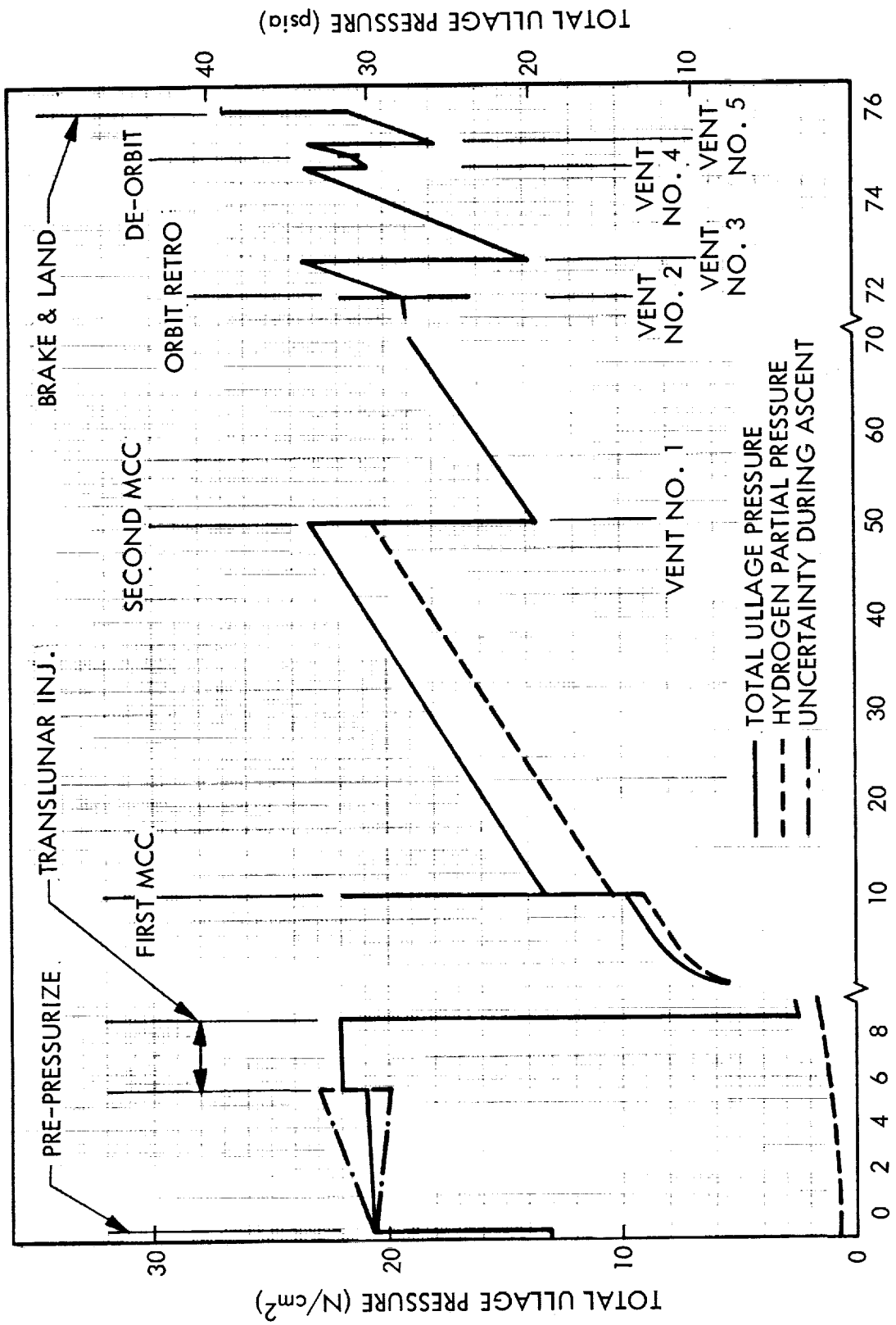

Fig. 3-18 Ullage Pressure-Time History for S-IVB/LASS Fueled With LH_2 Initially Saturated at Triple Point

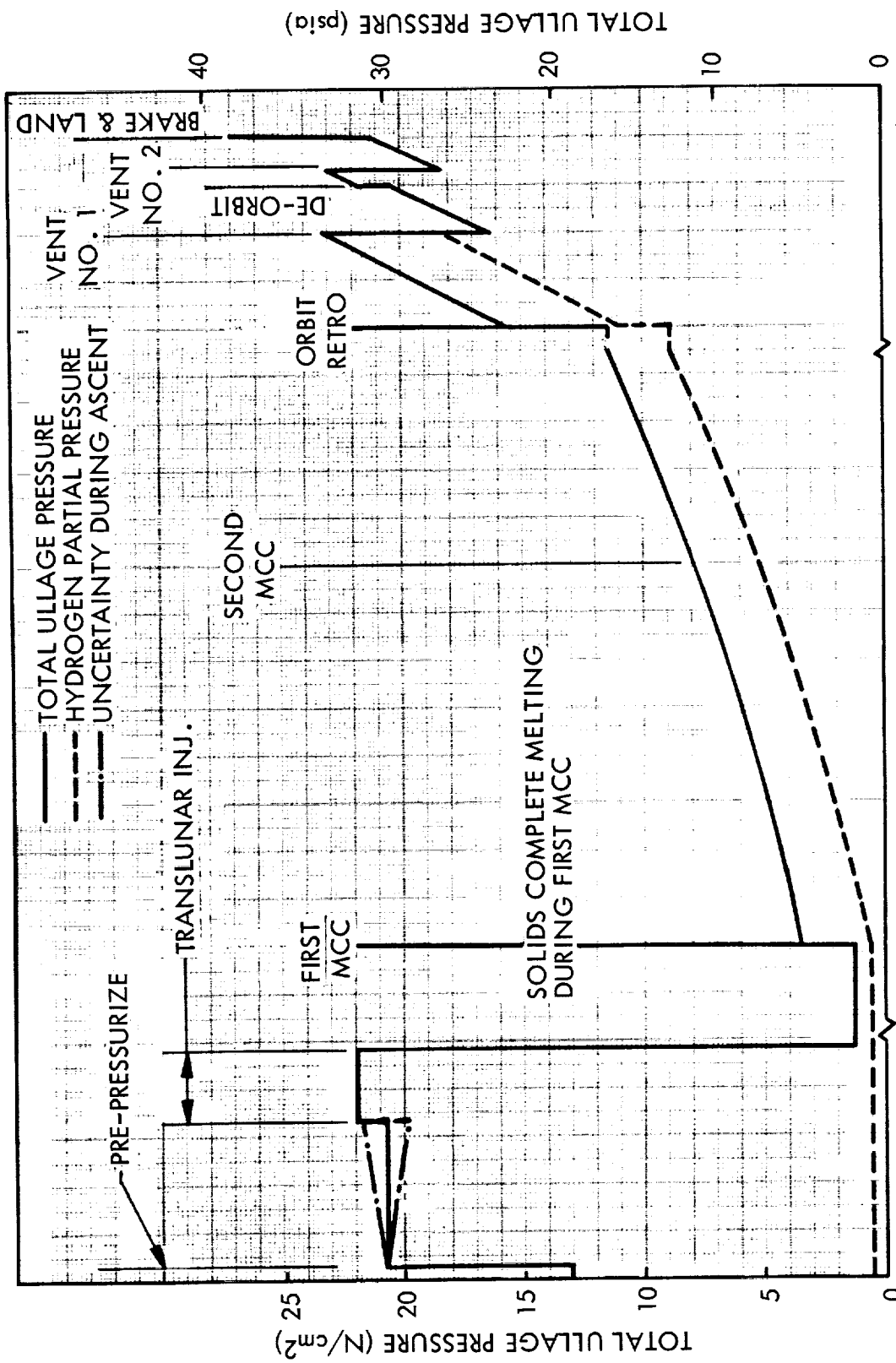

Fig. 3-19 Ullage Pressure-Time History for S-IVB/LASS Fueled With Initially 50% Slush Hydrogen

Table 3-7

SUMMARY OF HYDROGEN TANK VENTING HISTORY FOR THE SATURN S-IVB/LASS MISSION

Initial H_2 Condition	Vent No.	Time of Vent (hr)	Mass H_2 Vented, kg (lb)
LH_2 Sat. @ 13.1 N/cm^2 (19 psia)	1	0.65	638 (1406)
	2	15.0	602 (1327)
	3	49.2	580 (1278)
	4	72.0	214 (473)
	5	72.6	424 (936)
	6	74.4	233 (513)
	7	75.2	226 (498)
	Total		2917 (6431)
LH_2 Sat. @ T.P.	1	50.7	437 (964)
	2	72.0	340 (750)
	3	72.9	470 (1035)
	4	74.8	136 (299)
	5	75.3	261 (575)
	Total		1644 (3623)
50% Slush H_2 (nominal 4.5 to 1 mixture ratio)	1	74.0	116 (256)
	2	75.3	219 (482)
	Total		735 (738)

(4) The J-2/RL10 engine cluster is fired at full thrust for translunar injection; tank is repressurized with ambient helium, if required, to provide a minimum total ullage pressure of 22.1 N/cm^2 (32 psia) approximately 40 sec prior to ignition.

(5) Rapid cooling and pressure decay occur at engine shutdown due to low-gravity mixing.

(6) Ullage pressure rises during coast phases due to solar heating (vehicle is sun oriented).

(7) Vent cycle is initiated by pressure sensor at 23.4 N/cm^2 (34 psia); lower pressure limit is programmed at 13.8 N/cm^2 (20 psia) to allow for a further pressure rise to approximately 21.4 N/cm^2 (31 psia) for first MCC firing.

(8) Approximately 40 sec prior to RL10 ignition at 10-percent thrust for first MCC firing, the tank is repressurized with ambient helium to provide minimum partial pressure of 1 psia above saturated vapor pressure; total pressure may range between 21.4 N/cm^2 (31 psia) and 22.8 N/cm^2 (33 psia) as shown.

(9) Vent cycle is initiated by pressure sensor at 23.4 N/cm^2 (34 psia) and terminated at 13.8 N/cm^2 (20 psia) as required during translunar coast; each vent cycle includes (a) thrust axis alignment to the desired thrust vector, using the APS; (b) ullage orientation with RL10's at low-idle thrust prior to and during vent; and (c) reorienting vehicle to sunline using the APS after venting.

(10) Approximately 60 sec prior to J-2/RL10 engine cluster ignition, for braking into lunar orbit, tank is vented to 16.5 N/cm^2 (24 psia) and repressurized to 22.1 N/cm^2 (32 psia) with cryogenically stored helium heated through the O_2-H_2 burner system; rapid cooling and pressure decay occur at engine shutdown due to low-gravity mixing.

(11) Ullage pressure rises during coast in lunar orbit due to solar and lunar heating (increased heat flux compared to translunar flight).

(12) Venting in lunar orbit is initiated by ullage pressure rise to 23.4 N/cm^2 (34 psia); lower pressure limit is programmed to result in a total pressure of approximately 21 N/cm^2 (31 psia) prior to pressurization for deorbit firing.

(13) Approximately 40 sec prior to RL10 ignition at 10-percent thrust for deorbit firing, tank is repressurized with heated helium to provide 1-psia partial pressure above saturated conditions and a total pressure between 21.4 N/cm^2 (31 psia) and 22.8 N/cm^2 (33 psia) as shown.

(14) Venting after the deorbit firing is initiated by ullage pressure rise to 23.4 N/cm^2 (34 psia); lower limit is programmed to result in a total pressure of approximately 22.1 N/cm^2 (32 psia) prior to pressurization for the braking firing.

(15) Approximately 40 sec prior to J-2/RL10 engine cluster ignition for descent braking, tank is pressurized to 27.6 N/cm^2 (40 psia) with cryogenically-stored helium heated through the O_2-H_2 burner system.

It can be seen by inspection of the ullage pressure histories that variation of the predicted venting times could result in weight penalties for additional vents and for increased pressurization gas requirements. Further, it is apparent that errors in predicting heating rates and stratification effects would cause either premature or delayed venting times. However, the weight penalties associated with these effects can be minimized. One technique, which can be used for this purpose, is that of using the on-board computer, located in the Instrumentation Unit (I.U.), to monitor and control vent pressure limits so that repressurization requirements for the next firing are within design tolerances. The net effect of having an increased number of smaller vents is negligible insofar as their effect on total vented mass is concerned. The real penalty, however, is that of providing more impulse for settling the propellants. Approximately 170 kg (375 lb) of additional preflow, ullaging, and trapped propellants are required for each additional vent. There would also be a penalty associated with reorientation of the vehicle for additional vents, except that sufficient excess capability to satisfy this requirement exists in the present APS modules.

Effects of stratification causing premature venting can be minimized with use of a tank-pressure-actuated mixer system located in the hydrogen tank. Preliminary calculations show that such a system would weigh less than 4.5 kg (10 lb) for the mixer, motor, wiring, and controls. Power could be supplied from the I.U. fuel cells.

The venting mode used for this study assumes that the gravity environment provided by the RL10 engines in the idle mode is sufficient to prevent excessive venting of entrained liquid. This phenomenon was observed on the S-IVB/AS-203 orbital experiment (Ref. 3-5). The idle-mode settling force is approximately 5×10^{-3} g's for the S-IVB/LASS vehicle. This is approximately 13.5 times higher than the 3.7×10^{-4} g's provided on the AS-203 vehicle. Detailed investigations are required to determine whether a problem would exist for the venting mode selected.

3.6 PRESSURIZATION SYSTEM

General pressurization studies were completed and are discussed in subsection 2.6 of this report. The more important considerations which apply to the S-IVB/LASS vehicle are summarized below. Total pressurization system requirements are presented in Table 3-8 for optimized vehicles fueled with each of the three initial hydrogen conditions of interest.

A single technique was assumed, for study purposes, to expel hydrogen from the tank during operation of the engines. The expulsion pressurizing medium is warm hydrogen gas, which is bled from the engine. This is exactly the technique presently used on the Saturn V/S-IVB vehicle. Two candidate systems were considered for repressurization of the hydrogen tank prior to each engine start which requires NPSP. Tank-head idle-mode starts would not require repressurization unless the tank ullage pressure were to inadvertently drop below 13.8 N/cm^2 (20 psia). The repressurization systems considered are (1) a combination of ambiently stored helium for minor gas requirements and cryogenically stored helium, heated with the existing O_2-H_2 burner system, for major gas requirements, and (2) ambiently stored hydrogen gas for all requirements. The latter system would use a relatively low-pressure accumulator to store hydrogen collected from the engine bleed system during each firing.

The stored gas would then provide repressurization requirements for the next succeeding engine start cycle. The helium repressurization system was selected for study analyses primarily because it exists on the present S-IVB and is consistent with the

Table 3-8

SUMMARY OF PRESSURIZATION WEIGHT REQUIREMENTS FOR S-IVB/LASS MISSION

Mission Event		Initial Hydrogen Condition								
		Sat. @ 13.1 N/cm^2 (19 psia)			T.P. Liquid			50% Slush		
		Gas Wt., kg (lb)	Hdw. Wt., kg (lb)	Mode	Gas Wt., kg (lb)	Hdw. Wt., kg (lb)	Mode	Gas Wt., kg (lb)	Hdw. Wt., kg (lb)	Mode
Pre-Launch Press.		6 (13)	0 (0)	A	6 (13)	0 (0)	A	6 (13)	0 (0)	A
Translunar Injection	Repress.	0 (0)	0 (0)	–	0 (0)	0 (0)	–	0 (0)	0 (0)	–
	Expulsion	78 (171)	0 (0)	C	66 (146)	0 (0)	C	75 (165)	0 (0)	C
1st MCC	Repress.	5 (10.2)	64 (140)	D	76 (168)	114 (252)	B	131 (289)	196 (433)	B
	Expulsion	0 (0)	0 (0)	–	0 (0)	0 (0)	–	0 (0)	0 (0)	–
2nd MCC		No Pressurant Required								
Orbit Retro	Repress.	40 (88)	60 (132)	B	37.1 (81.7)	55 (122)	B	65 (144)	98 (216)	B
	Expulsion	12 (27)	0 (0)	C	14.4 (31.7)	0 (0)	C	15 (32)	0 (0)	C
Deorbit	Repress.	7 (16)	99 (219)	D	6 (13)	81 (178)	D	8.5 (18.7)	116 (256)	D
	Expulsion	0 (0)	0 (0)	–	0 (0)	0 (0)	–	0 (0)	0 (0)	–
Braking and Landing	Repress.	49 (107)	73 (161)	B	46 (102)	69 (153)	B	41.9 (92.3)	63 (139)	B
	Expulsion	17 (37)	0 (0)	C	21 (46)	0 (0)	C	28.1 (61.9)	0 (0)	C
Totals	He Gas	107 (234)			171 (378)			253 (557)		
	H_2 Gas	107 (235)			101 (224)			118 (259)		
	Hardware		296 (652)			319 (705)			473 (1044)	

Modes of Pressurization

A = Ground facility He at 55.6°K (100°R)

B = He stored in bottle at LH_2 temp., heated to 138.9°K (250°R) with gas burner, $M/M_{rqd.}$ = 2.5

C = GH_2 engine bleed at 111°K (200°R)

D = He from Isentropic blow-down of bottle at radiation equilibrium temp., 222.2°K (400°R), $M/M_{rqd.}$ = 14.7

"minimum-change" philosophy. System weight savings might be achieved with use of the hydrogen accumulator, but considerable analysis would be required to establish weight comparisons. Such analysis was considered irrelevant to this study since the choice of systems would not strongly influence the comparison of pressurant requirements for different initial hydrogen conditions.

The pressurization system analysis revealed one significant problem area peculiar to the S-IVB/LASS mission. The problem is that of starting the RL10 engines for the subcooled liquid- or slush-fueled vehicles to perform the first midcourse correction. As noted previously, propellant orientation prior to repressurization for major engine starts is achieved by starting and running the RL10's in a tank-head idle mode. The engines do not have an NPSP requirement for this mode. This means that the feed pumps are bypassed and propellants can be fed directly into the engine as liquids, vapors, or a combination of both. However, if the partial pressure of hydrogen is low and helium repressurization is used, the engines would not start or run in the idle mode because of the high relative concentration of helium.* This occurs for the first midcourse correction firing of S-IVB/LASS vehicles fueled with either triple-point liquid or 50-percent slush. Two alternates were considered in performing the study analyses: (1) substituting ambiently stored hydrogen gas for the first midcourse repressurization only, and (2) using the APS modules to provide impulse for settling the propellants for the midcourse firing. The second alternate was selected after analysis showed that system weights would be excessive if hydrogen gas were used for only one repressurization cycle. No problem exists for later firings since the bulk hydrogen will have heated considerably and the concentration of hydrogen in the ullage is then sufficient to start and run the engines.

*It was estimated by Pratt & Whitney that a maximum concentration of 10-percent helium (by volume) could be tolerated in the idle mode.

3.7 TANK-AFFECTED STRUCTURES

Structural modifications to the Saturn V/S-IVB vehicle which are necessary for it to perform the LASS mission were discussed in subsection 3.1. Estimates of the weight adjustments needed to obtain performance comparisons were taken from Ref. 3-1.

The only additional structural modifications considered during this study program were: (1) those associated with the addition of a liquid return line, shutoff valve, and disconnect for the recirculation tank loading system, and (2) minor changes in support structure for quantity- and quality-sensing instrumentation, feed-line screen and baffles, and additional pressurant bottles and plumbing. Weights were estimated for these modifications and are given in subsection 3.9. No detailed design work was performed during this study.

3.8 PERFORMANCE ANALYSIS

The velocity increment required to inject the S-IVB/LASS vehicle into a translunar trajectory varies with S-IVB ignition weight and with transit time. Figure 3-20 presents a plot of velocity requirements for a range of ignition weights and for two specific transit times. Values used in the study analyses were obtained from this figure for the 72-hr transit.

A preliminary performance analysis was conducted to determine optimum S-IVB ignition weights, propellant loadings, and mixture ratios. A summary of ignition weights, required velocity increments, mixture ratios, and specific impulse values used for this preliminary analysis is given in Table 3-9. For study purposes, the impulse increment provided by the RL10 engines during idle-mode settling of propellants and prior to scheduled impulse firings was assumed to contribute to the total velocity increment required from that firing. The impulse obtained from propellant settling prior to and during venting was neglected. Vented hydrogen weights used in the preliminary performance analysis were taken from the preliminary venting analysis. Figures 3-21 through 3-23 present the results of the preliminary performance analysis. Preliminary design points selected for the refined analysis are shown on the figures.

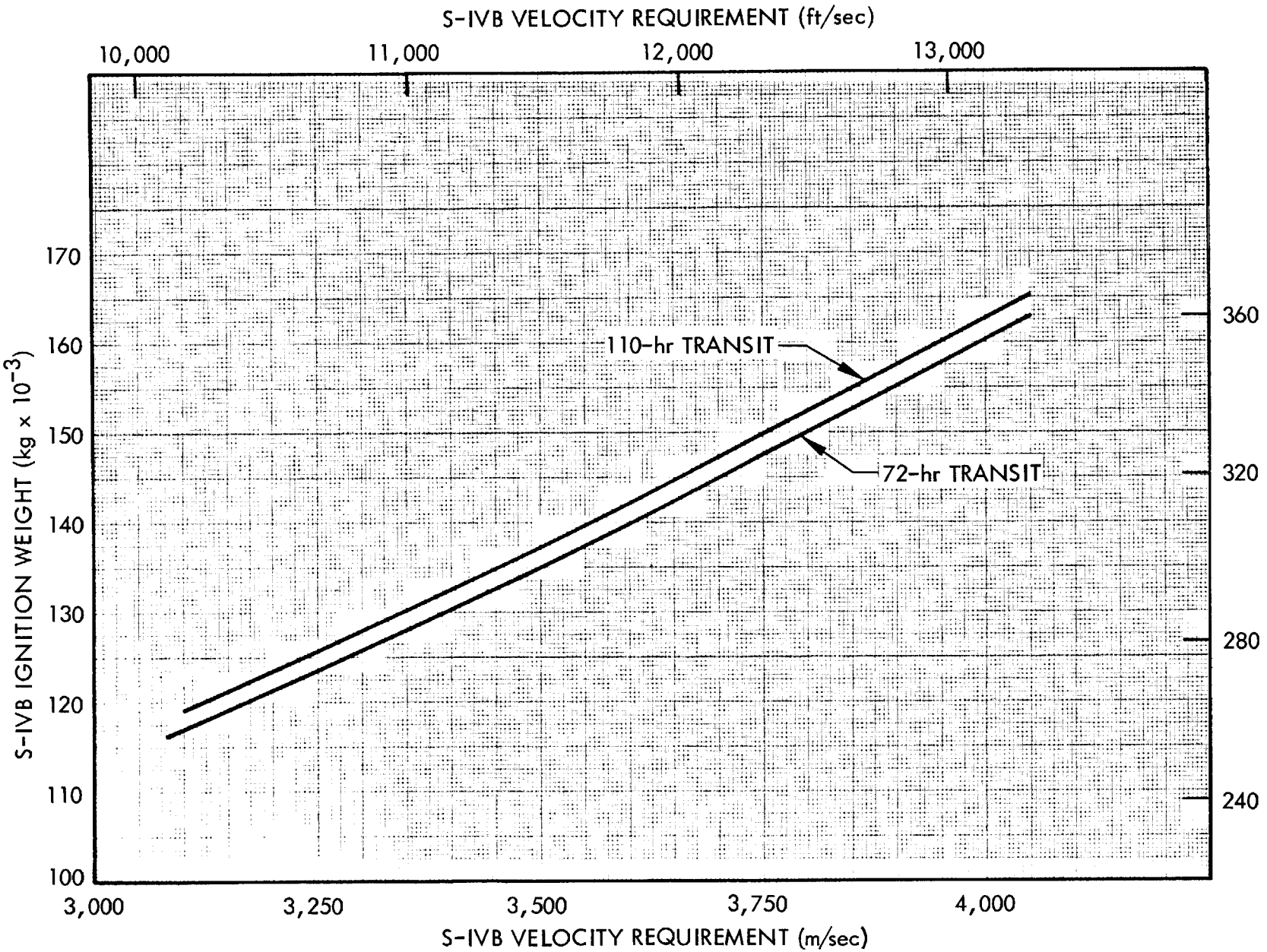

Fig. 3-20 S-IVB Velocity Requirement as a Function of Ignition Weight and Transit Time, S-IVB/LASS Mission

Table 3-9

SUMMARY OF PERFORMANCE DATA FOR S-IVB/LASS MISSION

Firing Description	Performance Analysis	Initial Hydrogen Condition	S-IVB Ignition Weight kg (lb)	Total Req'd ΔV, m/sec (fps)	RL10 Ullaging ΔV, m/sec (fps)	Net Firing ΔV, m/sec (fps)	Engine Mixture Ratio (O/H by Wt.)	J-2 + RL10 Specific Impulse m/sec, (sec)
1. Translunar Injection at 560 sec	Preliminary	Liquid Sat. @ 13.1 N/cm^2 (19 psia)/Triple Point Liquid or 50% Slush	117,936 (260,000)	3,109 (10,200)	0 (0)	3,109 (10,200)	4.4	4236/4233 (431.9/431.6)
							5.0	4205/4201 (428.8/428.4)
							5.6	4159/4159 (424.1/424.1)
			136,080 (300,000)	3,510 (11,515)		3,510 (11,515)	4.4	4236/4233 (431.9/431.6)
							5.0	4205/4201 (428.8/428.4)
							5.6	4159/4159 (424.1/424.1)
			154,224 (340,000)	3,871 (12,700)		3,871 (12,700)	4.4	4236/4233 (431.9/431.6)
							5.0	4205/4201 (428.8/428.4)
							5.6	4159/4159 (424.1/424.1)
	Final	13.1 N/cm^2 (19 psia) Liquid T.P. Liquid 50% Slush	128,029 (282,250)	3,338 (10,950)		3,338 (10,950)	5.5	4168 (425.0)
			136,565 (301,070)	3,519 (11,545)		3,519 (11,545)	4.8	4207 (429.0)
			137,661 (303,485)	3,542 (11,620)		3,542 (11,620)	4.5	4228 (431.1)
			138,439 (305,200)	3,562 (11,685)		3,562 (11,685)	4.2	4239 (432.2)
2. First MCC at 10 hr	All	All	–	87 (285)	12 (39)	75 (246)	5.0	4266 (435.0)
3. Second MCC at 50 hr	All	All	–	5 (15)	0 (0)	4.6 (15)	5.0	4021 (410.0)

Table 3-9 (Continued)

Firing Description	Performance Analysis	Initial Hydrogen Condition	S-IVB Ignition Weight kg, (lb)	Total Req'd ΔV, m/sec (fps)	RL10 Ullaging ΔV, m/sec (fps)	Net Firing ΔV, m/sec (fps)	Engine Mixture Ratio (O/H by Wt.)	J-2 + RL10 Specific Impulse m/sec, (sec)
4. Lunar Orbit Retro at 72 hr	Preliminary	All	–	982 (3,222)	20 (66)	962 (3,156)	4.4	4236 (431.9)
							5.0	4205 (428.8)
							5.6	4159 (424.1)
	Final	13.1 N/cm^2 (19 psia) Liquid T.P. Liquid 50% Slush					5.5	4168 (425.0)
							4.8	4217 (430.0)
							4.5	4231 (431.4)
							4.2	4242 (432.5)
5. Deorbit at 75 hr	All	All	–	31 (100)	16 (53)	47 (14)	5.0	4266 (435.0)
6. Descent Braking at 76 hr	Preliminary	All	–	1,804 (5,919)	24 (79)	1,780 (5,840)	4.4	4236 (431.9)
							5.0	4205 (428.8)
							5.6	4159 (424.1)
	Final	13.1 N/cm^2 (19 psia) Liquid T.P. Liquid 50% Slush					5.5	4168 (425.0)
							4.8	4217 (430.0)
							4.5	4231 (431.4)
							4.2	4242 (432.5)
7. Hover and Landing at 76 hr	All	All	–	280 (919)	0 (0)	280 (919)	5.0	4335 (442.0)

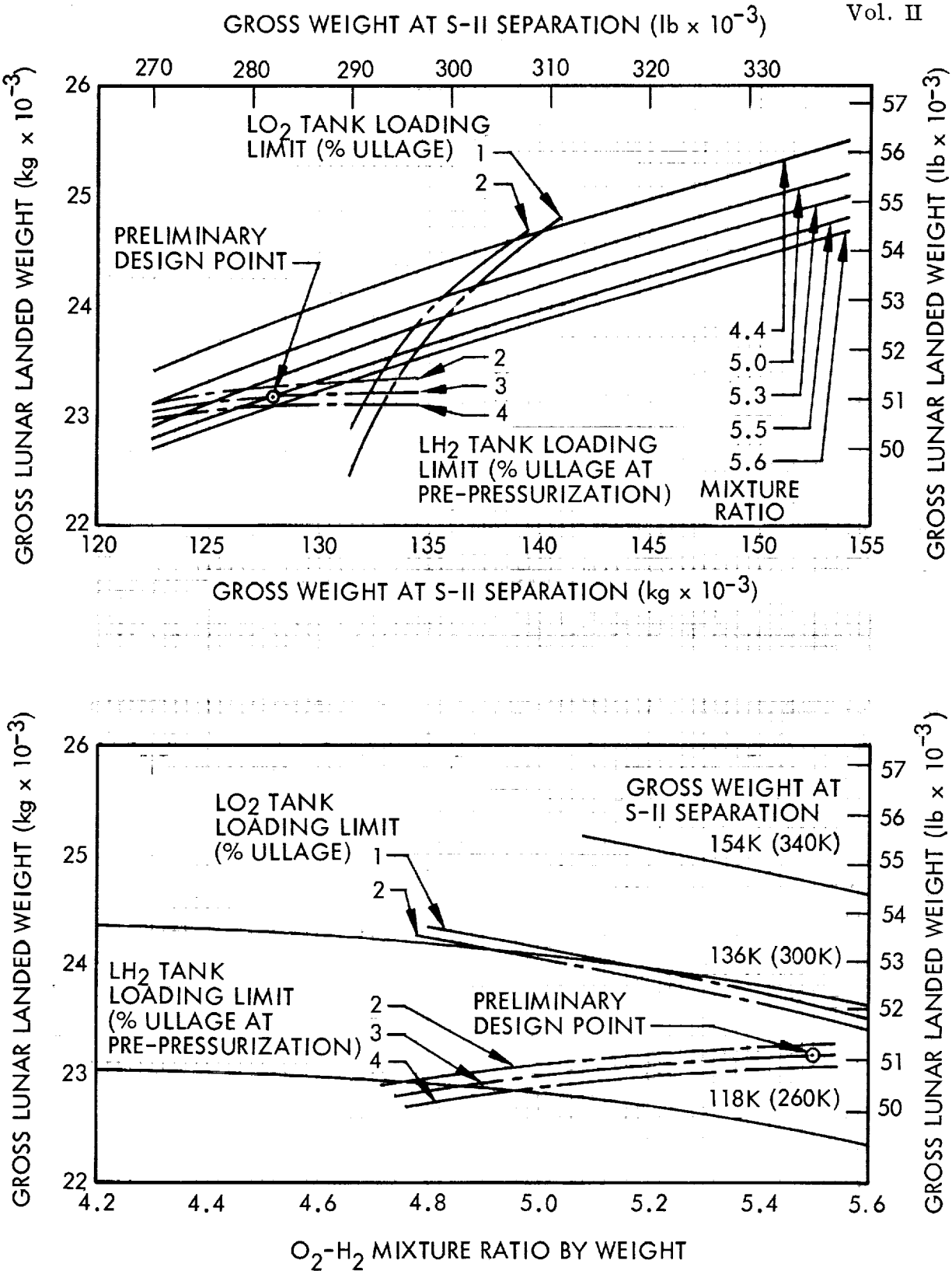

Fig. 3-21 Gross Lunar Landed Weight as a Function of Gross Weight (at S-II Separation) and Mixture Ratio for S-IVB/LASS Fueled With LH_2 Saturated at 13.1 N/cm^2 (19 psia)

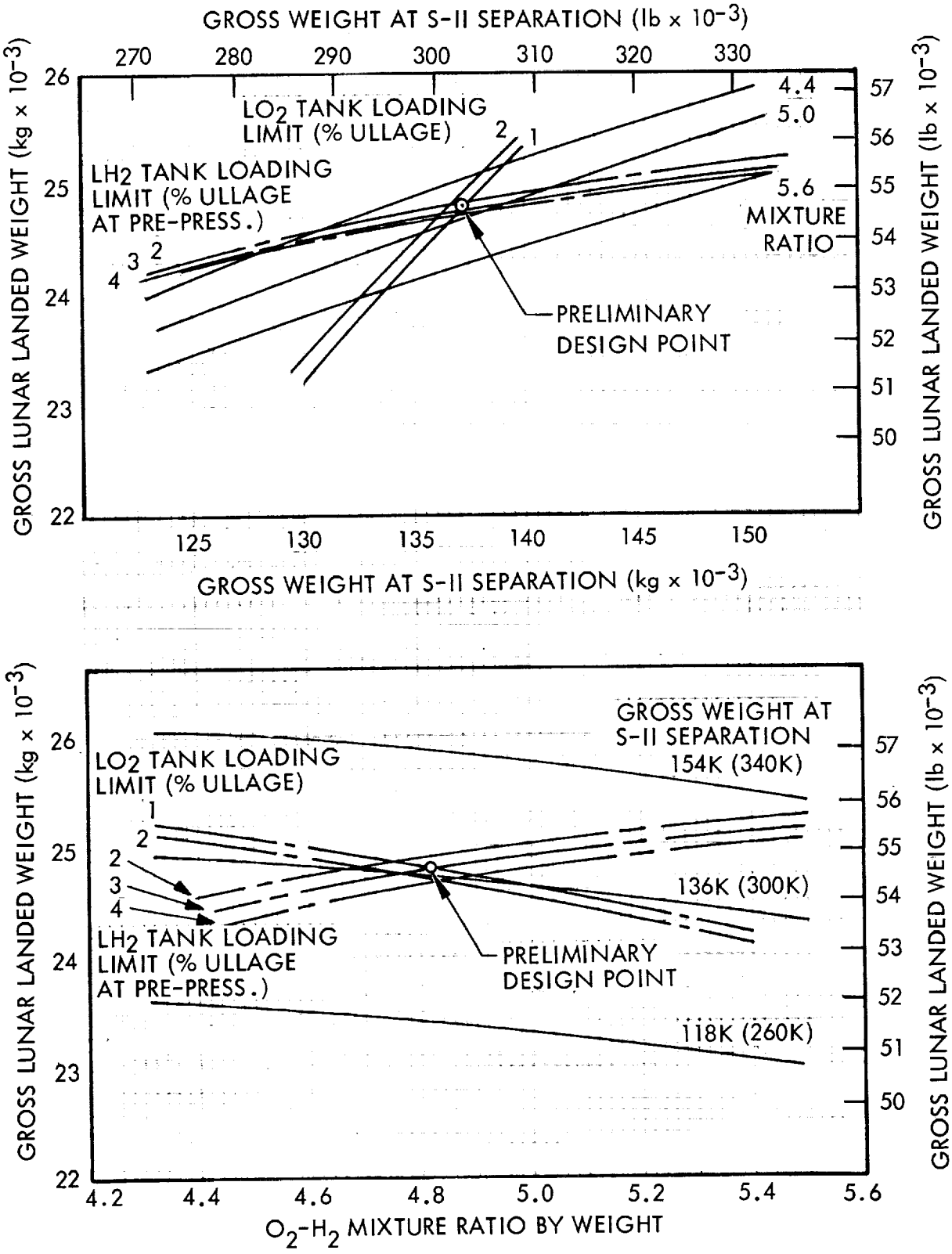

Fig. 3-22 Gross Lunar Landed Weight as a Function of Gross Weight (at S-II Separation) and Mixture Ratio for S-IVB/LASS Fueled With LH_2 at Triple Point

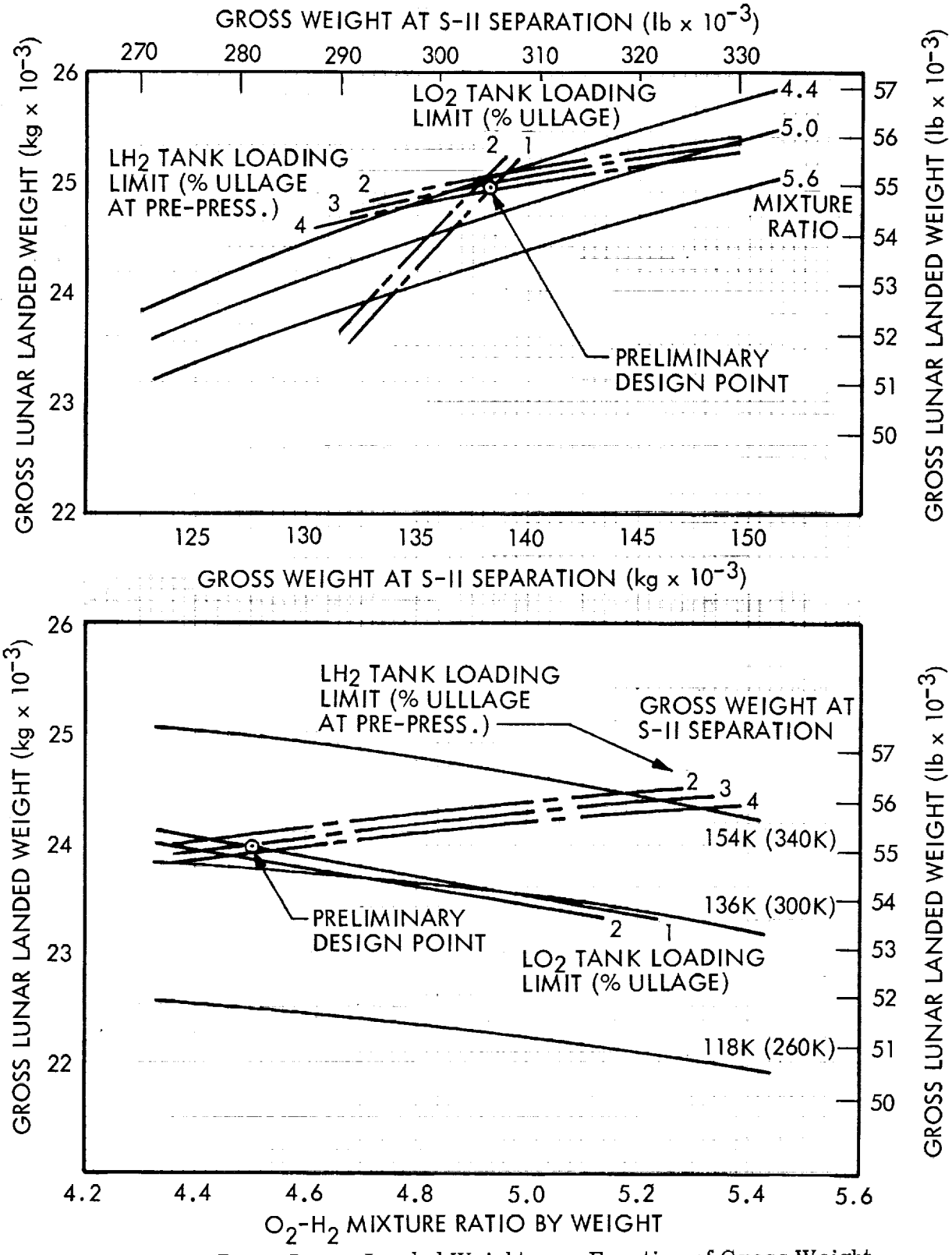

Fig. 3-23 Gross Lunar Landed Weight as a Function of Gross Weight (at S-II Separation) and Mixture Ratio for S-IVB/LASS Fueled With 50% Slush Hydrogen

A more refined performance analysis was then conducted using inputs from the preliminary performance analysis and the pressurization and venting studies discussed elsewhere in this report. Performance data used in this analysis are also summarized in Table 3-9. Results of the second performance analysis show that the design points selected for the saturated 13.1 N/cm^2 (19 psia) and triple-point liquid cases were approximately correct. However, an excess amount of liquid hydrogen residual resulted for the 50-percent slush case. This means that an additional payload gain could be achieved by off-loading hydrogen, or by further reducing the mixture ratio below the 4.5 to 1 limit for which guaranteed engine performance data are available. Further investigation is needed to determine the ullage pressure and venting histories and performance that would result from off-loading. However, an estimate of performance was calculated for the other alternative, namely, reducing the mixture ratio while increasing S-IVB ignition weight (and payload weight) to the point where both propellants are depleted to a reasonable residual weight. The ullage pressure and venting histories previously developed for a fully loaded hydrogen tank would be approximately correct for this alternative. *

Figure 3-24 shows the relationship of total tanked hydrogen weight to percent ullage volume. The maximum loading limits assumed for this study are those which correspond to 3-percent ullage volume at pre-pressurization. As shown, the resulting ullage volume at ignition for translunar injection is approximately 2 percent, which was considered to be satisfactory.

3.9 WEIGHT AND PAYLOAD SUMMARIES

Tables 3-10 through 3-13 present estimates of dry inert weights, firing-associated propellant weights, vent-associated propellant weights, and APS impulse requirements. These weights were used in both the preliminary and refined performance analyses of all S-IVB/LASS vehicles. Table 3-14 presents a detailed propellant summary for the vehicles analyzed in the refined performance analysis only.

*Discussions with representatives of both Pratt & Whitney Aircraft and Rocketdyne have indicated that a reduction in engine mixture ratio to the optimum of 4.2 to 1 appears to be entirely feasible.

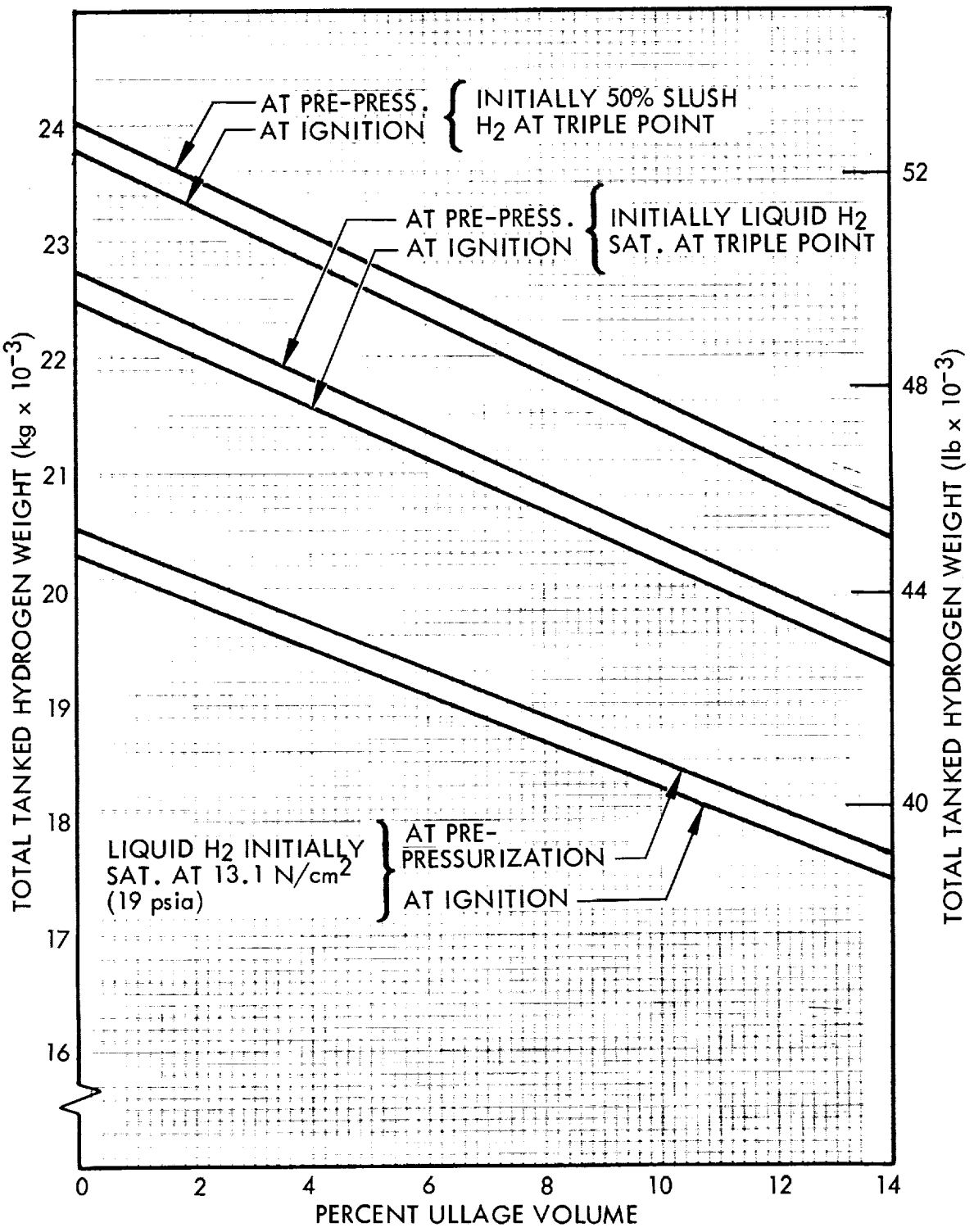

Fig. 3-24 Total Tanked Hydrogen Weight as a Function of Percent Ullage Volume at Pre-Pressurization and at Ignition for Translunar Firing

Table 3-10

ESTIMATE OF S-IVB/LASS DRY INERT WEIGHTS

Item	Ref. Source	LH_2 Sat. @ 13.1 N/cm^2 (19 psia) kg (lb)	LH_2 Sat. @ T.P. kg (lb)	50% Slush H_2 @ T.P. kg (lb)
Saturn V/S-IVB Basic Structure (Less 550 lb Battery Weight)	DAC 56365P	10,546 (23,250)	10,546 (23,250)	10,546 (23,250)
Landing Gear	↓	1,071 (2,360)	1,071 (2,360)	1,071 (2,360)
Power Supply (3 Fuel Cells Plus Peaking Batteries)	↓	724 (1,597)	724 (1,597)	724 (1,597)
Instrument Unit (Modified by Addition of Radiator and Removal of Sublimator)	↓	1,911 (4,212)	1,911 (4,212)	1,911 (4,212)
Structural Mods, Insulation, and Descent Electronics	↓	649 (1,430)	649 (1,430)	649 (1,430)
Two RL10 Engines and Associated Subsystems	↓	408 (900)	408 (900)	408 (900)
Additional Pressurization System Requirements	Present Lockheed Study	250 (550)	277 (610)	426 (940)
Additional Instrumentation and Wiring for P.U. System	↓	0 (0)	9 (20)	41 (90)
Liquid-Return Line, Control Valve, and Disconnect	↓	0 (0)	0 (0)	32 (70)
Total Dry Weight		15,559 (34,299)	15,595 (34,379)	15,808 (34,849)

Table 3-11

ESTIMATE OF S-IVB/LASS FIRING-ASSOCIATED AND LANDED PROPELLANT WEIGHTS

1. Firing Associated Impulse and Non-Impulse Propellants: kg (lb)

Firing Description		$O_2 - H_2$ Burner	Chilldown and Preflow	Ullage Orientation	Performance Reserves	Trapped in Lines and Engine	Totals
1st Firing	O_2	0 (0)	14 (30)	0 (0)	(Varies	86 (190)	(Varies
J-2 + 2 RLIO's	H_2	0 (0)	57 (125)	0 (0)	with M.R.)	16 (35)	with M.R.)
Full Thrust	Total	0 (0)	70 (155)	0 (0)	907 (2000)	102 (225)	1080 (2380)
2nd Firing	O_2	0 (0)	7 (15)	133 (293)	(Incl. in ΔV)	46 (101)	186 (409)
2 RLIO's	H_2	0 (0)	31 (69)	27 (59)		7 (15)	65 (143)
10% Thrust	Total	0 (0)	38 (84)	160 (352)		53 (116)	250 (552)
3rd Firing	O_2	0 (0)	7 (15)	0 (0)		46 (101)	53 (116)
2 RLIO's	H_2	0 (0)	31 (69)	0 (0)		7 (15)	38 (84)
2% Thrust	Total	0 (0)	38 (84)	0 (0)		53 (116)	91 (200)
4th Firing	O_2	4 (9)	14 (30)	232 (512)		86 (190)	336 (741)
J-2 + 2 RLIO's	H_2	4 (8)	57 (125)	47 (103)		16 (35)	123 (271)
Full Thrust	Total	8 (17)	70 (155)	279 (615)		102 (225)	459 (1012)
5th Firing	O_2	0 (0)	7 (15)	133 (293)		46 (101)	186 (409)
2 RLIO's	H_2	0 (0)	31 (69)	27 (59)		7 (15)	65 (143)
10% Thrust	Total	0 (0)	38 (84)	160 (352)		53 (116)	250 (552)
6th and 7th Firings	O_2	5 (10)	14 (30)	232 (512)		86 (190)	337 (742)
J-2 + 2 RLIO's	H_2	4 (9)	57 (125)	47 (103)		16 (35)	123 (272)
Full Thrust (Throt. Land.)	Total	9 (19)	70 (155)	279 (615)		102 (225)	460 (1014)
Sum of	O_2	9 (19)	63 (135)	730 (1610)	(Varies	396 (873)	(Varies
All	H_2	8 (17)	264 (582)	148 (324)	With M.R.)	69 (150)	With M.R.)
Firings	Total	17 (36)	324 (717)	878 (1934)	907 (2000)	465 (1023)	2590 (5710)

Table 3-11 (Continued)

2. Landed Non-Impulse Propellants: kg (lb)

Initial H_2 Condition		P.U. Reserves	Liquid Residuals	Vapor Residuals	Total Landed
LH_2 Sat. @ 19 psia	O_2	113 (250)	387 (853)	494 (1090)	995 (2193)
	H_2	113 (250)	243 (536)	762 (1679)	1118 (2465)
	Total	226 (500)	630 (1389)	1256 (2769)	2113 (4658)
LH_2 Sat. @ T.P.	O_2	113 (250)	325 (717)	494 (1090)	933 (2057)
	H_2	113 (250)	466 (1027)	763 (1683)	1343 (2960)
	Total	226 (500)	791 (1744)	1257 (2773)	2276 (5017)
50% Slush (4.5 to 1 M.R.)	O_2	113 (250)	154 (340)	494 (1090)	762 (1680)
	H_2	113 (250)	1902 (4193)	721 (1590)	2737 (6033)
	Total	226 (500)	1056 (4533)	1215 (2680)	3999 (7713)

Table 3-12

ESTIMATE OF S-IVB/LASS VENT-ASSOCIATED PROPELLANT WEIGHTS, DROPPED EACH VENT

Propellant	Preflow and Chill-down, kg (lb)	Ullage Orientation, kg (lb)	Trapped in Lines and Engine, kg (lb)	Total Dropped, kg (lb)
O_2	7 (15)	66 (146)	46 (101)	119 (262)
H_2	31 (69)	13 (29)	7 (15)	51 (113)
Total	38 (84)	79 (175)	53 (116)	170 (375)

Table 3-13

ESTIMATE OF APS IMPULSE REQUIREMENTS FOR S-IVB LASS

Mission Phase	Criteria	APS Function	N-sec (lb-sec) Impulse (2 Modules)		
			Nominal	3σ Dist.	Total
1. First Firing	Sep. and S-IVB Start; S-IVB Cutoff	Roll	0 (0)	7,117 (1,600)	
		Pitch	0 (0)	7,117 (1,600)	
		Yaw	0 (0)	4,003 (900)	
					18,237 (4,100)
2. Translunar Coast to 1st MCC @ 10 hr	±3° Deadband	Roll	10,853 (2,440)		
	±1° Deadband	Pitch	2,002 (450)		
		Yaw	4,359 (980)		
	3 Sun Orient. (Incl. 1st MCC) @ 0.4 deg/sec	Pitch	32,026 (7,200)		
	Propellant Vent	Roll		133 (30)	
		Pitch		623 (140)	
		Yaw		400 (90)	
					50,396 (11,330)
3. Translunar Coast – 1st to 2nd MCC @ 50 hr	±3° Deadband	Roll	43,412 (9,760)		
	±1° Deadband	Pitch	7,917 (1,780)		
		Yaw	17,481 (3,930)		
	8 Sun Orient. (Incl. 2nd MCC) @ 0.4 deg/sec	Pitch	85,402 (19,200)		
	Propellant Vent	Roll		445 (100)	
		Pitch		2,224 (500)	
		Yaw		1,334 (300)	
					158,215 (35,570)

Table 3-13 (Continued)

Mission Phase	Criteria	APS Function	N-sec (lb-sec) Impulse (2 Modules)		
			Nominal	3σ Dist.	Total
4. Translunar Coast – 2nd MCC to Retro @ 72 hr	±3° Deadband	Roll	23,886 (5,370)		
	±1° Deadband	Pitch	4,359 (980)		
		Yaw	9,608 (2,160)		
	4 Sun Orient. @ 0.4 deg/sec	Pitch	42,701 (9,600)		
	Propellant Vent	Roll		267 (60)	
		Pitch		1,245 (280)	
		Yaw		801 (180)	
					82,866 (18,630)
5. Lunar Orbit Retro to Deorbit @ 75 hr					(Negl.)
6. Deorbit to Braking @ 76 hr					(Negl.)
7. Descent and Landing	Control During Hover and Land	Pitch	890 (200)		
		Yaw	890 (200)		
					1,779 (400)

Table 3-14

SUMMARY OF S-IVB/LASS PROPELLANT WEIGHTS

Description	LH_2 Sat. @ 13.1 N/cm^2 (19 psia) r = 5.5[d], kg (lb)			LH_2 Sat. @ Triple Point r = 4.8[d], kg (lb)			50% Slush Hydrogen r = 4.5[d], kg (lb)			50% Slush Hydrogen r = 4.2[d], kg (lb)		
	O_2	H_2	Total	O_2	H_2	Total	O_2	H_2	Total	O_2	H_2	Total
Total Tanked Propellant	85,617 (188,750)	19,931 (43,940)	105,548 (232,690)	90,312 (199,100)	22,040 (48,590)	112,352 (247,690)	90,312 (199,100)	23,188 (51,120)	113,500 (250,220)	90,312 (199,100)	23,188 (51,120)	113,500 (250,220)
Usable Propellant[a]	88,323 (193,693)	15,201 (33,512)	98,524 (217,205)	88,085 (194,191)	18,359 (40,475)	106,444 (234,666)	88,846 (195,869)	19,674 (43,374)	108,520 (239,243)	88,228 (194,506)	20,876 (46,024)	109,104 (240,530)
Unusable Propellant[b]	2,294 (5,057)	4,730 (10,428)	7,024 (15,485)	2,227 (4,909)	3,681 (8,115)	5,908 (13,024)	1,466 (3,231)	3,514 (7,746)	4,980 (10,977)	2,084 (4,594)	2,312 (5,096)	4,395 (9,690)
Impulse Propellant:												
1. Translunar Firing[c]	60,469 (133,309)	10,991 (24,230)	71,460 (157,538)	64,582 (142,376)	13,468 (29,692)	78,050 (172,068)	64,612 (142,442)	14,360 (31,658)	78,972 (174,100)	64,271 (141,692)	15,294 (33,717)	79,565 (175,409)
2. First Midcourse	963 (2,124)	193 (426)	1,156 (2,550)	995 (2,194)	206 (455)	1,201 (2,649)	1,006 (2,217)	201 (444)	1,207 (2,661)	1,012 (2,231)	203 (447)	1,215 (2,678)
3. Second Midcourse	47 (103)	10 (21)	57 (124)	50 (111)	10 (23)	60 (134)	51 (112)	10 (23)	61 (135)	51 (112)	10 (23)	61 (135)
4. Retro to Lunar Orbit	8,995 (19,831)	1,639 (3,614)	10,634 (23,445)	9,242 (20,374)	1,924 (4,241)	11,166 (24,615)	9,408 (20,740)	2,085 (4,597)	11,493 (25,337)	9,296 (20,494)	2,205 (4,861)	11,501 (25,355)
5. Deorbit	239 (527)	48 (106)	287 (633)	245 (540)	50 (110)	295 (650)	251 (554)	50 (111)	301 (665)	252 (555)	50 (111)	302 (666)
6. Descent Braking	11,327 (24,971)	2,063 (4,549)	13,390 (29,520)	11,615 (25,606)	2,418 (5,331)	14,033 (30,937)	12,076 (26,622)	2,679 (5,905)	14,755 (32,527)	11,901 (26,237)	2,825 (6,228)	14,726 (32,465)
7. Hover and Landing	1,283 (2,829)	257 (566)	1,540 (3,395)	1,356 (2,990)	283 (623)	1,639 (3,613)	1,443 (3,182)	288 (636)	1,731 (3,818)	1,445 (3,185)	289 (637)	1,734 (3,822)

Table 3-14 (Continued)

Description	LH_2 Sat. @ 13.1 N/cm² (19 psia) r = 5.5(d), kg (lb)			LH_2 Sat. @ Triple Point r = 4.8(d), kg (lb)			50% Slush Hydrogen r = 4.5(d), kg (lb)			50% Slush Hydrogen r = 4.2(d), kg (lb)		
	O_2	H_2	Total	O_2	H_2	Total	O_2	H_2	Total	O_2	H_2	Total
Vented Propellants	0 (0)	2,917 (6,431)	2,917 (6,431)	0 (0)	1,643 (3,623)	1,643 (3,623)	0 (0)	335 (738)	335 (738)	0 (0)	499 (1,100)	499 (1,100)
Ullaging for Venting	464 (1,022)	92 (203)	556 (1,225)	464 (1,022)	92 (203)	556 (1,225)	132 (292)	26 (58)	158 (350)	132 (292)	26 (58)	158 (350)
Preflow and Chilldown	109 (240)	483 (1,065)	592 (1,305)	109 (240)	483 (1,065)	592 (1,305)	75 (165)	327 (720)	402 (885)	75 (165)	327 (720)	402 (885)
Trapped in Lines and Eng.	717 (1,580)	116 (255)	832 (1,835)	717 (1,580)	116 (255)	833 (1,835)	488 (1,075)	82 (180)	570 (1,255)	488 (1,075)	82 (180)	570 (1,255)
P.U. Reserves	113 (250)	113 (250)	226 (500)	113 (250)	113 (250)	226 (500)	113 (250)	113 (250)	226 (500)	113 (250)	113 (250)	266 (500)
Liquid Residuals	392 (865)	243 (536)	635 (1,401)	325 (717)	466 (1,027)	791 (1,744)	154 (340)	1,902 (4,193)	2,056 (4,533)	772 (1,703)	479 (1,055)	1,251 (2,758)
Vapor Residuals	494 (1,090)	762 (1,679)	1,256 (2,769)	494 (1,090)	763 (1,683)	1,257 (2,773)	494 (1,090)	721 (1,590)	1,215 (2,680)	494 (1,090)	778 (1,716)	1,272 (2,806)
$O_2 - H_2$ Burner	5 (10)	4 (9)	9 (19)	5 (10)	4 (9)	9 (19)	9 (19)	8 (17)	17 (36)	9 (19)	8 (17)	17 (36)

Notes: (a) Sum of impulse propellants which include ullaging for firings.
(b) Sum of all other propellants.
(c) Includes 907 kg (2,000 lb) of flight performance reserves.
(d) Mixture ratio given for 1st, 4th, and 6th firings; all others use r = 5.0.

A summary of S-IVB/LASS mission weights is presented in Table 3-15. In essence, these data show the final payload comparison for vehicles fueled with the three different initial hydrogen conditions of interest. Both of the 50-percent slush hydrogen-fueled cases, discussed previously in the Performance Analysis section of this report, are shown. These results indicate that the dry landed payload weight can be increased by 1628 kg (3590 lb), or 31.7 percent, when triple-point liquid hydrogen is used in lieu of saturated [at 13.1 N/cm^2 (19 psia)] liquid. Further, an additional increase in dry landed payload weight of 431 kg (950 lb) can be achieved with use of 50-percent slush hydrogen. This weight is 2059 kg (4540 lb), or 40.2 percent, greater than that for the saturated-liquid reference case. However, this payload increase, which represents the best performance that can be achieved with use of 50 percent slush hydrogen, requires an engine mixture ratio of 4.2 to 1 for the three full-thrust firings. If it is subsequently determined that the lowest feasible mixture ratio is in fact the 4.5 to 1 nominal limit discussed previously, then performance for the slush-fueled vehicle is degraded. The dry landed payload weight shown in Table 3-15 for such a case is only 1284 kg (2830 lb) greater than that for the saturated liquid reference case, but an additional 1660 kg (3660 lb) of liquid hydrogen residuals are landed on the lunar surface. Performance for this case could be improved by off-loading hydrogen on the launch pad, but the resulting loaded hydrogen, vented hydrogen, and payload weights were not determined in this analysis.

These results indicate that use of both triple-point liquid and slush hydrogen can substantially enhance performance for the S-IVB/LASS vehicle. The magnitude of the payload gains are somewhat greater than were originally predicted. Such improvement is possible because both the density increase and the heat absorption capabilities of the subcooled liquid and slush can be used to full advantage in this vehicle. This advantage occurs because a substantial firing (and use of hydrogen) early in the mission allows loading greater masses of the denser propellants without the problem of expansion as they warm up and melt. Also, since the S-IVB was originally designed for short-duration missions, application to a mission of this length and thermal environment results in a very large penalty for the saturated-liquid case. Some increase in performance could also be achieved with use of saturated [at 13.1 N/cm^2 (19 psia)] liquid

Table 3-15

SUMMARY OF S-IVB/ LASS MISSION WEIGHTS

Initial Hydrogen Condition	LH_2 Sat. at 13.1 N/cm^2 kg (lb)	LH_2 Sat. at T.P., kg (lb)	50% Slush Hydrogen, kg (lb)	
Tanked Oxygen Weight	85,617 (188,750)	90,312 (199,100)	90,312 (199,100)	90,312 (199,100)
Tanked Hydrogen Weight	19,931 (43,940)	22,040 (48,590)	23,188 (51,120)	23,188 (51,120)
Tanked Total Propellant Weight	105,548 (232,690)	112,352 (247,690)	113,500 (250,220)	113,500 (250,220)
Engine Mixture Ratio	5.5	4.8	4.5	4.2
Gross Translunar Ignition Weight	128,029 (282,250)	136,565 (301,070)	137,661 (303,485)	138,439 (305,200)
Less Expendables	71,639 (157,934)	78,230 (172,464)	79,151 (174,496)	79,745 (175,805)
Gross Weight Injected into Translunar Trajectory	56,390 (124,316)	58,336 (128,606)	58,509 (128,989)	58,694 (129,395)
Less Payload Shroud	1,452 (3,200)	1,452 (3,200)	1,452 (3,200)	1,452 (3,200)
Less Expendables	15,053 (33,185)	14,139 (31,170)	13,242 (29,193)	13,156 (29,003)
Gross Weight Injected into Lunar Orbit	39,886 (87,931)	42,745 (94,236)	43,816 (96,596)	44,086 (97,192)
Less Expendables	16,828 (37,098)	17,860 (39,373)	17,882 (39,423)	18,123 (39,953)
Gross Lunar Landed Weight	23,058 (50,833)	24,886 (54,863)	25,934 (57,173)	25,964 (57,239)
Less Residuals	2,369 (5,223)	2,532 (5,582)	3,713 (8,186)	2,965 (6,537)
Dry Lunar Landed Weight	20,689 (45,610)	22,354 (49,281)	22,221 (48,987)	22,998 (50,702)
Less Dry Inerts	15,558 (34,299)	15,594 (34,379)	15,808 (34,849)	15,808 (34,849)
Dry Landed Payload Weight	5,131 (11,311)[a]	6,760 (14,902)	6,413 (14,138)	7,191 (15,853)
Increase in Payload Weight kg (lb)		1,629 (3,591)	1,282 (2,827)	2,060 (4,542)
Increase in Payload Weight (%)		31.7	25.0	40.2

[a]Reference Case

hydrogen if the hydrogen tank size were increased to initially load more of that fuel. Hence, use of subcooled liquid and slush hydrogen can be expected to provide larger payload gains for existing vehicles such as the S-IVB where the tank size is not presently optimum for use of saturated liquid hydrogen.

Section 4
LUNAR MISSION VEHICLE APPLICATION STUDIES

4.1 VEHICLE/MISSION CHARACTERISTICS

The Lunar Mission Vehicle (LMV), used as a cryogenic service module to perform a selected advanced Apollo mission, was selected as the object of this study. The LMV launch configuration is shown in Fig. 4-1. A standard Saturn V booster with a 45,360-kg (100,000-lb) translunar injection capability was assumed. The mission profile and deployment of each module are generally identical to those for the present Saturn V/ Apollo mission. For example, the Lunar Excursion Module (LEM) is separated and docked to the Command Module (CM) for translunar flight after booster separation at injection. Primary LMV components include two 2.67-m (105-in.) diameter hydrogen tanks, two 1.44-m (57-in.) diameter oxygen tanks, and two RL10A3-3 engines. Figure 4-2 shows the hydrogen tank structural support concept, which is based on previous work at MSFC (Ref. 4.1).

Since the improved payload capability of the cryogenic LMV allows longer lunar stay times than are presently possible with the standard Apollo vehicles, a nominal 21-day advanced Apollo mission profile was chosen for the analysis. Vehicle definition and system weights are available from Phase II MIMOSA studies. The LMV is assumed to remain in lunar orbit for 17 days, with a 14-day LEM stay time on the lunar surface. Weight of the three-man CM was fixed at 5,278 kg (11,635 lb) for the study. Weight of the LEM was then maximized as the result of systems optimization for each initial hydrogen condition.

LMV propellant tanks were re-sized in each case to provide optimum performance for each initial hydrogen condition considered in the study.

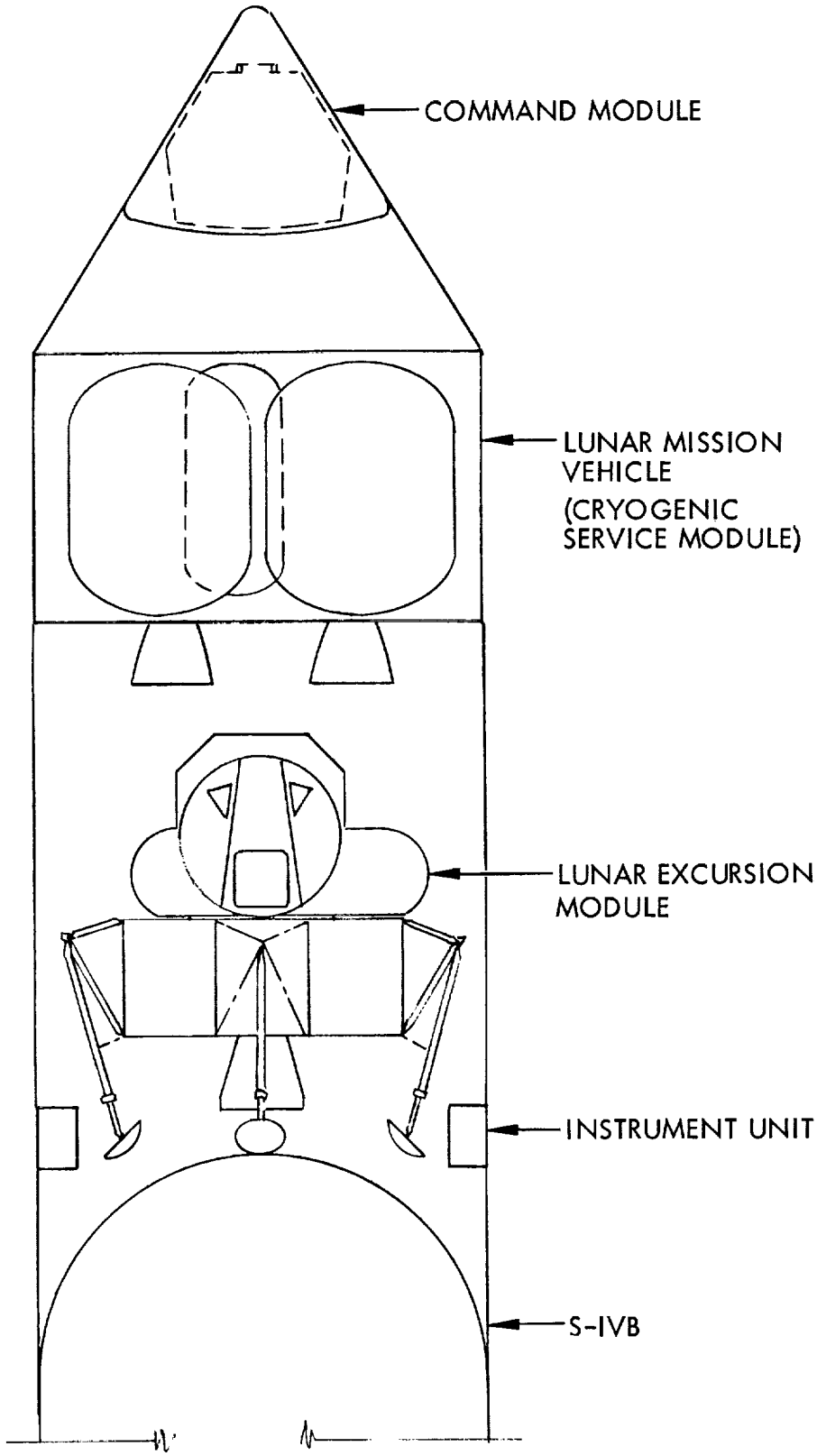

Fig. 4-1 Launch Configuration for LMV Applied to a Selected Advanced Apollo Mission

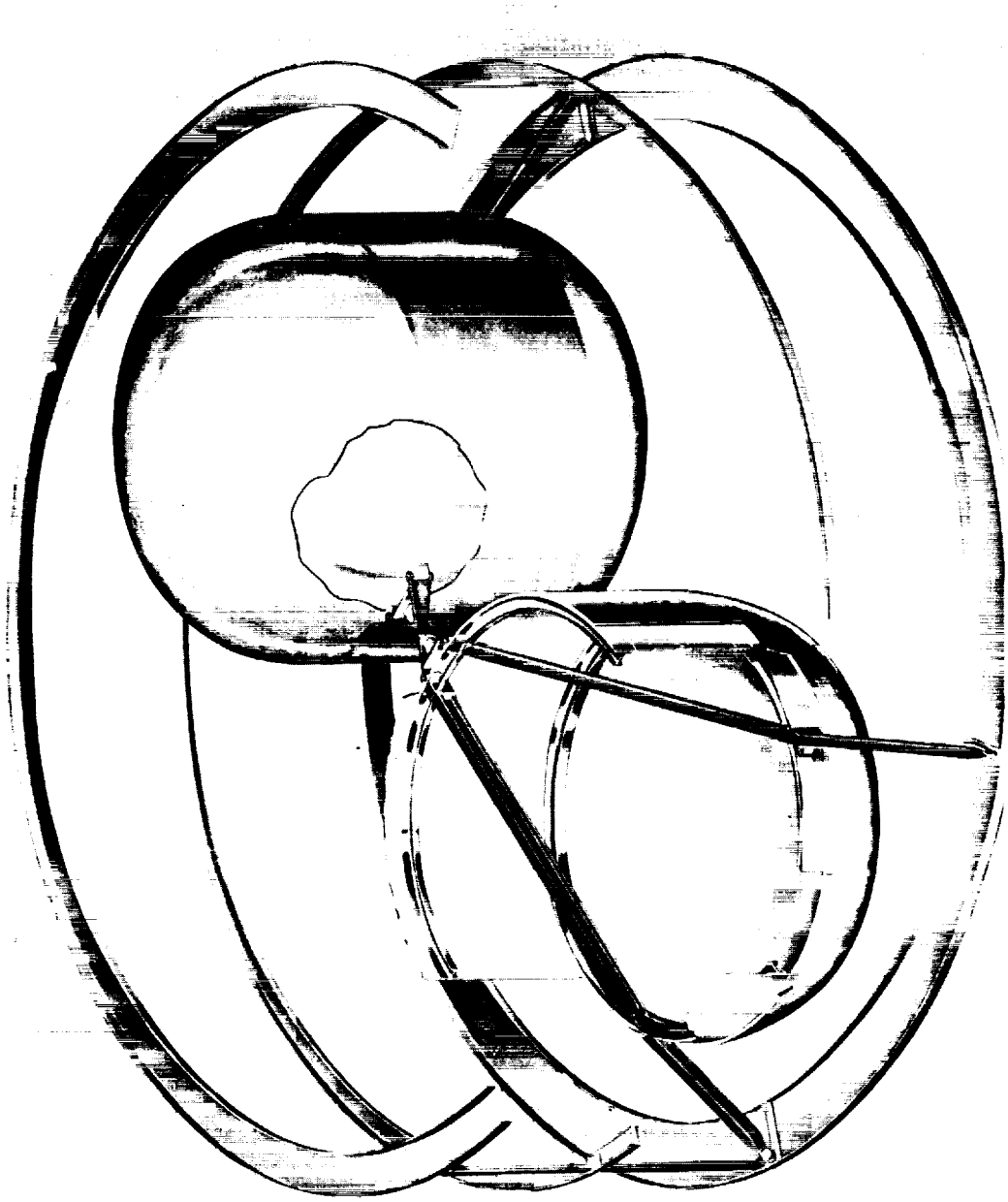

Fig. 4-2 LMV Liquid Hydrogen Tank Support Structure (from NASA/MSFC Internal Note IN-P and VE-SA-63-44)

4.2 PROPELLANT MANAGEMENT SYSTEM

Results of the propellant management system optimization analyses, described in Section 2, were applied in preliminary studies to the LMV/Advanced Apollo mission. These applications included tank fill and ground hold system tolerance effects, and instrumentation for quantity and quality measurements.

4.2.1 Tank Fill and Ground Hold

Techniques based on recirculation, injection of helium vapor, and operation of a cold-helium heat exchanger were applied to the LMV to obtain approximate requirements for tank fill and ground hold. The following LMV characteristics were assumed to perform the preliminary analyses:

- Loaded hydrogen weight = 1,225 kg (2,700 lb) for each of the two tanks
- Steady-state ground-hold heat rate = 3,252 to 32,523 w (11,100 to 111,000 Btu/hr) for each of the two tanks

Table 4-1 summarizes results of the preliminary tank fill and ground-hold analysis. As seen from these data, the recirculation technique is again the best method with which to fill or maintain the hydrogen tank. The discussion in subsection 3.2.1 for the S-IVB vehicle generally applies to the LMV also. There is one significant difference for this vehicle, i.e., slush quality degradation in the transfer line is now approximately 15 percent for a 50-percent supply. This is due to the fact that the required recirculation rate is much less, being approximately 28 percent of that required for the S-IVB. This degradation effect can be corrected by increasing the flow rate to the point where 50 percent slush is supplied to the tank.

4.2.2 System Tolerance Effects Study

Figure 4-3 shows individual payload penalties as a function of LMV system tolerance values that resulted from preliminary evaluation of the equations described in subsection 2.2.2. Results are similar to those for the Saturn V/S-IVB. The most

Table 4-1

PREDICTED TANK FILL AND GROUND-HOLD REQUIREMENTS FOR EACH OF THE LMV HYDROGEN TANKS*

Technique	Recirculation	GHe Injection	Cold GHe Heat Exchanger
Transient Cooldown			
T_1 of LH_2, ^oK (^oR)	–	20.33 (36.6)	20.33 (36.6)
T_2 of LH_2, ^oK (^oR)	–	13.83 (24.9)	13.83 (24.9)
T_1 of GHe, ^oK (^oR)	–	11.11 (20.0)	11.11 (20.0)
GHe flow rate, kg/hr (lb/hr)	–	4,173 (9,200)	5,489 (12,100)
Cooldown time, hr	–	0.40	1.0
Steady-state operation to maintain triple-point liquid or slush			
Degradation in transfer line, $\Delta X/X_1$	0.154	–	–
H_2 flow rate for X_a= 50% X_{b2} = 50%,kg/hr (lb/hr)	3,348 (7,380)	–	–
Recirculation period, hr	0.35	–	–
11.11^oK (20^oR) GHe flow-rate, kg/hr (lb/hr)	–	3,774 (8,320)	8,165 (18,000)
Slush formation in vehicle tank			
11.11^oK (20^oR) GHe required to form 50% slush, kg (lb)	–	1,148 (2,530)	2,350 (5,180)

*Q = 32,523 w (111,000 Btu/hr).

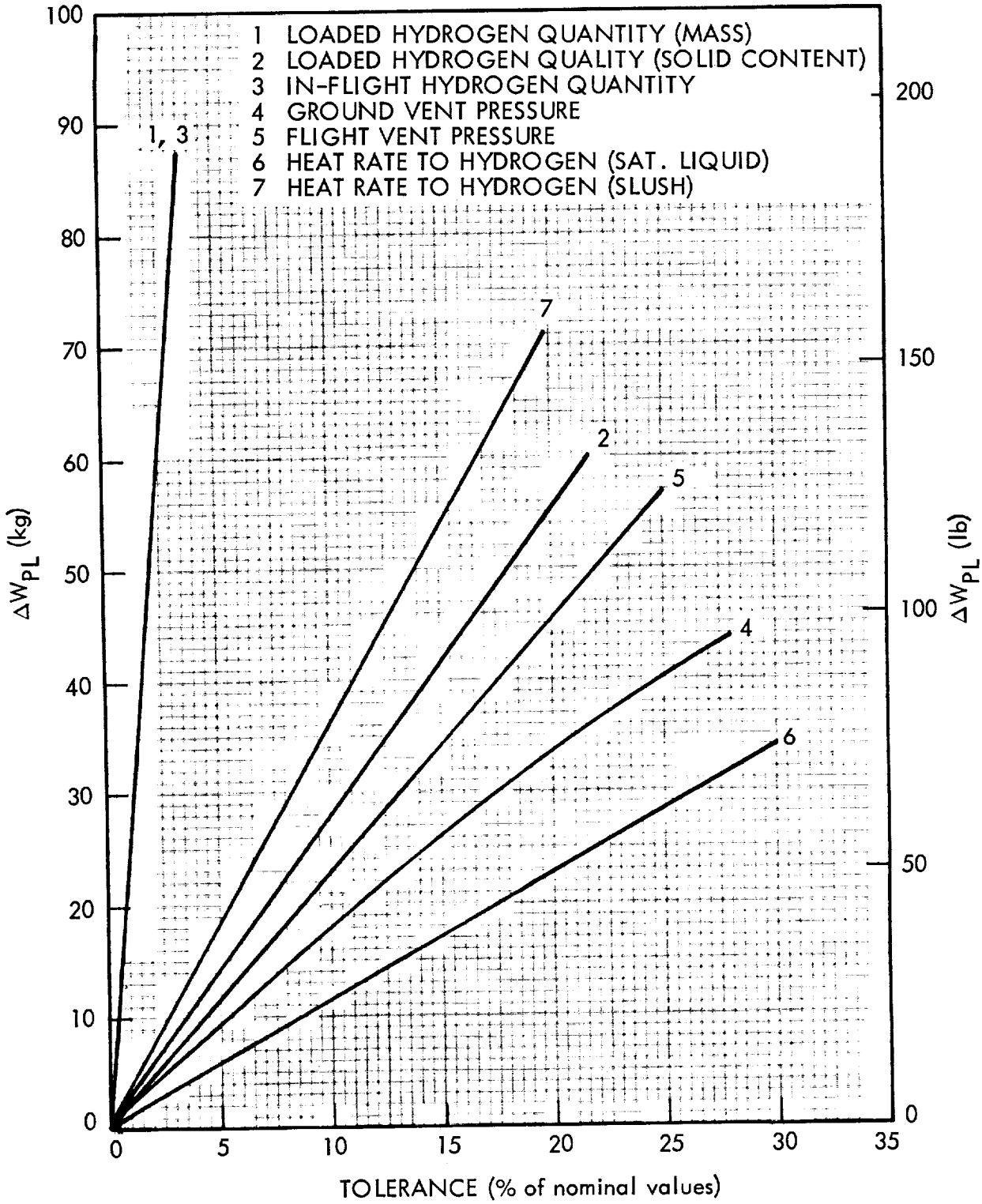

Fig. 4-3 Payload Penalties Resulting From LMV System Tolerances (Liquid- or Slush-Fueled Vehicles)

critical variables are the loaded hydrogen quantity and that available in flight (equal penalties for a given tolerance with this vehicle). Smaller penalties, listed in the order of their significance, are heat rate, loaded quality, flight-vent pressure, and ground-vent pressure.

Payload penalties for the LMV that correspond to presently predicted state-of-the-art tolerances on each variable are given in Table 4-2. Total system payload penalty, also given in the table was then obtained using a root mean square combination of the individual values.

4.2.3 Instrumentation Requirements

The following additions to or modifications of quantity- and quality-sensing instrumentation and control components were assumed in performing LMV application studies for subcooled liquid or slush:

- Replacement or recalibration of temperature and capacitance sensors
- Installation of liquid-recirculation lines, control valves, and a disconnect
- Installation of a gamma radiation (or x-ray) attenuation system for quality measurements
- Installation of screens at the hydrogen tank feed-line outlets to filter and retain solid hydrogen particles in the tank during expulsion of liquid for engine firings.

Weight differences for minor modification of other instrumentation and control components were assumed to be negligible.

4.3 PROPULSION SYSTEM

Two RL10A3-3 engines provide primary propulsion requirements for the LMV/advanced Apollo mission. These engines operate at a nominal mixture ratio of 5.0 to 1 and each develops 66,720 N (15,000 lb) of thrust. Specific impulse values of 4,315 m/sec (440 sec) for saturated liquid hydrogen and 4,307 m/sec (439.2 sec) for

Table 4-2

PAYLOAD PENALTIES RESULTING FROM PREDICTED HYDROGEN SYSTEM TOLERANCES FOR THE LMV

Variable[a]	Nominal Value	Predicted Tolerance (%)	Tolerance Value	Payload Penalty
Loaded H_2 Quantity	2,345 kg (5,170 lb)	1	24 kg (52 lb)	25 kg (55 lb)
Loaded H_2 Solid Fraction	50%	10	(b)/5%	(b)/27 kg [(b)/60 lb]
In-flight H_2 Quantity	variable	2	47 kg (104 lb)	49 kg (108 lb)
Ground Vent Pressure	11.7 N/cm^2 (17 psia)	5	0.59 N/cm^2/(b) [0.85 psia/(b)]	9 kg/(b) [20 lb/(b)]
Flight Vent Pressure	19.3 N/cm^2 (28 psia)	5	0.96 N/cm^2 (1.4 psia)	12 kg (26 lb)
Heat Rate to Hydrogen	13/43 w (434/1470 Btu/hr)	25	3/11 w (109/368 Btu/hr)	27/91 kg (60/200 lb)
Total System Payload	6,350 kg (14,000 lb)	0.96/ 1.68	–	63/110 kg (139/243 lb)

(a) When two values are given, the first applies to liquid-fueled systems and the second to slush-fueled systems; single values apply to both.

(b) Not applicable.

triple-point liquid hydrogen were used in the analysis.* This small difference is the estimated effect of low-temperature (triple-point) hydrogen on specific impulse at a constant mixture ratio of 5.0 to 1. This occurs only during the first firing. Two full-thrust firings are required to retro into lunar orbit and to achieve transearth injection velocity after the 17-day coast period in lunar orbit.

All other propulsion requirements for translunar and transearth midcourse corrections, attitude control, ullaging of propellants for engine start or vent, etc., are provided by an auxiliary propulsion system (APS). This system uses earth-storable propellants and is assumed to deliver a specific impulse of 2,942 m/sec (300 sec).

4.4 INSULATION SYSTEM

The LMV hydrogen tank insulation is a multilayer composite consisting of alternate layers of 0.006-mm (0.25-mil) Mylar, aluminized on both sides, and 0.071-mm (2.8-mil) Dexiglas paper spacers. Basic thermal and physical property data were previously established (Ref. 4-2), and are under continuing investigation. A button attachment method was assumed for this analysis. The insulation is installed without a substrate, and is purged with helium gas during ground-hold operations. During ascent the helium outgases and the insulation gradually attains its steady-state value of conductivity in space.

Effective thermal conductivity values range from 1.7×10^{-7} w/cm°K (1×10^{-5} Btu/hr ft°R) to 1.7×10^{-6} w/cm°K (1×10^{-4} Btu/hr ft°R). A value of 3.5×10^{-7} w/cm°K (2×10^{-5} Btu/hr ft°R) was used in this analysis. An assumed density of 80.1 kg/m^3 (5.0 lb/ft^3) was used to calculate insulation weights, which vary with thickness.

A preliminary optimization of insulation thickness for the LMV was obtained using the method described in subsection 2.4. A more exact optimization was then obtained using a numerical evaluation of system weights for several thicknesses. Secondary effects such as outgasing of the helium purge gas and pressurant heating were considered in the second analysis.

*Final Pratt & Whitney values are 4,350 m/sec (444 sec) for saturated liquid hydrogen and 4,343 m/sec (443.2 sec) for triple-point liquid hydrogen.

4.4.1 Preliminary Optimization

For preliminary calculations of insulation parameters for this vehicle, a uniform heating rate through the multilayer insulation blankets was assumed. Random vehicle orientation with respect to the sun was considered. The multifiring technique was used to optimize the insulation thickness, however, because of the time spacing of the propellant usage for the two firings. Preliminary calculations were based on a total mission duration of 120 hr, which corresponds to a standard Apollo mission profile. Since the selected mission duration is 21 days or 504 hr, the preliminary values have no meaning with respect to the final analysis, and are not shown. However, a numerical optimization was performed for the 120-hr mission, and results correlated well with those from the preliminary analysis.

4.4.2 Final Optimization

Final insulation optimization for the LMV as with the other study vehicles was performed in two steps: heat transfer considerations, and final optimization procedure and results.

4.4.2.1 Significant Heat Transfer Considerations

It was again convenient for this vehicle, as with the S-IVB, to separate the advanced Apollo mission profile into chronological time periods. In this case, six periods were considered: ground hold, ascent, cooldown, earth parking orbit, lunar transit, and lunar orbit. Heating environments are significantly different during each of these time periods. Calculation of heat transfer to the hydrogen tanks during each period included consideration of insulation, structural supports, plumbing penetrations, and pressurant gases.

Ground Hold. A 90-sec ground-hold period was assumed during which topping or recirculation of the hydrogen tanks was terminated. A constant heating rate was assumed for each insulation thickness considered during this period. Thermal conductivity of the multilayer insulation at this time was assumed to be that of helium purge gas at the average insulation temperature.

Ascent. Outgasing of helium purge gas from the multilayer insulation occurs rapidly during ascent. At 82 sec after liftoff the thermal conductivity is approximately 80 percent of that during ground hold, but it decreases to near the steady-state evacuated value at approximately 140 sec. Complete reduction to the steady-state value is assumed to occur before orbit injection (at 720 sec).

Cooldown. Temperature of the outer shroud increases rapidly between liftoff and maximum aerodynamic heating, then gradually cools off to a steady-state value in earth parking orbit at approximately 0.4 hr.

Other Time Periods. Heat transfer during the earth parking orbit, lunar transit, and lunar orbit periods was calculated using steady-state average temperatures consistent with each environment and a constant thermal conductivity value of 3.46×10^{-7} w/cm°K (2×10^{-5} Btu/hr ft °R). The average temperatures were taken from previous calculations for a similar mission.

Heat transfer to tanks filled with triple-point liquid or slush hydrogen was calculated using corrected average temperature differentials for each time period.

Figures 4-4, 4-5, and 4-6 present the total accumulated heat transfer to each LMV hydrogen tank as a function of time. The values presented were obtained from the analysis just described.

4.4.2.2 Final Optimization Procedure and Results

Optimum hydrogen tank insulation thickness depends upon minimizing the sum of those system weights that vary with insulation thickness and the resulting hydrogen boiloff. For a nonexistent vehicle such as the LMV, this sum includes weights for the hydrogen tank, insulation, boiloff, pressurization system, and residual. Also included are weights for APS impulse propellants required for ullage orientation during hydrogen venting and vehicle structure, which varies with the size and weight of the hydrogen tank. Payload weight, which is the LEM weight in this case, is maximized as the sum of the weights described above is minimized. Those weights

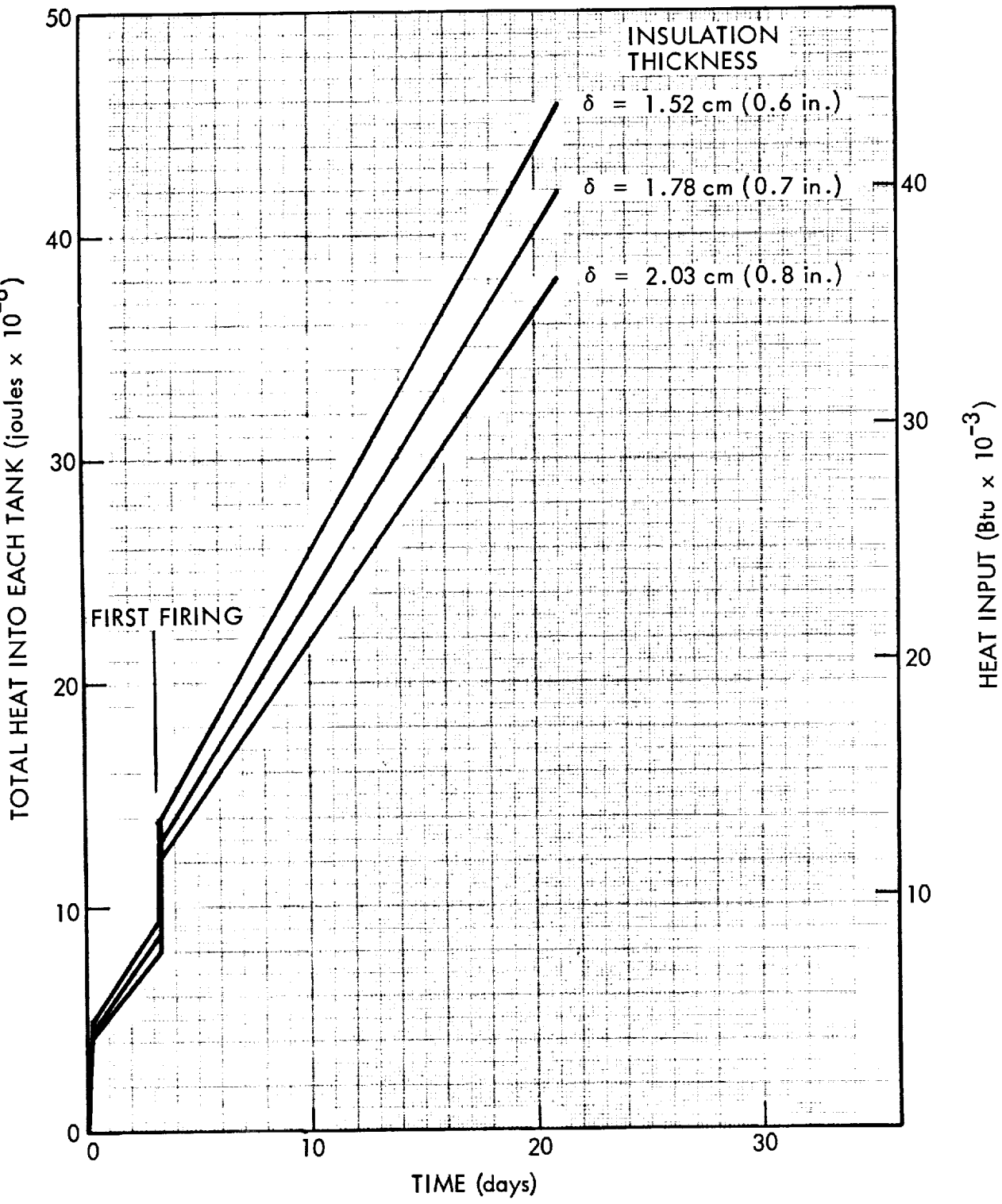

Fig. 4-4 Total Heat Transferred to Each LMV LH_2 Tank [Initially Saturated LH_2 at 11.7 N/cm^2 (17 psia)]

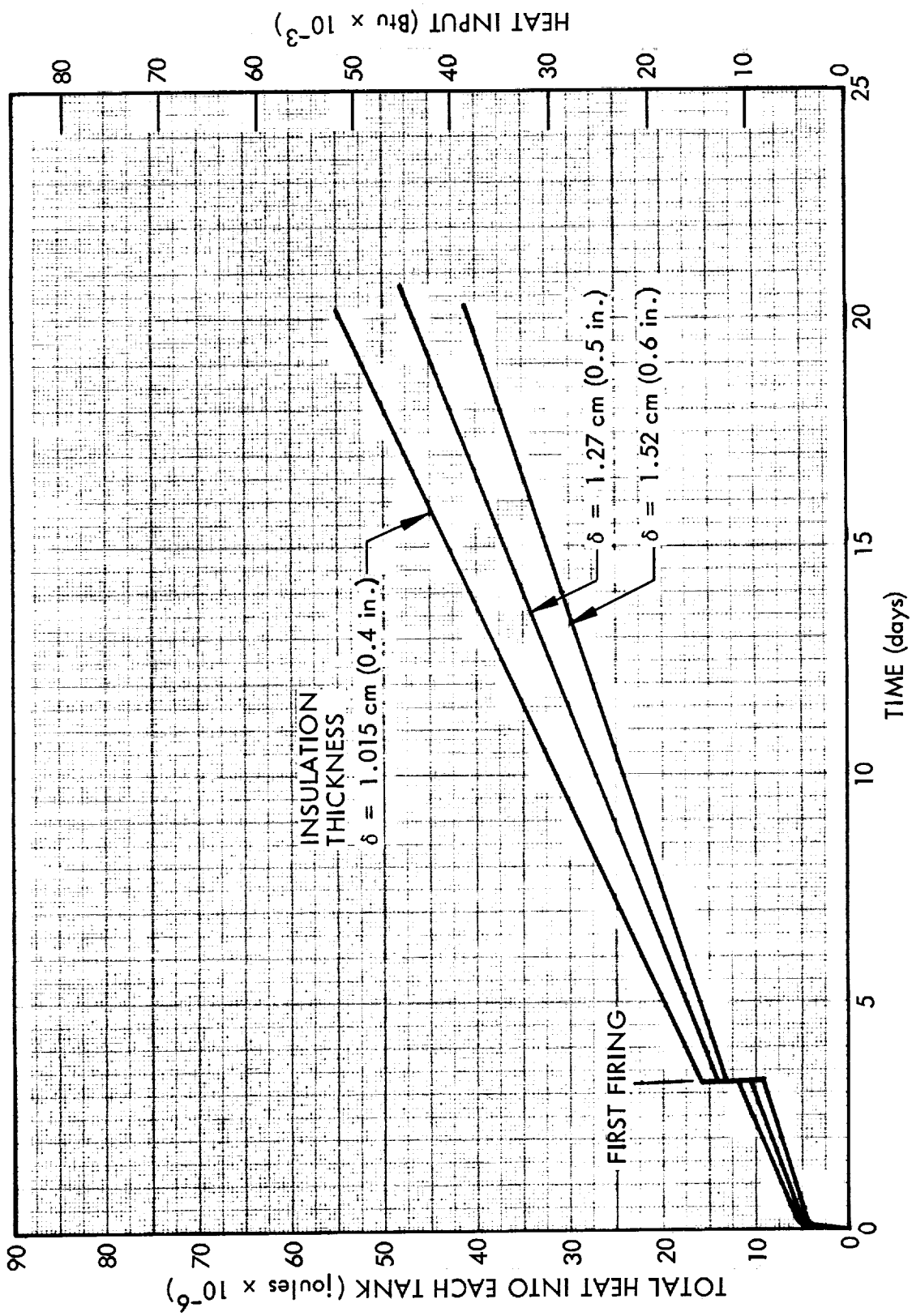

Fig. 4-5 Total Heat Transferred to Each LMV Hydrogen Tank (Initially Triple-Point LH_2)

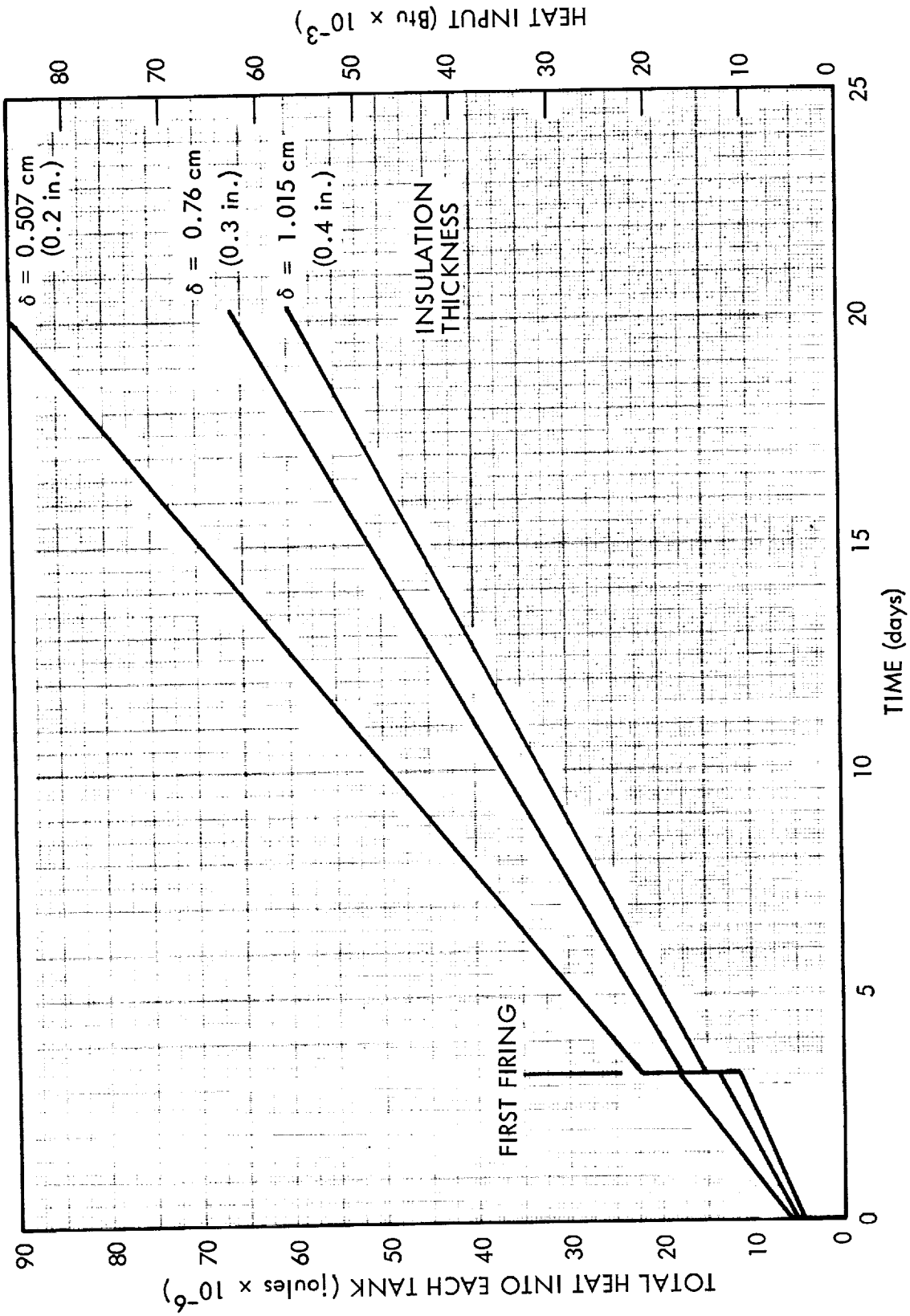

Fig. 4-6 Total Heat Transferred to Each LMV Hydrogen Tank (Initially 50-Percent Slush Hydrogen)

dropped prior to the lunar orbit retro firing must be multiplied by $1/\mu_1$ before they are summed. Similarly, those weights which are not dropped until after the trans-earth injection firing must be multiplied by μ_2 before summing.

The optimum hydrogen tank insulation thickness for each initial hydrogen condition was obtained from a plot of the weight sum described above as a function of the insulation thickness. Since only the relative weight for each thickness was needed to obtain the shape of the optimization curve, weight increments with respect to a convenient reference were used for each variable. The relationship of incremental payload weight to the important system weights is given by

$$\Delta W_{PL} = -\frac{1}{\mu_1} \Delta W_{BO_1} - \Delta W_{BO_2} - \Delta W_{UP} - \mu_2 (\Delta W_V + \Delta W_I) \quad (4.1)$$

The boiloff prior to lunar orbit retro, ΔW_{BO_1}, is zero for all cases considered. ΔW_V was taken as the sum of tank, pressurization system, residual, and structure weight increments, which vary as a function of hydrogen tank volume. Therefore, the sum of $\Delta W_{BO_2} + \Delta W_{UP} + \mu_2 (\Delta W_V + \Delta W_I)$ was used to plot the optimization curves. Results are presented in Figs. 4-7, 4-8, and 4-9.

4.5 VENTING SYSTEM

Ullage pressure histories were determined for LMV's fueled with initially saturated liquid at a pressure of 11.7 N/cm^2 (17 psia), triple-point liquid, and 50-percent slush hydrogen. In the case of saturated liquid at 11.7 N/cm^2 (17 psia), where the optimum insulation system results in venting, the pressure history also includes vent pressure limits and vent cycle times. Figures 4-10, 4-11, and 4-12 present these histories as a function of mission time.

Venting analysis for the LMV is based on the equations developed in subsection 2.5, which assume a mixed thermal model and distribution of heat to both liquid and vapor within the tank. A tank-pressure-actuated mixer system can be used for the LMV, as for the S-IVB, to ensure mixing and to minimize stratification effects. Such a system is estimated to weigh approximately 4.54 kg (10 lb), exclusive of power, which

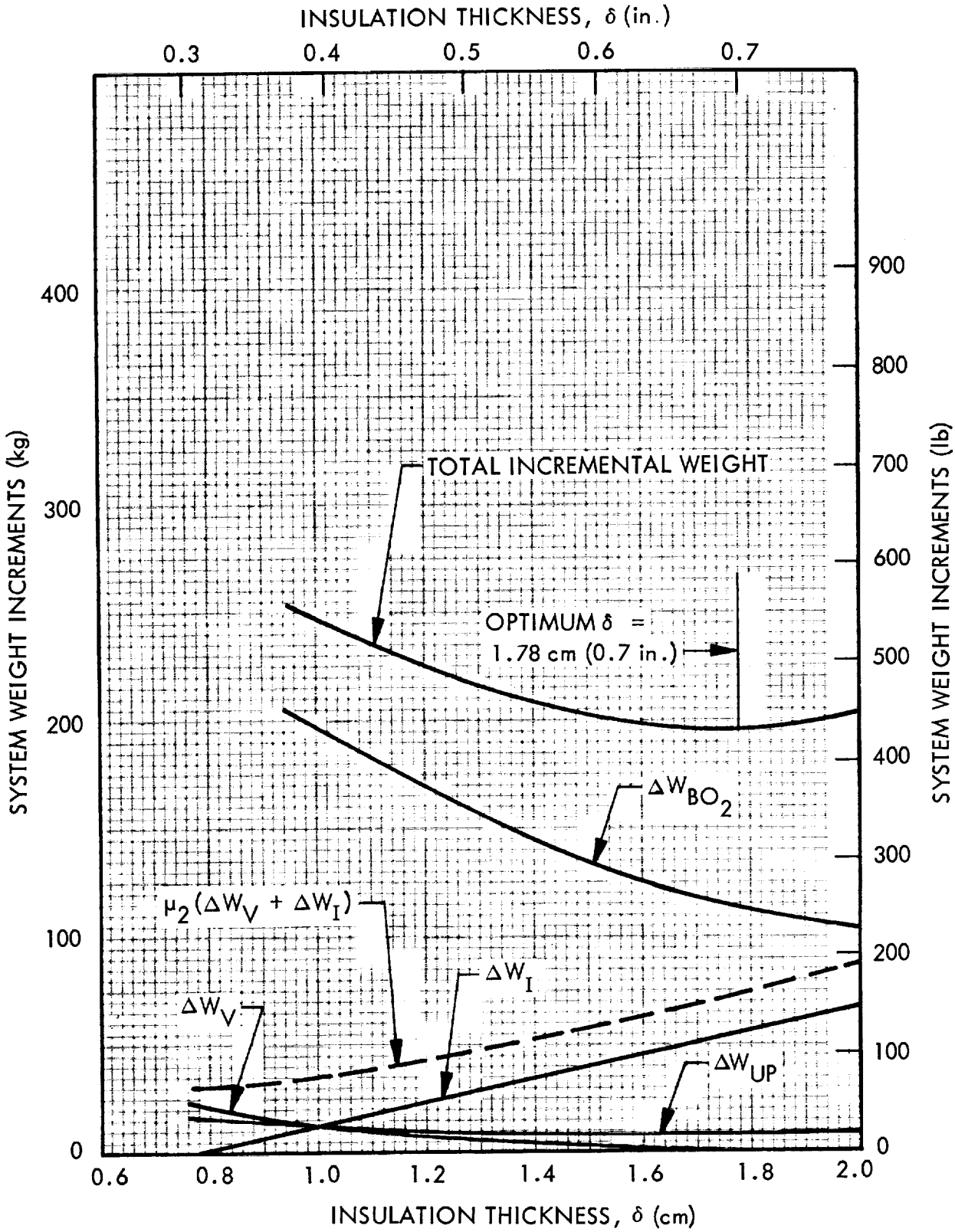

Fig. 4-7 Optimum Insulation Thickness for LMV With Saturated LH_2 at 11.7 N/cm^2 (17 psia)

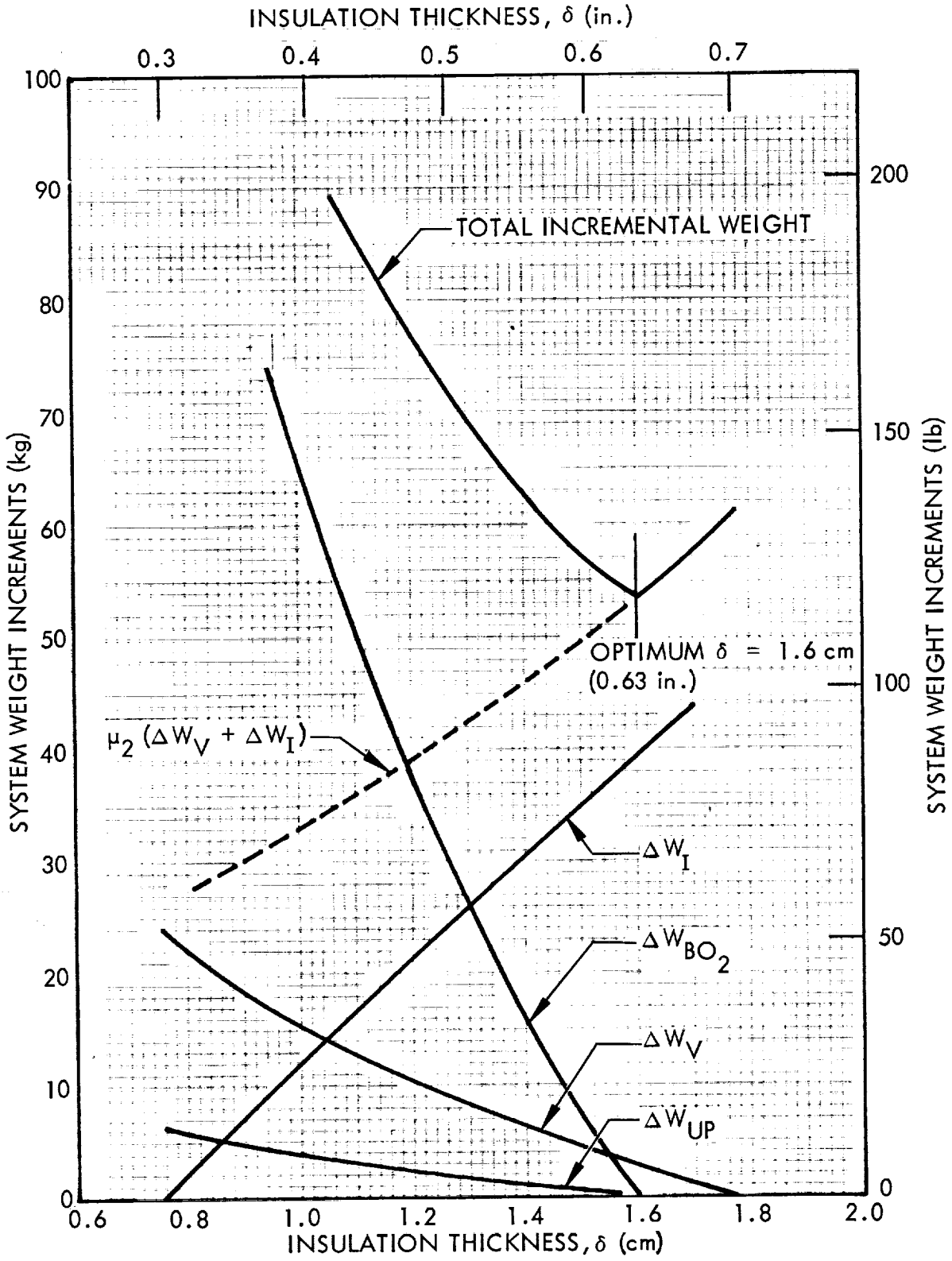

Fig. 4-8 Optimum Insulation Thickness for LMV With Triple-Point LH_2

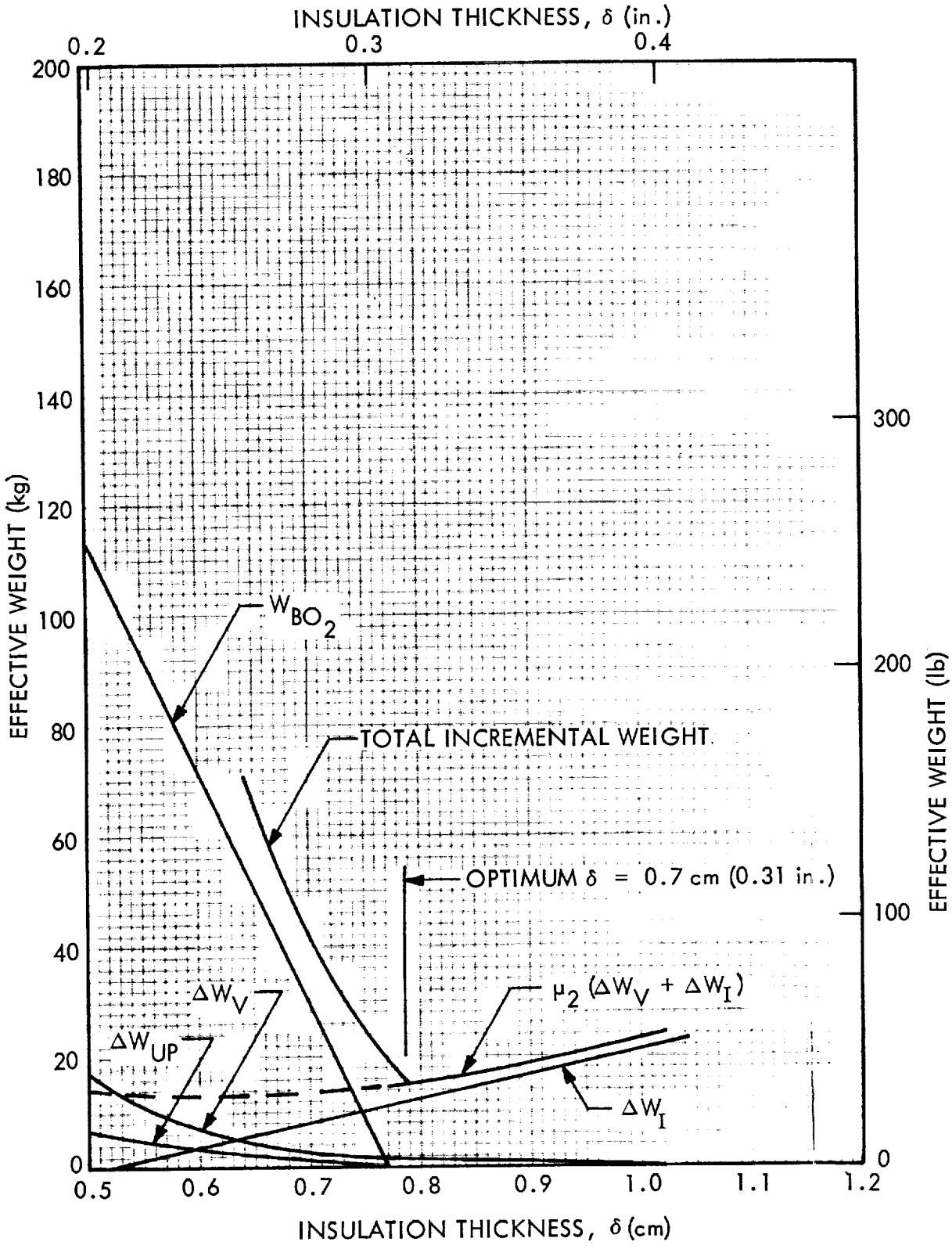

Fig. 4-9 Optimum Insulation Thickness for LMV With 50-Percent Slush Hydrogen

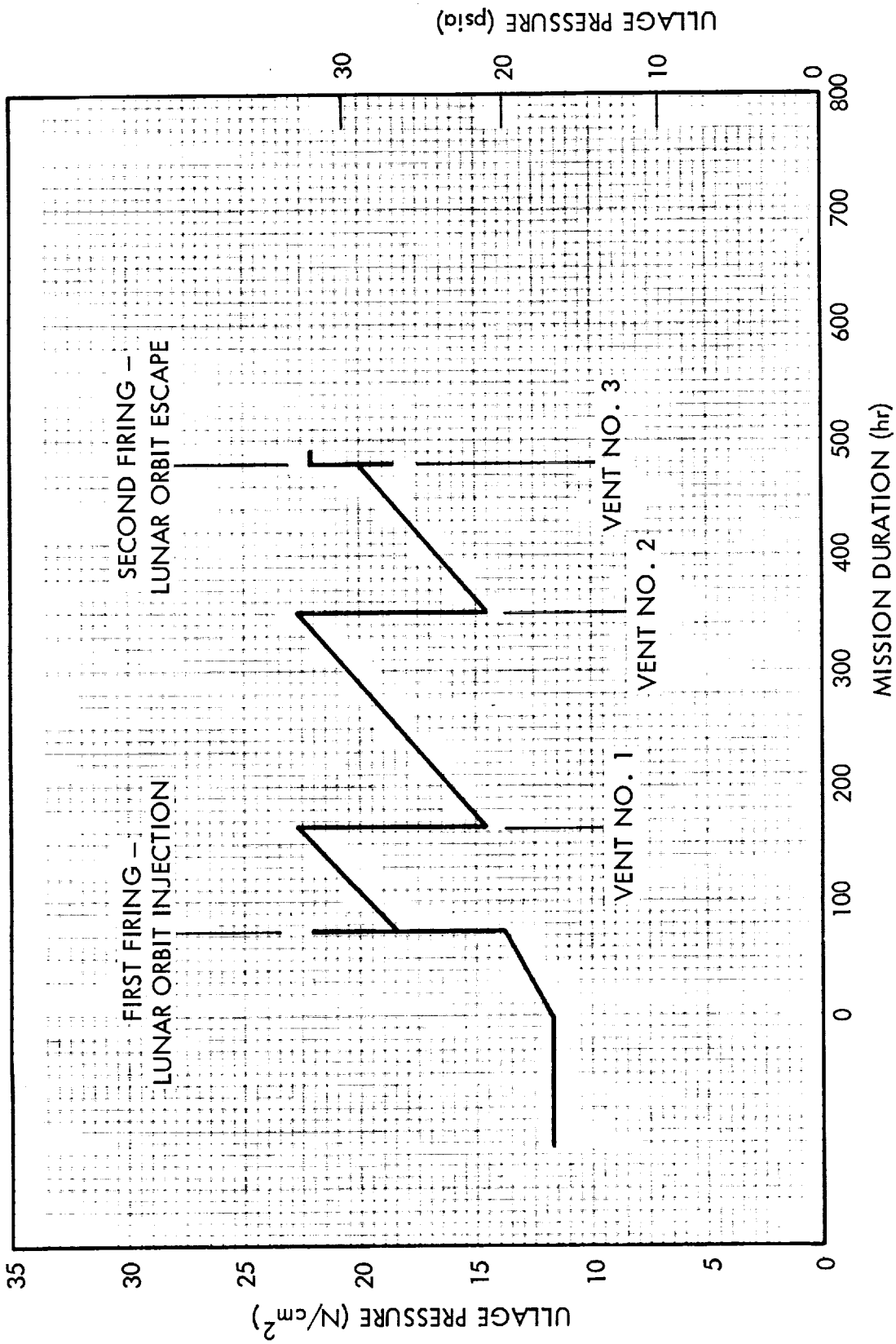

Fig. 4-10 Ullage Pressure-Time History for LMV With LH_2 [Initially Saturated at 11.7 N/cm^2 (17 psia)]

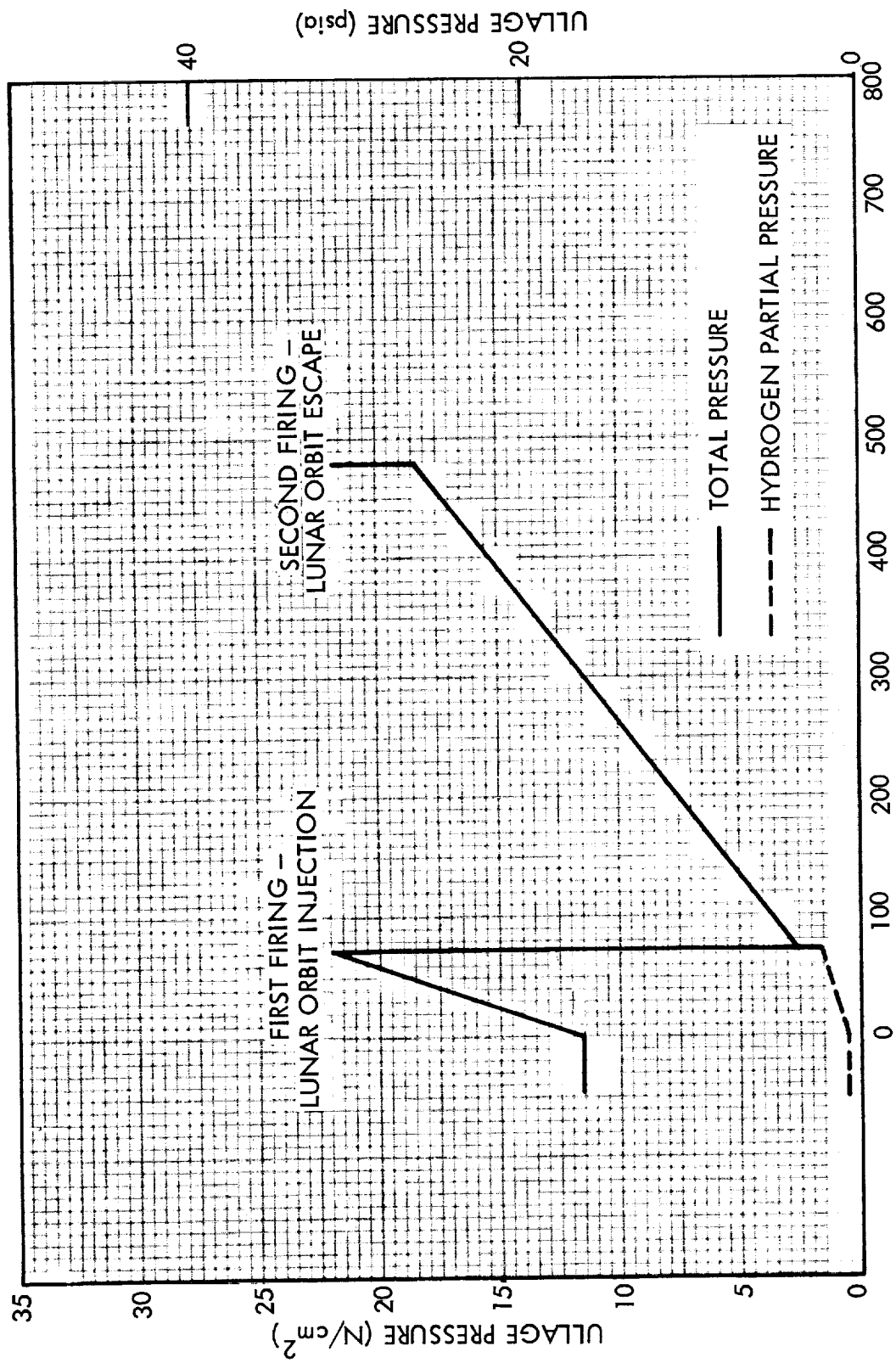

Fig. 4-11 Ullage Pressure-Time History for LMV With LH_2 (Initially Saturated at Triple Point)

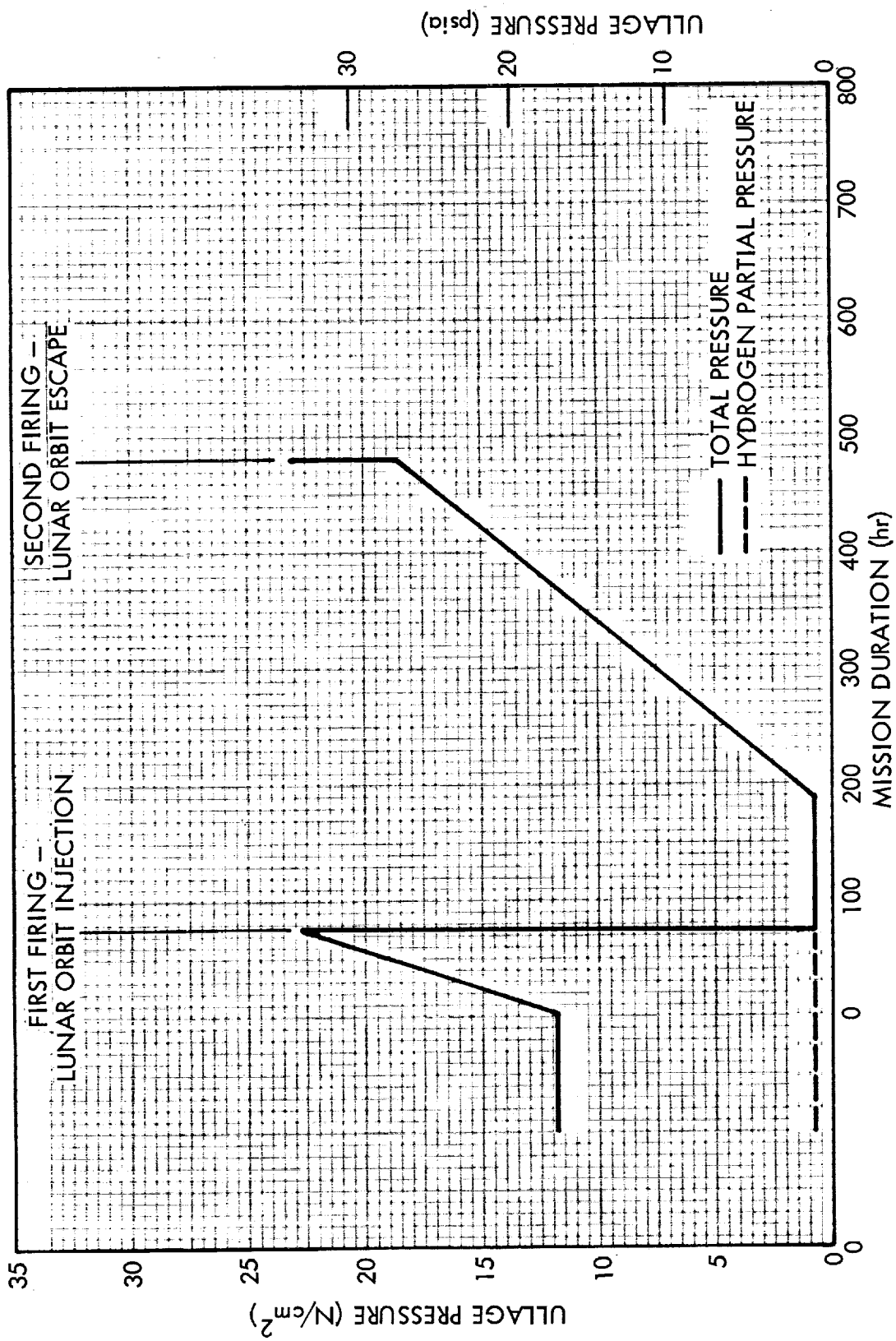

Fig. 4-12 Ullage Pressure-Time History for LMV (Initially 50-Percent Slush Hydrogen)

could be supplied from CM fuel cells. The vented hydrogen weights obtained from the analysis for the initially saturated liquid-fueled vehicle at a pressure of 11.7 N/cm^2 (17 psia) are given in Table 4-3.

Table 4-3

SUMMARY OF HYDROGEN VENTING FOR A SATURATED LIQUID-FUELED LMV

Vent No.	Time of Vent		Mass H_2 Vented	
	(hr)	(days)	(kg)	(lb)
1	168	7.0	54.9	121
2	352	14.7	53.1	117
3	486	20.2	9.1	20

No venting analysis was performed during the study for the oxidizer tanks. However, based on results of previous studies, some type of thermal conditioning is required to avoid venting, since the oxygen tanks are separately supported and insulated. A value of 68 kg (150 lb) of vented oxygen was assumed for each case in this study to account for this effect.

4.6 PRESSURIZATION SYSTEM

An ambiently stored helium system was assumed for repressurization requirements to start the engines for each primary firing. Hydrogen propellant expulsion requirements are provided by use of heated hydrogen vapor at 111°K (200°R) from the engine bleed system. Since the performance analysis is based on differences in system weight for each of the initial hydrogen conditions of interest, no attempt was made to evaluate pressurant requirements for the oxygen system. Table 4-4 presents a summary of the hydrogen tank helium pressurant and storage-bottle requirements for the LMV.

Table 4-4

SUMMARY OF HYDROGEN TANK HELIUM PRESSURANT AND STORAGE-BOTTLE REQUIREMENTS FOR THE LMV

Initial Hydrogen Condition[a]	Sat. Liquid at 11.7 N/cm^2 (17 psia) kg	(lb)	Triple-Point Liquid kg	(lb)	50% Slush, kg	(lb)
Orbit Retro Repressurization	0.136	(0.3)	Negligible		Negligible	
Transearth Injection Repressurization	4.08	(9.0)	3.99	(8.8)	3.71	(8.2)
Total Helium Weight	4.22	(9.3)	3.99	(8.8)	3.71	(8.2)
Total Helium and Storage-Bottle Weight	27.31	(60.2)	26.04	(57.4)	24.31	(53.6)

(a)Helium stored at 166.7°K (300°R).

4.7 TANK-AFFECTED STRUCTURE

Since the LMV is not an existing vehicle, both propellant loadings and propellant-tank volumes were varied to achieve a maximum payload weight. This results in various-sized hydrogen tanks for use of saturated liquid, triple-point liquid, and slush hydrogen. The tank volume variation is obtained by varying the length of the tank cylindrical section. An equal variation is required in the length of the external shell. Corresponding variations in structural weight were included in the volume-dependent weight increment ΔW_V shown in Figs. 4-7, 4-8, and 4-9 and were used to obtain optimum insulation thicknesses.

Additional structural differences considered in the study were those associated with installation of liquid-return lines, shutoff valves, a disconnect, and additional instrumentation and controls for the slush-fueled vehicle.

4.8 PERFORMANCE ANALYSIS

The velocity increment required to inject the LMV/CM/LEM assembly into lunar orbit is 990 m/sec (3,250 ft/sec). The corresponding velocity increment required

to inject the LMV/CM assembly into a transearth trajectory after 17 days in orbit is 1,076 m/sec (3,530 ft/sec).

Since the object of the performance analysis was to maximize the LEM weight separated in lunar orbit, this analysis was necessarily accomplished as a part of the final insulation optimization procedure. An iterative procedure was used to select the LEM weight and the LMV propellant load, tank size, insulation thickness and weight, boiloff weight, tank-volume-dependent inert weight, and ullage propellant weight which, when combined with other fixed weights, satisfied the limiting translunar injected gross weight of 45,360 kg (100,000 lb). Figure 4-13 presents the results of this analysis. In this figure, LEM separated weight is shown as a function of hydrogen tank insulation thickness for LMV's fueled with each of the three initial hydrogen conditions of interest.

LMV inert weights, as a function of hydrogen tank volume, and the fixed CM weight of 5,278 kg (11,635 lb) were taken from data to be presented in the MIMOSA final report (not yet published).

4.9 WEIGHT AND PAYLOAD SUMMARIES

Tables 4-5 and 4-6 are summaries of the propellant and mission weights obtained from the LMV analysis. LEM payload weights are given in Table 4-6 for vehicles fueled with liquid hydrogen, initially saturated at 11.7 N/cm^2 (17 psia) and the triple-point, as well as with 50-percent slush hydrogen.

These results indicate that the separated LEM weight can be increased by approximately 227 kg (500 lb), or 1.2 percent, when triple-point liquid hydrogen is used rather than liquid hydrogen initially saturated at 11.7 N/cm^2 (17 psia). Further, an additional increase of approximately 59 kg (130 lb) can be obtained when 50-percent slush hydrogen is used. This weight is approximately 284 kg (627 lb), or 1.5 percent, greater than that for the saturated liquid-reference case.

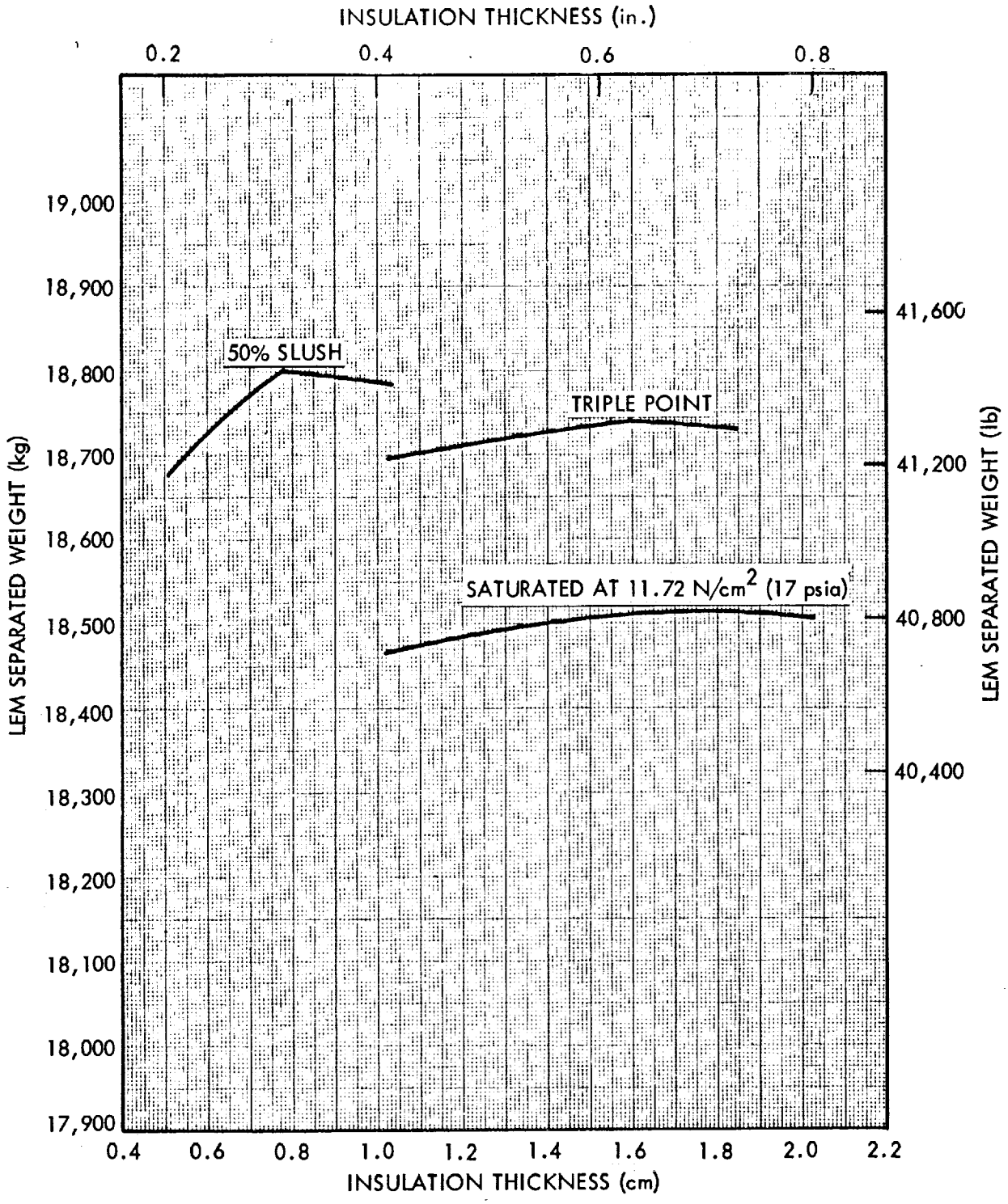

Fig. 4-13 LEM Weight Separated in Lunar Orbit vs. LMV Hydrogen Tank Insulation Thickness

The percent increase in payload weights, obtained with use of triple-point liquid and slush hydrogen, is not very large when compared to the total weight of the separated LEM vehicle. However, since this weight increase can be used entirely for extending mission time or data gathering, a significant advantage in information return can be realized. Also, elimination of venting with use of these subcooled fuels does provide a significant benefit. This effect allows operation of hydrogen-fueled vehicles on a similar basis as that for earth-storable-fueled vehicles in that the complexity of venting hydrogen in a low-gravity environment can be avoided.

Table 4-5

SUMMARY OF LMV/ADVANCED APOLLO HYDROGEN WEIGHTS FOR TWO TANKS

Initial Hydrogen Condition	Sat. Liquid at 11.7 N/cm^2 (17 psia) kg (lb)	Triple-Point Liquid kg (lb)	50% Slush kg (lb)
Total Tanked	2,295 (5,060)	2,165 (4,774)	2,160 (4,762)
Usable[(a)]	2,028 (4,472)	2,027 (4,468)	2,027 (4,464)
Unusable[(b)]	267 (588)	139 (306)	135 (298)
Impulse Propellant			
Retro to Lunar Orbit	1,466 (3,231)	1,468 (3,236)	1,468 (3,236)
Transearth Injection	563 (1,241)	559 (1,232)	557 (1,228)
Vented	117 (258)	0 (0)	0 (0)
Preflow and Chilldown	63 (138)	63 (138)	63 (138)
Trapped	3 (6)	3 (6)	3 (6)
Liquid Residual	23 (50)	23 (50)	23 (50)
Vapor Residual	62 (136)	51 (112)	47 (104)

(a) Sum of impulse propellant.
(b) Sum of all other propellants.

Table 4-6

SUMMARY OF LMV/ADVANCED APOLLO MISSION WEIGHTS

Initial Hydrogen Condition	Sat. Liquid at 11.7 N/cm^2 (17 psia) kg (lb)	Triple-Point Liquid kg (lb)	50% Slush kg (lb)
Tanked Oxygen	10,551 (23,260)	10,535 (23,225)	10,525 (23,204)
Tanked Hydrogen	2,295 (5,060)	2,165 (4,774)	2,160 (4,762)
Tanked Storable Propellant	1,805 (3,979)	1,784 (3,932)	1,781 (3,927)
Engine Mixture Ratio	5.0	5.0	5.0
Gross Translunar Injected	45,360 (100,000)	45,360 (100,000)	45,360 (100,000)
Less Adapter	1,015 (2,238)	1,015 (2,238)	1,015 (2,238)
Less Expendables	10,270 (22,642)	10,276 (22,654)	10,276 (22,654)
Gross Weight Injected Into Lunar Orbit	34,074 (75,120)	34,069 (75,108)	34,069 (75,108)
Less Separated LEM	18,514 (40,816)	18,740 (41,313)	18,799 (41,443)
Less Expendables	3,626 (7,994)	3,467 (7,643)	3,456 (7,618)
Gross Weight Injected Into Transearth Trajectory	11,934 (26,310)	11,863 (26,152)	11,815 (26,047)
Less Expendables	376 (830)	374 (825)	372 (820)
Gross Burnout	11,558 (25,480)	11,488 (25,327)	11,443 (25,227)
Less Residuals	378 (833)	367 (809)	363 (801)
Dry Burnout	11,180 (24,647)	11,121 (24,518)	11,080 (24,426)
LMV Dry Inert	3,070 (6,767)	3,011 (6,638)	2,969 (6,546)
Storable Propulsion System	197 (434)	197 (434)	197 (434)
Equip. and Apollo Expendables	2,418 (5,331)	2,418 (5,331)	2,418 (5,331)
Adapter	218 (480)	218 (480)	218 (480)
Command Module	5,278 (11,635)	5,278 (11,635)	5,278 (11,635)
Increase in LEM Weight	(a)	225 (497)	284 (627)
Increase in LEM Weight	(b)	1.22[(b)]	1.54[(b)]

(a) Based on reference vehicle.
(b) Percent weight increase.

Section 5
EARTH ORBITAL TANKER APPLICATION STUDIES

5.1 VEHICLE/MISSION CHARACTERISTICS

An uprated Saturn V earth orbital hydrogen tanker (EOHT) was selected by MSFC as a typical nonpropulsive vehicle candidate for subcooled liquid- and slush-hydrogen application studies. The reference vehicle design and mission profile were taken directly from a previous Lockheed investigation for MSFC (Ref. 5-1). In this application study, liquid hydrogen initially saturated at 11.7 N/cm^2 (17 psia) was used for the reference case. Figure 5-1 shows the tanker inboard profile.

The tanker is launched and injected into a 185-km (100-nm) circular earth orbit by an uprated Saturn V booster. An independent RL10 propulsion system, which is attached to the tanker then fires to place it in a 485-km (262-nm) circular orbit. The tanker coasts in this higher orbit for the 120-day mission duration, after which the tanked hydrogen is transferred into a receiving vehicle.

When boiloff and venting are required to deliver the propellant as saturated liquid under a pressure of 17.2 N/cm^2 (25 psia), venting is performed during S-II firing for ascent into earth orbit. At this time the hydrogen is oriented by booster acceleration. An isentropic blowdown venting model was assumed for this phase of the mission.

Three independent effects were evaluated in the tanker application studies. In the first study, tanker volumes and insulation thicknesses were optimized for each initial hydrogen condition. Considered in the study was delivery of saturated propellant under a pressure of 17.2 N/cm^2 (25 psia). This was to occur at the end of the mission, before transfer to the receiver. An insulation thermal conductivity value of 3.5×10^{-7} w/cm°K (2×10^{-5} Btu/hr ft°R) was used during investigation of the first effect. The optimization procedure and operating characteristics assumed

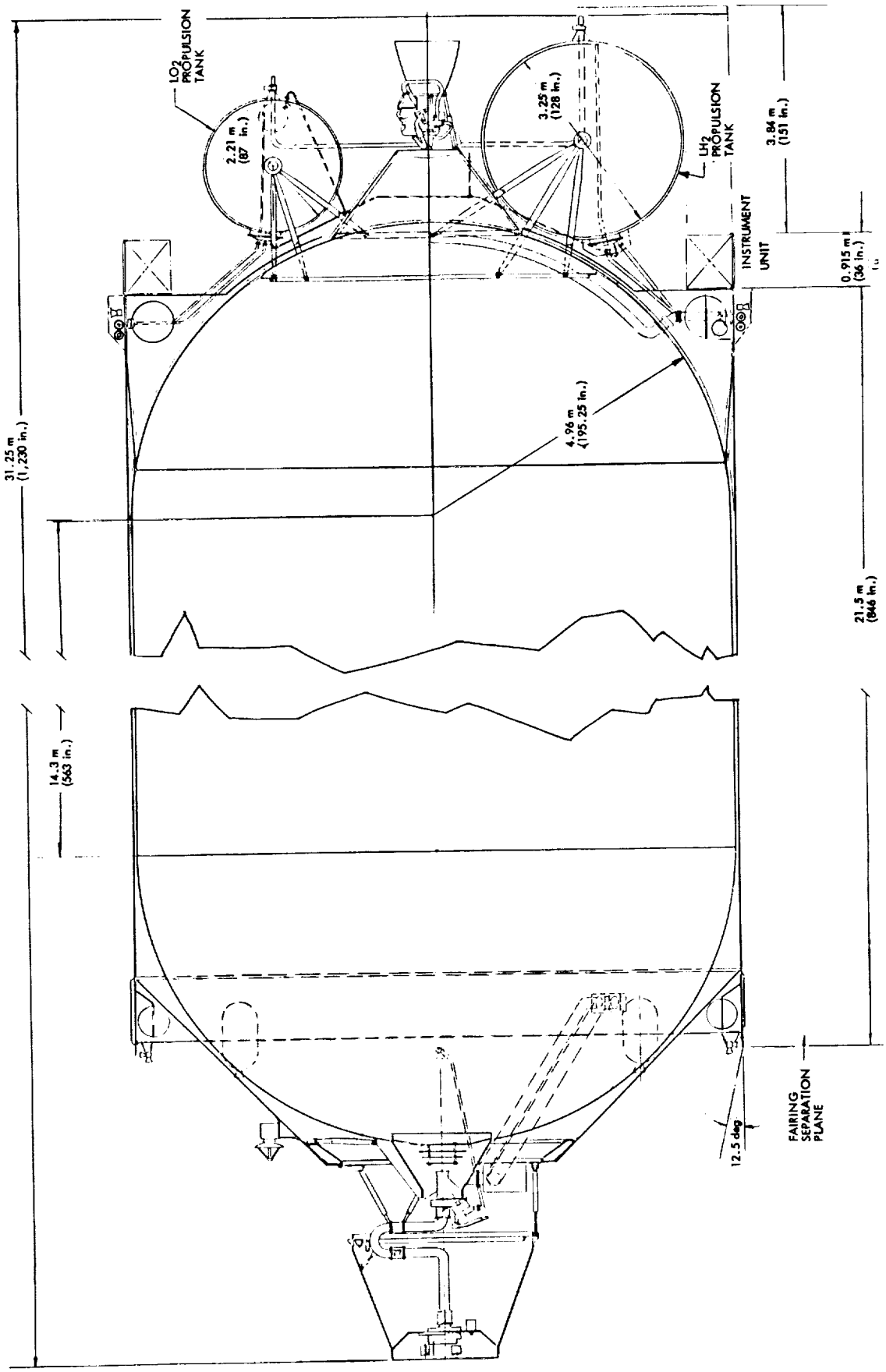

Fig. 5-1 Uprated Saturn V Liquid Hydrogen Tanker

in evaluating the second effect are identical to those used for the first, except that an insulation conductivity value of 1.7×10^{-6} w/cm°K (1×10^{-4} Btu/hr ft°R) was used. The third effect studied is that of delivering the propellant in a sufficiently subcooled condition so that it is just saturated at a pressure of 17.2 N/cm^2 (25 psia) after transfer to and cooling of the receiver tank. In this case the nominal thermal conductivity value of 3.5×10^{-7} w/cm°K (2×10^{-5} Btu/hr ft°R) was used.

5.2 PROPELLANT MANAGEMENT SYSTEM

Results of the systems optimization studies described in Section 2 were applied to the preliminary propellant management studies performed for the tanker. The three specific studies performed were tank fill and ground hold, system tolerance effects, and instrumentation for quantity and quality measurements. The results presented in this section correspond to preliminary vehicle/mission characteristics, and were not modified for final vehicle characteristics.

5.2.1 Tank Fill and Ground Hold

The following EOHT characteristics were assumed for the preliminary analyses:

- Loaded hydrogen weight = 109,771 kg (242,00 lb)
- Steady-state ground-hold heat rate = 71,199 to 711,990 w (243,000 to 2,430,000 Btu/hr)

Recirculation, helium-vapor injection, and cold-helium heat-exchanger operation were the techniques investigated in the preliminary analyses to obtain approximate tank-fill and ground-hold requirements. Results of these techniques are summarized in Table 5-1. As with the previous vehicle application studies, the recirculation technique was shown to be superior to the others. The discussion in subsection 3.2.1 for the S-IVB vehicle recirculation system also applies to the EOHT.

Table 5-1

PREDICTED TANK-FILL AND GROUND-HOLD REQUIREMENTS FOR THE EOHT VEHICLE[a]

Technique	Recirculation	GHe Injection	Cold GHe Heat Exchanger
Transient cooldown			
T_1 of LH_2, °K(°R)	–	20.33 (36.6)	20.33 (36.6)
T_2 of LH_2, °K(°R)	–	13.83 (24.9)	13.83 (24.9)
T_1 of GHe, °K(°R)	–	11.11 (20.0)	11.11 (20.0)
GHe flow rate, kg/hr(lb/hr)	–	106,596 (235,000)	140,616 (310,000)
Cooldown time, hr	–	1.0	2.0
Steady-state operation to maintain triple-point liquid or slush			
Degradation in transfer line, $\Delta X/X_1$	0.016	–	–
H_2 flowrate for $X_a = 50\%$, $X_{b2} = 50\%$, kg/hr(lb/hr)	76,658 (169,000)	–	–
Recirculation period, hr	1.4	–	–
11.11°K(20°R) GHe flow rate, kg/hr(lb/hr)	–	82,555 (182,000)	175,090 (386,000)
Slush formation in vehicle tank			
11.11°K(20°R)GHe required to form 50% slush, kg (lb)	–	102,060 (225,000)	219.996 (485,000)

[a] Q = 711,990 w (2,430,000 Btu/hr)

5.2.2 System Tolerance Effects Study

The equations described in subsection 2.2.2 were evaluated in a preliminary study to assess tanker payload penalties as a function of tolerance values on each hydrogen tank variable. For the EOHT, the most critical variable is loaded hydrogen quantity. Smaller penalties, listed in the order of their significance to payload, are heat rate to the hydrogen for a slush-fueled tanker, flight vent pressure, loaded hydrogen quality, ground vent pressure, and heat rate to the hydrogen for a saturated-liquid-fueled tanker.

Presently predicted state-of-the-art system tolerances on each variable result in the payload penalties summarized in Table 5-2 for the EOHT fueled with hydrogen at the three different initial conditions of interest. Corresponding total system payload penalties were obtained by combining the individual tolerance penalties using a root-mean-square probability that all would occur in a given mission. These total penalties are also given in Table 5-2.

5.2.3 Instrumentation Requirements

Quantity- and quality-sensing instrumentation and control components require modifications or additions for use of subcooled liquid or slush. For the EOHT, the important modifications and the components to which they apply are as follows:

- Replacement or recalibration of temperature and capacitance sensors
- Installation of recirculation-system liquid-return line, control valve, and disconnect
- Installation of a gamma radiation (or x-ray) attenuation system for quality measurements

Differences in weight were assumed to be negligible for necessary modifications to other vehicle instrumentation and control components.

Table 5-2

PAYLOAD PENALTIES RESULTING FROM PREDICTED HYDROGEN SYSTEM TOLERANCES FOR THE EOHT

Variable[a]	Nominal Value	Predicted Tolerance (%)	Tolerance Value	Payload Penalty
Loaded H_2 Quantity	111,132 kg (245,000 lb)	1	1111 kg (2,450 lb)	1,098 kg (2,420 lb)
Loaded H_2 Solid Fraction	50%	10	N.A./5%	N.A./1449 kg (N.A./3,194 lb)
Ground Vent Pressure	11.7 N/cm^2 (17 psia)	5	0.59 N/cm^2 (0.85 psia)[b]	522 kg[b] (1,150 lb)[b]
Flight Vent Pressure	17.2 N/cm^2 (25 psia)	5	0.86 N/cm^2 (1.25 psia)	803 kg (1,770 lb)
Heat Rate to the Hydrogen	226/1,026 w (772/3,500 Btu/hr)	25	57/256 w (193/875 Btu/hr)	1,261/5,724 kg (2,780/12,620 lb)
Total System Payload	109,771 kg (242,000 lb)	1.75/5.52	–	1,928/6,060 kg (4,250/13,360 lb)

(a) When two values are given, the first applies to the liquid-fueled systems and the second to slush-fueled systems; single values apply to both.

(b) Not applicable.

5.3 INSULATION SYSTEM

An aluminized Mylar/Dexiglas multilayer insulation system, identical in concept to that described in subsection 4.4 for the LMV, was assumed for EOHT studies. Again, the insulation system is installed directly on the outside of the tank without a substrate. The multilayers are purged with helium gas during ground hold and allowed to outgas during ascent.

A nominal effective thermal conductivity value of 3.5×10^{-7} w/cm °K (2×10^{-5} Btu/hr ft °R) was assumed for the study. However, the effect of higher conductivities, typical of state-of-the-art systems, was assessed by also considering a value of 1.7×10^{-6} w/cm°K (1×10^{-4} Btu/hr ft °R). An average installed insulation density of 80 kg/m^3 (5.0 lb/ft^3) was used to calculate insulation weights, which vary with thickness.

5.3.1 Preliminary Optimization

Preliminary optimization procedures discussed in subsection 2.4 were initially applied to obtain an estimate of the optimum insulation thickness for the tanker. As in the case of the Lunar Mission Vehicle, preliminary calculations were performed assuming a uniform heating rate through the multilayer insulation blankets. Also, no orientation of the vehicle with respect to the sun was assumed. Since the tanker is non-propulsive, the preliminary insulation optimization was obtained assuming that the propellant transfer at the end of the earth orbit period is equivalent to that for a single-firing propulsive stage. Venting was assumed to occur in space, as required, which results in a boiloff factor of 1.0. This assumption was modified in the final optimization analysis to one where all venting is accomplished during ascent and the propellants are oriented by booster acceleration. For this latter assumption, the boiloff factor is 0.25.

Optimized multilayer insulation thicknesses and the related parametric quantities obtained in the preliminary analysis for two initial propellant conditions are presented in Table 5-3.

Table 5-3

SUMMARY OF PRELIMINARY OPTMIZED MULTILAYER INSULATION THICKNESS AND RELATED QUANTITIES FOR THE EARTH ORBITAL HYDROGEN TANKER

Q_p = 117 w (400 Btu/hr)

K = 3.5×10^{-7} w/cm^{o}K (2×10^{-5} Btu/hr ft^{o}R)

A = 752 m^2 (8100 ft^2)

W_P = 111,132 kg (245,000 lb)

ΔT = 150^{o}K (270^{o}R)

ρ_I = 70.5 kg/m^3 (4.4 lb/ft^3)

θ_M = 120 days

Vent pressure = 17.2 N/cm^2 (25 psia)

BF = 1

q^* = 0.219 cm^{-1} (6.67 ft^{-1})

α = 0.831×10^{-6} m^2/hr (0.894×10^{-5} ft^2/hr)

	Initially Saturated Liquid at 17 psia	Initially 50% Solid at 1.02 psia
θ_M^* (hr)	1,830	19,800
ϕ, cm (ft)	7.193 (0.236)	48.768 (1.60)
δ_{OPT}, cm (in.)	4.90 (1.93)	0.556 (0.219)
W_{BO}, kg (lb)	1,574 (3,470)	0 (0)
W_I, kg (lb)	2,586 (5,700)	296 (652)
$W_{BO} + W_I$, kg (lb)	4,160 (9,170)	296 (652)

5.3.2 Final Optimization

Detailed numerical analyses were performed to obtain the final optimum insulation thicknesses for the EOHT. These analyses, conducted in a manner similar to that employed for the other study vehicles, included heat-transfer considerations and final optimization procedure and results.

5.3.2.1 Significant Heat Transfer Considerations

Heat transfer to the hydrogen was calculated independently for three chronological time periods, during which temperature and conductivity of the insulation are significantly different. These time periods are ground hold, ascent and cooldown, and steady-state earth orbit. Within each time period, heat transfer through insulation and structural and plumbing penetrations was considered.

Ground Hold. Thermal conductivity of the multilayer insulation during the 90-sec period after topping or recirculation ceases was taken as that of helium purge gas at the average insulation temperature.

Ascent and Cooldown. During ascent and cooldown analysis, two separate transient effects were considered. First, the thermal conductivity of the insulation was assumed to decrease rapidly with outgassing of the helium purge gas as the ambient pressure decreases. It was assumed to reach the steady-state evacuated values at 680 sec after launch. The second effect considered was the shroud and insulation temperature variations. Shroud temperature was assumed to increase to a maximum value during ascent, and then to gradually cool to the steady-state orbital value in approximately 0.4 hr. Corresponding variations in insulation temperature were assumed to occur during this time period.

Steady-state Earth Orbit. Heat transfer during the 120-day earth-orbit storage period was assumed to be constant. As described in subsection 5.1, two values of thermal conductivity were assumed in succeeding analyses to evaluate the effect of conductivity

variations. The nominal conductivity value assumed was 3.5×10^{-7} w/cm °K (2×10^{-5} Btu/hr ft° R), and the degraded value was 1.7×10^{-6} w/cm °K (1×10^{-4} Btu/hr ft °R). Environmental temperatures during the orbit period were taken from the tanker study (Ref. 5-2).

Temperatures were adjusted to calculate heat transfer to the triple-point liquid and slush-hydrogen tankers.

Figure 5-2 shows the total heat transferred to the hydrogen as a function of time for 120-day earth-orbital hydrogen tankers filled with saturated liquid, triple-point liquid, and slush hydrogen. The data presented in the figure give total heat transfer for the nominal conductivity value and for an assumed tanker surface area of 755 m^2 (8,125 ft^2). These data were adjusted in the analyses to consider the effects of degraded conductivity and variable surface area.

5.3.2.2 Final Optimization Procedure and Results

The object of the insulation optimization for the tanker was to select the insulation thickness that results in delivery of the maximum hydrogen quantity at the end of the orbital storage period. This was accomplished independently for saturated liquid, triple-point liquid, and 50-percent slush initial hydrogen conditions. A maximum delivered hydrogen quantity results when the sum of insulation, boiloff (multiplied by a dropped weight factor of 0.25), volume-dependent structure, and residual vapor weights is minimized. Total system weights are limited by booster capability, which is assumed to be 150,854 kg (332,570 lb) (Ref. 5-3). Of the weights shown in the reference weight summary, the 24,593-kg (54,218-lb) value is assumed to be constant and therefore does not vary in the optimization analyses. An iterative procedure was used to select the variable system weights so that

$$W_P + W_I + 0.25\, W_{BO} + \Delta W_V + \Delta W_R + \begin{Bmatrix} 24,593 \text{ kg} \\ (54,218 \text{ lb}) \end{Bmatrix} = \begin{Bmatrix} 150,854 \text{ kg} \\ (332,570 \text{ lb}) \end{Bmatrix} \qquad (5.1)$$

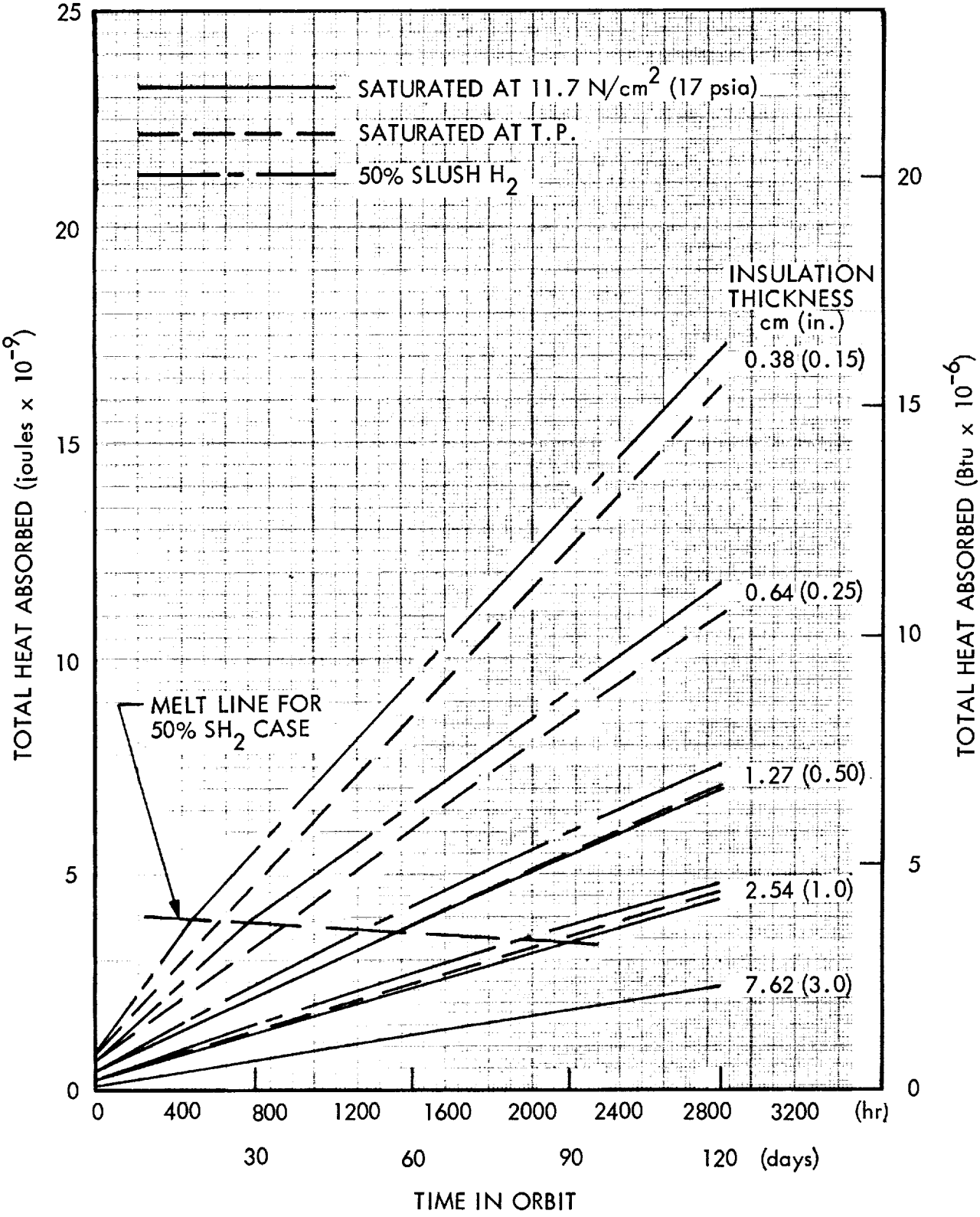

Fig. 5-2 Estimated Total Heat Transfer to Hydrogen Tank of EOHT

Optimum tanker insulation thickness for each initial hydrogen condition was obtained from a plot of system weight increments ($W_I + 0.25\ W_{BO} + \Delta W_V + \Delta W_R$) as a function of insulation thickness. Results are presented in Fig. 5-3 for the case of triple-point hydrogen. The data presented are based on the first set of conditions noted in subsection 5.1; i.e., the hydrogen delivered at the end of the orbital sotrage period is saturated under a pressure of 17.2 N/cm^2 (25 psia) prior to transfer and the insulation conductivity is 3.5×10^{-7} w/cm ^oK (2×10^{-5} Btu/hr ft ^oR).

The quantity of orbital-tanker hydrogen delivered at the end of the orbit storage period is shown in Fig. 5-4 as a function of insulation thickness. Results are shown for both the nominal thermal conductivity value and the degraded value, which corresponds to the second set of conditions discussed in subsection 5.1. It can be seen that only single points that result in zero boiloff were calculated for triple-point liquid and slush applications to the degraded conductivity value, since the curves for the nominal conductivity indicate that the zero-boiloff thicknesses are optimum.

Optimum insulation thickness values were obtained for the third set of conditions described in subsection 5.1 in the same manner as for the other two cases. This case considered transfer of subcooled hydrogen at the end of the orbit storage period as saturated liquid at 17.2 N/cm^2 (25 psia) after cooling down the receiving vehicle. Results of this analysis, summarized in subsection 5.7, were not plotted.

5.4 VENTING SYSTEM

The venting system required for the EOHT is similar to those previously discussed for the S-IVB and the LMV. Venting is assumed to occur, when required, as an isentropic blowdown of the tank ullage pressure with the propellants oriented by acceleration forces. For the final analysis, all venting was therefore assumed to occur during S-II firing for ascent. Sufficient subcooling is achieved during the vent period so that subsequent environmental heating of the hydrogen will result in saturation at the desired final conditions. A mixer system weighing approximately 4.5 kg (10 lb), excluding a power supply, can be used to minimize the effects of stratification in the tanker, as with the other study vehicles.

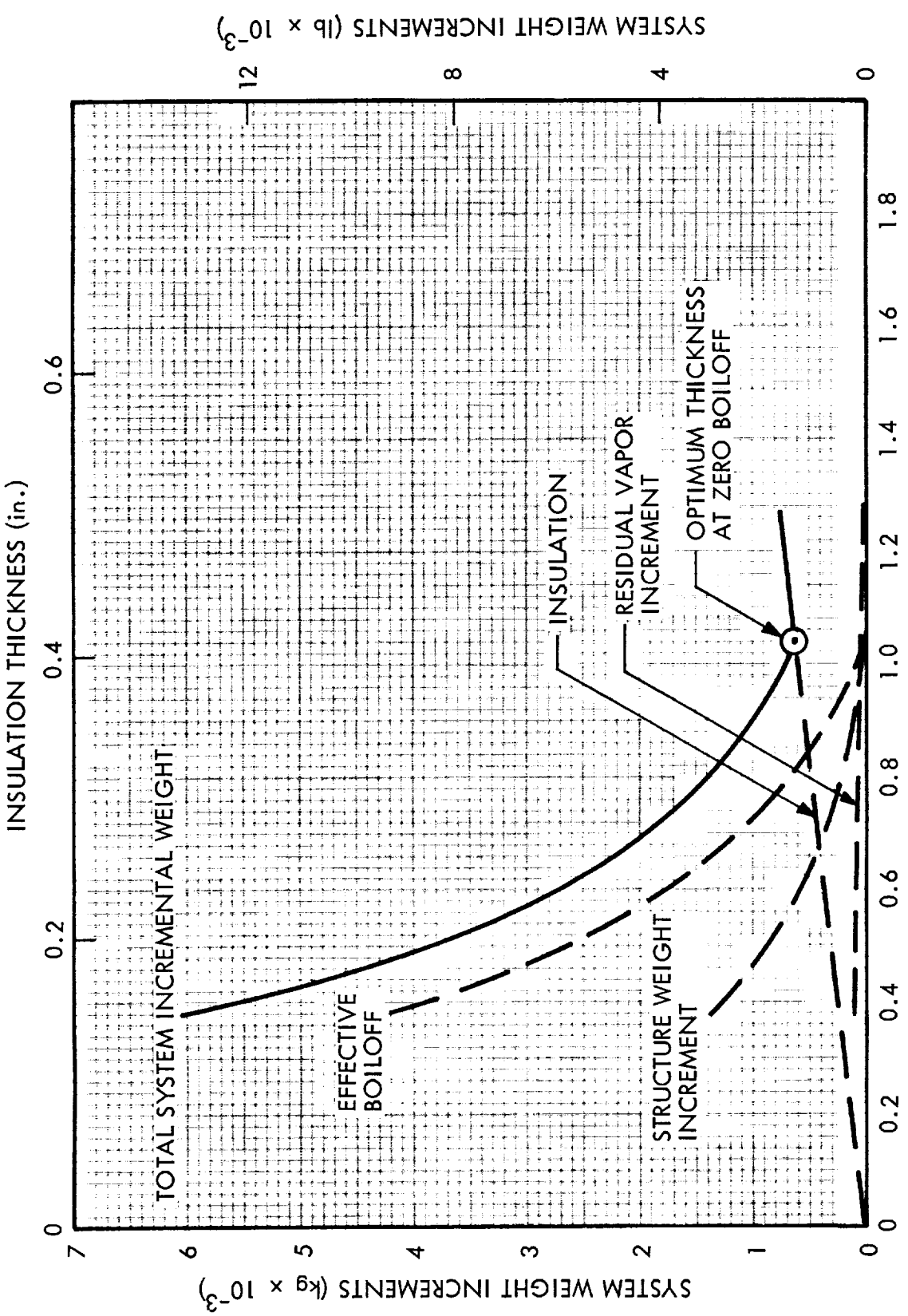

Fig. 5-3 Optimum Insulation Thickness for EOHT – Initially Triple-Point LH_2

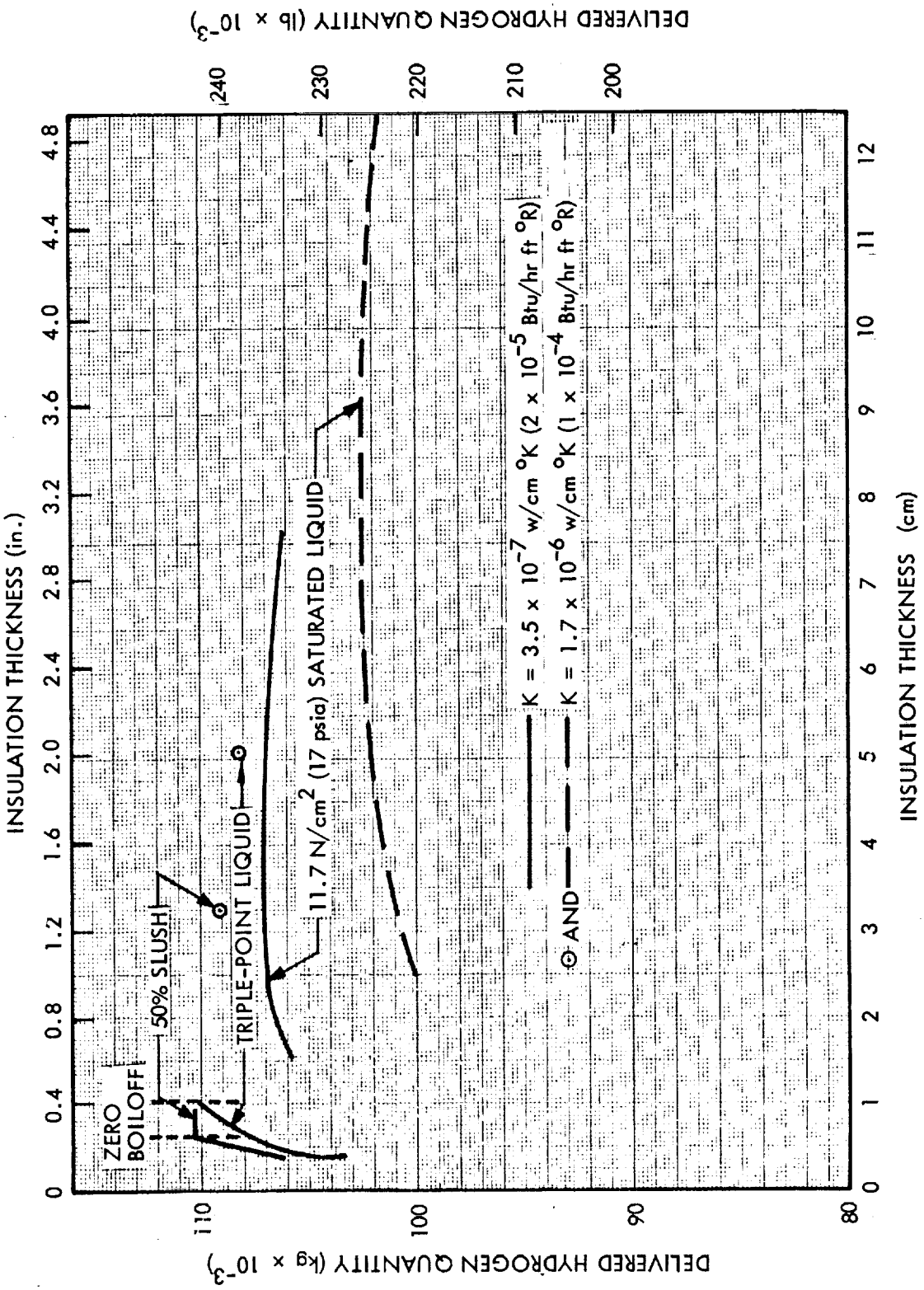

Fig. 5-4 Effect of Insulation Thickness on Quantity of Delivered Hydrogen

Figure 5-5 presents EOHT ullage pressure-time histories for hydrogen at the three specified initial conditions. Venting indicated for the triple-point liquid and 50-percent slush cases is that required to void the tank of the partial helium pressure used to prevent buckling of the tank during ground operations and the early ascent period. This venting results in loss of a negligible quantity of hydrogen. Venting analysis is based on the model and equations developed in subsection 2.5.

5.5 TANK-AFFECTED STRUCTURES

The tanker cylindrical section length, and therefore tank volume, was varied for each case considered in the analysis to maximize the delivered hydrogen quantity. A similar variation in the length of the external shell is required. This procedure was based on the assumption that the design should be optimized independently for each initial hydrogen condition, since the tanker is not yet an existing vehicle. Figure 5-3 shows the incremental variation in total tanker structure weight as a function of insulation thickness.

Installation of a liquid-return line, shutoff valve, and disconnect, plus additional instrumentation and controls for quality measurement, was also considered in the study.

5.6 PERFORMANCE ANALYSIS

Fixed performance capability for the uprated Saturn V launch vehicle was assumed for all cases considered in the analysis. This capability, discussed in subsection 5.3, results in a 150,854 kg (332,570 lb) gross tanker weight being injected into the 185-km (100-nm) earth orbit. When venting during ascent is required, the injected gross weight is reduced by effective boiloff weight ($0.25\ W_{BO}$) to account for the tradeoff of weight dropped during S-II firing.

No consideration was given in this analysis to the small variation that would be required in RL10 propulsion system weights for orbit adjustment to 485 km (262 nm) after injection.

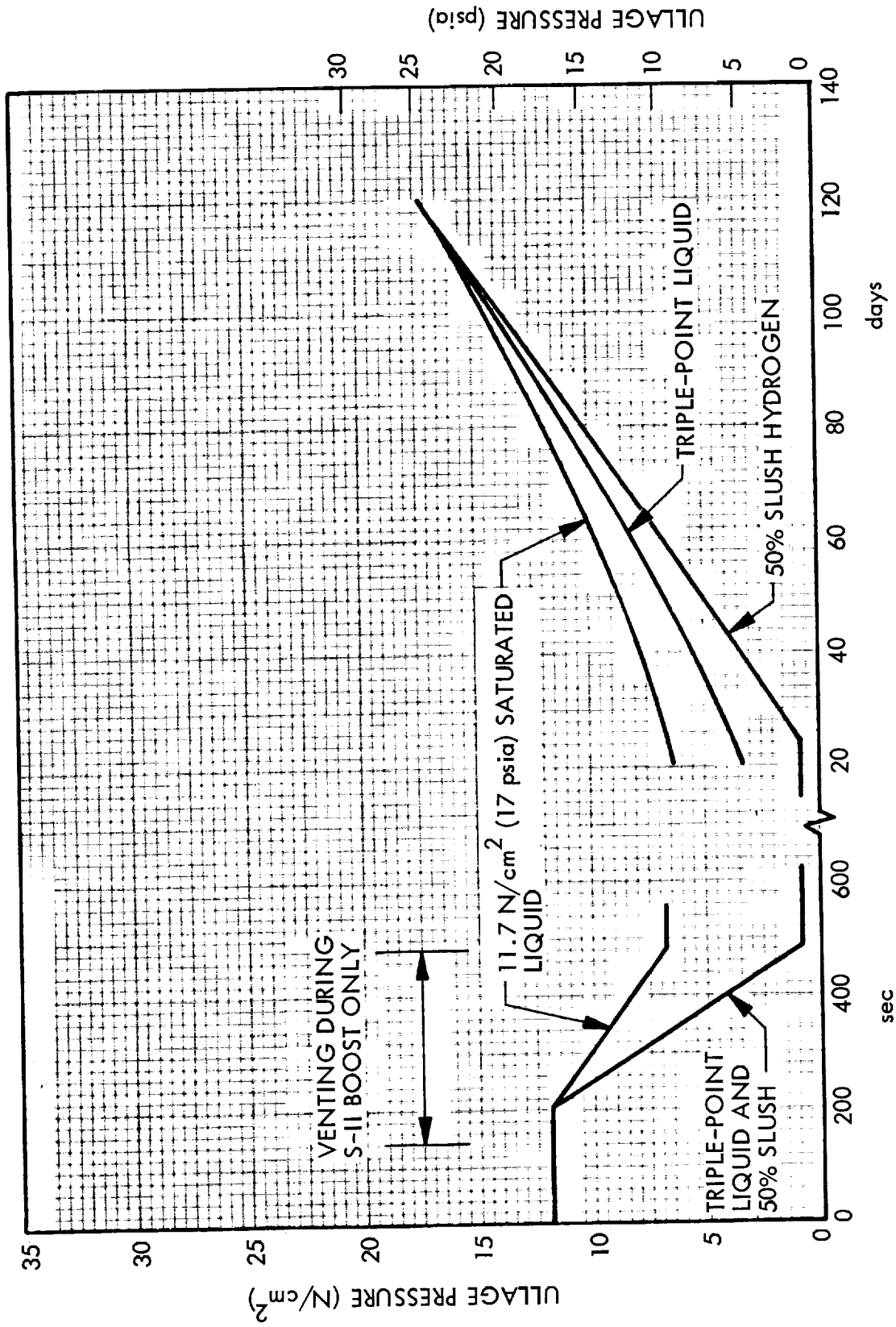

Fig. 5-5 Ullage Pressure History for Uprated Saturn V Orbital Tanker

5.7 WEIGHT AND PAYLOAD SUMMARIES

Tables 5-4, 5-5, and 5-6 are summaries of optimized tanker characteristics and delivered hydrogen weights that were obtained in the analysis. The three sets of limiting conditions, previously described in subsection 5.1, are as follows:

- Delivery of saturated liquid hydrogen before transfer at the end of the orbit storage period with a nominal effective insulation conductivity of 3.5×10^{-7} w/cm ^{o}K (2×10^{-5} Btu/hr ft ^{o}R)
- Identical conditions to the above, except with a degraded effective insulation conductivity of 1.7×10^{-6} w/cm ^{o}K (1×10^{-4} Btu/hr ft ^{o}R)
- Delivery of saturated liquid hydrogen after transfer and cooldown of the receiving vehicle with the nominal effective insulation conductivity

A summary of the EOHT total system weights, which corresponds to the first item above, is presented in Table 5-7.

As shown in Table 5-4, payload gains of 3,225 kg (7,110 lb), or 3 percent and 3,361 kg (7,410 lb), or 3.1 percent, can be obtained using triple-point liquid and 50-percent slush, respectively, compared to use of saturated liquid. These gains correspond to delivery of saturated liquid in the tanker, prior to transfer, with an insulation conductivity of 3.5×10^{-7} w/cm ^{o}K (2×10^{-5} Btu/hr ft ^{o}R).

Data presented in Table 5-5 show that payload gains of 5,747 kg (12,670 lb), or 5.6 percent, and 6,691 kg (14,750 lb), or 6.5 percent, can be obtained for the same respective initial hydrogen conditions, but with a degraded insulation conductivity of 1.7×10^{-6} w/cm ^{o}K (1×10^{-4} Btu/hr ft ^{o}R).

Similarly, Table 5-6 shows that payload gains of 10,750 kg (23,700 lb), or 10.9 percent, and 11,431 kg (25,200 lb), or 11.6 percent, can be obtained for the same respective initial hydrogen conditions and with the nominal insulation conductivity value; however, in this case, the payloads are evaluated after transfer and cooldown of the receiving vehicle.

Table 5-4

TANKER CHARACTERISTICS FOR DELIVERY OF SATURATED LIQUID BEFORE TRANSFER (NOMINAL INSULATION)[a]

Variable	11.7 N/cm^2 (17 psia) Saturated Liquid	Triple-Point Liquid	50% Slush
Optimum Insulation Thickness, cm (in.)	3.81 (1.5)	1.04 (0.41)	0.64 (0.25)
Tank Volume, m^3 (ft^3)	1,681 (59,350)	1,663 (58,725)	1,665 (58,800)
Ullage at Launch, %	4	13	17
Initial Propellant Load, kg (lb)	113,028 (249,180)	111,785 (246,440)	111,935 (246,770)
Propellant Boiloff, kg (lb)	4,441 (9,790)	0 (0)	0 (0)
Residual GH_2, kg (lb)	1,674 (3,690)	1,657 (3,653)	1,659 (3,657)
Delivered Hydrogen Payload, kg (lb)	106,914 (235,700)	110,139 (242,810)	110,275 (243,110)
Payload Gain, kg (lb) (%)	(b)	3,225(7,110)(3.0%)	3,361(7,410)(3.1%)

(a) $K = 3.5 \times 10^{-7}$ w/cm ^{o}K (2×10^{-5} Btu/hr ft ^{o}R)

(b) Based on reference vehicle

Table 5-5

TANKER CHARACTERISTICS FOR DELIVERY OF SATURATED LIQUID BEFORE TRANSFER (DEGRADED INSULATION)[a]

Variable	11.7 N/cm^2 (17 psia) Saturated Liquid	Triple-Point Liquid	50% Slush
Optimum Insulation Thickness, cm (in.)	6.35 (2.50)	5.08 (2.00)	3.18 (1.25)
Tank Volume, m^3 (ft^3)	1,757 (62,050)	1,634 (57,700)	1,647 (58,160)
Ullage at Launch, %	4	13	17
Initial Propellant Load, kg (lb)	118,412 (261,050)	109,703 (241,850)	110,660 (243,960)
Propellant Boiloff, kg (lb)	14,334 (31,600)	0 (0)	0 (0)
Residual GH_2, kg (lb)	1,751 (3,860)	1,628 (3,590)	1,642 (3,620)
Delivered Propellant Payload, kg (lb)	102,328 (225,590)	108,075 (238,260)	109,018 (240,340)
Payload Gain, kg (lb) (%)	(b)	5,747(12,670)(5.6%)	6,691(14,750)(6.5%)

(a) $K = 1.7 \times 10^{-6}$ w/cm ^{o}K (1×10^{-4} Btu/hr ft ^{o}R).

(b) Based on reference vehicle.

Table 5-6

TANKER CHARACTERISTICS FOR DELIVERY OF SATURATED LIQUID AFTER TRANSFER (NOMINAL INSULATION)[a]

Variable	11.7 N/cm^2 (17 psia) Saturated Liquid	Triple-Point Liquid	50% Slush
Optimum Insulation Thickness, cm (in.)	3.81 (1.50)	2.54 (1.00)	1.27 (0.50)
Tank Volume, m^3 (ft^3)	1,681 (59,350)	1,650 (58,280)	1,643 (58,000)
Ullage at Launch %	4	13	17
Initial Propellant Load, kg (lb)	113,028 (249,180)	110,923 (244,540)	111,608 (246,050)
Propellant Boiloff, kg (lb)	12,830 (28,290)	0 (0)	0 (0)
Residual GH_2, kg (lb)	1,674 (3,690)	1,644 (3,625)	1,653 (3,645)
Delivered Propellant Payload, kg (lb)	106,914 (235,700)	109,272 (240,900)	109,953 (242,400)
Received Usable Propellant, kg (lb)	98,522 (217,200)	109,272 (240,900)	109,953 (242,400)
Received Payload Gain, kg (lb) (%)	(b)	10,750(23,700)(10.9%)	11,431(25,200)(11.6%)

(a) $K = 3.5 \times 10^{-7}$ w/cm ^{o}K (2×10^{-5} Btu/hr ft ^{o}R).

(b) Based on reference vehicle.

Table 5-7

SUMMARY OF TOTAL SYSTEM WEIGHTS FOR THE EOHT
(NOMINAL CASE)

Item	Initial Hydrogen Condition		
	11.7 N/cm^2 (17 psia) Sat. Liquid	Triple-Point Liquid	50% Slush
Weights Considered Fixed for This Study, kg (lb)			
Primary Propulsion Propellant	7,212 (15,900)		
Secondary Propulsion Propellant	3,139 (6,920)		
Disposal Solid Rockets	2,188 (4,823)		
Propulsion System and Supports	1,270 (2,800)		
Secondary Propulsion System	308 (680)		
Docking System	816 (1,800)		
Propellant Transfer System	953 (2,100)		
Interstage Assembly	1,497 (3,300)		
Nose Shroud	2,862 (6,310)		
Docking Electronics	107 (235)		
Instrument Unit	1,792 (3,950)		
Additional Power Supply	318 (700)		
Additional Meteoroid Shield	2,132 (4,700)		
Weights Optimized for the Study Assumptions, kg (lb)			
Payload Tank, Shell, and Support	14,330 (31,595)	13,727 (30,265)	13,958 (30,773)
Insulation System	2,232 (4,920)	737 (1,624)	368 (812)
Vented Hydrogen	4,441 (9,790)	0 (0)	0 (0)
Residual Hydrogen Vapor	1,674 (3,690)	1,657 (3,653)	1,659 (3,657)
Delivered Liquid Hydrogen	106,914 (235,700)	110,139 (242,810)	110,275 (243,110)
Gross Weight	154,185 (339,913)	150,854 (332,570)	150,854 (332,570)

Section 6
REFERENCES

2-1 Aerojet-General Corporation, Cryogenic Flow Measurements, Technical Memo No. 149, Sacramento, California, 17 January 1962

2-2 B. L. Sutton (of Gilmore Industries, Inc.), "Measurement of Cryogenic Fuels by Weight," (paper presented to the Seventeenth Annual ISA Conference, October 1962)

2-3 Thomas and Morse, "Analytic Solution for the Phase Change in a Suddenly Pressurized Liquid Vapor System," in Vol. 8 of Advances in Cryogenic Engineering, K. D. Timmerhouse, ed., Plenum Press, New York, 1966

2-4 National Aeronautics and Space Administration, Experimental and Analytical Investigation of Interfacial Heat and Mass Transfer in a Pressurized Tank Coating Liquid Hydrogen, by W. A. Olsen, NASA TRD-3219, Lewis Research Center, Cleveland, Ohio, March 1966

2-5 J. R. O'Loughlin, "Dimensionless Mass Transfer Alignment Chart for Suddenly Pressurized Liquid-Vapor Systems," (paper presented at the Conference on Propellant Tank Pressurization and Stratification held at the Marshall Space Flight Center, Huntsville, Alabama, January 1965)

2-6 Lockheed Missiles & Space Comapny, Asymmetric Propellant Heating Computer Program, LMSC-A794909, Vol. IV, Sunnyvale, California, March 1966

3-1 Douglas Missiles and Space Systems Division of Douglas Aircraft Company, Lunar Applications of a Spent S-IVB/IU Stage (LASS), Report 56365P, by L. O. Schulte et al, Huntington Beach, California, September 1966

3-2 Lockheed Missiles & Space Company, Interim Lunar Exploration Data Book Exploration Equipment, LMSC-A820667, Sunnyvale, California, June 1966

3-3 D. L. Dearing, "Development of the Saturn S-IV and S-IVB Liquid Hydrogen Tank Internal Insulation," in Vol. 11, Advances in Cryogenic Engineering, K. D. Timmerhouse, ed., Plenum Press, New York, 1966

3-4 Douglas Missiles and Space Systems Division of Douglas Aircraft Company, LASS Mid-Study Summary Presentation, Report PP147, by L. O. Schulte et al, Huntington Beach, California, July 1966

3-5 Chrysler Corporation, Evaluation of AS-203 Low Gravity Orbital Experiment, Technical Report HSM-R421-67, Contract NAS 8-4016, Huntsville, Alabama, 13 January 1967

4-1 National Aeronautics and Space Administration, "S-VI Structural Design Study Development and Conclusions," NASA/MSFC Internal Note IN-P and VE-SA-63-44, MSFC P&VE Laboratories, Marshall Space Flight Center, Huntsville, Alabama, September 1963

4-2 Lockheed Missiles & Space Company, "Design of High Performance Insulation Systems – Vol. VI," Handbook of Thermal Design Data for Multilayer Insulation Systems, LMSC-A742593, Synnyvale, California, August 1965

5-1 -----, Orbital Tanker Design Data Study (Final Report), LMSC-A748410, Sunnyvale, California, May 1965

Section 7

CONVERSION FACTORS

Multiply	By	To Obtain
Atmosphere (atm)	14.6959	Pounds per square inch (lb/sq^2)
Atmosphere (atm)	101325	Newtons per square meter (N/m^2)
British thermal unit (Btu)	1054.8	Joules (joule), watt-second (w-sec), or newton-meters (N-m)
Btu per hour-foot-° R (Btu/hr-ft-° R)	1.731×10^{-2}	Watts per cm-° K (W/cm-° K)
Btu per ° R (Btu/° R)	1898.6	Joules per ° K (joule/° K)
Btu per pound-° R (Btu/lb-° R)	4.18674	Joules per gram-° K (joule/gm-° K)
Btu per pound (Btu/lb)	2.32597	Joules per gram (joule/gm)
Btu per pound (Btu/lb)	4.6891	Joules per GMole (joule/GMole)
Degrees Kelvin (° K)	1.8	Degrees Rankine (° R)
Degrees Rankine (° R)	0.556	Degrees Kelvin (° K)
Feet (ft)	0.3048	Meters (m)
Joules (joule), watt-seconds (w-sec), or newton-meters (N-m)	9.481×10^{-4}	British thermal units (Btu)
Joules per° K (joule/° K)	5.267×10^{-4}	Btu per ° R (Btu/° R)
Joules per gram-° K (joule/gm-° K)	0.23885	Btu per pound-° R (Btu/lb-° R)
Joules per gram (joule/gm)	0.42993	Btu per pound (Btu/lb)
Joules per GMole (joule/GMole)	0.21326	Btu per pound (Btu/lb)
Joules per GMole (joule/GMole)	0.4961	Joules per gram (joule/gm)
Joules per gram (joule/gm)	2.01572	Joules per GMole (joule/GMole)
Kilogram (kg)	2.205	Pounds-mass (lb-mass)
Kilogram per cubic meter (kg/m^3)	6.243×10^{-2}	Pounds per cubic foot (lb/ft^3)
Meters (m)	3.281	Feet (ft)
Newtons (N)	0.2248	Pounds-force (lb-force)
Newtons per square meter (N/m^2)	1.450×10^{-4}	Pounds per square inch ($lb/in.^2$)
Newtons per square meter (N/m^2)	9.869×10^{-6}	Atmosphere (atm)
Pounds-mass (lb-mass)	0.4536	Kilogram (kg)
Pounds per cubic foot (lb/ft^3)	16.02	Kilogram per cubic meter (kg/m^3)
Pounds-force (lb-force)	4.448	Newtons (N)
Pounds per square inch ($lb/in.^2$)	6.895×10^{3}	Newtons per square meter (N/m^2)
Pounds per square inch ($lb/in.^2$)	6.804×10^{-2}	Atmosphere (atm)
Watts per cm-° K (w/cm-° K)	57.78	Btu per hour-feet-° R (Btu/hr-ft-° R)